supplemento ai
rendiconti
del Circolo matematico di Palermo

VIIIth *international conference in "stochastic geometry, convex bodies, empirical measures & applications to mechanics and engineering train-transport"*

Taormina - Italy, 28-30 September, 2011

serie II - numero 84 - anno 2012

sede della società: Palermo - Via Archirafi, 34

SUPPLEMENTO

AI

RENDICONTI DEL CIRCOLO MATEMATICO DI PALERMO

DIREZIONE E REDAZIONE
Via Archirafi, 34 - Tel. 091.23891069 - 90123 Palermo (Italia)
E-mail: vetro@math.unipa.it

SUPPLEMENTO

AI

RENDICONTI DEL CIRCOLO MATEMATICO DI PALERMO

DIRETTORE: **P. VETRO**

VIIIth INTERNATIONAL CONFERENCE IN "STOCHASTIC GEOMETRY, CONVEX BODIES, EMPIRICAL MEASURES & APPLICATIONS TO MECHANICS AND ENGINEERING TRAIN-TRANSPORT"

Taormina - Italy, 28-30 September, 2011

Edited by:
Giuseppe Caristi

SERIE II - NUMERO 84 - ANNO 2012



PALERMO
SEDE DELLA SOCIETÀ
VIA ARCHIRAFI, 34

CONFERENCE DATA

Taormina, Italy, 28th - 30th September, 2011

Scientific Committee

M.I. Stoka (Torino - Italia); D. Bosq (Paris - France); V. Capasso (Milano - Italia); G. Caristi (Messina - Italia); P. Deheuvels (Paris - France); A. Duma (Hagen - Germany); P. Gruber (Wien - Austria); D. Lo Bosco (Reggio Calabria - Italia)

Host Organizations

University of Messina - Faculty of Economics

Organizing Committee

G. Caristi; D. Barilla; M. Bisaia; V. Bonanzinga; A. Feminò; G. Leonardi; A. Puglisi

Supported by

Autorità Portuale di Messina
Agricola Catalano
Sicily Region
Assembly Regional Sicilian
Province of Messina
N.G.I. Shipping Company
RFI

Contents

Preface

Bäsel U. - Duma A. – *Reconfiguration of convex cyclic quadrilaterals* pag. 11

Bäsel U. - Duma A. – *Reconfiguration of polygons* » 17

Banik S. - Rangayyan M. R. - Desautels J. E. L. – *Detection of architectural distortion using statistical measures of correlation and stationarity* » 33

Barilla D. - Feminó A. - Puglisi A. – *Laplace problems for regular lattices with eight obstacles* » 43

Barilla D. - Feminó A. - Puglisi A. – *Laplace type problems for three hexagonal lattices with "disk body test"* » 49

Bonanzinga V. – *Buffon's problem with a 3-star and a lattice of parallelograms* » 69

Bosq D. – *A note on Bayesian prediction* » 81

Broniatwski M. - Vajda I. – *Divergences in parametric setting without smoothing or grouping* » 91

Caristi G. - Stoka M. – *A Buffon-Laplace type problem for two Delone covex-concave octagonal lattices and obstacles* » 107

Caristi G. - Stoka M. – *A Buffon-Laplace type problem for two lattices of Delone with obstacles* » 127

Corriere F. - Di Vincenzo D. – *The global comfort criteria as a tool for the optimization of the safety, quality and efficiency in the railway tracks* » 157

Di Pino A. - Campolo M. G. – *Empirical analysis of married women's working time and paid- work equation estimation in Italy* » 167

Forgione A. F. – *The creditworthiness of construction companies* » 177

Cêrin Z. - Gianella G. M. – *Square in Euler triples from Pell and Pell-Lucas numbers* » 187

Heinrich L. – *Some new results on second-order chord power integrals of convex quadrangles* » 195

Lanfranchi M. - Gianetto C. - Souca M. L. – *The gap model applied to rural tourism - a theoretical approach* » 207

Lanfranchi M. – *An analysis of the agricultural activity in EU-27 using the multiple regression* » 219

Montrone S. - Perchinunno P. - De Blasi L. - L'Abbate S. – *A modified density-based algorithm for clustering* » 231

Sorrenti L. – *The chord length distribution function for a non convex polygon* » 241

Streit F. – *On score tests devised to discover late registration of events of point processes* » 251

Zirilli A. - Alibrandi A. – *A GLM approach or the customer satisfaction measurement in some bathing beaches of Messina province* » 259

Preface

The eightth International Conference on "Stochastic Geometry, Convex Bodies, Empirical Measure & Applications to Mechanics and Engineering Train-Transport" took place in Taormina from September 28th to 30th.

This volume collect the Proceedings of the eighth Conference, organized by the Research Group on Integral Geometry, Geometrical Probabilities and Convex Bodies, together Faculty of Economics of Messina University.

The conference was sponsored by the following:

- Messina University - Faculty of Economics
- Sicily Region
- Autorità portuale di Messina
- Province of Messina
- Agricola Catalano
- N.G.I. Shipping Company
- RFI

Our grateful acknowledgements.

We want to thank the *Scientific Committee of the Journal* "Rendiconti del Circolo Matematico di Palermo" for accepting to publish the Proceedings of the Conference in a supplement of the Journal.

Giuseppe Caristi

RENDICONTI DEL CIRCOLO MATEMATICO DI PALERMO
Serie II, Suppl. 84 (2012), pp. 11-16

Reconfiguration of Convex Cyclic Quadrilaterals

Uwe Bäsel Andrei Duma

Dedicated to Professor Peter M. Gruber
on the occasion of his 70th birthday

Abstract

At the beginning of the present paper we define for two arbitrary plane convex polygons $\mathbf{P_1}$ and $\mathbf{P_2}$ with equal perimeter and equal area the relation '$\mathbf{P_1}$ is polygon-rounder than $\mathbf{P_2}$'.

Then, a given cyclic quadrilateral $\mathbf{V_1}$ (with diameter equal to the diameter of the circumscribed circle) and a second cyclic quadrilateral $\mathbf{V_2}$, made from $\mathbf{V_1}$ by cutting it along its diameter and recomposing the two part ('reconfiguration'), are compared concerning their polygon-roundness.

AMS Classification: 60D05, 52A22

Keywords: Geometric probability, stochastic geometry, random sets, random convex sets, integral geometry

1 Introduction

Let $\mathbf{K}$ be a bounded convex body in the Ebene; with $\mathsf{D}(\mathbf{K})$ we denote its diameter (= maximum breadth) und with $\mathsf{d}(\mathbf{K})$ its width (= minimum breadth).

Let D be a positive real number equal to the diameter $\mathsf{D}(\mathbf{K})$. $\mathcal{R}_D$ is the lattice of Buffon consisting of equidistant parallel lines with distance D between consecutive lines. $\mathbf{K}$ is randomly placed onto the plane with $\mathcal{R}_D$. With $p_{\mathbf{K}}(s)$ we denote the probability that the intersection between $\mathbf{K}$ and one of the lines of $\mathcal{R}_D$ is a chord of $\mathbf{K}$ of length $\geq s$.

If $\mathbf{K}$ is a polygon $\mathbf{P}$, we denote by $\ell(\mathbf{P})$ the length of its shortest side. We put $s^*(\mathbf{P_1}, \mathbf{P_2}) := \min\{\mathsf{d}(\mathbf{P_1}), \mathsf{d}(\mathbf{P_2}), \ell(\mathbf{P_1}), \ell(\mathbf{P_2})\}$ and give the following

Definition 1. Let $\mathbf{P_1}$ and $\mathbf{P_2}$ be two bounded convex polygons with equal perimeter and equal area. $\mathbf{P_2}$ is *polygon-rounder* (abbreviated: *pg-rounder*) than $\mathbf{P_1}$ if for every s with $0 < s \leq s^*(\mathbf{P_1}, \mathbf{P_2})$ the inequality $p_{\mathbf{P_1}}(s) < p_{\mathbf{P_2}}(s)$ holds.

To this definition we give the following remarks:

1) In [1] the relation *rounder* is defined. If in any case the relation *rounder* holds, it trivially follows that *pg-rounder* holds, too. The inversion is not true in general.

2) For all considered polygons in [1] we have $s^*(\mathbf{P_1}, \mathbf{P_2}) := \min\{\mathsf{d}(\mathbf{P_1}), \mathsf{d}(\mathbf{P_2})\}$. Therefore, the restriction in the definition of *pg-rounder* is not needed in [1].

Let $\mathbf{V_1}$ be a convex cyclic quadrilateral with diameter $\mathsf{D}(\mathbf{V_1})$ whose vertices all lie on a circle with diameter $D = \mathsf{D}(\mathbf{V_1})$ as shown in Fig. 1. We generate the quadrilateral $\mathbf{V_2}$ with *reconfiguration* of $\mathbf{V_1}$ by means of cutting of $\mathbf{V_1}$ along D and recomposing the two parts (see [1]). We write $\mathbf{V_2} = \mathbf{V_1}(D)$.

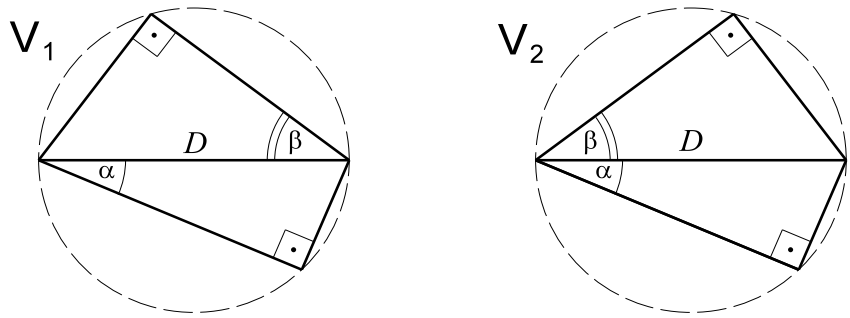


Fig. 1: The cyclic quadrilaterals $\mathbf{V_1}$ and $\mathbf{V_2}$

We assume the following:

i) $\alpha \neq \beta$, since otherwise $\mathbf{V_1}$ is a rectangle and this was already investigated in [1],

ii) $\alpha < \beta$, since α and β can be exchanged in the case $\alpha > \beta$ due to existing symmetry,

iii) $\beta \leq \pi/4$, since otherwise $\mathbf{V_1}$ und $\mathbf{V_2}$ can be exchanged, and

iv) $\beta < \pi/4$, since the case $\mathbf{V_1} = \mathbf{V_2}$ is uninteresting.

2 The intersection probability

For abbreviation we put $p_j(s)$ instead of $p_{\mathbf{V_j}}(s)$ for the probability that a random chord $\mathcal{R}_D \cap \mathbf{V_j}$ has a length $\geq s$.

From $\ell(\mathbf{V_1}) = \ell(\mathbf{V_2}) = D\sin\alpha$, $\mathsf{d}(\mathbf{V_1}) = D\sin\beta\cos(\beta-\alpha)$, $\mathsf{d}(\mathbf{V_2}) = D\cos\beta \times \sin(\alpha+\beta)$ and $\beta < \pi/4$ it follows $s^*(\mathbf{V_1}, \mathbf{V_2}) = D\sin\alpha < \mathsf{d}(\mathbf{V_1}) < \mathsf{d}(\mathbf{V_2})$.

Now we calculate $p_1(s)$ for $s \leq D\sin\alpha$. Let ϕ be the angle between the lines of $\mathcal{R}_D$ and the diagonal D of $\mathbf{V_1}$. For any ϕ and any s, $s \leq D\sin\alpha$, there are two different chords of length s in $\mathbf{V_1}$ that are parallel to the lines of $\mathcal{R}_D$ (and hence forming the angle ϕ with the diagonal D), so that every chord of $\mathbf{V_1}$, which is parallel to these two chords, has length $\geq s$ if and only if it lies between them. In order to get all possible situations for these chords exactly once, one has to consider ϕ in $[0, \pi]$. If we denote by $x_s(\phi)$ the distance between these two chords

of length s, we can use the following formula, that is due to Stoka (see [4, p. 14]), to calculate $p_1(s)$:

$$p_1(s) = \frac{\int_0^\pi x_s(\phi)\,\mathrm{d}\phi}{\int_0^\pi D\,\mathrm{d}\phi} = \frac{1}{\pi D}\int_0^\pi x_s(\phi)\,\mathrm{d}\phi\,. \tag{1}$$

The formula of $x_s(\phi)$ depends on the fact to which of the five subintervals $[0,\alpha]$, $[\alpha,\beta]$, $[\beta,\alpha+\pi/2]$, $[\alpha+\pi/2,\beta+\pi/2]$ and $[\beta+\pi/2,\pi]$ the angle ϕ belongs.

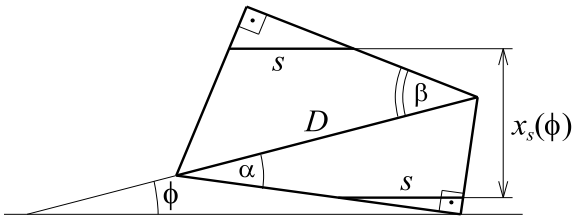


Fig. 2: $0 \le \phi \le \alpha$

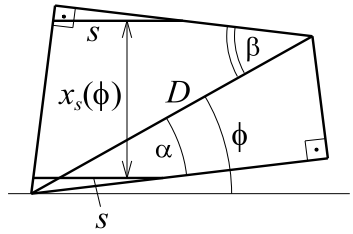


Fig. 3: $\alpha \le \phi \le \beta$

With the help of Fig. 2 we get for $\phi \in [0,\alpha]$ the following formula

$$\begin{aligned} x_s(\phi) = {} & D\cos\alpha\sin(\alpha-\phi) + D\sin\alpha\cos(\beta-\phi) \\ & - s\sin(\alpha-\phi)\cos(\alpha-\phi) - s\sin(\beta-\phi)\cos(\beta-\phi) \end{aligned}$$

and hence

$$\begin{aligned} \int_0^\alpha x_s(\phi)\,\mathrm{d}\phi = {} & D\cos\alpha - D\cos^2\alpha - D\sin\beta\sin(\beta-\alpha) + D\sin^2\beta \\ & - \frac{s}{4} + \frac{s}{4}\cos 2\alpha - \frac{s}{4}\sin(2\beta-2\alpha) + \frac{s}{4}\cos 2\beta\,. \end{aligned} \tag{2}$$

With Fig. 3 we have for $\phi \in [\alpha,\beta]$

$$\begin{aligned} x_s(\phi) = {} & D\sin\beta\cos(\beta-\phi) - \frac{s}{\cos(\beta-\alpha)}\sin(\phi-\alpha)\cos(\beta-\phi) \\ & - s\sin(\beta-\phi)\cos(\beta-\phi) \end{aligned}$$

and therefore

$$\begin{aligned} \int_\alpha^\beta x_s(\phi)\,\mathrm{d}\phi = {} & D\sin\beta\sin(\beta-\alpha) - \frac{s}{2}(\beta-\alpha)\tan(\beta-\alpha) \\ & - \frac{s}{4} + \frac{s}{4}\cos(2\beta-2\alpha)\,. \end{aligned} \tag{3}$$

If $\phi \in [\beta,\alpha+\pi/2]$ (see Fig. 4), we get

$$\begin{aligned} x_s(\phi) &= D\sin\phi - \frac{s}{\cos(\beta-\alpha)}\big[\sin(\phi-\alpha)\cos(\phi-\beta) - \cos(\phi-\alpha)\sin(\phi-\beta)\big] \\ &= D\sin\phi - \frac{s}{\cos(\beta-\alpha)}\sin(2\phi-\alpha-\beta) \end{aligned}$$

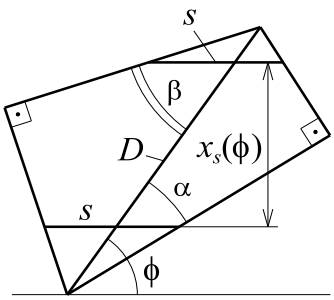


Fig. 4: $\beta \le \phi \le \alpha + \pi/2$

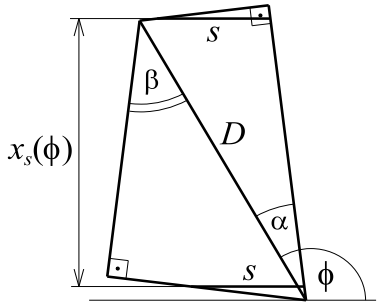


Fig. 5: $\alpha + \pi/2 \le \phi \le \beta + \pi/2$

and hence

$$\int_{\beta}^{\alpha+\pi/2} x_s(\phi)\,\mathrm{d}\phi = D(\cos\beta + \sin\alpha) - s\,. \tag{4}$$

If $\phi \in [\alpha + \pi/2, \beta + \pi/2]$, one has to use Fig. 5 to get the formula of x_s:

$$\begin{aligned} x_s(\phi) &= D\cos\alpha\sin(\phi-\alpha) + s\sin(\phi-\alpha)\cos(\phi+\alpha) \\ &\qquad - \frac{s}{\cos(\beta-\alpha)}\,\sin(\phi-\alpha)\cos(\phi-\beta) \\ &= D\cos\alpha\sin(\phi-\alpha) + \frac{s}{2}\,(\sin 2\phi - \sin 2\alpha) \\ &\qquad - \frac{s}{2\cos(\beta-\alpha)}\,\sin(2\phi-\alpha-\beta) - \frac{s}{2}\,\tan(\beta-\alpha)\,. \end{aligned}$$

It follows

$$\begin{aligned} \int_{\alpha+\pi/2}^{\beta+\pi/2} x_s(\phi)\,\mathrm{d}\phi &= D\cos\alpha\sin(\beta-\alpha) + \frac{s}{4}\,(\cos 2\beta - \cos 2\alpha) \\ &\qquad - \frac{s}{2}\,(\beta-\alpha)\sin 2\alpha - \frac{s}{2}\,(\beta-\alpha)\tan(\beta-\alpha)\,. \end{aligned} \tag{5}$$

Finally, we find with the help of Fig. 6

$$\begin{aligned} x_s(\phi) &= D\cos\beta\sin(\phi-\beta) + D\sin\alpha\cos(\phi-\alpha) \\ &\qquad + s\sin(\phi-\beta)\cos(\phi-\beta) + s\sin(\phi-\alpha)\cos(\phi-\alpha) \end{aligned}$$

and

$$\begin{aligned} \int_{\beta+\pi/2}^{\pi} x_s(\phi)\,\mathrm{d}\phi &= D\cos^2\beta - D\sin^2\alpha + D\sin\alpha\cos(\beta-\alpha) \\ &\qquad - \frac{s}{4}\left[\cos 2\beta + \cos 2\alpha + 1 + \cos(2\beta - 2\alpha)\right]. \end{aligned} \tag{6}$$

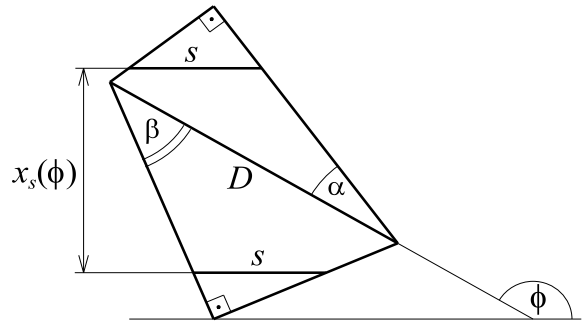


Fig. 6: $\beta + \pi/2 \le \phi \le \pi$

Overall, one gets

$$\int_0^\pi x_s(\phi)\,\mathrm{d}\phi = D\big(\sin\alpha + \cos\alpha + \sin\beta + \cos\beta\big) - \frac{s}{4}\big[7 + \cos(2\beta - 2\alpha) + \cos 2\alpha - \cos 2\beta + 2(\beta-\alpha)\sin 2\alpha + 4(\beta-\alpha)\tan(\beta-\alpha)\big] \quad (7)$$

and

$$p_1(s) = \frac{1}{\pi D}\Big\{D\big(\sin\alpha + \cos\alpha + \sin\beta + \cos\beta\big) - \frac{s}{4}\big[7 + \cos(2\beta - 2\alpha) + \cos 2\alpha - \cos 2\beta + 2(\beta-\alpha)\sin 2\alpha + 4(\beta-\alpha)\tan(\beta-\alpha)\big]\Big\}. \quad (8)$$

In the considerations above the assumption $\beta < \pi/4$ did not play any role; we only used $s \le D\sin\alpha$, since for every ϕ there are chords of length s in $\mathbf{V_1}$. In particular, we get with $\alpha = \beta$ from (8) the already known result for a rectangle with perimeter equal to $D(\sin\alpha + \cos\alpha + \sin\beta + \cos\beta)$.

If one puts $\pi/2 - \beta$ instead β in (8), one gets

$$p_2(s) = \frac{1}{\pi D}\Big\{D\big(\sin\alpha + \cos\alpha + \cos\beta + \sin\beta\big) - \frac{s}{4}\Big[7 + \cos(2\beta + 2\alpha) + \cos 2\alpha + \cos 2\beta + 2\left(\frac{\pi}{2} - \alpha - \beta\right)\sin 2\alpha + 4\left(\frac{\pi}{2} - \alpha - \beta\right)\tan\Big(\frac{\pi}{2} - \alpha - \beta\Big)\Big]\Big\}. \quad (9)$$

Hence, the inequality

$$p_1(s) > p_2(s) \quad \text{for all } 0 < s \le D\sin\alpha \quad (10)$$

is equivalent to

$$2\cos 2\beta + (\pi - 4\beta)\sin 2\alpha - \big[\cos(2\beta - 2\alpha) + \cos(2\beta + 2\alpha)\big] + 4\left[\Big(\frac{\pi}{2} - \alpha - \beta\Big)\tan\Big(\frac{\pi}{2} - \alpha - \beta\Big) - (\beta - \alpha)\tan(\beta - \alpha)\right] > 0\,. \quad (11)$$

But now we need the assumption $0 < \alpha < \beta < \pi/4$ to compare $p_1(s)$ with $p_2(s)$, i.e. for the decision if (11) holds; from this assumption follows

$$0 < \beta - \alpha < \pi/2 - \alpha - \beta\,, \quad \cos 2\beta > 0\,, \quad \pi - 4\beta > 0\,, \quad \sin 2\alpha > 0$$

and

$$2\cos 2\beta - \big[\cos(2\beta - 2\alpha) + \cos(2\beta + 2\alpha)\big] \;=\; 2\cos 2\beta\,(1 - \cos 2\alpha) \;>\; 0\,.$$

Furthermore, we have $(\pi - 4\beta)\sin 2\alpha > 0$.

The function $\gamma \mapsto \gamma \tan\gamma$ is strictly increasing in the interval $]0, \pi/2[$, hence

$$\Big(\frac{\pi}{2} - \alpha - \beta\Big)\tan\Big(\frac{\pi}{2} - \alpha - \beta\Big) - (\beta - \alpha)\tan(\beta - \alpha) \;>\; 0\,.$$

So the inequalities (11) and (10) hold and the promised result is proved:

Theorem. $\mathbf{V_1}$ *is pg-rounder than* $\mathbf{V_2}$.

References

[1] U. Bäsel, A. Duma: Reconfiguration of Parallelograms, to be published in *Rend. Circ. Mat. Palermo*, Suppl.

[2] A. Duma, S. Rizzo: Chord length distribution functions for an arbitrary triangle, *Rend. Circ. Mat. Palermo*, Serie II, Suppl. **81** (2009), 141-157.

[3] A. Duma, S. Rizzo: Die Sehnenlängenverteilung zu einem Trapez mit zwei geraden Winkeln, *FernUniversität Hagen: Seminarberichte aus der Fakultät für Mathematik und Informatik*, **83** (2010) 129-142.

[4] A. Duma, M. I. Stoka: Schnitte eines 'kleinen' gleichseitigen Dreiecks mit den Gittern von Buffon und Laplace, *FernUniversität Hagen: Seminarberichte aus der Fakultät für Mathematik und Informatik*, **79** (2008) 13-22.

Uwe BÄSEL

HTWK Leipzig
Fakultät für Maschinen- und Energietechnik,
04251 Leipzig, Germany

baesel@me.htwk-leipzig.de

Andrei DUMA

FernUniversität in Hagen
Fakultät für Mathematik und Informatik
58084 Hagen, Germany

Mathe.Duma@FernUni-Hagen.de

RENDICONTI DEL CIRCOLO MATEMATICO DI PALERMO
Serie II, Suppl. 84 (2012), pp. 17-31

Reconfiguration of Polygons

Uwe Bäsel Andrei Duma

Dedicated to Professor Peter M. Gruber
on the occasion of his 70th birthday

Abstract

At the beginning of the present paper we define for two arbitrary plane convex bodies $\mathbf{K_0}$ and $\mathbf{K_1}$ with equal perimeter and equal area the relations '$\mathbf{K_1}$ is rounder than $\mathbf{K_0}$' and '$\mathbf{K_1}$ is as round as $\mathbf{K_0}$'.

Then parallelograms and kites, made from parallelograms by cutting them along one of its diagonals and recomposing the two parts ('reconfiguration'), are compared concerning their roundness.

In the last section we compare the roundness of triangles and quadrilaterals, made from the triangles by cutting them along its smallest height.

AMS Classification: 60D05, 52A22

Keywords: Geometric probability, stochastic geometry, random sets, random convex sets, integral geometry

1 Introduction

Let $\mathbf{K}$ be a bounded convex body in the plane with diameter (= maximum breadth) $\mathsf{D}(\mathbf{K})$ and s^* the greatest real number s so that for every direction there exists a chord of $\mathbf{K}$ with length s. In [9, pp. 163-164, Theorem 12.18] it is shown that $s^* \equiv \mathsf{d}(\mathbf{K})$, where $\mathsf{d}(\mathbf{K})$ is the width (= minimum breadth) of $\mathbf{K}$.

For an ellipse $\mathbf{E}$, $\mathsf{D}(\mathbf{E})$ is the length of the major axis and $\mathsf{d}(\mathbf{E})$ the length of the minor axis; for a triangle $\mathbf{T}$, $\mathsf{D}(\mathbf{T})$ is the length of the longest side and $\mathsf{d}(\mathbf{T})$ the length of the smallest height; for a parallelogram $\mathbf{P_0}$, $\mathsf{D}(\mathbf{P_0})$ is the length of the longer diagonal and $\mathsf{d}(\mathbf{P_0})$ the length of the smaller height etc.

Let D a positive real number that is greater than the diameter of every convex body we consider. $\mathcal{R}_D$ is the lattice of Buffon consisting of equidistant parallel lines with distance D between consecutive lines. With $p_{\mathbf{K}}(s)$ we denote the probability that the intersection between a body $\mathbf{K}$ and one of the lines of $\mathcal{R}_D$ is a chord of $\mathbf{K}$ of length $\geq s$, where $\mathbf{K}$ is randomly placed onto the plane.

For two convex bodies $\mathbf{K_0}$ and $\mathbf{K_1}$ with equal perimeter and equal area one may ask the question 'Which of them is rounder?'. In order to investigate this property we suggest the following definition that is close to geometrical imagination.

Definition 1. Let $\mathbf{K_0}$ and $\mathbf{K_1}$ be convex bodies with equal perimeter and equal area. $\mathbf{K_1}$ is *rounder* than $\mathbf{K_0}$, if $p_{\mathbf{K_0}}(s) < p_{\mathbf{K_1}}(s)$ for all $s \leq \min\{\mathtt{d}(\mathbf{K_0}), \mathtt{d}(\mathbf{K_1})\}$.

It intuitively means (and that makes the term 'rounder' plausible) that for every $s \leq \min\{\mathtt{d}(\mathbf{K_0}), \mathtt{d}(\mathbf{K_1})\}$ there are 'more' chords of lengths $\geq s$ in $\mathbf{K_1}$ than in $\mathbf{K_0}$.

Definition 2. $\mathbf{K_1}$ is as *round* as $\mathbf{K_0}$ if $p_{\mathbf{K_0}}(s) = p_{\mathbf{K_1}}(s)$ for all $s \leq \min\{\mathtt{d}(\mathbf{K_0}), \mathtt{d}(\mathbf{K_1})\}$.

Due to the classical result of Barbier [1] we have

$$p_{\mathbf{K_0}}(0) = p_{\mathbf{K_1}}(0) = \frac{\mathrm{per}}{\pi D},$$

where per is the perimenter of $\mathbf{K_0}$ as well as of $\mathbf{K_1}$.

2 Reconfiguration of a convex polygon

Let $\mathbf{P}$ a convex polygon and g a line, which separates $\mathbf{P}$ into the two parts $\mathbf{P'}$ and $\mathbf{P''}$. Let M be the midpoint of the chord $\sigma := \mathbf{P} \cap g$ and h the line perpendicular to g and passing through M. We reflect the polygon $\mathbf{P'}$ along the line h and recompose it with $\mathbf{P''}$ along σ. So we get a polygon with equal perimeter and equal area as $\mathbf{P}$. This polygon could be convex. If it is convex (and only in this case), we denote it by $\mathbf{P}(\sigma)$. We say that $\mathbf{P}(\sigma)$ is generated with *reconfiguration* by means of cutting of $\mathbf{P}$ along σ. The question, which one of $\mathbf{P}$ and $\mathbf{P}(\sigma)$ is rounder than the other one, cannot be answered in general. (This can be easily seen from the fact that the operator *reconfiguration* $\mathbf{P} \mapsto \mathbf{P}(\sigma)$ is involutional.) For the existence of $\mathbf{P}(\sigma)$ we have to consider the following situations:

i) Let M_1 and M_2 be points (but no end-points) of two non-adjacent sides of $\mathbf{P}$ and σ the chord $\overline{M_1M_2}$. On one side of σ there are the angles α_1 between σ and a_1, and α_2 between σ and a_2, on the other side of σ there are the angles β_1 and β_2, see Fig. 1.

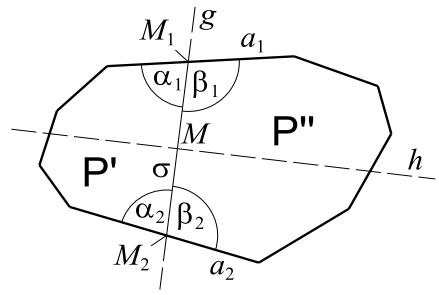


Figure 1: M_1 and M_2 are no end-points

This method delivers a convex polygon, which is then denoted by $\mathbf{P}(\sigma)$, if and only if $\alpha_1 = \alpha_2$ (and hence $\beta_1 = \beta_2$).

ii) Let a and b adjacent sides of $\mathbf{P}$ with common vertex M_1, $M_2 \in \partial\mathbf{P}$ is a point which belongs neither to a nor to b, and $\sigma := \overline{M_1M_2}$; therefore M_2 is a vertex or is not a vertex of $\mathbf{P}$. We denote by α_1 the angle between a and σ, and by β_1 the angle between b and σ. α_2 and β_2 are the angles in M_2 between $\mathbf{P}$ and σ as shown in the Fig. 2 and 3: Independent from the fact whether M_2 is a vertex of $\mathbf{P}$ or not, we have: $\mathbf{P}(\sigma)$ (and therefore its convexity) exists if an only if $\alpha_1 + \beta_2 \leq \pi$ and $\alpha_2 + \beta_1 \leq \pi$.

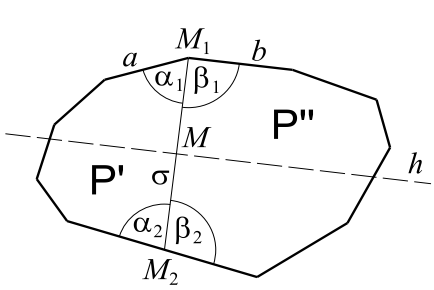


Figure 2: M_1 is vertex, M_2 is no vertex

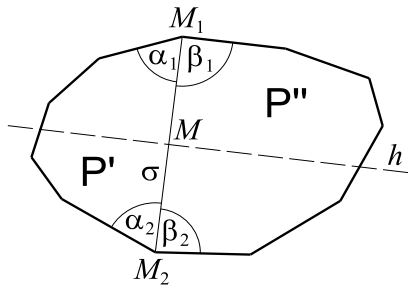


Figure 3: M_1 and M_2 are vertices

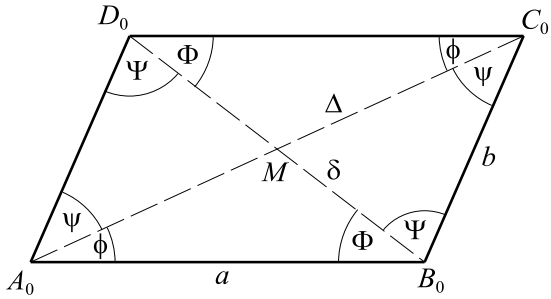


Figure 4: The parallelogram $\mathbf{P_0}$

Let particularly be $\mathbf{P_0}$ the parallelogram with the sides a and b, where $a \geq b$, and the diagonals Δ and δ, where $\delta \leq \Delta$ (see Fig. 4). For the diagrammed angles ϕ, ψ, Φ and Ψ we have: $\phi \leq \psi$, $\alpha := \phi + \psi \leq \pi/2$, $\Phi \leq \Psi$, $\pi - \alpha = \Phi + \Psi \geq \pi/2$, $\phi \leq \Phi$ and $\psi \leq \Psi$. Let $\mathbf{P_1} = \mathbf{P_0}(\Delta)$ and $\mathbf{P_2} = \mathbf{P_0}(\delta)$ the kites shown in Fig. 5.

For $a = b$ (i.e. $\mathbf{P_0}$ is a rhombus) one gets the uninteresting case $\mathbf{P_0} = \mathbf{P_1} = \mathbf{P_2}$, which we exclude; therefore we assume $a > b$ and hence $\phi < \psi$, $\phi < \pi/4$, $\Phi < \Psi$ and $\Psi > \pi/4$ for the following calculations. Notice that for $\phi + \psi = \Phi + \Psi = \pi/2$ (i.e. $\mathbf{P_0}$ ist a rectangle) we have: $\mathbf{P_0} \neq \mathbf{P_1} = \mathbf{P_2}$ (and $\delta = \Delta$).

Remark 1. From $a > b$, $a \sin\phi = b \sin\psi$ and $\phi < \Phi$ it follows:

i) $\mathsf{D}(\mathbf{P_0}) = \Delta$, $\mathsf{d}(\mathbf{P_0}) = b \sin\alpha$,

ii) $\mathsf{D}(\mathbf{P_1}) = \Delta$, $\mathsf{d}(\mathbf{P_1}) = a \sin 2\phi$,

iii) $\mathsf{D}(\mathbf{P_2}) = \max(a, \delta, 2a\sin\Phi)$, $\mathsf{d}(\mathbf{P_2}) = \begin{cases} a\sin 2\Phi\,, & \text{if} \quad 2\Phi < \pi/2\,, \\ a\,, & \text{if} \quad 2\Phi \geq \pi/2\,, \end{cases}$

iv) $\mathsf{d}(\mathbf{P_0}) < \mathsf{d}(\mathbf{P_1}) < \mathsf{d}(\mathbf{P_2})$.

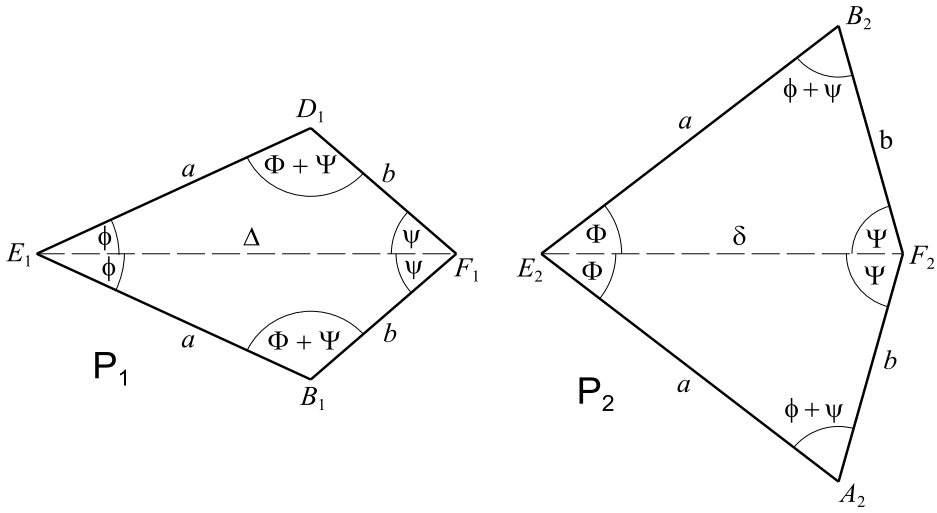


Figure 5: $\mathbf{P_1}$ and $\mathbf{P_2}$

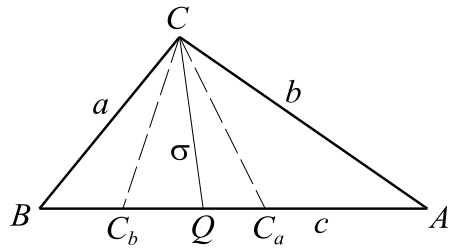


Figure 6: The triangle $\mathbf{T}$

Let $\mathbf{T}$ be an triangle with side lengths $a \leq b \leq c$ and angles $A \leq B \leq C$ (see Fig 6). For the points C_a and C_b of the side $\overline{AB}$ we assume $\left|\overline{AC_b}\right| = b$ and $\left|\overline{AC_a}\right| = a$. If Q is a point of the side $\overline{AB}$ and $\sigma := \overline{CQ}$, then exists $\mathbf{T}(\sigma)$ (i.e. $\mathbf{T}(\sigma)$ is convex) if and only if Q is a point of the line segment $\overline{C_aC_b}$, because then we have

$$\measuredangle(BQC) + \measuredangle(QCA) \leq \measuredangle(BQC) + \measuredangle(CQA) \leq \pi \quad \text{and}$$
$$\measuredangle(AQC) + \measuredangle(QCB) \leq \measuredangle(AQC) + \measuredangle(CQB) \leq \pi\,.$$

In particular, we can take as $\overline{CQ}$ the height h_c of $\mathbf{T}$ through the vertex C (due to $A \leq B \leq C$). In this case we have $\mathsf{D}(\mathbf{T}(h_c)) = \sqrt{c^2 + h_c^2}$ and $\mathsf{d}(\mathbf{T}(h_c)) = \frac{a}{2}\,\sin 2B = a\sin B\cos B = h_c\cos B < h_c = \mathsf{d}(\mathbf{T})$.

If $\mathbf{T}$ has only acute angles (i.e. $C < \pi/2$), one may also consider $\mathbf{T}(h_a)$ and $\mathbf{T}(h_b)$, where h_a and h_b are the heights of $\mathbf{T}$ through the vertices A and B repectively.

3 Reconfiguration of a parallelogram

Let $\mathbf{P_0}$, $\mathbf{P_1} := \mathbf{P_0}(\Delta)$ and $\mathbf{P_2} := \mathbf{P_0}(\delta)$ as shown in Fig. 4 and 5. For $s \le \mathtt{d}(\mathbf{P_0}) = b\sin\alpha$ one finds (see [7]):

$$p_0(s) = p_{\mathbf{P_0}}(s) = 2\,\frac{a+b-s[1+(\pi/2-\alpha)\cot\alpha]}{\pi D}\,. \tag{1}$$

If $s \le \mathtt{d}(\mathbf{P_1})$, then for every direction there are exactly two parallel chords of length s in $\mathbf{P_1}$. With $x_s(\chi)$ we denote the distance between the chords of length s in $\mathbf{P_1}$ forming the angle χ with Δ. Due to the symmetry of $\mathbf{P_1}$ with respect to Δ, one has to consider χ in $[0,\pi/2]$ to get all possible positions of $\mathbf{P_1}$ relative to $\mathcal{R}_D$ exactly once. The term of $x_s(\chi)$ depends on the belonging of χ to the intervals $[0,\phi[$, $[\phi,\psi[$ and $[\psi,\pi/2]$.

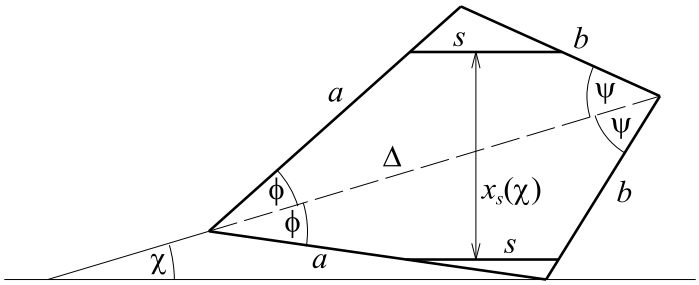


Figure 7: $\chi \in [0,\phi[$

For $\chi \in [0,\phi[$ one gets with the help of Fig. 7

$$\begin{aligned} x_s(\chi) &= (a\sin\phi + b\sin\psi)\cos\chi - \frac{s}{\sin\alpha}\big[\sin(\phi-\chi)\sin(\chi+\psi) \\ &\qquad + \sin(\psi-\chi)\sin(\phi+\chi)\big] \\ &= (a\sin\phi + b\sin\psi)\cos\chi - \frac{s}{2\sin\alpha}\big[\cos(2\chi+\psi-\phi) \\ &\qquad + \cos(2\chi+\phi-\psi) - 2\cos\alpha\big] \end{aligned}$$

and hence

$$\int_0^{\phi} x_s(\chi)\,\mathrm{d}\chi = a\sin^2\phi + b\sin\phi\sin\psi - \frac{s}{4} + s\phi\cot\alpha - \frac{s}{4}\,\frac{\sin(3\phi-\psi)}{\sin\alpha}\,. \tag{2}$$

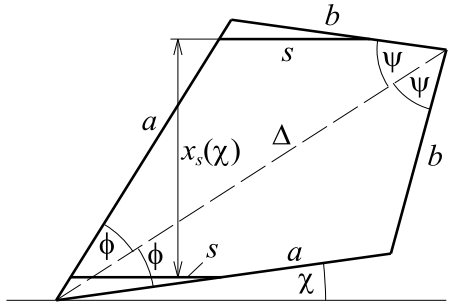


Figure 8: $\chi \in [\phi, \psi[$

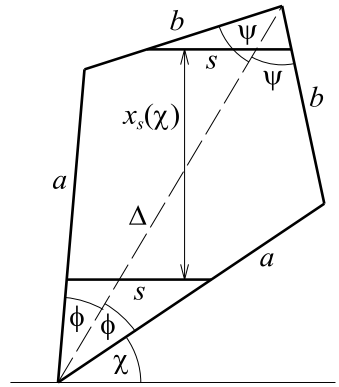


Figure 9: $\chi \in [\psi, \pi/2]$

For $\chi \in [\phi, \psi[$ we use Fig. 8 in order to get the term of $x_s(\chi)$:

$$\begin{aligned} x_s(\chi) &= a\sin(\phi+\chi) - \frac{s}{\sin 2\phi}\,\sin(\chi-\phi)\sin(\phi+\chi) - \frac{s}{\sin\alpha}\,\sin(\psi-\chi)\sin(\phi+\chi) \\ &= a\sin(\phi+\chi) - \frac{s}{2\sin 2\phi}\,(\cos 2\phi - \cos 2\chi) \\ &\qquad - \frac{s}{2\sin\alpha}\,\big[\cos(2\chi+\phi-\psi) - \cos\alpha\big]\,. \end{aligned}$$

In this case we get

$$\begin{aligned} \int_\phi^\psi x_s(\chi)\,\mathrm{d}\chi &= a\cos 2\phi - a\cos(\phi+\psi) - \frac{s}{2} - \frac{s}{2}\,(\psi-\phi)\cot 2\phi \\ &\qquad + \frac{s}{4}\,\frac{\sin 2\psi}{\sin 2\phi} + \frac{s}{4}\,\frac{\sin(3\phi-\psi)}{\sin\alpha} + \frac{s}{2}\,(\psi-\phi)\cot\alpha\,. \end{aligned} \tag{3}$$

Finally one finds for $\chi \in [\psi, \pi/2]$ with Fig. 9

$$\begin{aligned} x_s(\chi) &= (a\cos\phi + b\cos\psi)\sin\chi - \frac{s}{\sin 2\phi}\,\sin(\chi-\phi)\sin(\phi+\chi) \\ &\qquad - \frac{s}{\sin 2\psi}\,\sin(\chi-\psi)\sin(\chi+\phi) \\ &= (a\cos\phi + b\cos\psi)\sin\chi - \frac{s}{2\sin 2\phi}\,(\cos 2\phi - \cos 2\chi) \\ &\qquad - \frac{s}{2}\left(\cot 2\psi - \frac{\cos 2\chi}{\sin 2\psi}\right) \end{aligned}$$

and therefore

$$\begin{aligned} \int_\psi^{\pi/2} x_s(\chi)\,\mathrm{d}\chi &= a\cos\phi\cos\psi + b\cos^2\psi - \frac{s}{4} - \frac{s}{2}\Big(\frac{\pi}{2}-\psi\Big)\cot 2\phi \\ &\qquad - \frac{s}{2}\Big(\frac{\pi}{2}-\psi\Big)\cot 2\psi - \frac{s}{4}\,\frac{\sin 2\psi}{\sin 2\phi}\,. \end{aligned} \tag{4}$$

In summary, we get with (2), (3) and (4)

$$\int_0^{\pi/2} x_s(\chi)\,\mathrm{d}\chi = a+b-s+\frac{s}{2}\,\alpha\cot\alpha-\frac{s}{2}\Big[\Big(\frac{\pi}{2}-\phi\Big)\cot 2\phi + \Big(\frac{\pi}{2}-\psi\Big)\cot 2\psi\Big]. \tag{5}$$

Due to a formula of Stoka (see [4, p. 14]) it holds for $s \le \mathsf{d}(\mathbf{P_1})$

$$p_1(s) := p_{\mathbf{P_1}}(s) = \frac{\int_0^{\pi/2} x_s(\chi)\,\mathrm{d}\chi}{\int_0^{\pi/2} D\,\mathrm{d}\chi} = \frac{2}{\pi D}\Big[a+b-s+\frac{s}{2}\,(\phi+\psi)\cot(\phi+\psi) - \frac{s}{2}\Big\{\Big(\frac{\pi}{2}-\phi\Big)\cot 2\phi+\Big(\frac{\pi}{2}-\psi\Big)\cot 2\psi\Big\}\Big]. \tag{6}$$

We wrote $\phi+\psi$ instead of α in this formula, since the calculation of $p_2(s) := p_{\mathbf{P_2}}(s)$ for $s \le \mathsf{d}(\mathbf{P_2})$ is analogue to the calculation of $p_1(s)$. One only has to replace the angles ϕ and ψ in formula (6) by the angles Φ and Ψ and gets

$$p_2(s) = \frac{2}{\pi D}\Big[a+b-s+\frac{s}{2}\,(\Phi+\Psi)\cot(\Phi+\Psi) - \frac{s}{2}\Big\{\Big(\frac{\pi}{2}-\Phi\Big)\cot 2\Phi+\Big(\frac{\pi}{2}-\Psi\Big)\cot 2\Psi\Big\}\Big]. \tag{7}$$

4 Rectangle as special case and further examples

If $\mathbf{P_0}$ is an rectangle with side lenghts a and b, $b<a$, we have with the notations from above $\mathbf{P_1}=\mathbf{P_2}$, $\phi<\pi/4$, $\psi=\pi/2-\phi$, $\mathsf{d}(\mathbf{P_0})=b<2a^2b/(a^2+b^2)=\mathsf{d}(\mathbf{P_1})$. From (6) one gets for $s \le 2a^2b/(a^2+b^2)$

$$p_1(s) = \frac{2}{\pi D}\left[a+b-s-\frac{s}{2}\left(\frac{\pi}{2}-2\phi\right)\cot 2\phi\right].$$

In this case it follows from (1) that $p_0(s) = \frac{2}{\pi D}\,(a+b-s)$ for $s \le b$, hence $p_1(s) < p_0(s)$ for $0 < s \le \mathsf{d}(\mathbf{P_0}) < \mathsf{d}(\mathbf{P_1})$, i.e. $\mathbf{P_0}$ is rounder than $\mathbf{P_1}$ according to our definition.

Now our aim is to compare the 'roundness' of the three quadrilaterals $\mathbf{P_0}$, $\mathbf{P_1}$ and $\mathbf{P_2}$ for an arbitraray $\mathbf{P_0}$ (as in section 3). At first we consider some examples in order to get from (1), (6) and (7) hints to existing general relations.

Example 1. Let $\mathbf{P_0}$ have the angles $\alpha=\phi+\psi=\pi/3$, $\Phi=\pi/6$, therefore $\Psi=\pi/2$, $a=2b$, $\delta=\sqrt{3}\,b$ and $\Delta=\sqrt{7}\,b$. It follows

$$\sin\phi=\frac{\sqrt{3}}{2\sqrt{7}},\quad \cos\phi=\frac{5}{2\sqrt{7}},\quad \cot\phi=\frac{5}{\sqrt{3}},\quad \cot 2\phi=\frac{11\sqrt{3}}{15},$$
$$\sin\psi=\frac{\sqrt{3}}{\sqrt{7}},\quad \cos\psi=\frac{2}{\sqrt{7}},\quad \cot\psi=\frac{2}{\sqrt{3}},\quad \cot 2\psi=\frac{1}{4\sqrt{3}},$$

$$\cot(\phi+\psi)=\frac{1}{\sqrt{3}}\,,\quad \cot(\Phi+\Psi)=-\frac{1}{\sqrt{3}}\,,\quad \cot 2\Psi=\infty\,,\quad \cot 2\Phi=\frac{1}{\sqrt{3}}\,.$$

Taking

$$\lim_{\eta\,\to\,\pi/2}\Big(\frac{\pi}{2}-\eta\Big)\cot 2\eta=-\frac{1}{2}$$

into acount, we find with (1) and (7)

$$\begin{aligned} p_0(s) &= \frac{2}{\pi D}\left[3b-s\left(1+\frac{\pi}{6\sqrt{3}}\right)\right] \quad \text{for} \quad s\le\frac{\sqrt{3}}{2}\,b\,,\\ p_2(s) &= \frac{2}{\pi D}\left[3b-s\left(\frac{3}{4}+\frac{\pi}{2\sqrt{3}}\right)\right] \quad \text{for} \quad s\le\sqrt{3}\,b\,. \end{aligned}$$

Hence $p_0(s)>p_2(s)$ for $0<s\le\sqrt{3}\,b/2$, i.e. $\mathbf{P_0}$ is rounder than $\mathbf{P_2}$ (and – it may be subjective – it corresponds to our perception). Note that $\mathbf{P_2}$ is an equilateral triangle with side length $2b$; the above result for $p_2(s)$ is confirmed by the result in [4]. The calculation of $p_1(s)$ for $s\le 5\sqrt{3}\,b/7$ is more complicated. We have

$$\begin{aligned} p_1(s) &= \frac{2}{\pi D}\left[3b-s+\frac{s}{2}\left\{\frac{\pi}{3\sqrt{3}}-\left(\frac{\pi}{2}-\arcsin\frac{\sqrt{3}}{2\sqrt{7}}\right)\frac{11}{5\sqrt{3}}\right.\right.\\ &\qquad\left.\left.-\left(\frac{\pi}{2}-\arcsin\frac{\sqrt{3}}{\sqrt{7}}\right)\frac{1}{4\sqrt{3}}\right\}\right]\\ &= \frac{2}{\pi D}\left[3b-s\left(1+\frac{107\pi}{240\sqrt{3}}-\frac{11}{10\sqrt{3}}\arcsin\frac{\sqrt{3}}{2\sqrt{7}}-\frac{1}{8\sqrt{3}}\arcsin\frac{\sqrt{3}}{\sqrt{7}}\right)\right]\\ &\approx \frac{2}{\pi D}\big(3b-1,5454\,s\big)\,. \end{aligned}$$

From

$$1+\frac{\pi}{6\sqrt{3}}\approx 1,3023\quad\text{and}\quad \frac{3}{4}+\frac{\pi}{2\sqrt{3}}\approx 1,6569$$

we get

$$p_0(s)>p_1(s)>p_2(s)\ \text{ for }\ 0<s\le\frac{\sqrt{3}}{2}\,b\,,$$

in this example; this means that $\mathbf{P_0}$ is rounder than $\mathbf{P_1}$ and $\mathbf{P_1}$ rounder than $\mathbf{P_2}$.

Example 2. For $\phi=\pi/6$ and $\psi=\pi/4$, hence $\alpha=5\pi/12$ and $\Phi+\Psi=7\pi/12$, one gets (for fixed b) the lengths

$$a=\sqrt{2}\,b\,,\quad \delta=\sqrt{4-\sqrt{3}}\,b\quad\text{and}\quad \Delta=\frac{\sqrt{6}+\sqrt{2}}{2}\,b$$

and the values

$$\cot(\phi+\psi)=2-\sqrt{3}\,,\quad \cot 2\phi=\frac{1}{\sqrt{3}}\quad\text{and}\quad \cot 2\psi=0\,,$$

which yields

$$p_0(s) = \frac{2}{\pi D}\left[\sqrt{2}\,b + b - s\left(1 + \frac{2-\sqrt{3}}{12}\,\pi\right)\right] \approx \frac{2}{\pi D}\big(\sqrt{2}\,b + b - 1,0701s\big)\,,$$
$$p_1(s) = \frac{2}{\pi D}\left[\sqrt{2}\,b + b - s + \frac{s}{2}\left\{\frac{5\pi}{12}\big(2-\sqrt{3}\big) - \frac{\pi}{3\sqrt{3}}\right\}\right]$$
$$\approx \frac{2}{\pi D}\big(\sqrt{2}\,b + b - 1,1266s\big)$$

and therefore $\mathbf{P_0}$ is rounder than $\mathbf{P_1}$ in this case.

Now we calculate $p_2(s)$ for $s \le \mathsf{d}(\mathbf{P_2})$. We have

$$\sin\Psi = \frac{\sqrt{3}+1}{2\sqrt{4-\sqrt{3}}} \approx 0,9071\,, \quad \Psi \approx 1,1363\,\mathrm{rad}\,, \quad \Phi = \frac{7\pi}{12} - \Psi \approx 0,6963\,\mathrm{rad}\,,$$
$$\cot 2\Phi \approx 0,1801\,, \quad \cot 2\Psi \approx -0,8454$$

and therefore with (7)

$$p_2(s) \approx \frac{2}{\pi D}\big(\sqrt{2}\,b + b - 1,1409s\big)\,.$$

Hence $\mathbf{P_1}$ is rounder than $\mathbf{P_2}$ and of course $\mathbf{P_0}$ is rounder than $\mathbf{P_2}$. Here we took into account that $\mathsf{d}(\mathbf{P_0}) < \mathsf{d}(\mathbf{P_1}) < \mathsf{d}(\mathbf{P_2})$.

5 $\mathbf{P_0}$ is rounder than $\mathbf{P_1}$

Let $\mathbf{P_0}$, $\mathbf{P_1}$ and $\mathbf{P_2}$ defined as in section 3. We notice that $\mathbf{P_0}$ is uniquely determined by $\phi \in]0,\pi/4[$ and $\psi \in]\phi,\pi/2-\phi[$ or by (Φ,Ψ) with $\Phi \in]0,\pi/2[$ and $\psi \in]\max(\Phi,\pi/2-\Phi),\pi-\Phi[$ except similarity of parallelograms (that plays no role for the comparison of $p_0(s)$, $p_1(s)$ and $p_2(s)$). The pair (ϕ,ψ) uniquely determines the pair (Φ,Ψ), which follows from

$$\cot\Phi = \frac{2\sin\psi}{\sin\phi\,\sin(\phi+\psi)} - \cot\phi\,, \quad \cot\Psi = \frac{2\sin\phi}{\sin\psi\,\sin(\phi+\psi)} - \cot\psi\,. \tag{8}$$

Otherwise (Φ,Ψ) uniquely determines (ϕ,ψ) because

$$\cot\phi = \frac{2\sin\Psi}{\sin\Phi\,\sin(\Phi+\Psi)} - \cot\Phi\,, \quad \cot\psi = \frac{2\sin\Phi}{\sin\Psi\,\sin(\Phi+\Psi)} - \cot\Psi\,. \tag{9}$$

From the geometrical viewpoint these facts are clear.

The inequality $p_0(s) > p_1(s)$ for all s with $0 < s \le b\sin\alpha = \mathsf{d}(\mathbf{P_0})$ is obviously equivalent to

$$\left(\frac{\pi}{2} - \phi\right)\cot 2\phi + \left(\frac{\pi}{2} - \psi\right)\cot 2\psi > \big[\pi - (\phi+\psi)\big]\cot(\phi+\psi)\,. \tag{10}$$

Remark 2. This simple formula is one of the reasons for the assumption $s \leq \min\{\mathsf{d}(\mathbf{K_0}), \mathsf{d}(\mathbf{K_1})\}$ in the definition of 'rounder'. Without this restriction for the values of s we had to deal with much more complicated formulas for $p_0(s)$ and $p_1(s)$ as well as a case distinction for $s > b\sin\alpha$; in this context the ratio s/b for $s > b\sin\alpha$ must be taken into consideration.

With

$$h:\,]0,\pi/2[\;\to\;\mathbb{R}\,,\quad t\;\mapsto\;h(t):=\Big(\frac{\pi}{2}-t\Big)\cot 2t$$

we can write (10) in the form

$$h(\phi)+h(\psi)>2\Big(\frac{\pi}{2}-\frac{\phi+\psi}{2}\Big)\cot\Big(2\,\frac{\phi+\psi}{2}\Big)=2\,h\Big(\frac{\phi+\psi}{2}\Big)\,.$$

This means that (10) is equivalent to the strict convexity (see [5, pp. 274, 277]) of h, wich we now prove.

Lemma 1. *The function*

$$h:\,]0,\pi/2[\;\to\;\mathbb{R}\,,\quad t\;\mapsto\;h(t):=\Big(\frac{\pi}{2}-t\Big)\cot 2t$$

is strictly convex.

Proof. With

$$h'(t)=-\cot 2t+\frac{2t-\pi}{\sin^2 2t}$$

we get

$$h''(t)=\frac{2}{\sin^2 2t}+\frac{2}{\sin^2 2t}-\frac{4(2t-\pi)}{\sin^2 2t}\cot 2t=\frac{4}{\sin^2 2t}\left[1-(2t-\pi)\cot 2t\right].$$

For $t\in\,]0,\pi/4]$ we have $(2t-\pi)\cot 2t\leq 0$ and hence $h''(t)>0$. For $t\in\,]\pi/4,\pi/2[$ we put $v=\pi-2t$, hence $v\in\,]0,\pi/2[\,;\,1-(2t-\pi)\cot 2t$ gets the form $1-v\cot v=1-v/\tan v$. Since $v<\tan v$ for all $v\in\,]0,\pi/2[\,,\;h''$ is positive in $\;]\pi/4,\pi/2[\;$ and therefore h is strictly convex. □

Due to the existing equivalence and this lemma we have proved:

Theorem 1. $\mathbf{P_0}$ *is rounder than* $\mathbf{P_1}$.

6 The comparison with $\mathbf{P_2}$

In order to compare $\mathbf{P_0}$ with $\mathbf{P_2}$, we use the equivalence between $p_0(s) > p_2(s)$ for $0 < s \leq \mathsf{d}(\mathbf{P_0}) = b\sin\alpha$ and

$$\Big(\frac{\pi}{2}-\Phi\Big)\cot 2\Phi+\Big(\frac{\pi}{2}-\Psi\Big)\cot 2\Psi>\big[\pi-(\Phi+\Psi)\big]\cot(\Phi+\Psi)\,.\qquad(11)$$

To prove this inequality, we consider the continuous extension $\widetilde{h}$ of the function h (see above) to the interval $]0,\pi[$ with $\widetilde{h}(t) := h(t) = (\pi/2 - t)\cot 2t$ for $t \neq \pi/2$ and $\widetilde{h}(\pi/2) = -1/2$. The continuous derivative of $\widetilde{h}$ is given by

$$-\cot 2t + \frac{2t-\pi}{\sin^2 2t} \text{ for } t \in]0,\pi/2[\cup]\pi/2,\pi[\quad \text{and} \quad 0 \text{ for } t = \pi/2\,.$$

From $\widetilde{h}(\pi/2 - t) = \widetilde{h}(\pi/2 + t)$ for all $t \in]0,\pi/2[$ it follows that the graph of $\widetilde{h}$ is symmetrical with respect to the line $t = \pi/2$. Therefore and due to the strict convexity of h, $\widetilde{h}$ is strict convex too. Hence we have shown that inequality (11) holds, and

Theorem 2. $\mathbf{P_0}$ *is rounder than* $\mathbf{P_2}$.

If a general roundness relation between $\mathbf{P_1}$ and $\mathbf{P_2}$ exists, then it could be only '$\mathbf{P_1}$ is rounder than (or as round as) $\mathbf{P_2}$', which follows from the examples 1 and 2.

We denote by F the function

$$F(\mu,\nu) := \Big(\frac{\pi}{2} - \mu\Big)\cot 2\mu + \Big(\frac{\pi}{2} - \nu\Big)\cot 2\nu - \frac{\pi}{2}\cot(\mu+\nu)\,.$$

The inequality $p_1(s) > p_2(s)$ for all $0 < s \leq \mathsf{d}(\mathbf{P_1}) = a\sin 2\phi$ is equivalent to

$$F(\Phi(\phi,\psi),\Psi(\phi,\psi)) > F(\phi,\psi)\,, \tag{12}$$

where Φ and Ψ as functions of ϕ and ψ are given by (8).

Unfortunately, we have not found a proof in this case as for the Theorems 1 and 2. On this account we numerically calculated and compared for all $k \in \{1,2,\ldots,44\}$ and $\ell \in \{1,2,\ldots,89-k\}$ the values

$$F\Big(\frac{\pi}{180}\,k,\,\frac{\pi}{180}\,\ell\Big) \quad \text{and} \quad F\Big(\Phi\Big(\frac{\pi}{180}\,k,\,\frac{\pi}{180}\,\ell\Big),\,\Psi\Big(\frac{\pi}{180}\,k,\,\frac{\pi}{180}\,\ell\Big)\Big)\,.$$

The result is that for all pairs (k,ℓ) the inequality

$$F\Big(\Phi\Big(\frac{\pi}{180}\,k,\,\frac{\pi}{180}\,\ell\Big),\,\Psi\Big(\frac{\pi}{180}\,k,\,\frac{\pi}{180}\,\ell\Big)\Big) > F\Big(\frac{\pi}{180}\,k,\,\frac{\pi}{180}\,\ell\Big)$$

holds. So we formulate the following

Conjecture. $\mathbf{P_1}$ is rounder than $\mathbf{P_2}$.

7 Reconfiguration of a triangle by cutting along its smallest height

Let $\mathbf{T}$ be the triangle considered at the end of section 2, i.e. with the side lengths $a \leq b \leq c$ and the angles $A \leq B \leq C$. We denote $\mathbf{T}(h_c)$ by $\mathbf{T_1}$ (see Fig. 10) and have $\mathsf{d}(\mathbf{T_1}) = \frac{a}{2}\sin 2B = h_c\cos B < h_c = \mathsf{d}(T)$. In order to calculate $p_{\mathbf{T_1}}$ – analogous to section 3 – we determine the distance $x_s(\chi)$ between the two chords

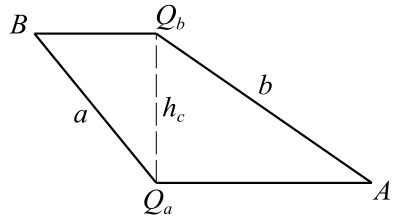


Figure 10: The quadrilateral $\mathbf{T_1}$

of $\mathbf{T_1}$ of lenghth $s \le \mathsf{d}(\mathbf{T_1})$ that form with $\overline{Q_aA}$ and $\overline{Q_bB}$ the angle χ. For the subintervals $[0, A[$, $[A, B[$ and $[B, \pi]$ there are different formulas for $x_s(\chi)$. So we find with Fig. 11 the formula

$$\begin{aligned} x_s(\chi) &= a \sin B \cos\chi - s\,\frac{\sin\chi \sin(A-\chi)}{\sin A} - s\,\frac{\sin\chi\sin(B-\chi)}{\sin B} \\ &= a \sin B \cos\chi - s\,\frac{\cos(A-2\chi)-\cos A}{2\sin A} - s\,\frac{\cos(B-2\chi)-\cos B}{2\sin B}\,. \end{aligned} \tag{13}$$

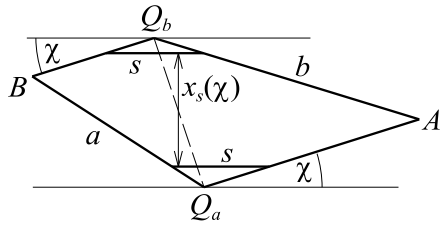


Figure 11: $0 \le \chi < A$

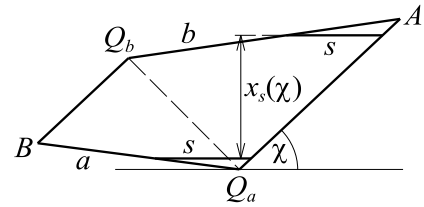


Figure 12: $A \le \chi < B$

If $\chi \in [A, B[$, we use Fig. 12 and find

$$\begin{aligned} x_s(\chi) &= b \cos A \sin\chi - s\,\frac{\sin\chi\sin(\chi-A)}{\sin A} - s\,\frac{\sin\chi\sin(B-\chi)}{\sin B} \\ &= b \cos A \sin\chi - s\,\frac{\cos A-\cos(A-2\chi)}{2\sin A} - s\,\frac{\cos(B-2\chi)-\cos B}{2\sin B}\,. \end{aligned} \tag{14}$$

Finally, we get for $\chi \in [B, \pi]$ with Fig. 13

$$\begin{aligned} x_s(\chi) &= b \cos A \sin\chi + a\sin(\chi-B) - s\,\frac{\sin\chi\sin(\chi-A)}{\sin A} - s\,\frac{\sin\chi\sin(\chi-B)}{\sin B} \\ &= b \cos A \sin\chi + a\sin(\chi-B) - s\,\frac{\cos A-\cos(A-2\chi)}{2\sin A} \\ &\quad - s\,\frac{\cos B-\cos(B-2\chi)}{2\sin B}\,. \end{aligned} \tag{15}$$

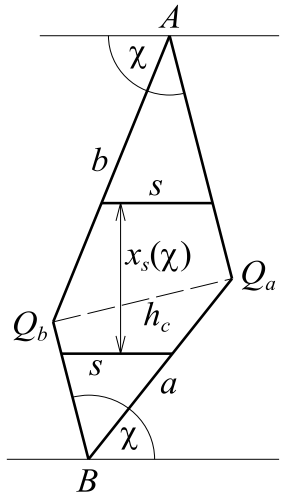


Figure 13: $B \le \chi \le \pi$

With

$$\int_0^A x_s(\chi)\,\mathrm{d}\chi = a\sin A\sin B - \frac{s}{4} - \frac{s}{4} + \frac{s}{2}\,A\cot A + \frac{s}{4}\,\cos 2A - \frac{s}{4}\,\sin 2A\cot B + \frac{s}{2}\,A\cot B - \frac{s}{4}\,,$$

$$\int_A^B x_s(\chi)\,\mathrm{d}\chi = b\cos^2 A - b\cos A\cos B - \frac{s}{4}\,\cos 2B + \frac{s}{4}\sin 2B\cot A - \frac{s}{4} - \frac{s}{2}\,(B-A)\cot A - \frac{s}{4} - \frac{s}{4}\,\cos 2A + \frac{s}{4}\,\sin 2A\cot B + \frac{s}{2}\,(B-A)\cot B\,,$$

$$\int_B^\pi x_s(\chi)\,\mathrm{d}\chi = b\cos A + b\cos A\cos B + a\cos B + a - \frac{s}{4} + \frac{s}{4}\,\cos 2B - \frac{s}{4}\,\sin 2B\cot A - \frac{s}{2}(\pi - B)\cot A - \frac{s}{4} - \frac{s}{4} - \frac{s}{2}\,(\pi - B)\cot B$$

we get

$$\int_0^\pi x_s(\chi)\,\mathrm{d}\chi = a + b + c - \frac{s}{2}\left[4 + (\pi - 2A)\cot A + (\pi - 2B)\cot B\right]$$

and hence

$$p_{\mathbf{T_1}}(s) = \frac{1}{\pi D}\Big[a + b + c - \frac{s}{2}\left\{4 + (\pi - 2A)\cot A + (\pi - 2B)\cot B\right\}\Big]\,. \qquad (16)$$

Remark 3. If $A = B =: \alpha$, then $\mathbf{T_1}$ is the parallelogram with the side lenghts a and $a\cos\alpha$ and the angles α and $\pi - \alpha$. In this case $p_{\mathbf{T_1}}$ is equal to

$$\frac{2}{\pi D}\Big[a + a\cos\alpha - s\Big\{1 + \Big(\frac{\pi}{2} - \alpha\Big)\cot\alpha\Big\}\Big]\,.$$

This is the result of formula (1), first proved by Stoka in 1975. In particular, it follows from Theorem 2 that the quadrilateral $\mathbf{T_1}$ (which is in this special case $\mathbf{P_0}$ with side lenghts a and $a\cos\alpha$ and angles α and $\pi - \alpha$) is rounder than $\mathbf{T}$ $(= \mathbf{P_2})$.

Therefore, we ask whether $\mathbf{T_1}$ is always rounder than $\mathbf{T}$. In this case the inequality $p_{\mathbf{T_1}}(s) > p_{\mathbf{T}}(s)$ holds for all $0 < s \le \mathtt{d}(\mathbf{T_1})$. From this we conclude with (16) and [2, p. 144, formula (2)]

$$(A + B)\cot C + A\cot A + B\cot B > 1\,. \tag{17}$$

With

$$\cot C = \frac{1 - \cot A\cot B}{\cot A + \cot B}$$

and $\cot A + \cot B > 0$ formula (17) yields

$$A\cot^2 A - \cot A + A + B\cot^2 B - \cot B + B > 0\,. \tag{18}$$

The function $f :]0, \pi/2[\to \mathbb{R}\,,\ f(x) := x\cot^2 x - \cot x + x$ has the limiting value $\lim_{x\to+0} = 0$, furthermore,

$$f'(x) = \cot^2 x - 2x\cot x\cdot\frac{1}{\sin^2 x} + \frac{1}{\sin^2 x} + 1 = \frac{2(\tan x - x)}{\sin^3 x\cos x} > 0\,.$$

Therefore, f is always positiv and hence (18) holds. So we have proved:

Theorem 3. $\mathbf{T_1}$ *is rounder than* $\mathbf{T}$.

References

[1] J.-É. Barbier: Note sur le problème de l'aiguille et le jeu du joint couvert. *Journal des mathématiques pures et appliquées*, 2d ser., **5** (1860), 273-286.

[2] A. Duma, S. Rizzo: Chord length distribution functions for an arbitrary triangle, *Rend. Circ. Mat. Palermo*, Serie II, Suppl. **81** (2009), 141-157.

[3] A. Duma, S. Rizzo: Die Sehnenlängenverteilung zu einem Trapez mit zwei geraden Winkeln, *Fernuniversität Hagen: Seminarberichte aus der Fakultät für Mathematik und Informatik*, **83** (2010) 129-142.

[4] A. Duma, M. I. Stoka: Schnitte eines 'kleinen' gleichseitigen Dreiecks mit den Gittern von Buffon und Laplace, *Fernuniversität Hagen: Seminarberichte aus der Fakultät für Mathematik und Informatik*, **79** (2008) 13-22.

[5] G. M. Fichtenholz: *Differential- und Integralrechnung*, Band 1, Deutscher Verlag der Wissenschaften, Berlin, 1969.

[6] L. A. Santaló: *Integral Geometry and Geometric Probability*, Addison-Wesley, London, 1976.

[7] M. I. Stoka: Probabilités géometriques de type "Buffon" dans le plan euclidien, *Atti Acc. Sci. Torino*, **110** (1975-76) 53-59.

[8] M. I. Stoka: *Probabilità e geometria*, Herbita, Palermo, 1982.

[9] F. A. Valentine: *Konvexe Mengen*, Hochschultaschenbuch 402/402a, Bibliographisches Institut, Mannheim, 1968.

Uwe BÄSEL

HTWK Leipzig
Fakultät für Maschinen- und Energietechnik,
04251 Leipzig, Germany

baesel@me.htwk-leipzig.de

Andrei DUMA

FernUniversität in Hagen
Fakultät für Mathematik und Informatik
58084 Hagen, Germany

Mathe.Duma@FernUni-Hagen.de

RENDICONTI DEL CIRCOLO MATEMATICO DI PALERMO
Serie II, Suppl. 84 (2012), pp. 33-42

Detection of architectural distortion using statistical measures of correlation and stationarity

Shantanu Banik[1], Rangaraj M. Rangayyan[1,2,⋆], and J.E.Leo Desautels[1]
[1]Department of Electrical and Computer Engineering,
Schulich School of Engineering, and [2]Department of Radiology,
University of Calgary, Calgary, Alberta, CANADA T2N 1N4
⋆To whom all correspondence should be addressed: ranga@ucalgary.ca

Abstract

Architectural distortion is a mammographic sign of early stages of breast cancer. We present methods for the recognition of architectural distortion in prior mammograms of interval-cancer cases using a set of statistical features obtained through the analysis of spatial and angular correlation and stationarity. Initial sites of architectural distortion were localized using a bank of Gabor filters and phase-portrait analysis. Statistical features were computed from the detected regions of interest. A set of selected features and a quadratic classifier provided a sensitivity of 0.80 at 5.4 false positives per patient.

1 Introduction

Early detection of cancer is of utmost importance to increase the possibility of survival through treatment at early stages of the disease. Architectural distortion is a hard-to-detect mammographic sign of early stages of breast cancer [1, 2]. Various computer-aided diagnosis (CAD) techniques [3] have been developed to enhance the sensitivity and accuracy of detection of breast cancer; however, they have been found to be effective only in the detection of comparatively more distinguishable masses and calcifications with satisfactory performance. The CAD systems available to date have been found to fail in detecting architectural distortion with a high level of accuracy [4]. In addition, studies on CAD of architectural distortion suggest that there is significant scope and need for more research on the detection of architectural distortion to facilitate early detection of breast cancer, for improvement in the prognosis of breast cancer patients [5], and to help in reducing the associated mortality rate.

The presence of architectural distortion is manifested by distortion of the normal architecture of the breast with no definite mass visible [6]. The patterns of distortion include subtle spiculations radiating from a point and focal retraction or distortion at the edge of the parenchyma. Such patterns may closely resemble the appearance of normal breast tissue overlapped in the projected mammographic image. Due to its subtle appearance and

variability in presentation, architectural distortion is the most commonly missed abnormality in false-negative cases [2]. For characterization of the variety of textural patterns related to architectural distortion in mammograms, several CAD methods have been proposed, including a multiscale method for the detection of stellate distortion [7], morphological image processing techniques with a concentration index [8], fractal analysis [9–11], multiresolution analysis [12], a point convergence index for radiating spiculation [13], Gabor filters and phase-portrait analysis [11, 14–16], texture analysis [11, 14], and characterization of angular spread [11, 17].

The aim of this study is to develop a CAD technique for the recognition of architectural distortion in screening mammograms acquired prior to the detection of breast cancer using a set of statistical features obtained through the analysis of spatial and angular correlation and stationarity [18]. The analysis of correlation is based on Mantel's nonparametric statistical test [19–21] to determine clustering trends in terms of space and difference in attributes. Mantel's test considers the location and attribute values in a 3D space $[x, y, Z(x, y)]$, where $Z(x, y)$ is a function of (x, y). Extending this notion to image analysis, statistical measures can be obtained based on the proximity of pixels for quantification of the amount of clustering of patterns in image data, to characterize the relationship between space and image intensity [18, 21]. In addition, for quantification of trends in data, a nonparametric test of stationarity, called the reverse arrangements (RA) test [22, 23], is used in the present study [18].

2 Methods

2.1 Experimental Setup and Database

For the present study, 158 mammographic images, including 52 images of 13 normal individuals and 106 prior mammographic images of 56 individuals diagnosed with breast cancer, were obtained from Screen Test: Alberta Program for the Early Detection of Breast Cancer [24]. All but two prior mammograms had been declared to be free of signs of breast cancer at the time of their screening and interpretation. The 106 prior mammograms of interval-cancer cases were analyzed independently by a radiologist specialized in screening mammography (J.E.L.D.). Parts of the images related to or suspected to contain architectural distortion were marked using rectangular boxes based on the reports available on subsequent imaging, biopsy, or by detailed inspection of the prior mammograms. One rectangular part per image was marked by the radiologist. The time interval between the diagnosis of cancer and the related prior mammograms ranged from 1.5 months to 24.5 months, with an average of 15 ± 7 months.

2.2 Detection of Potential Sites of Architectural Distortion

The potential sites of architectural distortion in the prior mammograms were detected initially by the analysis of oriented texture patterns with the application of a bank of Gabor filters [25, 26] and linear phase-portrait models [27, 28]. The procedures are summarized as follows [11, 14, 28]:

i Segment the breast portion in the given mammographic image using adaptive thresholding and morphological opening.

ii Apply a set of 180 Gabor kernels with angles spaced evenly over the range [$-\pi/2$, $\pi/2$] to obtain the magnitude response and orientation field by selecting the response and angle of the Gabor filter with the highest response at each pixel.

iii Select curvilinear structures (CLS) of interest (i.e., spicules and fibroglandular tissue) by separating them from confounding structures (i.e., edges of the pectoral muscle, parenchymal tissue, breast boundary, and noise) using the orientation field, the gradient field, the nonmaximal suppression technique, and additional conditions [28].

iv Filter the orientation field with a Gaussian filter and downsample by a factor of four to reduce noise and further computational requirements [14, 28].

v Apply linear phase-portrait modeling, with a sliding analysis window of size 10×10 pixels (at 800 μm/pixel) with one pixel per step, to the filtered orientation field with specific conditions to yield the phase-portrait map for node patterns [14, 28]. For each position of the window, cast a vote at the node position given by the corresponding fixed (equilibrium) point to form the node map.

vi Filter the node map with a Gaussian window of size 35×35 pixels with the empirically determined value of $\sigma = 6$ pixels (4.8 mm) in order to group votes placed in close proximity to one another.

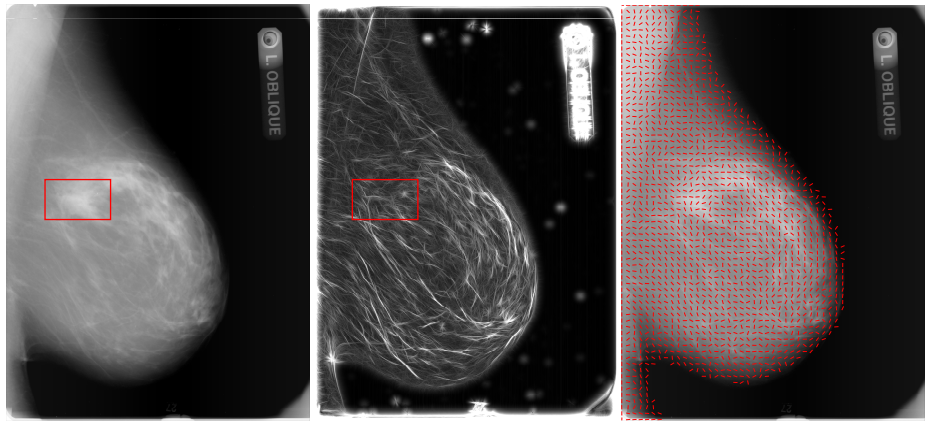
vii Analyze the node map by rank-ordering the peaks in the node map.

viii Cut a region of interest (ROI) of size 128×128 pixels (except at the edges) from the original image with the center of each ROI located at the center of the corresponding peak in the node map.

The peaks in the node map are expected to indicate potential sites of architectural distortion; however, the procedure also results in the detection of a number of false-positive (FP) sites [11, 14] (see Figures 1 and 2).

From the 158 mammograms in the study, a total of 4224 ROIs (2821 ROIs from the 106 prior mammograms of interval-cancer cases with 301 ROIs related to the parts with architectural distortion, and 1403 ROIs from the 52 normal prior mammograms) of size 128×128 pixels at 200 μm/pixel (except at the edges of the images) were automatically obtained. ROIs were labeled at the locations indicated by the peaks in the node maps, in decreasing order of the node value of the peak, up to a maximum of 30 ROIs per mammogram. The automatically detected ROIs with their centers within the rectangular regions of architectural distortion marked by the radiologist were identified as true-positive (TP) ROIs; the others were labeled as FP ROIs. Similarly, ROIs were obtained from the magnitude response and angle response images.

The results of application of the methods are illustrated in Figures 1 and 2 for a prior mammogram of an interval-cancer case. In Figure 1 (a), the rectangle shows the area of architectural distortion marked by the radiologist (J.E.L.D.). The magnitude image and the orientation field resulting from the Gabor filters are shown in parts (b) and (c), respectively. The node map is shown in Figure 2 (a); Figure 2 (b) illustrates all of the automatically detected ROIs obtained.

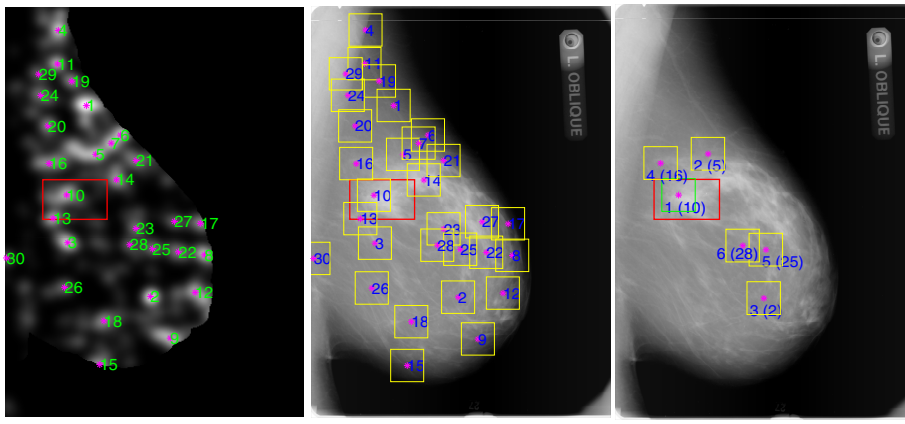


(a) (b) (c)

Figure 1: (a) A prior mammogram of an interval-cancer case with architectural distortion. The rectangle is of size 49.8 mm × 31.0 mm at 200 μm/pixel resolution, and indicates the site of architectural distortion identified by the radiologist. (b) Magnitude response obtained using a bank of 180 real Gabor filters. (c) Orientation field angle superimposed on the mammographic image; needles are drawn for every 18^{th} pixel.

2.3 Characterization of Architectural Distortion

Sites with architectural distortion are expected to possess spiculating patterns, resulting in high correlation in the radial direction from the center



(a) (b) (c)

Figure 2: (a) The node map at 800 μm/pixel resolution for the mammogram shown in Figure 1. Each asterisk mark (*) corresponds to a peak position detected automatically in the node map. The numbers next to the asterisk marks indicate the peaks in descending order of magnitude. (b) The 30 ROIs obtained through the application of Gabor filters and phase-portrait analysis are shown using yellow squares. The size of each ROI is 128×128 pixels (except at the edges of the image). (c) Reduction of FPs using the proposed features: only the top six ROIs based on the discriminant values are shown, with the associated average sensitivity of 0.8 at 5.4 FP/patient. The numbers outside the parentheses represent the ranking based on the discriminant values obtained by the quadratic classifier using manually selected features (Set-IV); the numbers within the parentheses represent the earlier ranking based on the node value.

of the site. Inspired by methods for the analysis of correlation [21] and Mantel's nonparametric statistical test [19] to determine clustering trends, six measures are proposed in the present work. The correlation measure, $M2$, quantifies the clusterability of the data, and the number of reverse arrangements, R^*, quantifies the trends found in the data.

Mantel's test was developed to determine clustering trends of disease in terms of geographic location (space) and time [19, 20] and is commonly used in ecology, where the data are usually estimates of the "distance" between objects such as species of organisms. Because distances are not independent of one another, changing the "position" of one object out of n would change $n-1$ of the distances (the distance from that object to each of the others); consequently, it is not possible to assess the relationship between the two matrices by simply evaluating the correlation coefficient between the two sets of distances and testing its statistical significance [21]. Mantel's test deals with this problem by considering the location and attribute (intensity) values in a 3D space $[x, y, I(x, y)]$, where (x, y) are spatial coordinates and $I(x, y)$ is an image attribute at (x, y). Extending this notion to

image analysis, measures can be obtained based on the proximity of pixels for quantification of the extent of clustering in image data, to characterize the relationship between space and image attributes. If correlation or spatial dependence exists between pixel attributes, pixels in close proximity will be coupled and have similar attribute values [20]. This property can be quantified as $M2 = \sum_{i=1}^{N1} \sum_{j=1}^{N2} W_{ij} U_{ij}$, where W_{ij} and U_{ij} are the Euclidean distance and the absolute value of the difference in attributes between the pixels at spatial locations i and j, and the summations are over all i and j (in the present work, $N1 = N2 = M \times N$, where $M \times N$ is the size of the ROI being analyzed). Here, W_{ij} and U_{ij} describe the spatial proximity and closeness of attributes of the pixels at spatial locations i and j, respectively. Because $M2$ quantifies clustering of image data, it can be used for quantitative analysis of texture [21].

The RA test [22, 23] involves, starting with the first data point, computing the number of times that subsequent points are less than the first data point. The count is known as a "reverse arrangement" and quantifies trends in the data that are indicative of nonstationarity. The sum of all reverse arrangements (R^*) can be used as a feature to quantify texture in images [21]. In the present work, in addition to $M2$ and R^* computed for each ROI with the original gray-scale values, the corresponding Gabor magnitude response, and the corresponding Gabor angle response, the node value was also used as a feature for classification of the ROIs.

Figure 2.3 illustrates two TP ROIs and two FP ROIs along with the corresponding parts of the Gabor magnitude and angle responses. The feature values obtained for the ROIs are also listed. Because the presence of architectural distortion changes the normal tissue patterns and is typically associated with a number of intersecting or spiculating structures, TP ROIs are expected to possess different $M2$ and R^* values than FP ROIs. All the features, except $M2$ for the original image ROIs, showed p-value< 0.001 indicating statistically highly significant differences [29] between the TP ROIs and FP ROIs.

3 Results

The results of receiver operating characteristic (ROC) analysis [30] of the individual features resulted in area under the ROC curve (A_z) of 0.53, 0.63, 0.66, 0.64, 0.58, and 0.55 for the $M2$ values for the ROIs from the original images, magnitude responses, and angle responses, and the R^* values obtained for the same, respectively. With the node value, i.e., the results after the application of Gabor filters and phase-portrait analysis, the A_z value obtained was 0.61; sensitivities of 0.8 and 0.9 were obtained at 11.6 and 19.6 FP/patient, respectively. The results indicate that node value

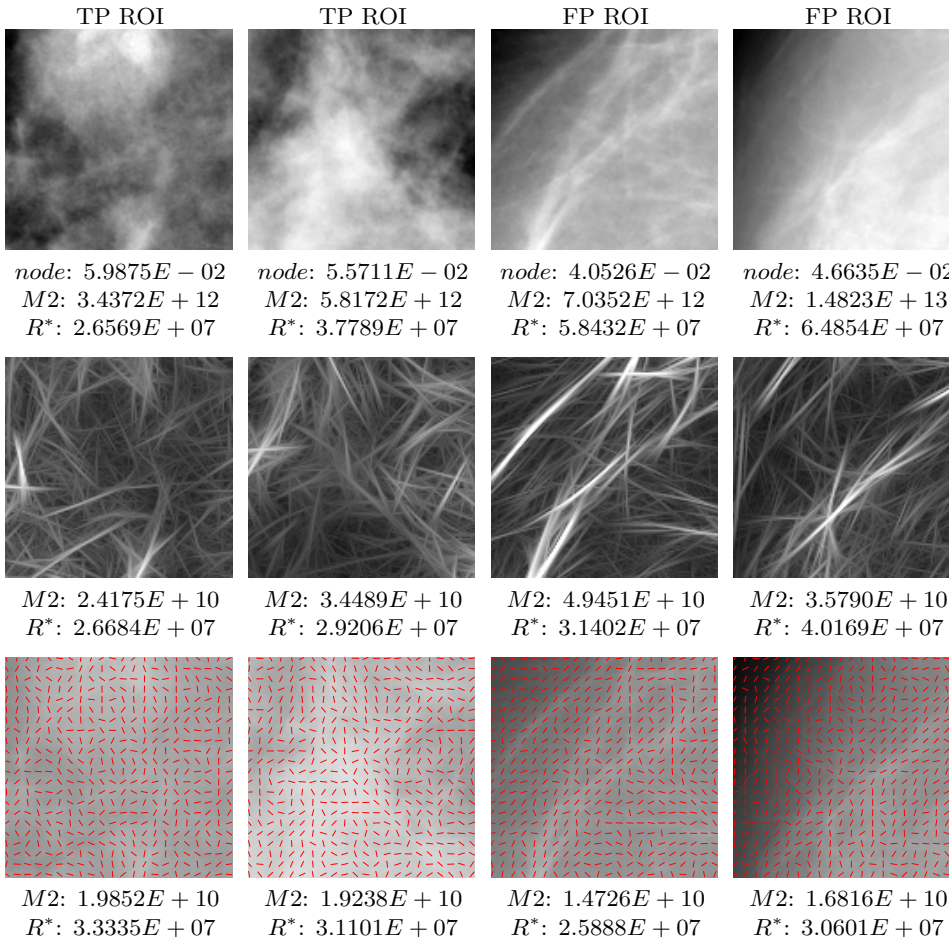


Figure 3: Examples of two TP and two FP ROIs. Each ROI from an original image (top row) is of size 128×128 pixels at 200 μm/pixel, or 25.6 mm×25.6 mm. The Gabor magnitude (middle row) and angle (bottom row) ROIs are also shown. The feature values are shown for each of the ROIs as well as their Gabor magnitude and angle responses.

alone is not adequate for accurate classification of the ROIs. A combination of all seven features including the node value resulted in $A_z = 0.76$ with an artificial neural network based on radial basis functions [31], with the validation performed using the leave-one-patient-out method.

The results of free-response ROC (FROC) analysis with several sets of selected features and using a quadratic classifier based on Bayesian decision theory [32] with the leave-one-patient-out method are shown in Table 1.

Table 1: Results of FROC analysis with sets of selected features, a quadratic classifier based on Bayesian decision theory, and the leave-one-patient-out method. Set-V was selected by stepwise regression; the other sets were manually selected.

Feature set	FP/patient at 80% sensitivity	FP/patient at 90% sensitivity
Node only	11.6	19.6
Set-I: All features	5.6	8.1
Set-II: $M2$- image, magnitude, angle; R^*- image, magnitude, angle	6.4	7.7
Set-III: Node value; $M2$- magnitude, angle; R^*- image, magnitude	5.7	8.2
Set-IV: Node value; $M2$- magnitude, angle; R^*- image, magnitude, angle	**5.4**	7.6
Set-V: Node value, $M2$- image, magnitude, angle; R^*- image, magnitude	6.0	7.7

The best results achieved represent a sensitivity of 0.8 at 5.4 FP/patient by using a combination of the node value, $M2$ values for the magnitude response and angle response ROIs, and R^* values for the image, magnitude response, and angle response ROIs.

4 Conclusion

The detection of architectural distortion in prior mammograms is an important but difficult problem. In this study, the detection of architectural distortion was performed using Gabor filters, linear phase-portrait analysis, and methods for statistical analysis of texture. The use of statistical measures of spatial and angular correlation and stationarity for the characterization of architectural distortion resulted in a sensitivity of detection of 0.8 at 5.4 FP/patient. The development of CAD techniques for the detection and localization of architectural distortion in prior mammograms is expected to lead to efficient detection of subtle signs of early stages of breast cancer at pre-mass-formation stages.

References

[1] M. J. Homer. *Mammographic Interpretation: A Practical Approach.* McGraw-Hill, New York, NY, 2nd edition, 1997.

[2] A. M. Knutzen and J. J. Gisvold. Likelihood of malignant disease for various categories of mammographically detected, nonpalpable breast lesions. *Mayo Clinic Proceedings*, 68:454–460, 1993.

[3] K. Doi. Diagnostic imaging over the last 50 years: research and development in

medical imaging science and technology. *Physics in Medicine and Biology*, 51:R5–R27, June 2006.

[4] J. A. Baker, E. L. Rosen, J. Y. Lo, E. I. Gimenez, R. Walsh, and M. S. Soo. Computer-aided detection (CAD) in screening mammography: Sensitivity of commercial CAD systems for detecting architectural distortion. *American Journal of Roentgenology*, 181:1083–1088, 2003.

[5] M. J. M. Broeders, N. C. Onland-Moret, H. J. T. M. Rijken, J. H. C. L. Hendriks, A. L. M. Verbeek, and R. Holland. Use of previous screening mammograms to identify features indicating cases that would have a possible gain in prognosis following earlier detection. *European Journal of Cancer*, 39:1770–1775, 2003.

[6] American College of Radiology (ACR). *Illustrated Breast Imaging Reporting and Data System (BI-RADS®)*. American College of Radiology, Reston, VA, 3rd edition, 1998.

[7] N. Karssemeijer and G. M. te Brake. Detection of stellate distortions in mammograms. *IEEE Transactions on Medical Imaging*, 15(5):611–619, October 1996.

[8] T. Matsubara, T. Ichikawa, T. Hara, H. Fujita, S. Kasai, T. Endo, and T. Iwase. Novel method for detecting mammographic architectural distortion based on concentration of mammary gland. *International Congress Series, Elsevier B.V.*, 1268:867–871, June 2004. Proceedings of the 18th International Congress and Exhibition on Computer Assisted Radiology and Surgery (CARS2004).

[9] Q. Guo, J. Shao, and V. F. Ruiz. Characterization and classification of tumor lesions using computerized fractal-based texture analysis and support vector machines in digital mammograms. *International Journal of Computer Assisted Radiology and Surgery*, 4(1):11–25, January 2009.

[10] G. D. Tourassi, D. M. Delong, and C. E. Floyd Jr. A study on the computerized fractal analysis of architectural distortion in screening mammograms. *Physics in Medicine and Biology*, 51(5):1299–1312, 2006.

[11] S. Banik, R. M. Rangayyan, and J. E. L. Desautels. Detection of architectural distortion in prior mammograms. *IEEE Transactions on Medical Imaging*, 30(2):279–294, February 2011.

[12] R. Nakayama, R. Watanabe, T. Kawamura, T. Takada, K. Yamamoto, and K. Takeda. Computer-aided diagnosis scheme for detection of architectural distortion on mammograms using multiresolution analysis. In *Proceedings of the 22nd International Congress and Exhibition on Computer Assisted Radiology and Surgery (CARS 2008)*, volume 3(1), pages S418–S419, Barcelona, Spain, June 2008.

[13] M. Nemoto, S. Honmura, A. Shimizu, D. Furukawa, H. Kobatake, and S. Nawano. A pilot study of architectural distortion detection in mammograms based on characteristics of line shadows. *International Journal of Computer Assisted Radiology and Surgery*, 4(1):27–36, January 2009.

[14] R. M. Rangayyan, S. Banik, and J. E. L. Desautels. Computer-aided detection of architectural distortion in prior mammograms of interval cancer. *Journal of Digital Imaging*, 23(5):611–631, October 2010.

[15] R. M. Rangayyan and F. J. Ayres. Gabor filters and phase portraits for the detection of architectural distortion in mammograms. *Medical and Biological Engineering and Computing*, 44:883–894, August 2006.

[16] Minavathi, Murali. S., and M. S. Dinesh. Model based approach for detection of architectural distortions and spiculated masses in mammograms. *International Journal on Computer Science and Engineering*, 3(11):3534–3546, November 2011.

[17] R. M. Rangayyan, S. Banik, and J. E. L. Desautels. Detection of architectural distortion in prior mammograms using measures of angular distribution. In R. M.

Summers and B. van Ginneken, editors, *Proceedings of SPIE Medical Imaging 2011: Computer Aided Diagnosis*, volume 7963, pages 796308: 1–9, Orlando, FL, February 2011.

[18] R. M. Rangayyan, S. Banik, and J. E. L. Desautels. Statistical measures of correlation and stationarity for the detection of architectural distortion in prior mammograms of interval-cancer cases. In *Proceedings of the 26th International Congress and Exhibition: Computer Assisted Radiology and Surgery*, Pisa, Italy, June 2012. In press.

[19] N. Mantel. The detection of disease clustering and a generalized regression approach. *Cancer Research*, 27(2):209–220, February 1967.

[20] O. Schabenberger and C. A. Gotway. *Statistical Methods for Spatial Data Analysis*. Chapman & Hall CRC, Boca Raton, FL, 2005.

[21] A. Khademi, D. Hosseinzadeh, A. Venetsanopoulos, and A. Moody. Nonparametric statistical tests for exploration of correlation and nonstationarity in images. In *Proceedings of the 16th International Conference on Digital Signal Processing*, pages 1–6, Santorini-Hellas, Greece, July 2009.

[22] T. Beck, T. Housh, J.Weir, J. Cramer, V. Vardaxis, G. Johnson, J. Coburn, M. Malek, and M. Mielke. An examination of the runs test, reverse arrangements test, and modified reverse arrangements test for assessing surface EMG signal stationarity. *Journal of Neuroscience Methods*, 156(1–2):242–248, 2006.

[23] P. Cappa, S. Silvestri, and S. Sciuto. On the robust utilization of non-parametric tests for evaluation of combined cyclical and monotonic drift. *Measurement Science and Technology*, 12:1439–1444, 2006.

[24] Alberta Cancer Board, www.cancerboard.ab.ca/screentest, Alberta, Canada. *Screen Test: Alberta Program for the Early Detection of Breast Cancer – 2001/03 Biennial Report*, 2004.

[25] D. Gabor. Theory of communication. *Journal of the Institute of Electrical Engineers*, 93:429–457, 1946.

[26] C. K. Chui. *An Introduction to Wavelets*, volume 1 of *Wavelet Analysis and its Applications*. Academic Press, San Diego, CA, 1992.

[27] A. R. Rao. *A Taxonomy for Texture Description and Identification*. Springer-Verlag, New York, NY, 1990.

[28] F. J. Ayres and R. M. Rangayyan. Reduction of false positives in the detection of architectural distortion in mammograms by using a geometrically constrained phase portrait model. *International Journal of Computer Assisted Radiology and Surgery*, 1:361–369, 2007.

[29] J. H. Ware, F. Mosteller, F. Delgado, C. Donnelly, and J. A. Ingelfinger. P values. In J.C. Bailar III and F. Mosteller, editors, *Medical Uses of Statistics*, pages 181–200. NEJM Books, Boston, MA, second edition, 1992.

[30] C. E. Metz. ROC methodology in radiologic imaging. *Investigative Radiology*, 21:720–733, 1986.

[31] S. Haykin. *Neural Networks: A Comprehensive Foundation*. Prentice Hall, Englewood Cliffs, NJ, second edition, 1999.

[32] R. O. Duda, P. E. Hart, and D. G. Stork. *Pattern Classification*. Wiley-Interscience, New York, NY, 2nd edition, 2001.

RENDICONTI DEL CIRCOLO MATEMATICO DI PALERMO
Serie II, Suppl. 84 (2012), pp. 43-48

Laplace problems for regular lattices with eight obstacles

D. Barilla, A. Feminó and A. Puglisi
Department SEA, University of Messina,
Via dei Verdi n.75, 98122 Messina, Italia.
E-mail:dbarilla@unime.it
E-mail:afemino@unime.it
E-mail:puglisia@unime.it

Abstract

In a previous paper [1] the authors compute the probability that a random rectangle r of constant sides l, m intersects a side of the lattice with the foundamental cell is a rectangle with sides a, b and with six obstacles. In this paper we consider the same foundamental cell but with eight obstacles. In particular when the rectangle r becomes a segment of length l, $(m = 0)$ we obtain the Laplace probability.

AMS Classification:60D05, 52A22.
Keywords:Geometric Probability, stochastic geometry, random sets, random convex sets and integral geometry.

1 Preliminaries

Let $\Re_1(a, b, c)$ be the regular lattice with fundamental cell is as in fig. 1.

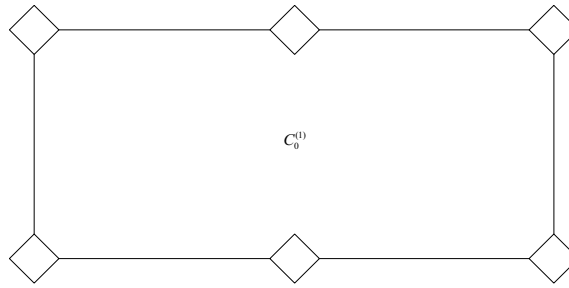


fig.1

Denoting with $C_0^{(1)}$ the fundamental cell, we have:

$$area\ C_0^{(1)} = 2ab - c^2. \tag{1}$$

The cell $C_0^{(1)}$ have six obstacles that are squares with diagonal of leght c with $c < \min(a, b)$.

Considering a segment s of random position and of leght l with $c < l < \min(a, b)$, we want compute the probabiltiy that this segment intersects a side of lattice. This probability is equal to probability $P_{int}^{(1)}$ that the segment s intersects the bounderay of the fundamental cell. The position of the segment s is determinated by the middle point p and by the angle φ that the segment form with the axis x. We consider the limit positions of the segment s that corrisponde at angle φ and let $\widehat{C}_0^{(1)}(\varphi)$ the dterminated figure from this position (see fig. 2):

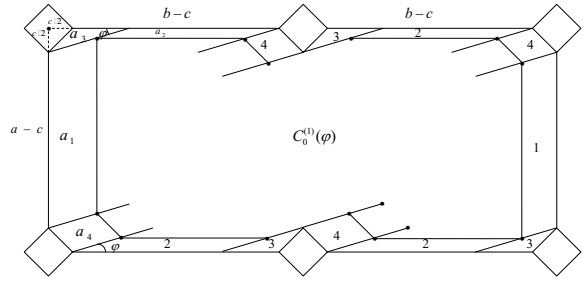


fig.2

Denoting with M_1 the set of segments s whose the middle point are in $C_0^{(1)}$ and N_1 the set of segments s whose the middle point are in $C_0^{(1)}$, we have that:

$$P_{int}^{(1)} = 1 - \frac{\mu(N_1)}{\mu(M_1)}, \tag{2}$$

where μ is the Lebesgue measure in Euclidean plane [5].

In order to compute the measures $\mu(M_1)$ and $\mu(N_1)$ we use the Poincaré kinematic measure [4]

$$dK = dx \wedge dy \wedge d\varphi,$$

where x, y are the coordinates of p and φ the defined angle. Then we have:

Theorem 1 *The probability that a segment s of random position and of length l (with $c < l < min(a, b)$) intersects a side of lattice $\Re_1(a, b, c)$ is*

$$P_{int}^{(1)} = \frac{2(a + 2b)l - l^2}{\pi(2ab - c^2)}. \tag{3}$$

2 Main results

Let $\Re_2(a, b, c)$ be the regular lattice with fundamental cell is as in fig. 3.

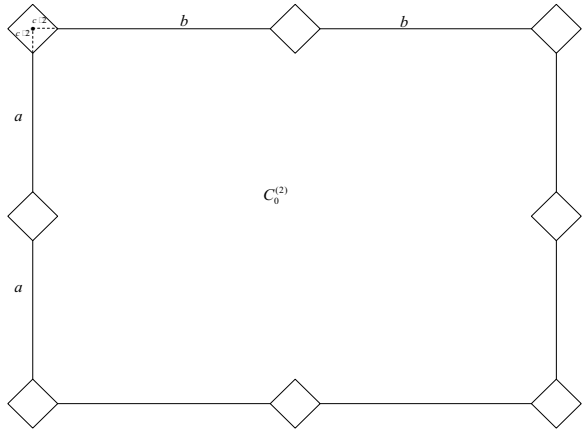


fig.3

Denoting with $C_0^{(2)}$ the fundamental cell, we have:

$$area\ C_0^{(2)} = 4ab - \frac{5c^2}{4}.$$

The cell $C_0^{(2)}$ have eight obstacles that are squares with diagonal of leght $2c$ with $c < \min(a, b)$.

Considering a segment s of random position and of leght l with $c < l < \min(a, b)$, we want compute the probabiltiy that this segment intersects a side of lattice. This probability is equal to probability $P_{int}^{(2)}$ that the segment s intersects the bounderay of the fundamental cell.

Denoting with $\widehat{C}_0^{(2)}(\varphi)$ the figure determinated by the limit positions of the segments s for a assigned value of φ (see fig. 4):

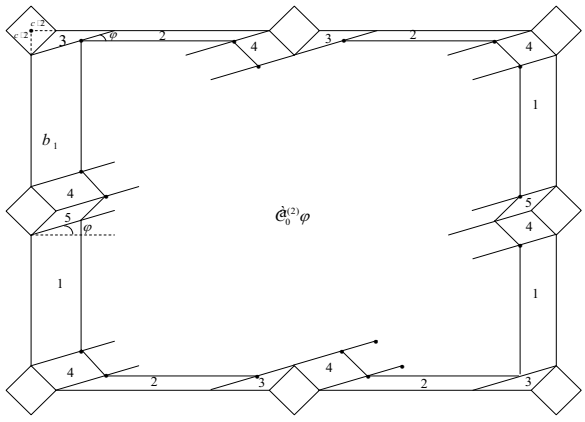


fig.4

From this figure we can write:

$$area\widehat{C}_0^{(2)}(\varphi) = areaC_0^{(2)} -$$

$$2\left[2areab_1(\varphi) + 2areab_2(\varphi) + 2areab_3(\varphi) + 3areab_4(\varphi) + areab_5(\varphi)\right]. \quad (4)$$

Considering of some results that we have obtained in a previous paper [2], follow that:

$$areab_1(\varphi) = \frac{(a-c)\,l}{2}\cos\varphi, \qquad areab_2(\varphi) + areab_3(\varphi) = \frac{(b-c)\,l}{2}\sin\varphi,$$

$$areab_4(\varphi) = \frac{cl}{4}(\sin\varphi + 2\cos\varphi) - \frac{l^2}{4}\sin 2\varphi. \quad (5)$$

In order to compute $areab_5(\varphi)$ we consider the fig.5

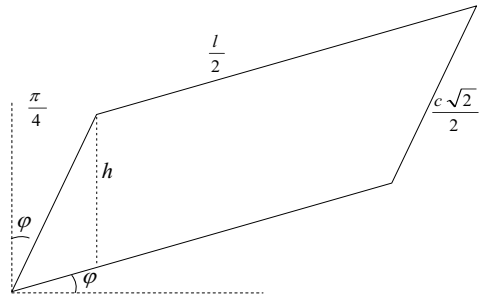


fig. 5

The parallelogram $b_5(\varphi)$ have the side $l/2$ and $c\sqrt{2}/2$ and the angles $\frac{\pi}{4} - \varphi$ and $\frac{3\pi}{4} + \varphi$. We have that:

$$h = \frac{c\sqrt{2}}{2}\sin\left(\frac{\pi}{4} - \varphi\right) = \frac{c}{2}(\cos\varphi - \sin\varphi),$$

then

$$areab_5(\varphi) = \frac{hl}{2} = \frac{cl}{4}(\cos\varphi - \sin\varphi) = \frac{cl}{4}(2\cos\varphi - \cos\varphi - \sin\varphi) =$$

$$\frac{cl}{4}\left(\frac{3}{2}\cos\varphi - \sin\varphi\right) + \frac{cl}{8}\cos\varphi,$$

i.e., considering that $c = 2l\sin\varphi$,

$$areab_5(\varphi) = -\frac{cl}{4}(\sin\varphi + \cos\varphi) + \frac{l^2}{2}\sin 2\varphi. \quad (6)$$

Considering (9) and (10) in (8) we obtain that:

$$area\widehat{C}_0^{(2)}(\varphi) = areaC_0^{(2)} -$$

$$\left[\left(2a+\frac{c}{2}\right) l\cos\varphi + (2b-c)\, l\sin\varphi - \frac{l^2}{2}\sin 2\varphi\right]. \tag{7}$$

Denoting with M_2 the set of segments s whose the middle point are in $C_0^{(2)}$ and N_2 the set of segments s whose the middle point are in $C_0^{(2)}$, we have that:

$$P_{int}^{(2)} = 1 - \frac{\mu(N_2)}{\mu(M_2)}. \tag{8}$$

Since $\varphi \in \left[0,\ \frac{\pi}{2}\right]$, we obtain that:

$$\mu(M_2) = \int_0^{\frac{\pi}{2}} d\varphi \iint\limits_{\left\{(x,y)\in C_0^{(2)}\right\}} dxdy = \frac{\pi}{2} areaC_0^{(2)} = \frac{\pi}{2}\left(4ab - \frac{5c^2}{2}\right), \tag{9}$$

and considering the (11)

$$\mu(N_2) = \int_0^{\frac{\pi}{2}} d\varphi \iint\limits_{\left\{(x,y)\in \widehat{C}_0^{(2)}(\varphi)\right\}} dxdy =$$

$$\frac{\pi}{2} areaC_0^{(2)} - \int_0^{\frac{\pi}{2}} \left[\left(2a+\frac{c}{2}\right) l\cos\varphi + (2b-c)\, l\sin\varphi - \frac{l^2}{2}\sin 2\varphi\right] d\varphi =$$

$$\frac{\pi}{2} areaC_0^{(2)} - \left[\left(2a+2b+\frac{5c}{2}\right) l - \frac{l^2}{2}\right]. \tag{10}$$

The (8), (9) and (10) give us that:

$$P_{int}^{(2)} = \frac{2\left(2a+2b-\frac{c}{2}\right) l - l^2}{\pi\left(4ab - \frac{5c^2}{4}\right)}. \tag{11}$$

When $c \to 0$, the obstacles becames points and the fundamental cell becames a rectangle with side $2a$ and $2b$. In this case the probability (11) becomes the Laplace probability:

$$P = \frac{2(2a+2b)\, l - l^2}{2\pi ab}. \tag{12}$$

References

[1] D. Barilla, P. Bartolomeo, G. Caristi, A. Puglisi , A Laplace type problem for a regular lattice with six obstacles , (to appear).

[2] Caristi G and Stoka M., A Laplace type problem for a regular lattice with obstacles (I), Atti Acc. Sci. Torino, (to appear).

[3] Caristi G and Stoka M., A Laplace type problem for a regular lattice with obstacles (II), Atti Acc. Sci. Torino, (to appear).

[4] Poincaré H., Calcul des probabilitiés, ed. 2, Carré, Paris, 1912.

[5] Stoka M., Probabilités géométriques de type Buffon dans le plan euclidean, Atti Acc. Sci. Torino, T. 110, pp. 53-59, 1975-1976.

RENDICONTI DEL CIRCOLO MATEMATICO DI PALERMO
Serie II, Suppl. 84 (2012), pp. 49-68

Laplace type problems for three hexagonal lattices with "disk body test "

D. Barilla, A. Feminó and A. Puglisi
Department S.E.A.
University of Messina
dbarilla@unime.it
afemino@unime.it
puglisi@unime.it

Abstract

In this paper we consider thre hexagonal lattices, and we compute the probability that a disk intersect a side of lattice.
Mathematical Subject Classification: 60D05, 52A22.
Keywords: Geometric Probability, stochastic geometry, random sets, random convex sets and integral geometry.

1 Regular Hexagonal Cell.

Let $\Re_1(a)$ be a lattice with fundamental cell$C_0^{(1)}$ a regular hexagon of side a.
We have

$$areaC_0^{(1)} = \frac{3\sqrt{3}}{2}a^2. \tag{1}$$

We want to determine the probability that a disk d of radius r with $r < \frac{a}{4}$ intersects a side of lattice, ie the probability $P_{int}^{(1)}$ that the disk intersects one of side of the cell $C_0^{(1)}$.

The position of the disk d is determined by its center.

To compute the probability $P_{int}^{(1)}$ we consider the positions limit of disk d in the cell $C_0^{(1)}$, which give us the figure

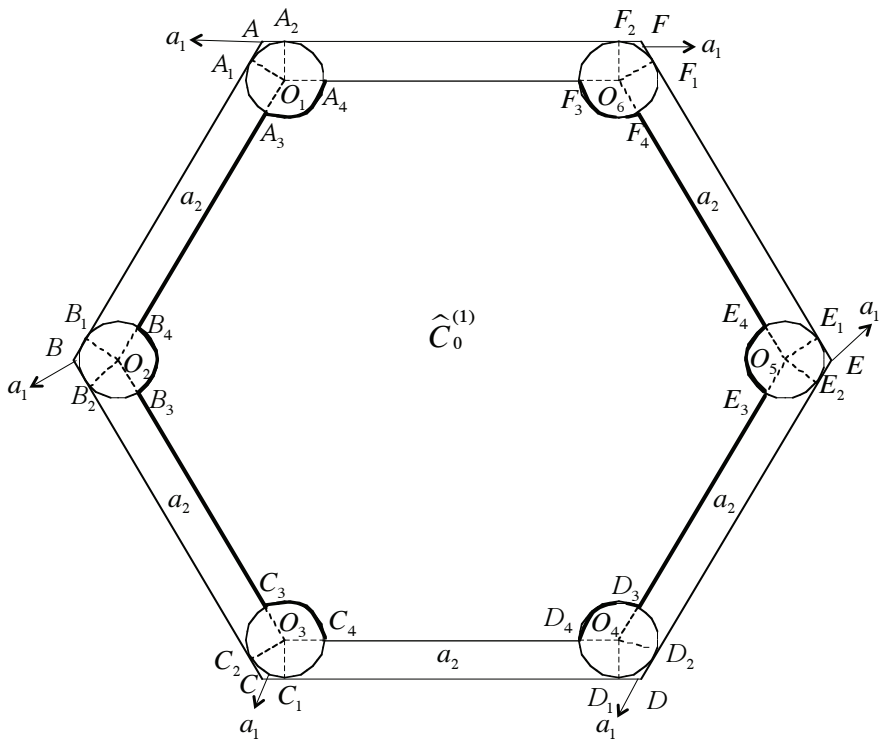


fig.1

Denoting with $\widehat{C}_0^{(1)}$ lhe figure determined by these positions, we can write

$$area\widehat{C}_0^{(1)} = areaC_0^{(1)} - 6aread - 6(areaa_1 + areaa_2). \tag{2}$$

To compute $areaa_1$ we consider the figure

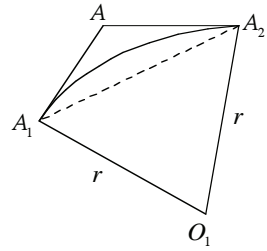


fig.2

we have

$$\widehat{AA_1O_1} = \widehat{AA_2O_1} = \frac{\pi}{2}, \quad \widehat{A_1AA_2} = \frac{2\pi}{3}, \quad \widehat{A_1O_1A_2} = \frac{\pi}{3}, \tag{3}$$

therefore

$$areaa_1 = \frac{4\sqrt{3} - r}{6} r^2. \tag{4}$$

Consider the figure

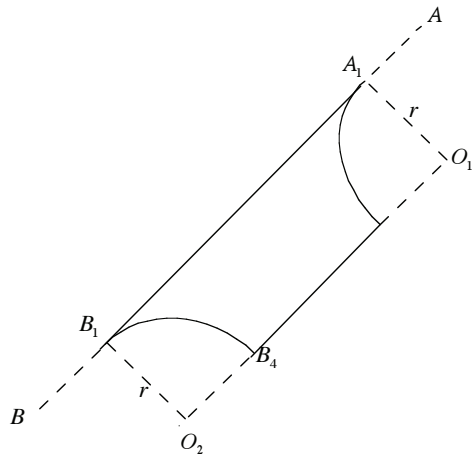


fig.3

With the formula (3) we have

$$|A_1B_1| = |AB| - 2\ |AA_1| = a - \frac{2\sqrt{3}}{3} r,$$

therefore

$$areaa_2 = a - \frac{2\sqrt{3}}{3} r - \frac{\pi r^2}{2} = ar - \frac{4\sqrt{3} + 3\pi}{6} r^2. \tag{5}$$

The relations (1), (2), (4) and (5) give us

$$area\widehat{C}_0^{(1)} = \frac{3\sqrt{3}}{2} a^2 - 6ar - 2\pi r^2. \tag{6}$$

Indicationg with $\mathcal{M}^{(1)}$ the set of disks that have the center inthe cell $C_0^{(1)}$, we have[2]:

$$P_{int}^{(1)} = 1 - \frac{\mu(\mathcal{N}^{(1)})}{\mu(\mathcal{M}^{(1)})} \tag{7}$$

where μ è the Lebesgue measure in the Euclidean plane.

To compute the measures $\mu(\mathcal{M}^{(1)})$ and $\mu(\mathcal{N}^{(1)})$ using the measure kinematic Poincarè [1] which, taking into account that a rotation around the center O of the disc leaves unchanged, reduces to

$$dK = dx \wedge dy,$$

where $x,\ y$ are the coordinates of O.

We have

$$\mu(\mathcal{M}^{(1)}) = \iint_{\left\{(x,y)\in C_0^{(1)}\right\}} dxdy = area C_0^{(1)} = \frac{3\sqrt{3}}{2}a^2 \tag{8}$$

and considering the formula (6),

$$\mu(\mathcal{N}^{(1)}) = \iint_{\left\{(x,y)\in \widehat{C}_0^{(1)}\right\}} dxdy = area \widehat{C}_0^{(1)} = \frac{3\sqrt{3}}{2}a^2 - 6ar - 2\pi r^2. \tag{9}$$

formulas(7), (8) e (9) give us

$$P_{int}^{(1)} = \frac{4\sqrt{3}}{3}\cdot\frac{r}{a} + \frac{4\sqrt{3}\pi}{9}\cdot\left(\frac{\pi}{a}\right)^2. \tag{10}$$

Da qui, poichè $r < a/4$, we have

$$P_{int}^{(1)} < 0,73$$

2 Two isosceles triangles + rectangle Cell.

Let $\Re_1(a)$ be a lattice with fundamental cell$C_0^{(1)}$ a regular hexagon of side a. Let $\Re_2(a)$ be a regular lattice with fundamental $C_0^{(2)}$ represented in figure

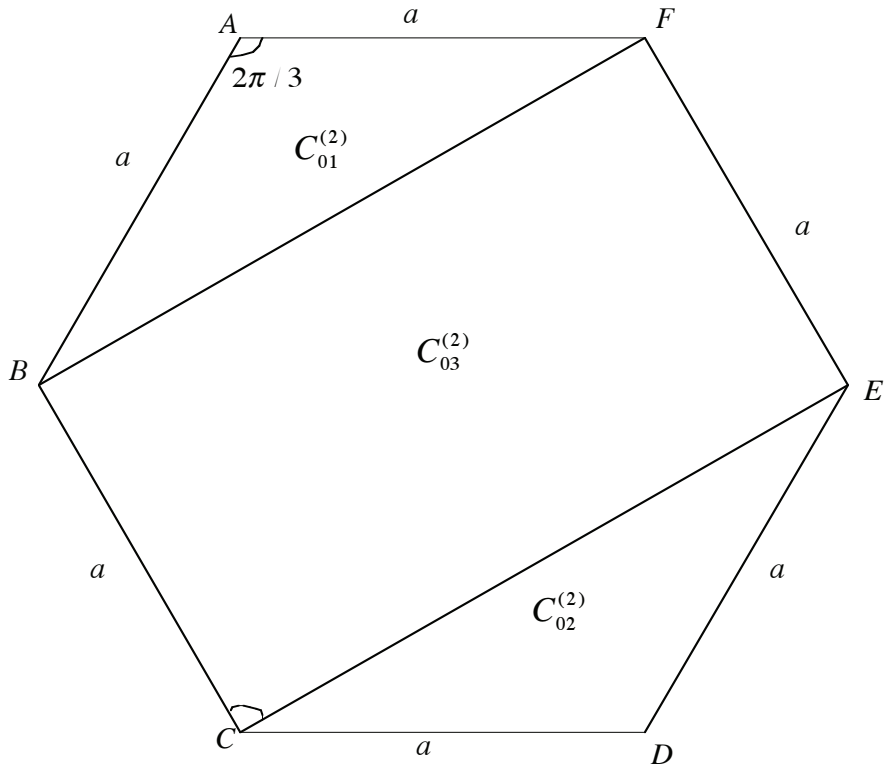


fig.4

We have

$$C_{01}^{(2)} = C_{02}^{(2)},\ \widehat{ABF} = \widehat{AFB} = \frac{\pi}{6},\ \ \widehat{BCE} = \widehat{CEF} =$$

$$\widehat{EFB} = \widehat{FBC} = \frac{\pi}{2},\quad |BF| = |CE| = a\sqrt{3}, \tag{11}$$

therefore

$$areaC_{01}^{(2)} = areaC_{02}^{(2)} = \frac{a^2\sqrt{3}}{4},\ areaC_{03}^{(2)} = a^2\sqrt{3},\ areaC_{0}^{(2)} = \frac{3\sqrt{3}}{2}a^2. \tag{12}$$

The "body test" is the same disk as the previous section.

We want to compute the probability $P_{int}^{(2)}$ that the disc intersects one side of the cell $C_0^{(2)}$.

Considering the limit positions of the disc d in the cell $C_{0i}^{(2)},\ (i = 1,\ 2,\ 3)$, we have the figure

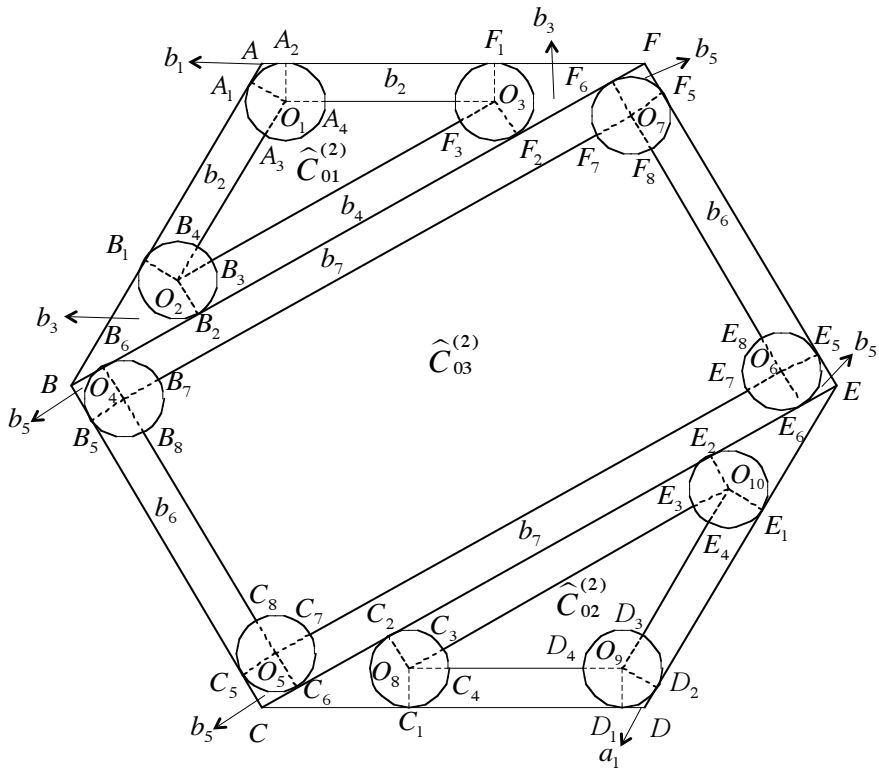


fig.5

Indicating with $\widehat{C}_{0i}^{(2)},\ (i = 1,\ 2,\ 3)$ the figure determined by these positions we have

$$area\widehat{C}_{01}^{(2)} = area\widehat{C}_{02}^{(2)} = areaC_{01}^{(2)} - 3aread -$$

$$(areab_1 + 2areab_2 + 2areab_3 + areab_4), \tag{13}$$

$$area\widehat{C}_{03}^{(2)} = areaC_{03}^{(2)} - 4aread - 2(2areab_5) + (areab_6) + (areab_7). \tag{14}$$

From Figure 1 and 5 appears

$$|AA_1| = |AA_2| = \frac{r\sqrt{3}}{3} \tag{15}$$

and

$$areab_1 = areaa_1 = \frac{3\sqrt{3} - \pi}{6} \cdot r^2. \tag{16}$$

Considering the figure

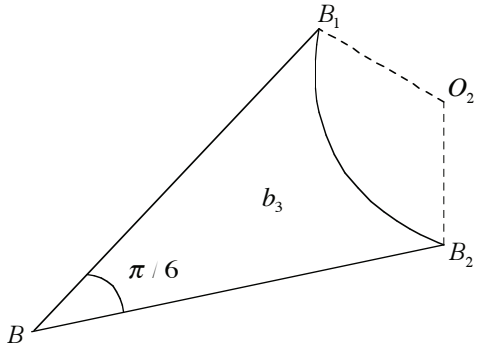


fig.6

we have

$$|BB_1| = |BB_2| = (2 + \sqrt{3})r \tag{17}$$

and

$$areab_3 = \frac{4\sqrt{3} - \pi}{24} \cdot r^2. \tag{18}$$

The figure

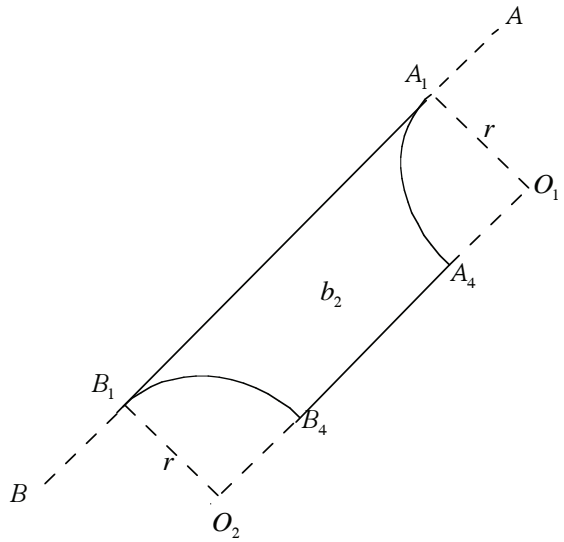


fig.7

and formulas (15) and (17) give us

$$|A_1B_1| = a - |AA_1| - |BB_1| = a - \frac{2(2\sqrt{3} + 3)}{3}r.$$

Therefore

$$areab_2 = ar - \frac{4(2\sqrt{3}+3)+3\pi}{6}r^2. \tag{19}$$

Considering the figure

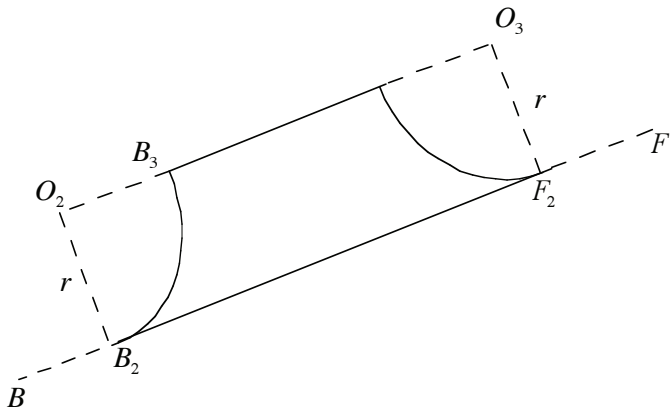


fig.8

Hence the formula (17) follows

$$|B_2F_2| = a\sqrt{3} - 2\,|BB_2| = a\sqrt{3} - 2(2+\sqrt{3})r.$$

then

$$areab_4 = \sqrt{3}ar - \frac{4(2+\sqrt{3})-\pi}{2}r^2. \tag{20}$$

Replacing in (13) expressions (16), (18), (19) and (20) we obtain

$$area\widehat{C}_{01}^{(2)} = area\widehat{C}_{02}^{(2)} = areaC_{01}^{(2)} - 2ar + \frac{27\pi - 4\sqrt{3}}{12}r^2. \tag{21}$$

The figure

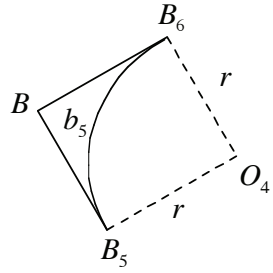


fig.9

give us

$$areab_5 = r^2 - \frac{\pi r^2}{4}, \tag{22}$$

while the figure

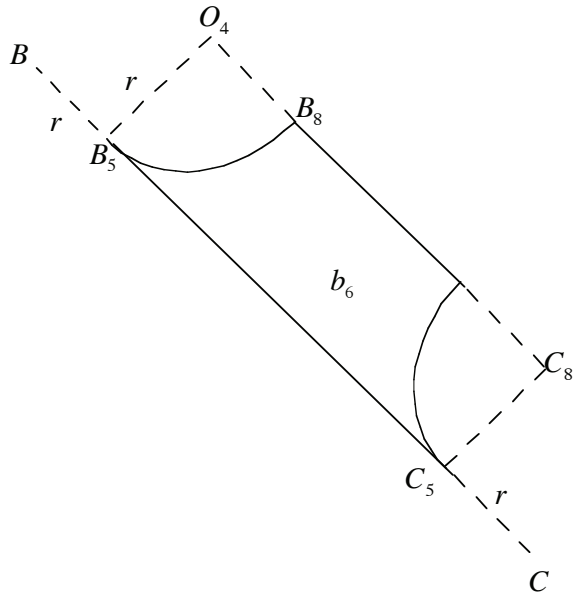


fig.10

follow

$$|B_5C_5| = a - 2r,$$

then

$$areab_6 = (a - 2r)r - \frac{\pi r^2}{2}. \tag{23}$$

Considering the figure

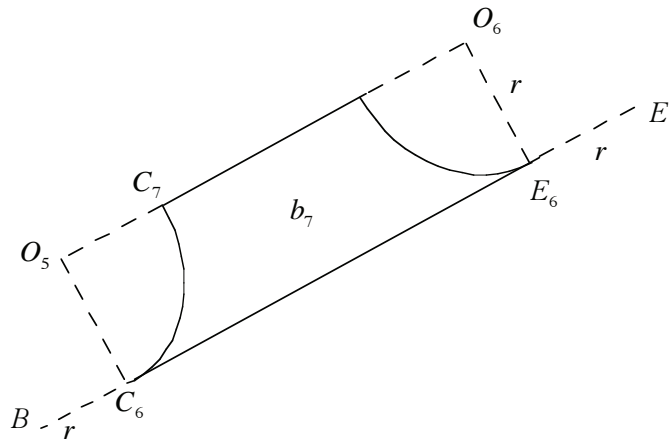


fig.11

we have

$$|C_6E_6| = a\sqrt{3} - 2r,$$

therefore

$$areab_7 = (a\sqrt{3} - 2r)r - \frac{\pi r^2}{2}. \tag{24}$$

Replacing in (14) the relation (22), (23) and (24) we obtain

$$area\widehat{C}_{03}^{(2)} = areaC_{03}^{(2)} - 2a(1+\sqrt{3})r + (4-r)r^2. \tag{25}$$

With the same notations of section 1 we have

$$P_{int}^{(2)} = 1 - \frac{2\mu(\mathcal{N}_1^{(2)}) + \mu(\mathcal{N}_3^{(2)})}{2\mu(\mathcal{M}_1^{(2)}) + \mu(\mathcal{M}_3^{(2)})} \tag{26}$$

and taking account the formulas (12), (21) and (25)

$$\mu(\mathcal{M}_1^{(2)}) = \iint_{\left\{(x,y)\in C_{01}^{(2)}\right\}} dxdy = areaC_{01}^{(2)} = \frac{a^2\sqrt{3}}{4}, \tag{27}$$

$$\mu(\mathcal{M}_3^{(2)}) = \iint_{\left\{(x,y)\in C_{03}^{(2)}\right\}} dxdy = areaC_{03}^{(2)} = a^2\sqrt{3}, \tag{28}$$

$$\mu(\mathcal{N}_1^{(2)}) = \iint_{\left\{(x,y)\in \widehat{C}_{01}^{(2)}\right\}} dxdy = area\widehat{C}_{01}^{(2)} = \frac{a^2\sqrt{3}}{4} - 2ar + \frac{27\pi - 4\sqrt{3}}{12}r^2, \tag{29}$$

$$\mu(\mathcal{N}_3^{(2)}) = \iint_{\left\{(x,y)\in\widehat{C}_{03}^{(2)}\right\}} dxdy = area\widehat{C}_{03}^{(2)} = a^2\sqrt{3} - 2(1+\sqrt{3})ar + (4-\pi)r^2. \tag{30}$$

The relations (26), (27), (28), (29) and (30) give us

$$P_{int}^{(2)} = \frac{4(1+\sqrt{3})}{3}\cdot\frac{r}{a} - \frac{(7\pi-8)\sqrt{3}}{9}\cdot\left(\frac{r}{a}\right)^2 \cong 3,64\cdot\frac{r}{a} - 2,68\cdot\left(\frac{r}{a}\right)^2. \tag{31}$$

3 Two isocele triangles + two right triangles cell

Let $\Re_3(a)$ be a regular lattice with the fundamental cell $C_0^{(3)}$ represented in figure

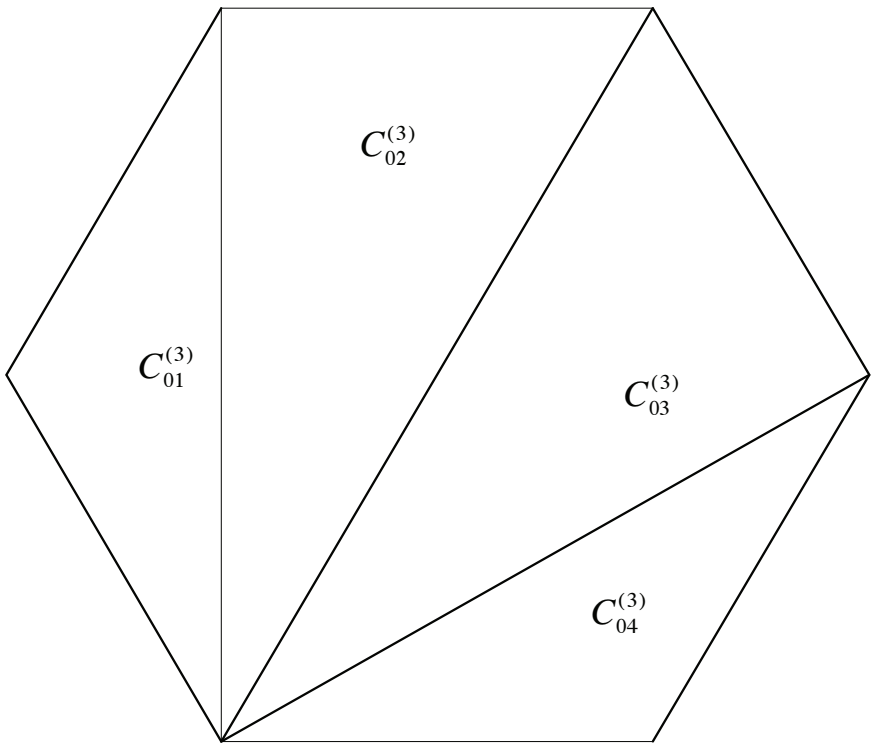


fig.12

We have

$$C_{01}^{(3)} = C_{04}^{(3)},\ C_{02}^{(3)} = C_{03}^{(3)},$$

$$\widehat{BAC} = \widehat{ACB} = \widehat{ECF} = \frac{\pi}{6},$$

$$\widehat{CFE} = \frac{\pi}{3}, \quad \widehat{CEF} = \frac{\pi}{2}, \tag{32}$$

$$|AC| = |CE| = a\sqrt{3}, \quad |CF| = 2a,$$

then

$$areaC_{01}^{(3)} = areaC_{04}^{(3)} = \frac{a^2\sqrt{3}}{4}, \; areaC_{02}^{(3)} = areaC_{03}^{(3)} = \frac{a^2\sqrt{3}}{2}. \tag{33}$$

The "body test" is the same disk as the previous section.

We want to compute the probability $P_{int}^{(3)}$ that the disc intersects one side of the cell $C_0^{(3)}$.

Considering the limit positions of the disc d in the cell $C_{0i}^{(3)}$, $(i = 1,\ 2,\ 3, 4)$, we have figure

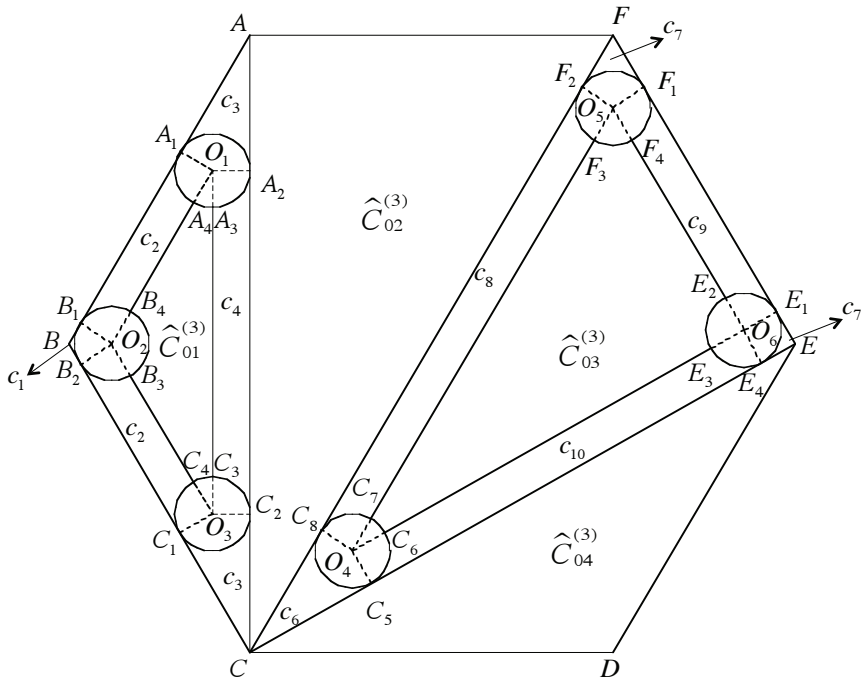


fig.13

Indicating with $\widehat{C}_{0i}^{(3)}$, $(i = 1,\ 2,\ 3, 4)$the figure determined by these positions, we have the formulas

$$area\widehat{C}_{01}^{(3)} = areaC_{04}^{(3)} = areaC_{01}^{(3)} - 3aread-$$

$$(areac_1 + 2areac_2 + 2areac_3 + areac_4), \tag{34}$$

$$area\widehat{C}_{02}^{(3)} = areaC_{03}^{(3)} = areaC_{02}^{(3)} - 3aread-$$

$$(areac_5 + areac_6 + ... + 2areac_{10}). \tag{35}$$

The figure

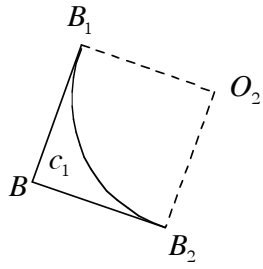


fig.14

give us

$$|BB_1| = |BB_2| = \frac{r\sqrt{3}}{3}, \tag{36}$$

therefore

$$areac_1 = \frac{r^2}{6}(2\sqrt{3} - \pi). \tag{37}$$

From figure

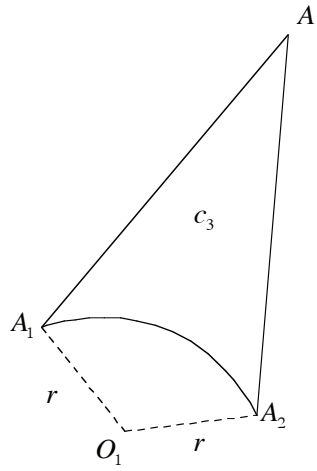


fig.15

follow

$$|AA_1| = |AA_2| = (2+\sqrt{3})r \tag{38}$$

and

$$areac_3 = \left(2+\sqrt{3}-\frac{5\pi}{12}\right)r^2. \tag{39}$$

Considering figure

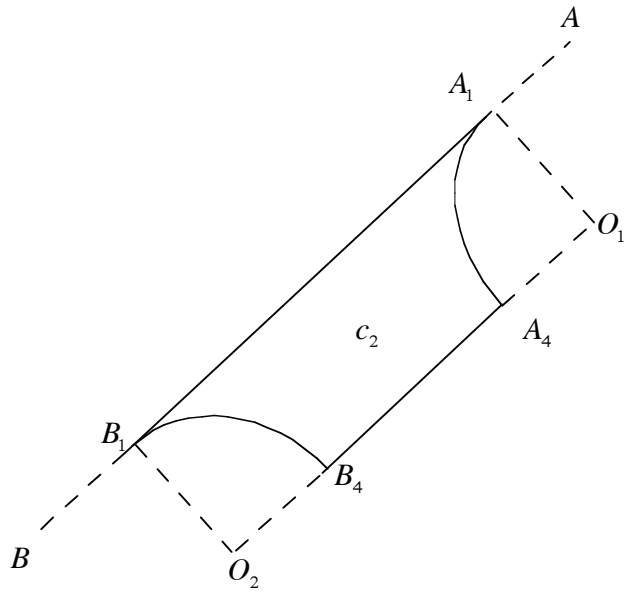


fig.16

and by relations (36) and (38) we have

$$|A_1B_1| = a - \frac{2(3+2\sqrt{3})}{3}r, \tag{40}$$

then

$$areac_2 = \left[a - \frac{2\left(3+2\sqrt{3}\right)}{3}r\right]r - \frac{\pi r^2}{2} =$$

$$ar - \frac{3\pi + 4\left(3+2\sqrt{3}\right)}{6}r^2. \tag{41}$$

Finally, the figure

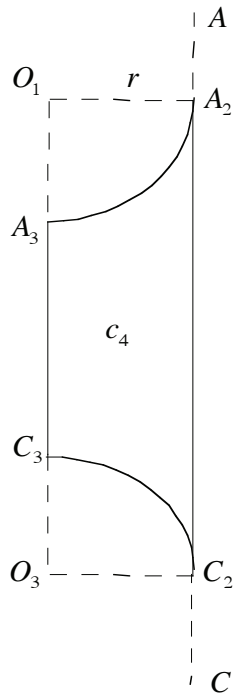


fig.17

p and by the solution (38) we can write

$$|A_2C_2| = |HC| - 2\,|AA_2| = a\sqrt{3} - 2(2+\sqrt{3})r.$$

Then

$$areac_4 = \left[a\sqrt{3} - 2\left(2+\sqrt{3}\right)r\right]r - \frac{\pi r^2}{2} =$$

$$\sqrt{3}ar - \frac{4\left(2+\sqrt{3}\right)+\pi}{2}r^2. \tag{42}$$

Replacing in the formula (34) expressions (37), (39), (41) and (42) we obtain

$$area\widehat{C}_{01}^{(3)} = areaC_{04}^{(3)} = \frac{a^2\sqrt{3}}{4} - \left(2+\sqrt{3}\right)ar + \left(4 + \frac{7\sqrt{3}}{3} - \frac{\pi}{2}\right)r^2. \tag{43}$$

The figure

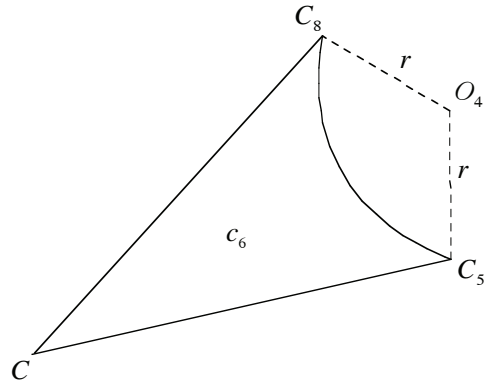


fig.18

and formula (38) gives us

$$|CC_5| = |CC_8| = |AA_1| = \left(2 + \sqrt{3}\right) r \tag{44}$$

and

$$areac_6 = \left(2 + \sqrt{3} - \frac{5\pi}{12}\right) r^2. \tag{45}$$

Now consider the figure

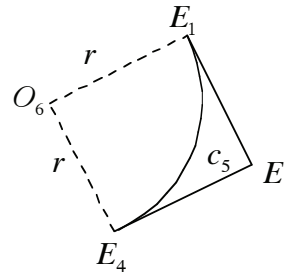


fig.19

from here it takes

$$areac_5 = r^2 - \frac{\pi r^2}{4}. \tag{46}$$

From figure

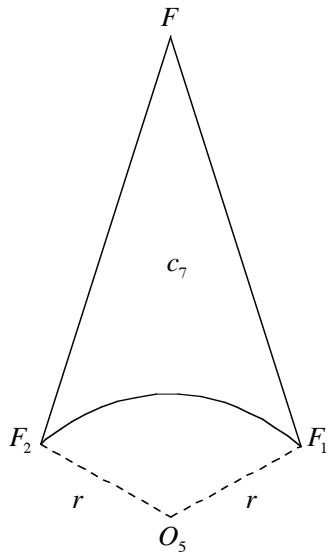


fig.20

follow

$$\widehat{F_1FF_2} = \frac{\pi}{3}, \quad |FF_1| = |FF_2| = r\sqrt{3}, \tag{47}$$

then

$$areac_7 = r^2\sqrt{3} - \frac{\pi}{6}r^2. \tag{48}$$

Figure

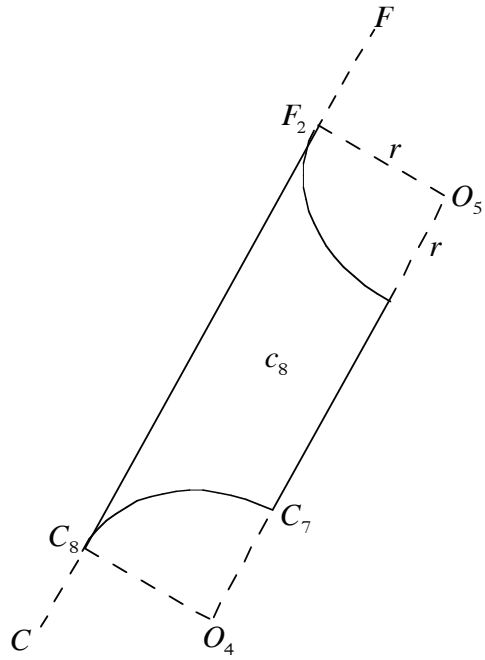


fig.21

and relations (44) and (47) give us

$$|F_2C_8| = |CF| - |CC_8| - |FF_2| = 2a - 2\left(1+\sqrt{3}\right)r,$$

therefore

$$areac_8 = 2ar - \left[2\left(1+\sqrt{3}\right) + \frac{\pi}{2}\right] r^2. \tag{49}$$

Considering figure

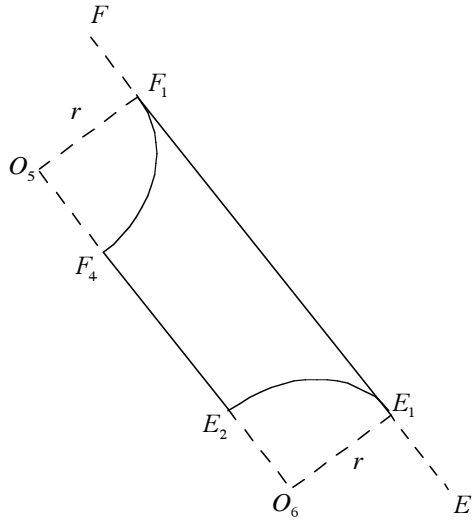


fig.22

and formula (47), we can write

$$|E_1F_1| = a - \left(1 + \sqrt{3} + \frac{\pi}{2}\right) r^2. \tag{50}$$

Finally, considering figure

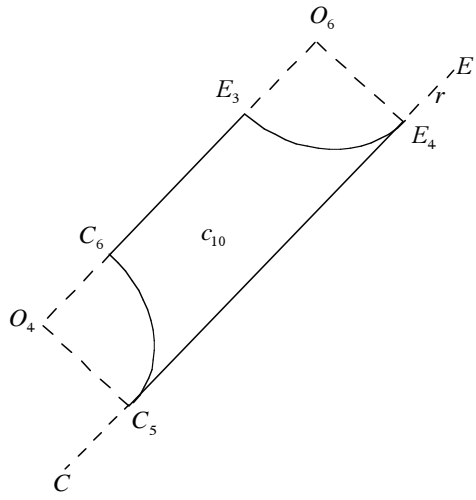


fig.23

from here and with (44), we have

$$|C_5E_4| = a\sqrt{3} - \left(3 + \sqrt{3}\right) r.$$

Therefore

$$areac_{10} = \sqrt{3}ar - \left(3 + \sqrt{3} + \frac{\pi}{2}\right) r^2. \tag{51}$$

Replacing in the formula (36) relations (45), (46), (48), (49), (50) and (51) we obtain

$$area\widehat{C}_{02}^{(3)} = area\widehat{C}_{03}^{(3)} = \frac{a^2\sqrt{3}}{2} - \left(3\sqrt{3}\right) ar + \left(3 + 2\sqrt{3} - \frac{2\pi}{3}\right) r^2. \tag{52}$$

With the notations of the first section, we have

$$P_{int}^{(3)} = 1 - \frac{2\mu(\mathcal{N}_1^{(3)}) + 2\mu(\mathcal{N}_2^{(3)})}{2\mu(\mathcal{M}_1^{(3)}) + 2\mu(\mathcal{M}_2^{(3)})} \tag{53}$$

$$\mu(\mathcal{M}_1^{(3)}) = \iint_{\left\{(x,y)\in C_{01}^{(3)}\right\}} dxdy = areaC_{01}^{(3)} = \frac{a^2\sqrt{3}}{4}, \tag{54}$$

$$\mu(\mathcal{M}_2^{(3)}) = \iint_{\left\{(x,y)\in C_{02}^{(3)}\right\}} dxdy = areaC_{02}^{(3)} = \frac{a^2\sqrt{3}}{2}, \tag{55}$$

and by the formulas (43) and (52)

$$\mu(\mathcal{N}_1^{(3)}) = \iint_{\left\{(x,y)\in \widehat{C}_{01}^{(3)}\right\}} dxdy = area\widehat{C}_{01}^{(3)} = \frac{a^2\sqrt{3}}{4} - \left(2 + \sqrt{3}\right) ar + \left(4 + \frac{7\sqrt{3}}{3} - \frac{\pi}{2}\right) r^2 \tag{56}$$

$$\mu(\mathcal{N}_2^{(3)}) = \iint_{\left\{(x,y)\in \widehat{C}_{02}^{(3)}\right\}} dxdy = area\widehat{C}_{02}^{(3)} = \frac{a^2\sqrt{3}}{2} - \left(3 + \sqrt{3}\right) ar + \left(3 + 2\sqrt{3} - \frac{2\pi}{3}\right) r^2. \tag{57}$$

and by the formulas (43) and (52)

$$P_{int}^{(3)} = \frac{4\left(6 + 5\sqrt{3}\right)}{9} \cdot \frac{r}{a} - \frac{4\left(13 + 7\sqrt{3 - \frac{7\sqrt{3}\pi}{6}}\right)}{9} \cdot \left(\frac{r}{a}\right)^2 \cong 4,51 \cdot \frac{r}{a} - 2,08 \cdot \left(\frac{r}{a}\right)^2.$$

References

[1] Poincaré H., Calcul des probabilitiés, ed. 2, Carré, Paris, 1912.

[2] Stoka M., Probabilités géométriques de type Buffon dans le plan euclidien, Atti Acc. Sci. Torino, T. 110, pp. 53-59, 1975-1976.

RENDICONTI DEL CIRCOLO MATEMATICO DI PALERMO
Serie II, Suppl. 84 (2012), pp. 69-80

BUFFON'S PROBLEM WITH A 3-STAR AND A LATTICE OF PARALLELOGRAMS

V. Bonanzinga

Abstract

This paper deals with a Buffon's problem for a star with three needles and a lattice of parallelograms. We compute the probabilities of exactly i intersections of the star $S_{3,\ell}$ and the lattice $\mathcal{R}_{a,b,\alpha}$ with the condition $\frac{\pi}{3} \leq \alpha \leq \frac{\pi}{2}$ (see figure 1).

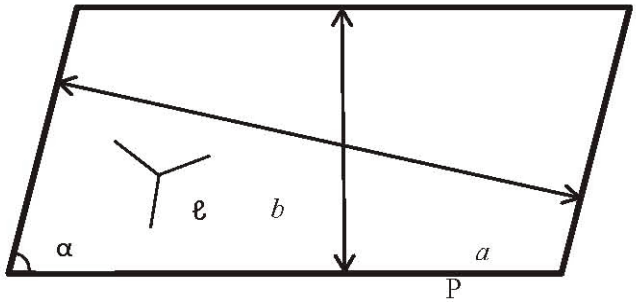


Figure 1: Star $S_{3,\ell}$ and lattice $\mathcal{R}_{a,b,\alpha} = \mathcal{R}_a \cup \mathcal{R}_b$.

AMS Subject Classification: 60D05, 52A22
Key words: Geometric probability, stochastic geometry, random sets and random convex sets.

1. Introduction

Stars $S_{n,\ell}$ with n needles and plane lattices of parallel lines are studied in [1]. Stars $S_{3,\ell}$ and $S_{5,\ell}$ and a lattice of rectangles are considered in [2]. Stars $S_{4,\ell}$ and $S_{6,\ell}$ and a lattice of rectangles are investigated in [3]. Stars $S_{n,\ell}$ with n needles and a lattice of rectangles are examined in [4]. Among other test bodies stars $S_{3,\ell}$ and lattices with obstacles are considered in [5]. Stars $S_{n,\ell}$ with an even number of n needles and a lattice of parallelograms are studied in [6]. We denote by $\mathcal{R}_{a,b,\alpha}$ the lattice of parallelograms of heights a and b and angle

$\alpha \in (0, \frac{\pi}{2}]$, $\lambda := \frac{\ell}{a}$ and $\mu := \frac{\ell}{b}$, where ℓ is the length of the needles of the star. The angle φ between a needle of the star and the x-axis in the direction of the parallel lines $\mathcal{R}_a$ is a random variable uniformly distributed in $[0,\pi]$. $\mathcal{R}_{a,b,\alpha}$ can be considered as union of the lattice $\mathcal{R}_a$ of parallel lines distance a apart and the lattice $\mathcal{R}_b$ of parallel lines distance b apart.

2. A 3-star: multiple intersections

Theorem 3.1 *A star $S_{3,\ell}$ is thrown at random onto the lattice $R_{a,b,\alpha}$. If $\frac{\pi}{3} \le \alpha \le \frac{\pi}{2}$ and $\min(a,b) \ge \ell\sqrt{3}$, the maximum number of intersections is 4. The probabilities* $\mathrm{p}(i,\alpha)$, *$i \in \{0,1,2,3,4\}$ of exactly i intersections are given by:*

$$(1)\quad p(0,\alpha) = 1 - \left(\frac{3\sqrt{3}}{\pi}(\lambda+\mu) - \frac{3}{4\pi}\lambda\mu\left(3(\pi-2\alpha)\cos\alpha + \left(6+\sqrt{3}\,\pi\right)\sin\alpha\right)\right)$$

$$(2)\quad \mathrm{p}(1,\alpha) = \frac{6}{\pi}\left(\sqrt{3}-1\right)(\lambda+\mu) - \frac{\lambda\mu}{2\pi}\left(3\left(3\pi-2\sqrt{3}-6\alpha\right)\cos\alpha + \left(5\sqrt{3}\pi+18-6\sqrt{3}\alpha\right)\sin\alpha\right)$$

$$(3)\quad \mathrm{p}(2,\alpha) = \frac{3}{\pi}\left(2-\sqrt{3}\right)(\lambda+\mu) + \frac{\lambda\mu}{\pi}\left(3\left(\pi-3\sqrt{3}-2\alpha\right)\cos\alpha + \left(4\sqrt{3}\pi+6-9\sqrt{3}\alpha\right)\sin\alpha\right)$$

$$(4)\quad \mathrm{p}(3,\alpha) = -\frac{\lambda\mu}{2\pi}\left(3\left(\pi-6\sqrt{3}-2\alpha\right)\cos\alpha + \left(7\sqrt{3}\pi+6-18\sqrt{3}\alpha\right)\sin\alpha\right)$$

$$(5)\quad \mathrm{p}(4,\alpha) = \frac{\lambda\mu}{4\pi}\left(3\left(\pi-4\sqrt{3}-2\alpha\right)\cos\alpha + \left(5\sqrt{3}\pi+6-12\sqrt{3}\alpha\right)\sin\alpha\right).$$

Proof We denote by B the set of stars with 3 needles with the center B_S belongs to the parallelogram P. Then, as in figure 2, 3, 4 and 5, the test body intersects one time (respectively, two, three and four times) the sides of the parallelogram P (i.e. the sides of the lattice $R_{a,b,\alpha}$) if and only if $B_S \in \tau_1(\varphi)$ (respectively $B_S \in \tau_2(\varphi)$, $B_S \in \tau_3(\varphi)$ and $B_S \in \tau_4(\varphi)$).

Hence, putting $C_i = \left\{(x,y) \in \tau_i(\varphi): \varphi \in \left[0, \frac{\pi}{3}\right]\right\}$, i=1,2,..,4 we have:

$$(6) \quad p(i,\alpha) = \frac{\mu(C_i)}{\mu(B)},\ i = 1,2,\dots,4,$$

where μ is the Lebesgue measure in the Euclidean plane. We can compute the previous measures using the elementary kinematic measure of Poincaré [7]

$$dK = dx \wedge dy \wedge d\varphi,$$

where x, y are the coordinate of B_S. Taking into account the symmetries we have

$$(7) \quad \mu(B) = \int_0^{\frac{\pi}{3}} d\varphi \iint_{(x,y)\in P} dxdy = \frac{\pi}{3}\frac{ab}{sin\alpha}.$$

We distinguish four intervals: $0 \le \varphi \le \frac{\pi}{2} - \alpha$; $\frac{\pi}{2} - \alpha \le \varphi \le \frac{\pi}{6}$; $\frac{\pi}{6} \le \varphi \le \frac{2\pi}{3} - \alpha$; $\frac{2\pi}{3} - \alpha \le \varphi \le \frac{\pi}{3}$, as in figure 2, 3, 4 and 5, respectively.

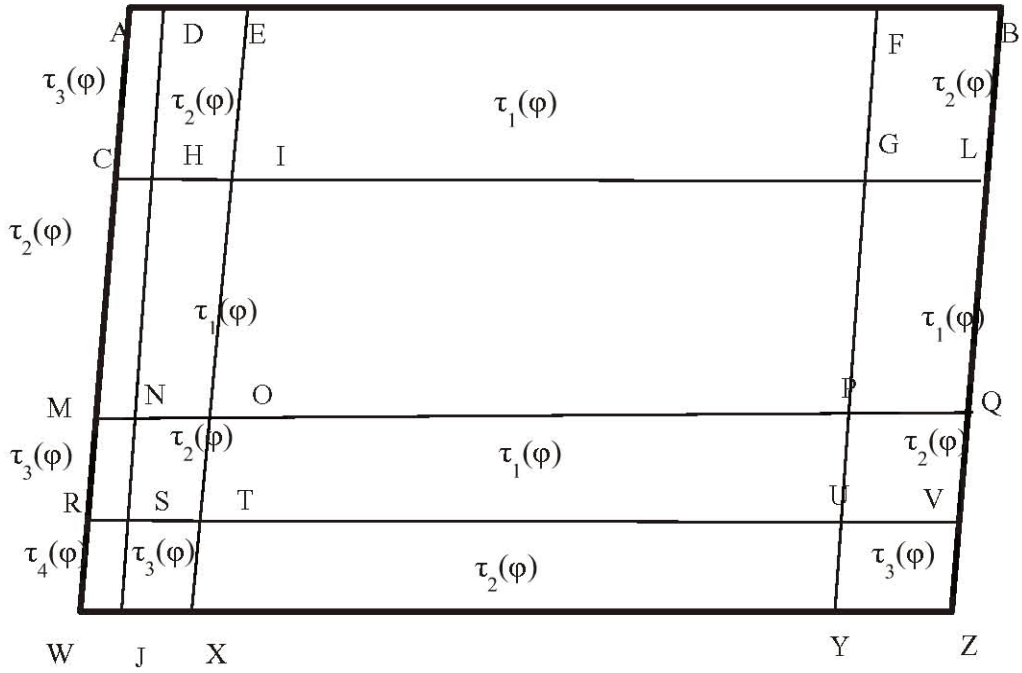


Fig. 2

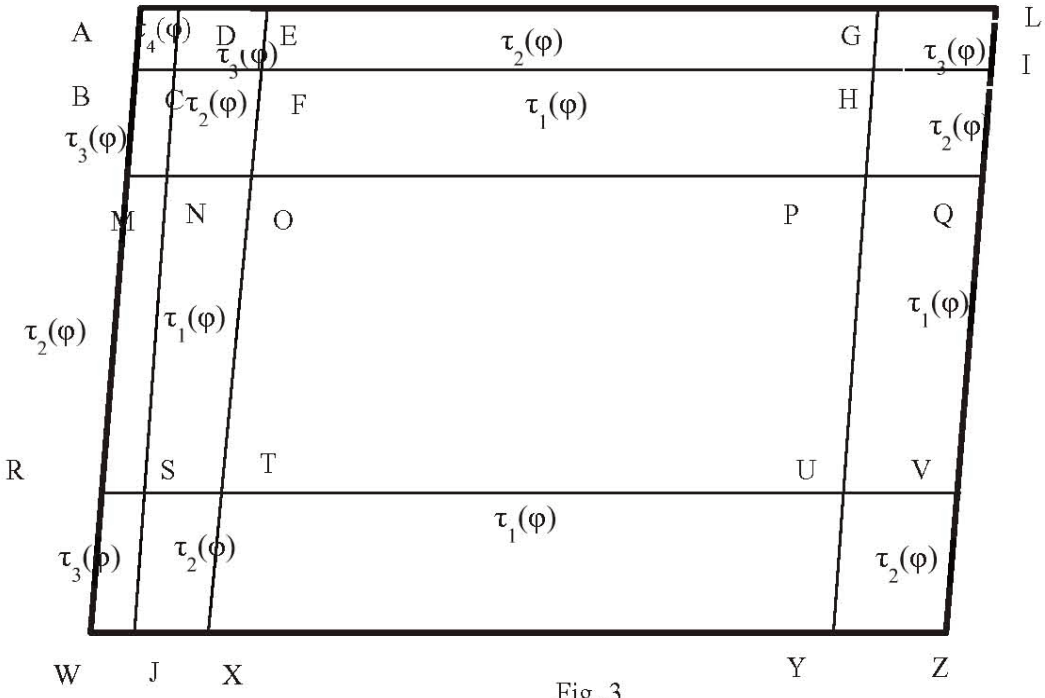

A
B
C
D
E
F
G
H
I
L
M
N
O
P
Q
R
S
T
U
V
W
J
X
Y
Z
$\tau_1(\varphi)$
$\tau_2(\varphi)$
$\tau_3(\varphi)$
$\tau_4(\varphi)$

Fig. 3

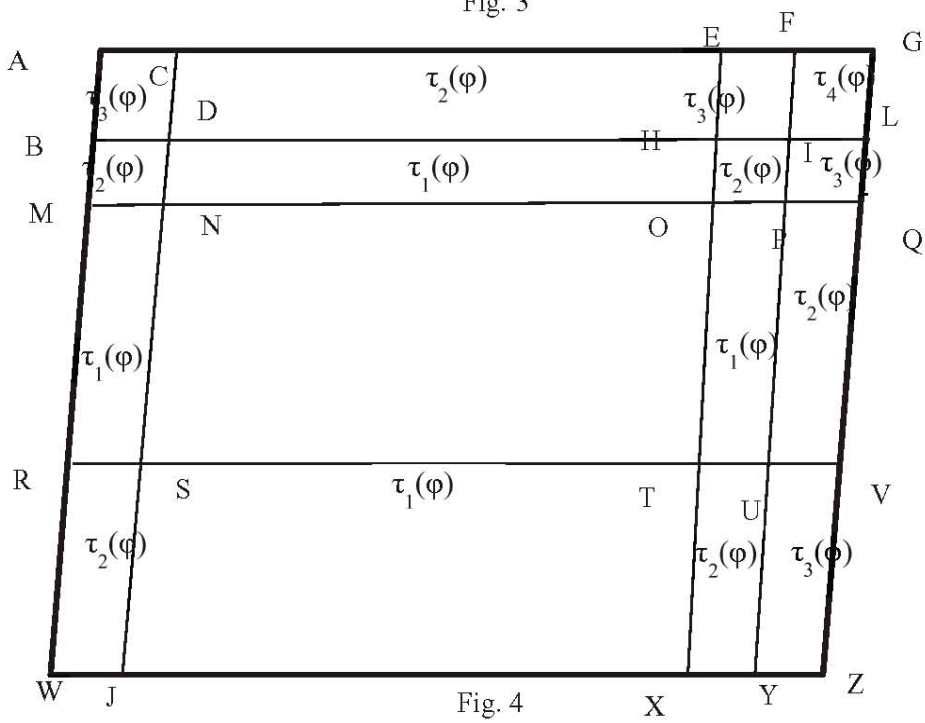

A
B
C
D
E
F
G
H
I
L
M
N
O
P
Q
R
S
T
U
V
W
J
X
Y
Z
$\tau_1(\varphi)$
$\tau_2(\varphi)$
$\tau_3(\varphi)$
$\tau_4(\varphi)$

Fig. 4

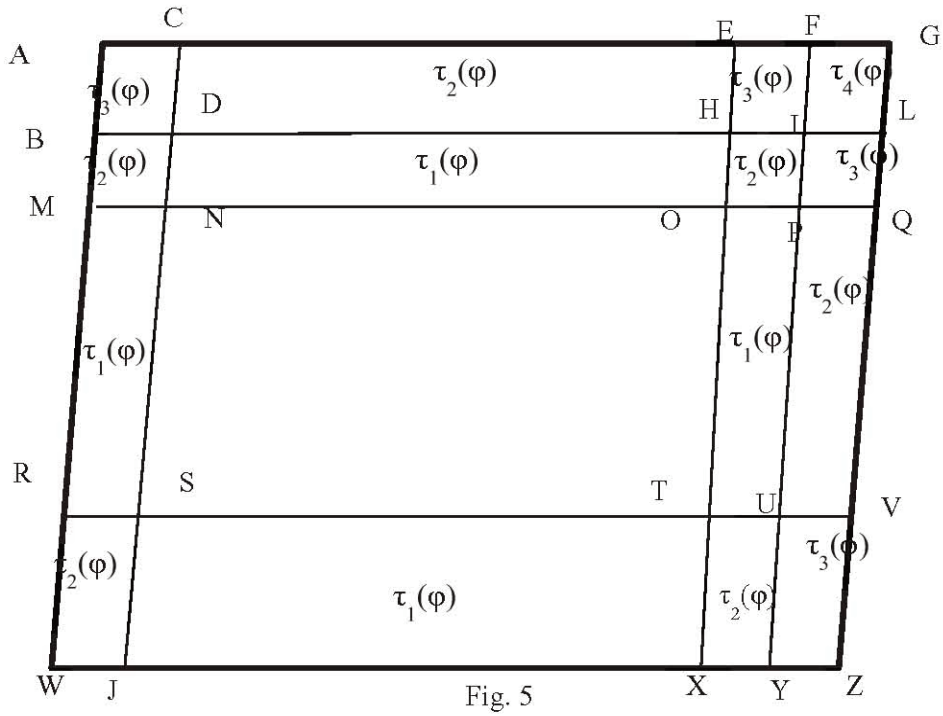


Fig. 5

In order to compute $\mu(C_1)$ we observe that for $0 \le \varphi \le \frac{\pi}{2} - \alpha$, as in figure 2, $\tau_1(\varphi)$ is union of the parallelogram EFGI, of side EI=$\ell\left(\frac{1}{2}cos\varphi cot\alpha - \frac{1}{2}sin\varphi + \frac{\sqrt{3}}{2}cos\varphi + \frac{\sqrt{3}}{2}sin\varphi cot\alpha\right)$ and height $h = a - \frac{\sqrt{3}}{2}\ell sin\varphi - \frac{3}{2}\ell cos\varphi$, the parallelogram OPUT of side OT=$\ell\left(-\frac{3}{2}cos\varphi cot\alpha + \frac{3}{2}sin\varphi + \frac{\sqrt{3}}{2}cos\varphi + \frac{\sqrt{3}}{2}sin\varphi cot\alpha\right)$ and height h, the parallelogram HION of side HN=$\frac{b}{sin\alpha}$-$\ell\sqrt{3}cos\varphi - \sqrt{3}\ell sin\varphi cot\alpha$ and height $h_1 = \sqrt{3}\ell sin\varphi$, and the parallelogram GLQP side GP=HN and height $h_2 = \ell cos\varphi$. Therefore

Area $\tau_1(\varphi)$= $\ell\left(-cos\varphi cot\alpha + sin\varphi + \sqrt{3}cos\varphi + \sqrt{3}sin\varphi cot\alpha\right)\left(a - \frac{\sqrt{3}}{2}\ell sin\varphi - \frac{3}{2}\ell cos\varphi\right) + \left(\frac{b}{sin\alpha} - \ell\sqrt{3}cos\varphi - \sqrt{3}\ell sin\varphi cot\alpha\right)\left(\sqrt{3}\ell sin\varphi + \ell cos\varphi\right)$.

For $\frac{\pi}{2} - \alpha \le \varphi \le \frac{\pi}{6}$, as in figure 3, $\tau_1(\varphi)$ is union of the parallelogram FHPO, of side FO=$\frac{3}{2}\ell cos\varphi cot\alpha - \frac{3}{2}\ell sin\varphi + \frac{\sqrt{3}}{2}\ell cos\varphi + \frac{\sqrt{3}}{2}\ell sin\varphi cot\alpha$ and height $h = a - \frac{\sqrt{3}}{2}\ell sin\varphi - \frac{3}{2}\ell cos\varphi$, the parallelogram TUYX of side

TX=$-\frac{1}{2}\ell cos\varphi cot\alpha+\frac{1}{2}\ell sin\varphi+\frac{\sqrt{3}}{2}\ell cos\varphi+\frac{\sqrt{3}}{2}\ell sin\varphi cot\alpha$ and height h, the parallelogram PQVU of side PU=$\frac{b}{sin\alpha}$-$\sqrt{3}\ell cos\varphi-\sqrt{3}\ell sin\varphi cot\alpha$ and height $h_2=\ell(cos\varphi)$, and the parallelogram NOTS of side NS=PU and height $h_1=\sqrt{3}\ell sin\varphi$. Therefore:

Area $\tau_1(\varphi)$= $\ell\left(+cos\varphi cot\alpha-sin\varphi+\sqrt{3}cos\varphi+\sqrt{3}sin\varphi cot\alpha\right)\left(a-\frac{\sqrt{3}}{2}\ell sin\varphi-\frac{3}{2}\ell cos\varphi\right)+\left(\frac{b}{sin\alpha}-\sqrt{3}\ell cos\varphi-\sqrt{3}\ell sin\varphi cot\alpha\right)\ell\left(\sqrt{3}sin\varphi+cos\varphi\right)$.

For $\frac{\pi}{6}\leq\varphi\leq\frac{2\pi}{3}-\alpha$, as in figure 4, $\tau_1(\varphi)$ is union of the parallelogram DHON, of side DN=$\frac{3}{2}\ell cos\varphi cot\alpha-\frac{3}{2}\ell sin\varphi+\frac{\sqrt{3}}{2}\ell cos\varphi+\frac{\sqrt{3}}{2}\ell sin\varphi cot\alpha$ and height $h=a-\frac{\sqrt{3}}{2}\ell sin\varphi-\frac{3}{2}\ell cos\varphi$, the parallelogram STXJ of side SJ=$-\frac{1}{2}\ell cos\varphi cot\alpha+\frac{1}{2}\ell sin\varphi+\frac{\sqrt{3}}{2}\ell cos\varphi+\frac{\sqrt{3}}{2}\ell sin\varphi cot\alpha$ and height h, the parallelogram OPUT of side OT=$\frac{b}{sin\alpha}$-$\sqrt{3}\ell cos\varphi-\sqrt{3}\ell sin\varphi cot\alpha$ and height $h_3=\ell\left(\frac{3}{2}cos\varphi-\frac{\sqrt{3}}{2}sin\varphi\right)$, and the parallelogram NSRM of side NS=OT and height $h_4=\ell\left(\frac{1}{2}cos\varphi+\frac{\sqrt{3}}{2}sin\varphi\right)$. Therefore:

Area $\tau_1(\varphi)$= $\ell\left(cos\varphi cot\alpha-sin\varphi+\sqrt{3}cos\varphi+\sqrt{3}sin\varphi cot\alpha\right)\left(a-\frac{\sqrt{3}}{2}\ell sin\varphi-\frac{3}{2}\ell cos\varphi\right)+\left(\frac{b}{sin\alpha}-\sqrt{3}\ell cos\varphi-\sqrt{3}\ell sin\varphi cot\alpha\right)(2\ell cos\varphi)$.

For $\frac{2\pi}{3}-\alpha\leq\varphi\leq\frac{\pi}{3}$, as in figure 5, $\tau_1(\varphi)$ is union of the parallelogram DHON, of side DN=$-\frac{3}{2}\ell cos\varphi cot\alpha+\frac{3}{2}\ell sin\varphi-\frac{\sqrt{3}}{2}\ell cos\varphi-\frac{\sqrt{3}}{2}\ell sin\varphi cot\alpha$ and height $h=a-\frac{\sqrt{3}}{2}\ell sin\varphi-\frac{3}{2}\ell cos\varphi$, the parallelogram STXJ of side SJ=$-\frac{1}{2}\ell cos\varphi cot\alpha+\frac{1}{2}\ell sin\varphi+\frac{\sqrt{3}}{2}\ell cos\varphi+\frac{\sqrt{3}}{2}\ell sin\varphi cot\alpha$ and height h, the parallelogram OPUT of side OT=$\frac{b}{sin\alpha}$+$\frac{3}{2}\ell cos\varphi cot\alpha-\frac{3}{2}\ell sin\varphi-\frac{\sqrt{3}}{2}\ell cos\varphi-\frac{\sqrt{3}}{2}\ell sin\varphi cot\alpha$ and height $h_3=\ell\left(\frac{3}{2}cos\varphi-\frac{\sqrt{3}}{2}sin\varphi\right)$, and the parallelogram NSRM of side NS=OT and height $h_4=\ell\left(\frac{1}{2}cos\varphi+\frac{\sqrt{3}}{2}sin\varphi\right)$. Therefore:

Area $\tau_1(\varphi)$= $\ell(-2cos\varphi cot\alpha+2sin\varphi)\left(a-\frac{\sqrt{3}}{2}\ell sin\varphi-\frac{3}{2}\ell cos\varphi\right)+\left(\frac{b}{sin\alpha}+\frac{3}{2}\ell cos\varphi cot\alpha-\frac{3}{2}\ell sin\varphi-\frac{\sqrt{3}}{2}\ell cos\varphi-\frac{\sqrt{3}}{2}\ell sin\varphi cot\alpha\right)(2\ell cos\varphi)$.

Hence, integrating Area $\tau_1(\varphi)$ in the respective intervals we have:

$$\mu(C_1) = \frac{1}{6}\frac{\ell\left(12\left(-1+\sqrt{3}\right)(a+b) + 3\ell\left(2\sqrt{3} - 3\pi + 6\alpha\right)cos\alpha - \ell\left(18 + 5\sqrt{3}\pi - 6\sqrt{3}\alpha\right)sin\alpha\right)}{sin\alpha},$$

And by formulas (6) and (7) we obtain the probability (2).

In order to compute $\mu(C_2)$ we observe that for $0 \le \varphi \le \frac{\pi}{2} - \alpha$, as in figure 2, $\tau_2(\varphi)$ is union of the parallelogram DEHI, of side DH=EI=$\ell\left(\frac{1}{2}cos\varphi cot\alpha - \frac{1}{2}sin\varphi + \frac{\sqrt{3}}{2}cos\varphi + \frac{\sqrt{3}}{2}sin\varphi cot\alpha\right)$ and height $h_1 = \sqrt{3}\ell sin\varphi$, , the parallelogram FBLG of side FG=DH and height $h_2 = \ell cos\varphi$, the parallelogram CHNM of side CM=HN= $\frac{b}{sin\alpha}$-$\ell\sqrt{3}cos\varphi - \sqrt{3}\ell sin\varphi cot\alpha$ and height $h_5 = \ell\left(\frac{1}{2}cos\varphi - \frac{\sqrt{3}}{2}sin\varphi\right)$, the parallelogram NOTS of side NS=OT=$\ell\left(-\frac{3}{2}cos\varphi cot\alpha + \frac{3}{2}sin\varphi + \frac{\sqrt{3}}{2}cos\varphi + \frac{\sqrt{3}}{2}sin\varphi cot\alpha\right)$ and height and height $h_1 = \sqrt{3}\ell sin\varphi$, the parallelogram PQVU of side PU=NS and height $h_2 = \ell cos\varphi$, and the parallelogram TUYX of side TX= $\ell cos\varphi cot\alpha - \ell sin\alpha$ and height $h = a - \frac{\sqrt{3}}{2}\ell sin\varphi - \frac{3}{2}\ell cos\varphi$. Therefore

Area $\tau_2(\varphi)$=$\ell\left(-cos\varphi cot\alpha + sin\varphi + \sqrt{3}cos\varphi + \sqrt{3}sin\varphi cot\alpha\right)\left(\ell cos\varphi + \sqrt{3}\ell sin\varphi\right) + \ell(cos\varphi cot\alpha - sin\varphi)\left(a - \frac{\sqrt{3}}{2}\ell sin\varphi - \frac{3}{2}\ell cos\varphi\right) + \left(\frac{b}{sin\alpha} - \ell\sqrt{3}cos\varphi - \sqrt{3}\ell sin\varphi cot\alpha\right)\left(\ell\frac{1}{2}cos\varphi - \frac{\sqrt{3}}{2}\ell sin\varphi\right)$.

For $\frac{\pi}{2} - \alpha \le \varphi \le \frac{\pi}{6}$, as in figure 3, $\tau_2(\varphi)$ is union of the parallelogram EGHF, of side EF=$-\ell cos\varphi cot\alpha + \ell sin\varphi$ and height $h = a - \frac{\sqrt{3}}{2}\ell sin\varphi - \frac{3}{2}\ell cos\varphi$, the parallelogram CFON of side FO=$\frac{3}{2}\ell cos\varphi cot\alpha - \frac{3}{2}\ell sin\varphi + \frac{\sqrt{3}}{2}\ell cos\varphi + \frac{\sqrt{3}}{2}\ell sin\varphi cot\alpha$ and height $h_1 = \sqrt{3}\ell sin\varphi$, the parallelogram HIQP of side HP=FO, the parallelogram STYJ of side TX=$-\frac{1}{2}\ell cos\varphi cot\alpha + \frac{1}{2}\ell sin\varphi + \frac{\sqrt{3}}{2}\ell cos\varphi + \frac{\sqrt{3}}{2}\ell sin\varphi cot\alpha$ and height $h_1 = \sqrt{3}\ell sin\varphi$, the parallelogram UVZY of side UY=TX and height $h_2 = \ell(cos\varphi)$, and the parallelogram MNSR of side MS=PU= $\frac{b}{sin\alpha}$-$\sqrt{3}\ell cos\varphi - \sqrt{3}\ell sin\varphi cot\alpha$ and height $h_5 = \ell\left(\frac{1}{2}cos\varphi - \frac{\sqrt{3}}{2}sin\varphi\right)$. Therefore:

Area $\tau_2(\varphi)$= $\ell(-cos\varphi cot\alpha + sin\varphi)\left(a - \frac{\sqrt{3}}{2}\ell sin\varphi - \frac{3}{2}\ell cos\varphi\right) + \left(\frac{b}{sin\alpha} - \sqrt{3}\ell cos\varphi - \sqrt{3}\ell sin\varphi cot\alpha\right)\ell\left(\frac{1}{2}cos\varphi - \frac{\sqrt{3}}{2}sin\varphi\right) + \ell\left(cos\varphi cot\alpha - sin\varphi + \sqrt{3}cos\varphi + \sqrt{3}sin\varphi cot\alpha\right)\left(\ell cos\varphi + \sqrt{3}\ell sin\varphi\right)$.

For $\frac{\pi}{6} \leq \varphi \leq \frac{2\pi}{3} - \alpha$, as in figure 4, $\tau_2(\varphi)$ is union of the parallelogram CEHD, of side CD=$\ell sin\varphi - \ell cos\varphi cot\alpha$ and height $h = a - \frac{\sqrt{3}}{2}\ell sin\varphi - \frac{3}{2}\ell cos\varphi$, the parallelogram BDNM of side DN=$\frac{3}{2}\ell cos\varphi cot\alpha - \frac{3}{2}\ell sin\varphi + \frac{\sqrt{3}}{2}\ell cos\varphi + \frac{\sqrt{3}}{2}\ell sin\varphi cot\alpha$ and height $h_4 = \ell\left(\frac{1}{2}cos\varphi + \frac{\sqrt{3}}{2}sin\varphi\right)$, the parallelogram HIPO of side HO=DN and height $h_3 = \ell\left(\frac{3}{2}cos\varphi - \frac{\sqrt{3}}{2}sin\varphi\right)$, the parallelogram PQVU of side PU=OT= $\frac{b}{sin\alpha}$-$\sqrt{3}\ell cos\varphi - \sqrt{3}\ell sin\varphi cot\alpha$ and height $h_5 = \ell\left(\frac{1}{2}cos\varphi - \frac{\sqrt{3}}{2}sin\varphi\right)$, the parallelogram RSJW of side RW= SJ=$-\frac{1}{2}\ell cos\varphi cot\alpha + \frac{1}{2}\ell sin\varphi + \frac{\sqrt{3}}{2}\ell cos\varphi + \frac{\sqrt{3}}{2}\ell sin\varphi cot\alpha$ and height $h_4 = \ell\left(\frac{1}{2}cos\varphi + \frac{\sqrt{3}}{2}sin\varphi\right)$ and the parallelogram TUYX of side TU= SJ and height $h_3 = \ell\left(\frac{3}{2}cos\varphi - \frac{\sqrt{3}}{2}sin\varphi\right)$. Therefore:

Area $\tau_2(\varphi)$= $\ell(sin\varphi - cos\varphi cot\alpha)\left(a - \frac{\sqrt{3}}{2}\ell sin\varphi - \frac{3}{2}\ell cos\varphi\right) + \left(\frac{b}{sin\alpha} - \sqrt{3}\ell cos\varphi - \sqrt{3}\ell sin\varphi cot\alpha\right)\ell\left(\frac{\sqrt{3}}{2}sin\varphi - \frac{1}{2}cos\varphi\right) + 2\ell cos\varphi\left(\ell cos\varphi cot\alpha - \ell sin\varphi + \sqrt{3}\ell cos\varphi + \sqrt{3}\ell sin\varphi cot\alpha\right)$.

For $\frac{2\pi}{3} - \alpha \leq \varphi \leq \frac{\pi}{3}$, as in figure 5, $\tau_2(\varphi)$ is union of the parallelogram CEHD, of side CD= $=\frac{1}{2}\ell cos\varphi cot\alpha - \frac{1}{2}\ell sin\varphi + \frac{\sqrt{3}}{2}\ell cos\varphi + \frac{\sqrt{3}}{2}\ell sin\varphi cot\alpha$ and height $h = a - \frac{\sqrt{3}}{2}\ell sin\varphi - \frac{3}{2}\ell cos\varphi$, the parallelogram BDNM of side DN= $=-\frac{3}{2}\ell cos\varphi cot\alpha + \frac{3}{2}\ell sin\varphi - \frac{\sqrt{3}}{2}\ell cos\varphi - \frac{\sqrt{3}}{2}\ell sin\varphi cot\alpha$ and height $h_4 = \ell\left(\frac{1}{2}cos\varphi + \frac{\sqrt{3}}{2}sin\varphi\right)$, the parallelogram HIPO of side HO=DN and height $h_3 = \ell\left(\frac{3}{2}cos\varphi - \frac{\sqrt{3}}{2}sin\varphi\right)$, the parallelogram PQVU of side PU=OT = $\frac{b}{sin\alpha}+\frac{3}{2}\ell cos\varphi cot\alpha - \frac{3}{2}\ell sin\varphi - \frac{\sqrt{3}}{2}\ell cos\varphi - \frac{\sqrt{3}}{2}\ell sin\varphi cot\alpha$ and height $h_6 = \ell\left(\frac{\sqrt{3}}{2}sin\varphi - \frac{1}{2}cos\varphi\right)$, the parallelogram RSJW of side RW=SJ= $\frac{1}{2}\ell sin\varphi - \frac{1}{2}\ell cos\varphi cot\alpha + \frac{\sqrt{3}}{2}\ell cos\varphi + \frac{\sqrt{3}}{2}\ell sin\varphi cot\alpha$ and height $h_4 = \ell\left(\frac{1}{2}cos\varphi + \frac{\sqrt{3}}{2}sin\varphi\right)$ and the parallelogram TUYX of side TX=SJ and height $h_3 = \ell\left(\frac{3}{2}cos\varphi - \frac{\sqrt{3}}{2}sin\varphi\right)$. Therefore:

Area $\tau_2(\varphi)= \ell\left(-\frac{1}{2}\ell sin\varphi+\frac{1}{2}\ell cos\varphi cot\alpha+\frac{\sqrt{3}}{2}\ell cos\varphi+\frac{\sqrt{3}}{2}\ell sin\varphi cot\alpha\right)\left(a-\frac{\sqrt{3}}{2}\ell sin\varphi-\frac{3}{2}\ell cos\varphi\right)+\left(\frac{b}{sin\alpha}+\frac{3}{2}\ell cos\varphi cot\alpha-\frac{3}{2}\ell sin\varphi-\frac{\sqrt{3}}{2}\ell cos\varphi-\frac{\sqrt{3}}{2}\ell sin\varphi cot\alpha\right)\ell\left(\frac{\sqrt{3}}{2}sin\varphi-\frac{1}{2}cos\varphi\right)+(2\ell cos\varphi)(\ell sin\varphi-\ell cos\varphi cot\alpha).$

Hence, integrating in the respective intervals we have:

$$\mu(C_2)=\frac{1}{3}\frac{\ell\left(-3(-2+\sqrt{3})(a+b)-3\ell(3\sqrt{3}-\pi+2\alpha)cos\alpha+\ell(6+4\sqrt{3}\pi-9\sqrt{3}\alpha)sin\alpha\right)}{sin\alpha},$$

and by formulas (6) and (7) we obtain the probability (3).

In order to compute $\mu(C_3)$ we observe that for $0\le\varphi\le\frac{\pi}{2}-\alpha$, as in figure 2, $\tau_3(\varphi)$ is union of the parallelogram ADHC, of side DH=EI=$\ell\left(\frac{1}{2}cos\varphi cot\alpha-\frac{1}{2}sin\varphi+\frac{\sqrt{3}}{2}cos\varphi+\frac{\sqrt{3}}{2}sin\varphi cot\alpha\right)$ and height $h_5=\ell\left(\frac{1}{2}cos\varphi-\frac{\sqrt{3}}{2}sin\varphi\right)$ the parallelogram MNSR of side NS=OT=$\ell\left(-\frac{3}{2}cos\varphi cot\alpha+\frac{3}{2}sin\varphi+\frac{\sqrt{3}}{2}cos\varphi+\frac{\sqrt{3}}{2}sin\varphi cot\alpha\right)$ and height , $h_5=\ell\left(\frac{1}{2}cos\varphi-\frac{\sqrt{3}}{2}sin\varphi\right)$, the parallelogram STXJ of side SJ = TX= $\ell cos\varphi cot\alpha-\ell sin\alpha$ and height $h_1=\sqrt{3}\ell sin\varphi$ and the parallelogram UVZY side UY=TX and height $h_2=\ell cos\varphi$. Therefore
Area $\tau_3(\varphi)= \ell\left(-cos\varphi cot\alpha+sin\varphi+\sqrt{3}cos\varphi+\sqrt{3}sin\varphi cot\alpha\right)\left(\frac{1}{2}\ell cos\varphi-\frac{\sqrt{3}}{2}\ell sin\varphi\right)+(\ell cos\varphi cot\alpha-\ell sin\varphi)\left(\sqrt{3}\ell sin\varphi+\ell cos\varphi\right).$
For $\frac{\pi}{2}-\alpha\le\varphi\le\frac{\pi}{6}$, as in figure 3, $\tau_3(\varphi)$ is union of the parallelogram DEFC of side EF=$\ell sin\varphi-\ell cos\varphi cot\alpha$ and height $h_1=\sqrt{3}\ell sin\varphi$, the parallelogram GLIH of side GH=EF and height $h_2=\ell(cos\varphi)$, the parallelogram BCNM of side CN=FO=$\frac{3}{2}\ell cos\varphi cot\alpha-\frac{3}{2}\ell sin\varphi+\frac{\sqrt{3}}{2}\ell cos\varphi+\frac{\sqrt{3}}{2}\ell sin\varphi cot\alpha$ and height $h_5=\ell\left(\frac{1}{2}cos\varphi-\frac{\sqrt{3}}{2}sin\varphi\right)$, and the parallelogram RSJW of side SJ=TX= $-\frac{1}{2}\ell cos\varphi cot\alpha+\frac{1}{2}\ell sin\varphi+\frac{\sqrt{3}}{2}\ell cos\varphi+\frac{\sqrt{3}}{2}\ell sin\varphi cot\alpha$ and height h_5.
Therefore:
Area $\tau_3(\varphi)= (\ell sin\varphi-\ell cos\varphi cot\alpha)\ell\left(\sqrt{3}sin\varphi+cos\varphi\right)+\ell\left(\frac{1}{2}cos\varphi-\frac{\sqrt{3}}{2}sin\varphi\right)+\left(\ell cos\varphi cot\alpha-\ell sin\varphi+\sqrt{3}\ell cos\varphi+\sqrt{3}\ell sin\varphi cot\alpha\right).$
For $\frac{\pi}{6}\le\varphi\le\frac{2\pi}{3}-\alpha$, as in figure 4, $\tau_3(\varphi)$ is union of the parallelogram ACDB, of side AB=$\ell sin\varphi-\ell cos\varphi cot\alpha$ and height $h_4=\ell\left(\frac{1}{2}cos\varphi+\frac{\sqrt{3}}{2}sin\varphi\right)$, the

parallelogram EFIH of side EH=AB and height $h_3 = \ell\left(\frac{3}{2}cos\varphi - \frac{\sqrt{3}}{2}sin\varphi\right)$, the parallelogram ILQP of side IP = $=\frac{\sqrt{3}}{2}\ell cos\varphi + \frac{3}{2}\ell cos\varphi cot\alpha - \frac{3}{2}\ell sin\varphi + \frac{\sqrt{3}}{2}\ell sin\varphi cot\alpha$ and height $h_6 = \ell\left(\frac{\sqrt{3}}{2}sin\varphi - \frac{1}{2}cos\varphi\right)$, and the parallelogram UVZY of side UY=$-\frac{1}{2}\ell cos\varphi cot\alpha + \frac{1}{2}\ell sin\varphi + \frac{\sqrt{3}}{2}\ell cos\varphi + \frac{\sqrt{3}}{2}\ell sin\varphi cot\alpha$ and height h_6. Therefore:

Area $\tau_3(\varphi)$= $(\ell sin\varphi - \ell cos\varphi cot\alpha)2\ell cos\varphi + \ell\left(\frac{\sqrt{3}}{2}sin\varphi - \frac{1}{2}cos\varphi\right)$ $\left(\ell cos\varphi cot\alpha + \sqrt{3}\,\ell cos\varphi - \ell sin\varphi + \sqrt{3}\ell sin\varphi cot\alpha\right)$.

For $\frac{2\pi}{3} - \alpha \leq \varphi \leq \frac{\pi}{3}$, as in figure 5, $\tau_3(\varphi)$ is union of the parallelogram ACDB, of side CD=$\frac{1}{2}\ell cos\varphi cot\alpha - \frac{1}{2}\ell sin\varphi + \frac{\sqrt{3}}{2}\ell cos\varphi + \frac{\sqrt{3}}{2}\ell sin\varphi cot\alpha$ and height $h_4 = \ell\left(\frac{1}{2}cos\varphi + \frac{\sqrt{3}}{2}sin\varphi\right)$, the parallelogram EFIH of side EH=CD and height $h_3 = \ell\left(\frac{3}{2}cos\varphi - \frac{\sqrt{3}}{2}sin\varphi\right)$, the parallelogram ILQP of side IP= - $\frac{3}{2}\ell cos\varphi cot\alpha + \frac{3}{2}\ell sin\varphi - \frac{\sqrt{3}}{2}\ell cos\varphi - \frac{\sqrt{3}}{2}\ell sin\varphi cot\alpha$ and height $h_6 = \ell\left(\frac{\sqrt{3}}{2}sin\varphi - \frac{1}{2}cos\varphi\right)$, and the parallelogram UVZY of side UY=$-\frac{1}{2}\ell cos\varphi cot\alpha + \frac{1}{2}\ell sin\varphi + \frac{\sqrt{3}}{2}\ell cos\varphi + \frac{\sqrt{3}}{2}\ell sin\varphi cot\alpha$ and height h_6. Therefore:

$$\text{Area } \tau_3(\varphi) = \left(\frac{1}{2}\ell cos\varphi cot\alpha - \frac{1}{2}\ell sin\varphi + \frac{\sqrt{3}}{2}\ell cos\varphi + \frac{\sqrt{3}}{2}\ell sin\varphi cot\alpha\right)2\ell cos\varphi + \\ + (-2\ell cos\varphi cot\alpha + 2\ell sin\varphi)\ell\left(\frac{\sqrt{3}}{2}sin\varphi - \frac{1}{2}cos\varphi\right).$$

Hence, integrating Area $\tau_3(\varphi)$ in the respective intervals we have:

$$\mu(C_3) = \frac{1}{6}\frac{\ell\left(3\ell\left(6\sqrt{3} - \pi + 2\alpha\right)cos\alpha + \ell\left(-6 - 7\sqrt{3}\pi + 18\sqrt{3}\alpha\right)sin\alpha\right)}{sin\alpha},$$

And by formulas (6) and (7) we obtain the probability (4).

In order to compute $\mu(C_4)$ we observe that for $0 \leq \varphi \leq \frac{\pi}{2} - \alpha$, as in figure 2, $\tau_4(\varphi)$ is the parallelogram RSJW, of side RW= $\ell cos\varphi cot\alpha - \ell sin\alpha$ and height $h_5 = \ell\left(\frac{1}{2}cos\varphi - \frac{\sqrt{3}}{2}sin\varphi\right)$. Therefore

Area $\tau_4(\varphi)$= $(\ell cos\varphi cot\alpha - \ell sin\varphi)\ell\left(\frac{1}{2}cos\varphi - \frac{\sqrt{3}}{2}sin\varphi\right)$.

For $\frac{\pi}{2} - \alpha \leq \varphi \leq \frac{\pi}{6}$, as in figure 3, $\tau_4(\varphi)$ is the parallelogram ADCB of side AB=$\ell sin\varphi - \ell cos\varphi cot\alpha$ and height $h_5 = \ell\left(\frac{1}{2}cos\varphi - \frac{\sqrt{3}}{2}sin\varphi\right)$. Therefore:

Area $\tau_4(\varphi)$= $(\ell sin\varphi - \ell cos\varphi cot\alpha\ )\ell\left(\frac{1}{2}cos\varphi - \frac{\sqrt{3}}{2}sin\varphi\right)$.

For $\frac{\pi}{6} \leq \varphi \leq \frac{2\pi}{3} - \alpha$, as in figure 4, $\tau_4(\varphi)$ is the parallelogram FGLI, of side FI=AB=$\ell sin\varphi - \ell cos\varphi cot\alpha$ and height $h_5 = \ell\left(\frac{1}{2}cos\varphi - \frac{\sqrt{3}}{2}sin\varphi\right)$.

Therefore:

Area $\tau_4(\varphi)$= $(\ell sin\varphi - \ell cos\varphi cot\alpha\ )\ell\left(\frac{1}{2}cos\varphi - \frac{\sqrt{3}}{2}sin\varphi\right)$.

For $\frac{2\pi}{3} - \alpha \leq \varphi \leq \frac{\pi}{3}$, as in figure 5, $\tau_4(\varphi)$ is the parallelogram FGLI, of side FI=$\frac{1}{2}\ell cos\varphi cot\alpha - \frac{1}{2}\ell sin\varphi + \frac{\sqrt{3}}{2}\ell cos\varphi + \frac{\sqrt{3}}{2}\ell sin\varphi cot\alpha$ and height $h_5 = \ell\left(\frac{1}{2}cos\varphi - \frac{\sqrt{3}}{2}sin\varphi\right)$. Therefore:

Area $\tau_4(\varphi)$= $\left(\frac{1}{2}\ell cos\varphi cot\alpha - \frac{1}{2}\ell sin\varphi + \frac{\sqrt{3}}{2}\ell cos\varphi + \frac{\sqrt{3}}{2}\ell sin\varphi cot\alpha\right)$ $\ell\left(\frac{1}{2}cos\varphi - \frac{\sqrt{3}}{2}sin\varphi\right)$.

Hence, integrating Area $\tau_4(\varphi)$ in the respective intervals we have:

$$\mu(C_4) = \frac{1}{12}\frac{\ell^2\left((3\pi - 12\sqrt{3} - 6\alpha)cos\alpha + (6 + 5\sqrt{3}\pi - 12\sqrt{3}\alpha)sin\alpha\right)}{sin\alpha},$$

And by formulas (6) and (7) we obtain the probability (5).

By (2), (3), (4) and (5) we obtain (1).

Remark For α=$\frac{\pi}{2}$, we obtain

$$p(0,\alpha) = 1 - \left(\frac{3\sqrt{3}}{\pi}(\lambda + \mu) - \frac{3}{4\pi}\lambda\mu\left(6 + \sqrt{3}\,\pi\right)\right)$$

$$p(1,\alpha) = \frac{6}{\pi}\left(\sqrt{3} - 1\right)(\lambda + \mu) - \frac{\lambda\mu}{2\pi}\left(5\sqrt{3}\pi + 18 - 6\sqrt{3}\alpha\right)$$

$$p(2,\alpha) = \frac{3}{\pi}\left(2 - \sqrt{3}\right)(\lambda + \mu) + \frac{\lambda\mu}{\pi}\left(4\sqrt{3}\pi + 6 - 9\sqrt{3}\alpha\right)$$

$$p(3,\alpha) = -\frac{\lambda\mu}{2\pi}\left(7\sqrt{3}\pi + 6 - 18\sqrt{3}\alpha\right)$$

$$\mathrm{p}(4,\alpha)=\frac{\lambda\mu}{4\pi}\left(5\sqrt{3}\pi+6-12\sqrt{3}\alpha\right).$$

the same results contained in [2] and [3].

Acknowledgements

The author would like to thank Prof. U. Bäsel for his helpful suggestions and for several discussions on the subject of the present paper.

References

[1] U. Bäsel, *Buffon's problem with a star of needles*, VI International Conference "Stochastic geometry, convex bodies, empirical measures and applications to mechanics and engineering of train transport", Milazzo, 2007.
[2] U. Bäsel, *Buffon's problem with a star of needles and a lattice of rectangles,* FernUniversität Hagen, Seminarberichte Band, 79, 2008, 1-11.
[3] U. Bäsel, V. Bonanzinga, L. Fiorino, *Buffon's problem with a star of needles and a lattice of rectangles II,* Communications to SIMAI Congress, Vol. 3, 2009, 1-7.
[4] U. Bäsel, *Buffon's problem with a star of needles and a lattice of rectangles III,* FernUniversität Hagen, Seminarberichte Band, 81 (2008), 69-74.
[5] A. Duma, M. Stoka, *Geometrische Wahrscheinlichkeiten für Hindernisse und nicht-konvexe Testkörper in der Ebene*, FernUniversität Hagen, Seminarberichte Band, 78 (2007), 37-51.
[6] U. Bäsel, *Geometrische Wahrscheinlichkeiten für Nadelsterne und Parallelogrammgitter*, FernUniversität Hagen, Seminarberichte Band 83, 2010, 29-48.
[7] H. Poincaré, *Calculus des probabilitiés*, ed. 2, Carré, Paris, 1912.

Vittoria BONANZINGA
University of Reggio Calabria
Faculty of Engineering – DIMET
Via Graziella (Feo di Vito)
vittoria.bonanzinga@unirc.it
vittoria.bonanzinga@tin.it

RENDICONTI DEL CIRCOLO MATEMATICO DI PALERMO
Serie II, Suppl. 84 (2012), pp. 81-90

A Note on Bayesian Prediction

Denis Bosq

Université Pierre et Marie Curie, Paris 6, France

Abstract

This paper deals with Bayesian prediction for stochastic processes. We give two equivalent definitions of a Bayesian predictor and study some simple properties. We derive some results, especially if the best predictor has a specific decomposition and we provide some examples.

Keywords : Bayesian prediction, unbiasedness, sufficiency

AMS classification : 62F15, 62M20

1 Introduction

Many papers are devoted to Bayesian estimation, but Bayesian prediction does not appear very much in statistical literature. However this topic is very important, especially if the number of observations is small.

In this short Note we study some properties of Bayesian predictors and give some examples.

First, we recall some general results concerning Statistical prediction (Section 2). In Section 3 we give two definitions of a Bayesian predictor and we note that it is always function of a P-sufficient statistic. Section 4 deals with the special case where the variable to predict is independent from the data. In Section 5 we specify the form of the Bayesian predictor if the best predictor has a special but rather general form. Finally, in Section 6, we try to answer the question of unbiasedness for a Bayesian predictor.

In addition, we study some examples of Bayesian predictors and compare them with classical predictors.

2 Statistical Prediction

Consider a random vector $Z = (X, Y)$ with values in the measurable space $(E \times \mathbb{R}, \mathcal{B} \otimes \mathcal{B}_{\mathbb{R}})$, where $\mathcal{B}$ is a $\sigma-$algebra over E and $\mathcal{B}_{\mathbb{R}}$ is the $\sigma-$algebra of Borel sets. The distribution P_θ of Z depends on an unknown parameter $\theta \in \Theta$ and $\mathcal{T}$ denotes a $\sigma-$algebra over Θ. X is supposed to be observed when Y is not observed, and one wants to predict Y given X.

A *Statistical predictor* of Y is a real random variable $p(X)$ where p is known. Now, if Y and $p(X)$ are square integrable for every θ in Θ, we have

$$E_\theta(p(X)-Y)^2 = E_\theta(p(X)-E_\theta(Y|X))^2 + E_\theta(E_\theta(Y|X)-Y)^2, \theta \in \Theta, \quad (2.1)$$

where, as usual, E_θ denotes expectation and $E_\theta(.|.)$ conditional expectation if Z has distribution P_θ.

It follows that, with respect to the quadratic risk, a predictor $p_1(X)$ is preferable to the predictor $p_2(X)$ if and only if

$$E_\theta(p_1(X)-E_\theta(Y|X))^2 \leq E_\theta(p_2(X)-E_\theta(Y|X))^2, \theta \in \Theta. \quad (2.2)$$

Thus, one may say that "predict Y " is equivalent to "predict $E_\theta(Y|X)$". In the following, we set

$$m(X,\theta) = E_\theta(Y|X).$$

Now, in order to obtain accurate predictions, it is necessary to use predictors that are function of a sufficient statistic. In the context of forecasting, the definition of such a statistic is rather restrictive :

Definition 2.1. A statistic $S(X)$ is said to be sufficient for predicting Y (or P-sufficient for Y) if

1. $S(X)$ is a sufficient statistic,
2. X and Y are conditionaly independent given $S(X)$.

Another interesting property is unbiasedness :

Definition 2.2. Suppose that $p(X)$ and Y are integrable. Then, $p(X)$ is said to be unbiased if

$$E_\theta p(X) = E_\theta Y, \ \theta \in \Theta.$$

Using these definitions we obtain conditions for optimality :

Proposition 2.1. *Let $p(X)$ be a square integrable unbiased predictor of Y and let $S(X)$ be a complete P-sufficient statistic. Then $E_\theta(p(X)|S(X))$ does not depend on θ and is the unique unbiased optimal predictor of Y (P_θ a.s. for all θ).*

Proof of the above result and other properties of statistical predictors appear in Bosq and Blanke [2007]. Here we only present an example :

Example 2.1. (Predicting a Poisson process)

Let $(N_t, t \geq 0)$ be an homogeneous Poisson process with intensity θ. One observes $(N_t, 0 \leq t \leq s)$ and wants to predict $N_{s+h}(s>0, h>0)$.Then N_s is a complete P-sufficient statistic and the unbiased predictor

$$p(N_s) = \frac{s+h}{s} N_s \tag{2.3}$$

is optimal for predicting N_{s+h}.

The quadratic error with respect to N_{s+h} is

$$E_\theta(N_{s+h} - p(N_s))^2 = \theta h(1 + \frac{h}{s})$$

when the quadratic error with respect to $E_\theta(N_{s+h}|N_s)$ is given by

$$E_\theta(\theta h + N_s - p(N_s))^2 = \frac{\theta h^2}{s}. \tag{2.4}$$

3 Bayesian predictors

In the Bayesian framework, one considers a random variable T with values in the measurable space $(\Theta,\mathcal{T})$. The distribution of (X,Y,T) has the form $f(x,y,\theta)d\lambda(x)d\mu(y)d\tau(\theta)$, where λ and μ are $\sigma-$finite measures and τ is the distribution of T, supposed to be non-degenerated. We assume that $f(x,y,\theta)$ is strictly positive for every (x,y,θ). In the following, expectations and conditional expectations with respect to (X,Y,T) will be denoted $E(.)$ or $E(.|.)$. Finally we suppose square integrability of $p(X)$ and Y with respect to E and $E_\theta, \theta \in \Theta$.

Now the quadratic Bayesian risk is given by

$$r(Y,p(X)) = \int_\Theta E_\theta(p(X) - Y)^2 d\tau(\theta) = E(p(X) - Y)^2,$$

hence the *Bayesian predictor (BP)* is

$$p_0(X) = E(Y|X) \tag{3.1}$$

or equivalently

$$p_0(X) = \int y f_{Y|X}(y|x) d\mu(y)$$

where

$$f_{Y|X}(y|x) = \frac{\int f(X,y,\theta)d\tau(\theta)}{\int f(X,y,\theta)d\mu(y)d\tau(\theta)}.$$

We now provide a useful alternative form of the BP; recall that $m(X,\theta) = E_\theta(Y|X)$.

Lemma 3.1. *It is equivalent to predict Y or to "predict" $m(X,T)$, hence*

$$p_0(X) = E(m(X,T)|X). \tag{3.2}$$

Proof. Let $p(X)$ be a predictor. Integrating (2.1) with respect to τ, one obtains

$$r(Y, p(X)) = E(Y - m(X,T))^2 + r(m(X,T), p(X)),$$

thus, it is equivalent to minimize $r(Y, p(X))$ or to minimize $r(m(X,T), p(X))$ and (3.2) follows. □

Note that it is easy to verify the formula

$$m(X,T) = E(Y|X,T) \tag{3.3}$$

thus, from (3.3) and (3.2), one finds again (3.1).

Lemma 3.2. *P-sufficient statistic*

If (X,Y) has a density of the form $g(S(x),y,\theta)$ then $S(X)$ is P-sufficient and $p_0(X)$ is a function of $S(X)$.

Proof. $S(X)$ is clearly sufficient, and the conditional density of Y given $X = x$ is

$$f_\theta(y|x) = \frac{g(S(x), y, \theta)}{\int g(S(x), y, \theta) d\mu(y)},$$

hence Y is independent of X given $S(X)$, thus $S(X)$ is a P-sufficient statistic.

Now we have

$$E(Y|X) = \frac{\int y g(S(x), y, \theta) d\mu(y) d\tau(\theta)}{\int g(S(x), y, \theta) d\mu(y) d\tau(\theta)},$$

which shows that $p_0(X)$ is a function of $S(X)$. □

4 Independence

In the current Section we consider the special case where X and Y are independent for each θ. Note that this is not equivalent to "X not observed" since the model (X,Y,T) induces a dependence between X and Y. If X is not observed one may put $p_0 = EY$.

We now study two examples of such a situation. A general result will appear in the next Section.

Example 4.1. If (X,Y) has distribution $\mathcal{B}(n,\theta) \otimes \mathcal{B}(1,\theta)$ where $\mathcal{B}$ denotes the Binomial distribution and $\theta \in]0,1[$, and if T has distribution $B(a,\, b)$ $(a > 0, b > 0)$, then

$$E_\theta(Y|X) = E_\theta(Y) = \theta$$

and, from lemma 3.1,

$$p_0(X) = E(T|X).$$

The distribution of (X, T) is

$$I_{]0,1[}(\theta)C_n^x\theta^x(1-\theta)^{n-x}\frac{\Gamma(a+b)}{\Gamma(a)\Gamma(b)}\theta^{a-1}(1-\theta)^{b-1}d\lambda(x)d\theta,$$

where λ is the counting measure over $\{1, ..., n\}$.

It is well known that the conditional distribution of T given X is the conjugate $B(a+X,\, n+b-X)$, hence

$$p_0(X) = \frac{a+X}{a+b+n}.$$

Comparison with the unbiased predictor (i.e. estimator) is easy to perform if $a = b$: elementary computations show that $p_0(X)$ is better than $\frac{X}{n}$, for each n, if

$$\theta(1-\theta) > \frac{a}{4(a+1)},$$

then, the length of the interval $]\theta_1, \theta_2[$ where $p_0(X)$ is better than $\frac{X}{n}$ is $(1+a)^{-\frac{1}{2}}$ and, if a is small, $p_0(X)$ is "often" preferable. For example, if $a = 0.02$, the length is greater than 0.99.

Example 4.2. If $(X, Y) \sim e(\theta) \otimes e(\theta)$ where $e(.)$ is the exponential distribution, and if $T \sim e(\eta)$ $(\theta > 0, \eta > 0)$, we have

$$(X, Y, T) \sim \eta\theta^2 \exp(-\theta(x+y+\theta))I_{x>0,y>0,\theta>0}dxdyd\theta,$$

hence $(X, Y) \sim \frac{2\eta}{(x+y+\eta)^3}I_{x>0,y>0}dxdy$, and $X \sim \frac{\eta}{(x+\eta)^2}I_{x>0}dx$. It follows that

$$p_0(X) = E(Y|X) = X + \eta.$$

Note that we also have

$$p_0(X) = E(m(X,T)|X) = E(\frac{1}{T}|X) = X + \eta.$$

Here the choice of the a priori distribution is not satisfactory since

$$E_\theta(X - \frac{1}{\theta})^2 = \frac{1}{\theta^2},$$

when

$$E_\theta(X + \eta - \frac{1}{\theta^2})^2 = \frac{1}{\theta^2} + \eta^2.$$

5 Decomposition of the conditional expectation

We now study the case where $m(X, \theta)$ has a specific form.

Proposition 5.1.

1. *Assume that*

$$E_\theta(Y|X) = A(X) + B(\theta)C(X) + D(\theta) \tag{5.1}$$

where A, B, C, D are square integrable with respect to the distribution of (X, T). Then

$$p_0(X) = A(X) + E(B(T)|X).C(X) + E(D(T)|X). \tag{5.2}$$

2. *In particular, if $E_\theta(Y|X) = A(X)$, then $p_0(X) = A(X)$.*

3. *If X and Y are independent, then $p_0(X) = E(D(T)|X)$ where $D(\theta) = E_\theta(Y)$.*

Proof. (5.1) entails

$$m(X, T) = A(X) + B(T)C(X) + D(T)$$

and, from Lemma 1

$$p_0(X) = E(m(X, T)|X)$$

hence (5.2).

Now, concerning the first particular case, the result is a direct consequence of (5.1) and (5.2). Note that, here, the a priori distribution is not involved.

In the second case one may remark that

$$E_\theta(Y|X) = E_\theta(Y)$$

and (5.2) gives the result. □

It should be noticed that it is not enough to compute the Bayesian estimator of θ for obtaining (5.2) since, in general,

$$E(B(T)|X) \neq B(E(T|X)$$

and the same for D. However the method works if B and D are linear.

Example 5.1. (continuation of example 2.3)

Here, the conditional expectation has the form

$$E_\theta(N_{s+h}|N_s) = \theta h + N_s \, , \theta > 0.$$

If the a priori distribution of T is $\Gamma(a,\, b)$ with density $b^a\theta^{a-1}e^{-b\theta}\Gamma(a)^{-1}I_{\mathbb{R}^+}(\theta)$, elementary computations show that the distribution of T given N_s is the conjugate $\Gamma(N_s + a, s + b)$, hence

$$E(T|N_s) = \frac{a + N_s}{b + s}$$

and, from Proposition 5.1, the Bayesian predictor is

$$p_0(N_s) = \frac{s + b + h}{s + b}\, N_s + \frac{ah}{s + b}.$$

In order to compare it with the unbiased optimal predictor (2.3) it suffices to compare (2.4) with

$$E_\theta(\theta h + N_s - p_0(N_s))^2 = \frac{\theta s + (a - \theta b)^2}{(s + b)^2}\, h^2.$$

Then, $p_0(X)$ is better than $p(X)$ if

$$\theta^2 - 2\theta(\frac{a+1}{b} + \frac{1}{2s}) + \frac{a^2}{2b} < 0.$$

In particular, if s is small, the BP is "often" better than the the unbiased predictor. We leave the complete discussion to the reader.

Example 5.2. Consider the gaussian process

$$X_t = \theta t + W_t\ , t \geq 0$$

where $(\mathrm{W}_t, t \geq 0)$ is a standard Wiener process. Then

$$E_\theta(X_{s+h}|\, X_u, 0 \leq u \leq s) = \theta h + X_s$$

hence

$$p_0(X) = E(T|X)\, h + X_s$$

with $X = (X_u, 0 \leq u \leq s)$ and $Y = X_{s+h}$.

6 Unbiasedness

A Bayesian estimator is not unbiased, except in some special cases. The next proposition underscores this fact :

Proposition 6.1. *(Blackwell-Girschick)*
If the risk function is quadratic and if $p(X)$ is an unbiased Bayesian estimator of $m(\theta)$, then

$$E(m(T) - p(X))^2 = 0.$$

i.e. the Bayes risk is 0.

Proof. See Lehmann and Casella [1998] p. 234-235. □

For a predictor, the situation appears to be more intricate :

Proposition 6.2. *Set*

$$\varphi(X,T) = m(X,T) - p_0(X)$$

- If $p_0(X)$ is unbiased, we have

$$\varphi(X,T) \perp L^2(\mathcal{B}_X) \cup L^2(\mathcal{B}_T)$$

where orthogonality is taken with respect to the distribution of (X,T) and where $\mathcal{B}_X$ (resp. $\mathcal{B}_T$) is the $\sigma-$algebra generated by X (resp. T).

- If $p_0(X)$ is unbiased and

$$m(X,\theta) = A(X) + B(\theta)C(X) + D(\theta)$$

then, $B(\theta)C(X) = 0$ entails

$$E(m(X,T) - p_0(X))^2 = 0 \tag{6.1}$$

when, if $B(\theta)C(X) \neq 0$, one may have

$$E(m(X,T) - p_0(X))^2 > 0.$$

Proof. - From Lemma 3.1 one has

$$\varphi(X,T) = m(X,T) - E(m(X,T)|X)$$

which implies that

$$\varphi(X,T) \perp L^2(\mathcal{B}_X).$$

Now, unbiasedness means that

$$E(m(X,T)|T) = E(p_0(X)|T)$$

that is

$$E(\varphi(X,T)|T) = 0$$

therefore

$$\varphi(X,T) \perp L^2(\mathcal{B}_T).$$

- If

$$m(X,\theta) = A(X) + D(\theta)$$

Proposition 5.1 gives

$$p_0(X) = A(X) + E(D(T)|X)$$

hence

$$E(\varphi(X,T))^2 = E(D(T) - E(D(T)|X))^2$$

and since $E(D(T)|X)$ is an unbiased Bayesian estimator of $D(\theta)$, Proposition 6.1 entails

$$E(\varphi(X,T)^2 = 0.$$

- Now, if $B(\theta)C(X) \neq 0$, consider the model

$$Y = \theta X + \varepsilon \ (|\theta| < 1)$$

where $(X, \varepsilon) \sim \mathcal{N}(0,1) \otimes \mathcal{N}(0,\ 1-\theta^2)$, then $Y \sim \mathcal{N}(0,1)$. Then we have

$$m(X,\theta) = \theta X$$

and, from Proposition 5.1,

$$p_0(X) = E(T|X).X.$$

But $(X,T) \sim \mathcal{N}(0,1) \otimes \tau$, so

$$p_0(X) = ET.X = \int_{-1}^{+1} \theta d\tau(\theta).X.$$

It follows that $p_0(X)$ is unbiased, since

$$E_\theta(p_0(X)) = ET.E_\theta(X) = 0 = E_\theta Y.$$

However

$$E(\varphi(X,T))^2 = EX^2.VT > 0$$

because τ is not degenerated. □

Example 6.1. (Autoregressive process)

Consider the AR(1) process (cf Brockwell and Davis, 1991)

$$X_n - \theta = \rho(X_{n-1} - \theta) + \varepsilon_n,\ n \in \mathbb{Z},\ (\theta \in \mathbb{R})$$

where (ε_n) is a strong white noise and ρ is known ($|\rho| < 1$). Then, if $X = (X_1, ..., X_n)$ and $Y = X_{n+1}$ we have

$$m(X,\theta) = E_\theta(X_{n+1}|\ X_1, ..., X_n) = \rho X_n + \theta(1-\rho) := A(X) + D(\theta),$$

thus

$$p_0(X) = \rho X_n + (1-\rho)E(T|X)$$

and (6.1) applies. As an application one can show that

$$p_0(X) = \rho X_n + (1-\rho)\bar{X}_n$$

is not Bayesian since this should imply

$$\bar{X}_n = T \; a.s.$$

Note that, on the contrary, if ρ is unknown, one can obtain the situation described at the end of the proof of Proposition 6.2. For a study of Bayesian prediction for AR(1) processes we refer to Díaz [1990].

Example 6.2. (continuation of example 2.3)
Recall that

$$m(N_s, \theta) = N_s + h\theta := A(X) + B(\theta),$$

so, whatever the a priori distribution τ, the BP is not unbiased.

References

D. Bosq and D. Blanke. *Prediction and inference in large dimensions*. Wiley series in probability and statistics. Wiley-Dunod, 2007.

P. J. Brockwell and R. A. Davis. *Time Series : Theory and Methods*. Springer-Verlag, New-York, 2nd edition, 1991.

J. Díaz. Bayesian forecasting for AR(1) models with normal coefficients. *Comm. Statist. Theory Methods*, 19(6):2229–2246, 1990.

E. L. Lehmann and G. Casella. *Theory of point estimation*. Springer, New-York, 2nd edition, 1998.

RENDICONTI DEL CIRCOLO MATEMATICO DI PALERMO
Serie II, Suppl. 84 (2012), pp. 91-106

Divergences in parametric setting without smoothing or grouping

Michel Broniatowski* , Igor Vajda†
*LSTA, Université Pierre et Marie Curie

Abstract

This paper reviews simple estimators based on the minimization of a divergence between the empirical measure and a model of continuous distributions. The technique which is developped here makes use of simple duality arguments. It has the benefit of requiring neither smoothing nor grouping, as is usually done for these problems. Also the class of estimators contains the Maximum Likelihood one as a special case. Influence functions are presented. Extensions of divergence concepts are exposed and a discussion on invariance is considered.

1 Introduction

The present paper presents an overview on the dual representation for divergences between probability measures with an emphasis on possible extensions towards statistical estimation criterions in parametric families. It is mostly based on Broniatowski and Vajda (2010) contribution to this domain; we refer to Bronniatowski and Keziou (2006) for an alternative approach, also based on duality arguments, in relation to the non parametric case. The basic notation is as follows.

Let $\phi : (0, \infty) \mapsto \mathbb{R}$ be twice differentiable strictly convex function with $\phi(1) = 0$ and (possibly infinite) continuous extension to $t = 0+$ denoted by $\phi(0)$, and let $\mathbf{\Phi}$ be the class of all such functions. For every $\phi \in \mathbf{\Phi}$ we consider the adjoint function

$$\phi^*(t) = t\phi(1/t) \quad \text{where} \quad \phi^* \in \mathbf{\Phi},\ (\phi^*)^* = \phi.$$

For every $\phi \in \mathbf{\Phi}$ we consider *ϕ-divergence* of probability measures P and Q on a measurable space $(\mathcal{X}, \mathcal{A})$ with densities p, q w.r.t. a dominating σ-finite measure λ. In this paper we deal with P, Q which are

either measure-theoretically equivalent (i.e. satisfying $pq > 0$ λ-a. s., in symbols $P \equiv Q$) or measure-theoretically orthogonal (i.e. satisfying $pq = 0$ λ-a. s., in symbols $P \perp Q$). Thus, by Liese and Vajda (1987 or 2006), for all P, Q under consideration

$$D_\phi(P,Q) = \begin{cases} \int \phi\,(p/q)\,\mathrm{d}Q & \text{if} \quad P \equiv Q \\ \phi(0) + \phi^*(0) & \text{if} \quad P \perp Q \end{cases}$$

where the range of values is

$$0 \le D_\phi(P,Q) \le \phi(0) + \phi^*(0)$$

and $D_\phi(P,Q) = 0$ iff $P = Q$ or $D_\phi(P,Q) = \phi(0) + \phi^*(0)$ if (for $\phi(0) + \phi^*(0) < \infty$ iff) $P \perp Q$. Another important property is the skew symmetry

$$D_\phi(Q,P) = D_{\phi^*}(P,Q).$$

We shall deal mainly with the power divergences (or Cressie-Read divergences)

$$D_\alpha(P,Q) := D_{\phi_\alpha}(P,Q) \quad \text{of real powers } \alpha \in \mathbb{R} \tag{1}$$

for the power functions $\phi_\alpha \in \mathbf{\Phi}$ defined by

$$\phi_\alpha(t) = \frac{t^\alpha - \alpha t + \alpha - 1}{\alpha(\alpha-1)} \quad \text{if} \quad \alpha(\alpha-1) \neq 0 \tag{2}$$

and otherwise by the corresponding limits

$$\phi_0(t) = -\ln t + t - 1, \qquad \phi_1(t) = \phi_0^*(t) = t \ln t - t + 1. \tag{3}$$

It is easy to verify for all $\alpha \in \mathbb{R}$ the relation

$$\phi_\alpha^* = \phi_{1-\alpha} \text{ so that } \; D_\alpha(Q,P) = D_{1-\alpha}(P,Q).$$

For $P \equiv Q$ we get

$$D_\alpha(P,Q) = \begin{cases} \frac{1}{\alpha(\alpha-1)} \left[\int (p/q)^\alpha \,\mathrm{d}Q - 1 \right] & \text{if} \qquad \alpha(\alpha-1) \neq 0 \\ \int \ln(p/q)\,\mathrm{d}P = D_0(Q,P) & \text{if} \qquad \alpha = 1 \end{cases} \tag{4}$$

and for $P \perp Q$ similarly

$$D_\alpha(P,Q) = \begin{cases} 1/\alpha(1-\alpha) & \text{if} \quad 0 < \alpha < 1 \\ \infty & \text{otherwise.} \end{cases} \tag{5}$$

The special cases $D_2(P,Q)$ or $D_1(P,Q)$ are sometimes called Pearson or Kullback divergences and $D_{-1}(P,Q) = D_2(Q,P)$ or $D_0(P,Q) = D_1(Q,P)$ reversed Pearson or reverse Kullback divergences, respectively.

The ϕ-divergences and power divergences will be applied in the *standard statistical estimation model* with i.i.d. observations $X_1, \ldots, X_n$ governed by P_{θ_0} from a family $\mathcal{P} = \{P_\theta : \theta \in \Theta\}$ of probability measures on $(\mathcal{X}, \mathcal{A})$ indexed by a set of parameters $\Theta \subset \mathbb{R}^d$. The parameter θ_0 is assumed to be identifiable and the family $\mathcal{P}$ measure-theoreticaly equivalent in the sense

$$P_\theta \neq P_{\theta_0} \quad \text{and} \quad P_\theta \equiv P_{\theta_0} \quad \text{for all } \theta,\, \theta_0 \in \Theta \;\; \text{with} \;\; \theta \neq \theta_0. \tag{6}$$

Further, the family is assumed to be *continuous* (nonatomic) in the sense

$$P_\theta(\{x\}) = 0 \quad \text{for all} \;\; x \in \mathcal{X},\; \theta \in \Theta \tag{7}$$

and dominated by a σ-finite measure λ with densities

$$p_\theta = \mathrm{d}P_\theta/\mathrm{d}\lambda \quad \text{for all } \theta \in \Theta. \tag{8}$$

In this model the parameter θ_0 is assumed to be estimated on the basis of observations $X_1, \ldots, X_n$ by measurable functions $\theta_n : \mathcal{X}^n \mapsto \Theta$ called estimates. Collection of estimates for various sample sizes n is an estimator. Estimators are denoted in this paper by the same symbols θ_n as the corresponding estimates.

The assumed strict convexity of $\phi(t)$ at $t = 1$ together with the identifiability of θ_0 assumed in (6) means that $D_\phi(P_\theta, P_{\theta_0}) \geq 0$ for all θ, $\theta_0 \in \Theta$ with the equality iff $\theta = \theta_0$. In other words, the unknown parameter θ_0 is the unique minimizer of the function $D_\phi(P_\theta, P_{\theta_0})$ of variable $\theta \in \Theta$,

$$\theta_0 = \mathrm{argmin}_\theta D(P_\theta, P_{\theta_0}) \quad \text{for every } \theta_0 \in \Theta. \tag{9}$$

Further, the observations $X_1, \ldots, X_n$ are in a statistically suffi cient manner represented by the empirical probability measure

$$P_n = \frac{1}{n} \sum_{i=1}^{n} P_{X_i} \tag{10}$$

where P_x denotes the Dirac probability measure with all mass concentrated at $x \in \mathcal{X}$. The empirical probability measures P_n are known to converge weakly to P_{θ_0} as $n \to \infty$. Therefore by plugging in (9) the measures P_n for P_{θ_0} one intuitively expects to obtain the estimator

$$\theta_n = \theta_{n,\phi} := \text{argmin}_{\boldsymbol{\theta}} D_\phi\left(P_{\boldsymbol{\theta}}, P_n\right) \tag{11}$$

which estimates $\boldsymbol{\theta_0}$ consistently in the usual sense of the convergence $\theta_n \to \boldsymbol{\theta_0}$ for $n \to \infty$. However, the reality is different: the problem is that for the continuous family $\mathcal{P}$ under consideration and the discrete family $\mathcal{P}_{dis}$ of all pmṡ with finite support, obviously containing the empirical distributions (10)

$$P_{\boldsymbol{\theta}} \perp P_n \Rightarrow D_\phi(P_{\boldsymbol{\theta}}, P_n) = \phi(0) + \phi^*(0) \quad \text{when } P_{\boldsymbol{\theta}} \in \mathcal{P} \text{ and } P_n \in \mathcal{P}_{dis}. \tag{12}$$

This means that the estimates θ_n proposed in (11) are trivial, with the argmin $= \Theta$.

In the following two sections we list and motivate several modifications of the minimum divergence rule (11) which allow to bypass the problem (12). Some of them are new and some known from the previous literature. We illustrate the general forms of these estimators by applying them to the basic standard statistical families. We denote by $\mathbb{L}_1(Q)$ the set of all absolutely Q-integrable functions $f : \mathcal{X} \mapsto \mathbb{R}$ and put for brevity

$$Q \cdot f = \int f \, \mathrm{d}Q \quad \text{for } f \in \mathbb{L}_1(Q). \tag{13}$$

The space $\mathcal{Q}$ is defined as the set of p.mṡ

$$\mathcal{Q} : = \mathcal{P} \cup \mathcal{P}_{dis}.$$

2 Subdivergences and superdivergences

We denote by

$$\boldsymbol{\ell}_{\boldsymbol{\theta},\tilde{\theta}} = p_{\boldsymbol{\theta}} / p_{\tilde{\theta}}$$

the likelihood ratios between the densities $p_{\boldsymbol{\theta}}$ and $p_{\tilde{\theta}}$.

Define the nonincreasing functions

$$\phi^{\#}(t) = \phi(t) - t\phi'(t) \quad \text{for every } \phi \in \boldsymbol{\Phi}$$

and assume that $\mathcal{P}$ is such that

$$\left\{\phi\left(\boldsymbol{\ell}_{\boldsymbol{\theta},\tilde{\theta}}\right),\ \phi'\left(\boldsymbol{\ell}_{\boldsymbol{\theta},\tilde{\theta}}\right),\ \phi^{\#}\left(\boldsymbol{\ell}_{\boldsymbol{\theta},\tilde{\theta}}\right)\right\} \subset \mathbb{L}_1(Q) \quad \text{for all } \theta, \tilde{\theta} \in \Theta \text{ and } Q \in \mathcal{Q}.$$

(which obviously holds for $Q = P_n$).

For all pairs $\theta,\, \tilde{\theta} \in \Theta$ we consider the functions $L_\phi(\theta,\, \tilde{\theta}) = L_\phi(\theta,\, \tilde{\theta},\, x)$ of variable $x \in \mathcal{X}$ defined by the formula

$$L_\phi(\theta,\, \tilde{\theta}) = P_\theta \cdot \phi'(\boldsymbol{\ell}_{\theta,\tilde{\theta}}) + \phi^{\#}(\boldsymbol{\ell}_{\theta,\tilde{\theta}}).$$

2.1 Dual version of $\phi-$divergences.

Liese and Vajda (2006) in parametric setting, Broniatowski and Keziou (2006) in measure space setting obtained the so called dual version of the divergence between P and Q. We present the simple argument developped by Liese and Vajda (2006), which has the merit of strict pertinence in the present parametric setting. By strict convexity

$$\phi(t) \geq \phi(s) + \phi'(s)(t - s)$$

with the equality only for $t = s$. Putting in this inequality $t = \boldsymbol{\ell}_{\theta,\theta_0}$, $s = \boldsymbol{\ell}_{\theta,\tilde{\theta}}$ and integrating both sides over P_{θ_0} we get

$$D_\phi\left(P_\theta, P_{\theta_0}\right) = \max_{\tilde{\theta}\in\boldsymbol{\Theta}} \underline{\mathrm{D}}_{\phi,\tilde{\theta}}\left(P_\theta, P_{\theta_0}\right) \quad \text{for all } \theta, \theta_{\mathbf{0}} \in \Theta$$

with

$$\underline{\mathrm{D}}_{\phi,\tilde{\theta}}\left(P_\theta, Q\right) = Q \cdot L_\phi(\,\theta, \tilde{\theta}) = P_\theta \cdot \phi'(\boldsymbol{\ell}_{\theta,\tilde{\theta}}) + Q \cdot \phi^{\#}(\boldsymbol{\ell}_{\theta,\tilde{\theta}}), \quad (P_\theta,\, Q) \in \mathcal{P} \otimes \mathcal{Q}$$

and immediately follows

Theorem 1 *For each $(P_\theta, P_{\theta_0}) \in \mathcal{P} \otimes \mathcal{P}$ and $\phi \in \boldsymbol{\Phi}$, the ϕ-divergence $D_\phi\left(P_\theta, P_{\theta_0}\right)$ is maximum of the finite expectations $\underline{D}_{\phi,\tilde{\theta}}\left(P_\theta, P_{\theta_0}\right)$ over $\tilde{\theta} \in \Theta$ attained at the unique point $\tilde{\theta} = \theta_{\mathbf{0}}$. In other words,*

$$D_\phi\left(P_\theta, P_{\theta_0}\right) = \max_{\tilde{\theta}\in\boldsymbol{\Theta}} \underline{D}_{\phi,\tilde{\theta}}\left(P_\theta, P_{\theta_0}\right) \quad \textit{for all } \theta, \theta_{\mathbf{0}} \in \Theta$$

where the equality holds iff $\tilde{\theta} = \theta_{\mathbf{0}}$.

From the above result it is natural to introduce the following two definitions

Definition 2 *θ is the escort parameter.*

Definition 3 *$\underline{D}_{\phi,\tilde{\theta}}\left(P_\theta, Q\right)$ is a **subdivergence** of P_θ, Q with parameters $(\phi, \tilde{\theta}) \in \boldsymbol{\Phi} \otimes \boldsymbol{\Theta}$.*

Now we introduce the family of suprema $\bar{\mathrm{D}}_\phi(P_\theta, Q) := \sup_{\tilde\theta\in\Theta} \underline{\mathrm{D}}_{\phi,\tilde\theta}(P_\theta, Q)$ for all $(P_\theta, Q) \in \mathcal{P}\otimes\mathcal{Q}$

parametrized by $\phi \in \mathbf{\Phi}$. This family extends the ϕ-divergences $D_\phi(P,Q)$ from the domain $\mathcal{P}\otimes\mathcal{P}$ to $\mathcal{P}\otimes\mathcal{Q}$ allowing therefore $\mathcal{Q}$ to be discrete. Indeed, by the above Theorem ,

$$\bar{\mathrm{D}}_\phi(P_\theta, Q) = D_\phi(P_\theta, Q) \quad \text{for all } (P_\theta, Q) \in \mathcal{P}\otimes\mathcal{P}\ .$$

This justifies us to interpret $\bar{\mathrm{D}}_\phi(P_\theta, Q)$ as ***superdivergences*** of $(P_\theta, Q) \in \mathcal{P}\otimes\mathcal{Q}$ with parameters $\phi \in \mathbf{\Phi}$.

Also

$$\min_\theta \bar{\mathrm{D}}_\phi(P_\theta, P_{\theta_0}) = D_\phi(P_{\theta_0}, P_{\theta_0}) = 0.$$

2.2 Estimators

Note that if $Q = P_n \in \mathcal{P}_{dis}$ then the superdivergence values $\bar{\mathrm{D}}_\phi(P_\theta, P_n)$ differ from the constant divergence values $D_\phi(P_\theta, P_n) \equiv \phi(0) + \phi^*(0)$.

The subdivergences $\underline{\mathrm{D}}_{\phi,\tilde\theta}(P_\theta, P_n)$ and superdivergences $\bar{\mathrm{D}}_\phi(P_\theta, P_n)$ can replace the divergences $D_\phi(P_\theta, P_n)$ as optimality criteria in definition of M-estimators. Let us consider the families of functionals $\tilde{T}_{\phi,\theta} : \mathcal{Q} \mapsto \Theta$ and $T_\phi : \mathcal{Q} \mapsto \Theta$ defined by

$$\tilde{T}_{\phi,\theta}(Q) = \mathrm{argmax}_{\tilde\theta}\ \underline{\mathrm{D}}_{\phi,\tilde\theta}(P_\theta, Q) \quad \text{for } (\phi,\theta) \in \mathbf{\Phi}\otimes\mathbf{\Theta}$$

and

$$T_\phi(Q) = \mathrm{argmin}_\theta\ \bar{\mathrm{D}}_\phi(P_\theta, Q) \quad \text{for } \phi \in \mathbf{\Phi}$$

respectively. Replacing the general argument Q by P_n we obtain the

maximum subdivergence estimators (briefly, the $\max\underline{\mathrm{D}}_\phi$-estimators)

$$\begin{aligned}\tilde\theta_{\phi,\theta,n} = \tilde{T}_{\phi,\theta}(P_n) &= \mathrm{argmax}_{\tilde\theta}\ \underline{\mathrm{D}}_{\phi,\tilde\theta}(P_\theta, P_n)\\ &= \mathrm{argmax}_{\tilde\theta}\ \left[P_\theta\cdot\phi'(\boldsymbol{\ell}_{\theta,\tilde\theta}) + P_n\cdot\phi^{\#}(\boldsymbol{\ell}_{\theta,\tilde\theta})\right]\\ &= \mathrm{argmax}_{\tilde\theta}\left[P_\theta\cdot\phi'\left(\frac{p_\theta}{p_{\tilde\theta}}\right) + \frac{1}{n}\sum_{i=1}^n \phi^{\#}\left(\frac{p_\theta(X_i)}{p_{\tilde\theta}(X_i)}\right)\right]\end{aligned}$$

with escort parameters $\theta \in \mathbf{\Theta}$, and the ***minimum superdivergence estimators*** (briefly, the $\min\bar{\mathrm{D}}_\phi$-estimators)

$$\begin{aligned}\theta_{\phi,n} = T_\phi(P_n) &= \mathrm{argmin}_\theta\ \bar{\mathrm{D}}_\phi(P_\theta, P_n) = \mathrm{argmin}_\theta \sup_{\tilde\theta}\ \underline{\mathrm{D}}_{\phi,\tilde\theta}(P_\theta, P_n)\\ &= \mathrm{argmin}_\theta \sup_{\tilde\theta}\left[P_\theta\cdot\phi'(\boldsymbol{\ell}_{\theta,\tilde\theta}) + P_n\cdot\phi^{\#}(\boldsymbol{\ell}_{\theta,\tilde\theta})\right]\\ &= \mathrm{argmin}_\theta \sup_{\tilde\theta}\left[P_\theta\cdot\phi'\left(\frac{p_\theta}{p_{\tilde\theta}}\right) + \frac{1}{n}\sum_{i=1}^n \phi^{\#}\left(\frac{p_\theta(X_i)}{p_{\tilde\theta}(X_i)}\right)\right].\end{aligned}$$

We can prove easily that the $\max\underline{\mathrm{D}}_\phi$-estimators are as well as the $\min\bar{\mathrm{D}}_\phi$-estimators are Fisher consistent.

$$\tilde{T}_{\phi,\boldsymbol{\theta}}(P_{\boldsymbol{\theta}_0}) = \mathrm{argmax}_{\tilde{\boldsymbol{\theta}}}\ \underline{\mathrm{D}}_{\phi,\tilde{\boldsymbol{\theta}}}\left(P_{\boldsymbol{\theta}}, P_{\boldsymbol{\theta}_0}\right) \ = \boldsymbol{\theta_0} \text{ for } (\phi,\boldsymbol{\theta}) \in \boldsymbol{\Phi}\otimes\boldsymbol{\Theta}$$

Remark: The remarkable property of the above construction is that it completely avoids any type of smoothing or grouping in the defintion of the estimators; these techniques have been widely developped in order to avoid the lack of absolute continuity between the (atomic) empirical measure P_n and the (continuous) distributions in the model $\mathcal{P}$.

The $\min\bar{\mathrm{D}}_\phi$-estimators $\theta_{\phi,n}$ were proposed independently by Liese & Vajda (2006) under the name **modified ϕ-divergence estimators** and Broniatowski & Keziou (2006) under the name **minimum dual ϕ-divergence estimators** . The $\max\underline{\mathrm{D}}_\phi$-estimators $\tilde{\theta}_{\phi,\boldsymbol{\theta},n}$ were proposed by Broniatowski and Keziou (2009) and called **dual ϕ-divergence estimators** . Both types of these estimators were in the cited papers motivated by the mentioned Fisher consistency and by the property easily verifiable from that $\phi(t) = -\ln t$ implies

$$\tilde{\theta}_{\phi,\boldsymbol{\theta},n} = \mathrm{argmax}_{\tilde{\boldsymbol{\theta}}}\ \Sigma_{i=1}^n \ln p_{\tilde{\boldsymbol{\theta}}}(X_i) \ \text{ and } \ \theta_{\phi,n} = \mathrm{argmax}_{\boldsymbol{\theta}}\ \Sigma_{i=1}^n \ln p_{\boldsymbol{\theta}}(X_i) \tag{14}$$

where the left equality holds for all escort parameters $\theta \in \Theta$. In other words, the logarithmic choice $\phi(t) = -\ln t$ reduces all the variants of the $\max\underline{\mathrm{D}}_\phi$-estimator as well as the $\min\bar{\mathrm{D}}_\phi$-estimator to the MLE. It is challenging to investigate the extent to which the $\max\underline{\mathrm{D}}_\phi$-estimators $\tilde{\theta}_{\phi,\boldsymbol{\theta},n}$ and the $\min\bar{\mathrm{D}}_\phi$-estimator $\theta_{\phi,n}$ as extensions of the MLE are effi cient and robust under various specifications of ϕ, θ and ϕ respectively.

2.3 Power divergences

We restrict ourselves to special subclasses of the power divergences $D_\alpha(P,Q)$ $D_{\phi_\alpha}(P,Q)$. For the power functions ϕ_α we get the functions

$$\mathring{\phi}_\alpha(t) := t\phi'_\alpha(t) = \begin{cases} \frac{t^\alpha - t}{\alpha - 1} & \text{for } \alpha \neq 1 \\ \lim_{\alpha\to 1} \frac{t^\alpha - t}{\alpha - 1} = t\ln t & \text{for } \alpha = 1 \end{cases}$$

and

$$\phi^{\#}_\alpha(t) = \phi_\alpha(t) - \mathring{\phi}_\alpha(t) = \begin{cases} \frac{1}{\alpha}\left(1 - t^\alpha\right) & \text{for } \alpha \neq 0 \\ \lim_{\alpha\to \mathbf{0}} \frac{1}{\alpha}\left(1 - t^\alpha\right) = -\ln t & \text{for } \alpha = 0. \end{cases}$$

They lead to the $\max\underline{\mathrm{D}}_\alpha$-estimators (briefly, ***power subdivergence estimators***)

$$\tilde\theta_{\alpha,\theta,n} = \mathrm{argmax}_{\tilde\theta}\left[P_{\tilde\theta}\cdot\mathring{\phi}_\alpha\left(\frac{p_\theta}{p_{\tilde\theta}}\right) + P_n\cdot\phi_\alpha^{\#}\left(\frac{p_\theta}{p_{\tilde\theta}}\right)\right]$$

with power parameters $\alpha\in\mathbb{R}$ and escort parameters $\theta\in\Theta$ and to the $\min\bar{\mathrm{D}}_\alpha$-estimators (briefly, ***power superdivergence estimators***)

2.4 Power subdivergence estimators

We study the $\max\underline{\mathrm{D}}_\alpha$-estimators $\tilde\theta_{\alpha,\theta,n}$ with the divergence power parameters $\alpha\geq 0$ and the escort parameters $\theta\in\Theta$. As said above, for $\alpha=0$ they coincide with the MLE's . Therefore we restrict ourselves to $\alpha>0$.We present the Influence Functions for those estimators.

For a density p_θ twice differentiable with respect to $\theta\in\Theta\subset\mathbb{R}^d$, we put

$$s_\theta = \frac{\mathrm{d}}{\mathrm{d}\theta}\ln p_\theta \quad\text{and}\quad \mathring{s}_\theta = \left(\frac{\mathrm{d}}{\mathrm{d}\theta}\right)^{\mathrm{t}} s_\theta$$

By assumptions, the argminima $\tilde\theta_{\alpha,\theta,n} = \tilde T_{\alpha,\theta}(P_n)$ are for all $\alpha>0$ solutions of the equations

$$P_{\tilde\theta}\cdot\left(\frac{p_\theta}{p_{\tilde\theta}}\right)^\alpha s_{\tilde\theta} - \frac{1}{n}\sum_{i=1}^n\left(\frac{p_\theta(X_i)}{p_{\tilde\theta}(X_i)}\right)^\alpha s_{\tilde\theta}(X_i) = 0$$

in the variable $\tilde\theta\in\Theta$.

The Influence Functions of the $\max\underline{\mathrm{D}}_\alpha$-estimators $\tilde\theta_{\alpha,\theta,n}$ under consideration are at P_{θ_0} given by the formula

$$\mathrm{IF}(x;\tilde T_{\alpha,\theta},\theta_{\mathbf{0}}) = \boldsymbol{I}_{\alpha,\theta}(\theta_{\mathbf{0}})^{-1}\left[\left(\frac{p_\theta(x)}{p_{\theta_0}(x)}\right)^\alpha s_{\theta_0}(x) - P_{\theta_0}\cdot\left(\frac{p_\theta}{p_{\theta_0}}\right)^\alpha s_{\theta_0}\right] \quad\text{if}\quad \alpha>0$$

$$\mathrm{IF}(x;\tilde T_{\mathbf{0},\theta},\theta_{\mathbf{0}}) = \boldsymbol{I}(\theta_{\mathbf{0}})^{-1}s_{\theta_0}(x) \qquad\text{otherwise}\quad(\alpha=0)$$

where

$$\boldsymbol{I}_{\alpha,\theta}(\theta_{\mathbf{0}}) = P_{\theta_0}\cdot\left(\frac{p_\theta}{p_{\theta_0}}\right)^\alpha s_{\theta_0}^{\mathrm{t}} s_{\theta_0} \qquad \text{if}\quad \alpha>0$$

$$\boldsymbol{I}(\theta_{\mathbf{0}}) = P_{\theta_0}\cdot s_{\theta_0}^{\mathrm{t}} s_{\theta_0} \qquad \text{if}\quad \alpha=0.$$

If the escort parameter θ coincides with the true parameter $\theta_{\mathbf{0}}$ then

$$\mathrm{IF}(x;\tilde T_{\alpha,\theta_0},\theta_{\mathbf{0}}) = \boldsymbol{I}(\theta_{\mathbf{0}})^{-1}s_{\theta_0}(x) \quad\text{for all}\ \alpha\geq 0.$$

In the MLE case $\alpha=0$ we get for all escort parameters θ the classical MLE influence function with the classical Fisher information matrix. This influence function is obtained also if the escort parameter θ coincides with the true parameter $\theta_{\mathbf{0}}$ as in this case the estimators with all power parameters $\alpha\geq 0$ reduce to the MLE .

2.5 The choice of the escort parameter

This important problem is currently being studied. It can be argued that for the escort parameter different from the unknown value θ_0 the ***maximum subdivergence estimators*** suffer of a lack of Fisher consistency under misspecification (see Broniatowski and Vajda 2010) for examples; this induces to consider escort parameters defined as preliminary estimators, possibly with good robustness properties. We refer to Toma and Broniatowski (2011) for some considerations in this respect. See also Cherfi (2010).

3 Power superdivergence estimators

In this subsection we deal with the $\min\bar{\mathrm{D}}_\alpha$-estimators $\theta_{\alpha,n}$ with the power parameters $\alpha \geq 0$. For $\alpha = 0$ they coincide with the MLE's. It holds

Theorem 4 *The $\min\bar{D}_\alpha$-estimators $\theta_{\alpha,n} = T_\alpha(P_n)$ are solutions of the equations*

$$\frac{\alpha}{1-\alpha} P_{\tilde{\tau}_{\alpha,\theta}} \cdot \left(\frac{p_\theta}{p_{\tilde{\tau}_{\alpha,\theta}}} \right)^\alpha s_\theta + \frac{1}{n} \sum_{i=1}^{n} \left(\frac{p_\theta(X_i)}{p_{\tilde{\tau}_{\alpha,\theta}}(X_i)} \right)^\alpha s_\theta(X_i) = 0.$$

Corollary 5 *The influence functions $IF(x; T_\alpha, \theta)$ of all $\min\bar{D}_\alpha$-estimators $\theta_{\alpha,n} = T_\alpha(P_n)$ with power parameters $0 < \alpha < 1$ at $P_\theta \in \mathcal{P}$ coincide with the influence function*

$$IF(x; T_0, \theta) = \boldsymbol{I}(\theta)^{-1} s_\theta(x)$$

of the MLE $\theta_{0,n} = T_0(P_n)$. Henceforth are not robust in most cases .

4 Decomposable pseudodistances

The ϕ-divergences $D_\phi(P, Q)$, $\phi \in \mathbf{\Phi}$ can be characterized by the *information processing property*, i. e. by the complete invariance w.r.t. the statistically suffi cient transformations of the observation space $(\mathcal{X}, \mathcal{A})$. This property is useful but probably not unavoidable in the minimum distance estimation based on similarity between theoretical and empirical distributions. Hence we admit in the rest of the paper general *pseudodistances* $\mathfrak{D}(P, Q)$ which may not satisfy the information processing property.

Definition 6 *We say that* $\mathfrak{D} : \mathcal{P} \otimes \mathcal{P}^+ \mapsto \mathbb{R}$ *is a pseudodistance of probability measures* $P \in \mathcal{P} = \{P_\theta : \theta \in \Theta\}$ *and* $Q \in \mathcal{P}^+$ *if*

$$\mathfrak{D}(P_\theta, P_{\tilde{\theta}}) \geq 0 \quad \textit{for all } \theta, \tilde{\theta} \in \Theta \textit{ with } \mathfrak{D}(P_\theta, P_{\tilde{\theta}}) = 0 \quad \textit{iff } \theta = \tilde{\theta}.$$

An additional restriction imposed in this section on pseudodistances $\mathfrak{D}(P, Q)$ will be the *decomposability*.

Definition 7 *A pseudodistance* $\mathfrak{D}$ *on* $\mathcal{P} \otimes \mathcal{P}^+$ *is a* ***decomposable*** *if there exist functionals* $\mathfrak{D}^{\mathbf{0}} : \mathcal{P} \mapsto \mathbb{R}$, $\mathfrak{D}^{\mathbf{1}} : \mathcal{P}^+ \mapsto \mathbb{R}$ *and measurable mappings*

$$\rho_\theta : \mathcal{X} \mapsto \mathbb{R}, \qquad \theta \in \Theta$$

such that for all $\theta \in \Theta$ *and* $Q \in \mathcal{P}^+$ *the expectations* $Q \cdot \rho_\theta$ *exist and*

$$\mathfrak{D}(P_\theta, Q) = \mathfrak{D}^{\mathbf{0}}(P_\theta) + \mathfrak{D}^{\mathbf{1}}(Q) + Q \cdot \rho_\theta.$$

Definition 8 *We say that a functional* $T_{\mathfrak{D}} : \mathcal{Q} \mapsto \Theta$ *for* $\mathcal{Q} = \mathcal{P}^+ \cup \mathcal{P}_{emp}$ *defines a* ***minimum pseudodistance estimator*** *(briefly,* $\min \mathfrak{D}$*-estimator) if* $\mathfrak{D}(P_\theta, Q)$ *is a decomposable pseudodistance on* $\mathcal{P} \otimes \mathcal{P}^+$ *and the parameters* $T_{\mathfrak{D}}(Q) \in \Theta$ *minimize* $\mathfrak{D}^{\mathbf{0}}(P_\theta) + Q \cdot \rho_\theta$ *on* Θ, *in symbols*

$$T_{\mathfrak{D}}(Q) = \operatorname{argmin}_\theta \left[\mathfrak{D}^{\mathbf{0}}(P_\theta) + Q \cdot \rho_\theta\right] \qquad \textit{for all } Q \in \mathcal{Q}.$$

In particular, for $Q = P_n \in \mathcal{P}_{emp}$

$$\theta_{\mathfrak{D},n} := T_{\mathfrak{D}}(P_n) = \operatorname{argmin}_\theta \left[\mathfrak{D}^{\mathbf{0}}(P_\theta) + \frac{1}{n}\sum_{i=1}^n \rho_\theta(X_i)\right] \quad \textit{if } P_n = \frac{1}{n}\sum_{i=1}^n \delta_{X_i}.$$

An important property is

Theorem 9 *Every* $\min \mathfrak{D}$*-estimator*

$$\theta_{\mathfrak{D},n} = \operatorname{argmin}_\theta \left[\mathfrak{D}^{\mathbf{0}}(P_\theta) + \frac{1}{n}\sum_{i=1}^n \rho_\theta(X_i)\right]$$

is Fisher consistent in the sense that

$$T_{\mathfrak{D}}(P_{\theta_0}) = \operatorname{argmin}_\theta \mathfrak{D}(P_\theta, P_{\theta_0}) = \theta_{\mathbf{0}} \quad \textit{for all } \theta_{\mathbf{0}} \in \Theta.$$

The sum

$$\mathfrak{D}(P_\theta, Q) := \mathfrak{D}^{\mathbf{0}}_{\phi,\tau}(P_\theta) + \mathfrak{D}^{\mathbf{1}}_{\phi,\tau}(Q) + Q \cdot \rho_{\phi,\tau,\theta}$$

is a pseudodistance on $\mathcal{P}\otimes\mathcal{P}^+$ and the maximum subdivergence estimator

$$\theta_{\phi,\tau,n} = \operatorname{argmax}_\theta \left[P_\tau \cdot \phi' \left(\frac{p_\tau}{p_\theta} \right) + \frac{1}{n} \sum_{i=1}^{n} \phi^{\#} \left(\frac{p_\tau(X_i)}{p_\theta(X_i)} \right) \right]$$

with the divergence parameter $\phi \in \mathbf{\Phi}$ and escort parameter $\tau \in \Theta$ is the $\min \mathfrak{D}$-estimator for the decomposable pseudodistance .

4.1 Power pseudodistance estimators

A special class of pseudodistances $\mathfrak{D}_\psi(P_\theta, Q)$ defined on $\mathcal{P} \otimes \mathcal{P}^+$ by the integral formula

$$\mathfrak{D}_\psi(P_\theta, Q) = \int \psi(p_\theta, q)\, \mathrm{d}\lambda \quad \text{for } p_\theta = \frac{\mathrm{d}P_\theta}{\mathrm{d}\lambda}, q = \frac{\mathrm{d}Q}{\mathrm{d}\lambda}$$

where $\psi(s,t)$ are *reflexive* in the sense that they are nonnegative functions of arguments $s,t>0$ with $\psi(s,t)=0$ iff $s=t$. If a function ψ is reflexive and also *decomposable* in the sense

$$\psi(s,t) = \psi^{\mathbf{0}}(s) + \psi^{\mathbf{1}}(t) + \rho(s)\, t, \quad s,t \geq 0 \tag{15}$$

for some $\psi^{\mathbf{0}}, \psi^{\mathbf{1}}, \rho : (0,\infty) \to \mathbb{R}$ then the corresponding ψ-pseudodistance is a *decomposable pseudodistance* satisfying

$$\mathfrak{D}_\psi(P_\theta, Q) = \mathfrak{D}^{\mathbf{0}}_\psi(P_\theta) + \mathfrak{D}^{\mathbf{1}}_\psi(Q) + Q \cdot \rho_\theta$$

for

$$\mathfrak{D}^{\mathbf{0}}_\psi(P_\theta) = \int \psi^{\mathbf{0}}(p_\theta)\, \mathrm{d}\lambda, \quad \mathcal{D}^{\mathbf{1}}_\psi(Q) = \int \psi^{\mathbf{1}}(q)\, \mathrm{d}\lambda \ \text{ and } \ \rho_\theta = \rho(p_\theta).$$

The ϕ-divergences $D_\phi(P_\theta, Q)$ are special ψ-pseudodistances (**??**) for the functions

$$\psi(s,t) = \phi(s/t)\, t - \phi'(1)(s-t), \quad s,t>0 \tag{16}$$

since they are nonnegative and reflexive, and (16) implies $\mathfrak{D}_\psi(P_\theta, Q) = D_\phi(P_\theta, Q)$ for all $P \in \mathcal{P}, Q \in \mathcal{P}^+$ when $\phi \in \mathbf{\Phi}$ and ψ are related by (16). However, the functions (16) in general do not satisfy the decomposability condition (15) so that the ϕ-divergences are not in general decomposable pseudodistances. An exception is the logarithmic function $\phi = \phi_{\mathbf{0}} = -\log x + x - 1$ for which the $\min \mathfrak{D}_{\phi_0}$-estimator is the MLE.

the L_2-estimator is an example where the above setting applies. The quadratic function $\psi(s,t) = (s-t)^2$ is reflexive and also decomposable . Thus it defines the decomposable pseudodistance

$$\mathfrak{D}_\psi(P_\theta, Q) = \int (p_\theta - q)^2 \, \mathrm{d}\lambda = \|p_\theta - q\|^2$$

on $\mathcal{P} \otimes \mathcal{P}^+$ for $\mathcal{P}^+ \subset L_2(\lambda)$. It is easy to verify that

$$\mathfrak{D}^0_\psi(P_\theta) = \int p_\theta^2 \, \mathrm{d}\lambda \quad \mathcal{D}^1_\psi(Q) = \int q^2 \, \mathrm{d}\lambda_Q, \quad \text{and} \quad \rho_\theta = -2p_\theta.$$

The corresponding $\min \mathfrak{D}_\psi$-estimator is in this case the L_2-estimator

$$\theta_n = \mathrm{argmin}_\theta \left[\int p_\theta^2 \, \mathrm{d}\lambda - \frac{2}{n} \sum_{i=1}^n p_\theta(X_i) \right]$$

which is known to be robust but not effi cient (see e.g. Hampel et al. (1986)).

To build a smooth bridge between the robustness and effi ciency, one needs to replace the reflexive and decomposable functions ψ by families $\{\psi_\alpha : \alpha \geq 0\}$ of reflexive functions decomposable in the sense

$$\psi_\alpha(s,t) = \psi^0_\alpha(s) + \psi^1_\alpha(t) + \rho_\alpha(s)\, t \quad \text{for all } \alpha \geq 0 \quad (\text{cf. } (\mathbf{??}))$$

with the limits at satisfying for some constant $\varkappa$ all $s > 0$ the conditions

$$\psi^0_0(s) = \lim_{\alpha \downarrow 0} \psi^0_\alpha(s) = \varkappa \, s \quad \text{and} \quad \lim_{\alpha \downarrow 0} \rho_\alpha(s) = \rho_0(s) = -\ln s.$$

Then for all $\alpha \geq 0$ and $(P_\theta, Q) \in \mathcal{P} \otimes \mathcal{P}^+$ the family of ψ_α-pseudodistances

$$\mathfrak{D}_\alpha(P_\theta, Q) := \mathfrak{D}_{\psi_\alpha}(P_\theta, Q), \qquad \alpha \geq 0$$

satisfies the decomposability condition

$$\mathfrak{D}_\alpha(P_\theta, Q) = \mathfrak{D}^0_\alpha(Q) + \mathfrak{D}^1_\alpha(P_\theta) + Q \cdot \rho_{\alpha,\theta} \qquad (\text{cf. } (\mathbf{??}))$$

for

$$\mathfrak{D}^0_\alpha(P_\theta) = \int \psi^0_\alpha(p_\theta) \, \mathrm{d}\lambda, \quad \mathfrak{D}^1_\alpha(Q) = \int \psi^1_\alpha(q) \, \mathrm{d}\lambda \quad \text{and} \quad \rho_{\alpha,\theta} = \rho_\alpha(p_\theta).$$

The pseudodistances $\mathfrak{D}_\alpha(P_\theta, Q)$ are decomposable and define the family of $\min \mathfrak{D}_\alpha$-estimators

$$\begin{aligned} \theta_{\alpha,n} &= \arg\min_\theta \left[\mathfrak{D}^0_{\psi_\alpha}(P_\theta) + P_n \cdot \rho_{\alpha,\theta} \right] \\ &= \mathrm{argmin}_\theta \left[\int \psi^0_\alpha(p_\theta) \, \mathrm{d}\lambda + \frac{1}{n} \sum_{i=1}^n \rho_\alpha(p_\theta(X_i)) \right], \quad \alpha \geq 0. \end{aligned}$$

This family contains as a special case for $\alpha = 0$ the effi cient but non-robust MLE

$$\theta_{\mathbf{0},n} = \text{argmin}_\theta \left[\text{const} - \frac{1}{n} \sum_{i=1}^{n} \ln p_\theta(X_i) \right]$$

while for $\alpha > 0$ the $\theta_{\alpha,n}$'s are expected to be less effi cient but more robust than $\theta_{\mathbf{0},n}$.

Decomposable pseudodistances $\mathfrak{D}_\alpha(P_\theta, Q)$, defined on $\mathcal{P} \otimes \mathcal{Q}$ by the functions

$$\psi_\alpha(s,t) = t^{1+\alpha} \left[\alpha \phi_{1+\alpha}\left(\frac{s}{t}\right) + (1-\alpha)\phi_\alpha\left(\frac{s}{t}\right) \right], \quad \alpha \geq 0$$

of variables $s, t > 0$ where $\phi_{1+\alpha}$ and ϕ_α are the power functions are defined through

$$\psi^{\mathbf{0}}_\alpha(s) = \frac{s^{1+\alpha}}{1+\alpha}, \quad \psi^{\mathbf{1}}_\alpha(t) = \begin{cases} t\left[\frac{t^\alpha - 1}{\alpha} - \frac{t^\alpha}{1+\alpha}\right] \\ t \ln t - t \end{cases} \quad \text{and} \quad \rho_\alpha(s) = \begin{cases} -\frac{s^\alpha - 1}{\alpha} \text{ if } \alpha > 0 \\ -\ln s \text{ if } \alpha = 0. \end{cases}$$

Moreover, this family is continuous in the parameter $\alpha \downarrow 0$ and leads to MLE as its limit.

4.2 Relation with other estimation criterions

we call the pseudodistances $\mathfrak{D}_\alpha(P, Q)$ simply ***power pseudo– distances*** of orders $\alpha \geq 0$. The next theorem guarantees finiteness and continuity of these divergences. It is restricted to the families $\mathcal{P}$ satisfying for some $\beta > 0$ the condition

$$p^\beta,\ q^\beta, \ln p \in \mathbb{L}_1(Q) \quad \text{for all } P \in \mathcal{P},\ Q \in \mathcal{P}^+. \tag{17}$$

Theorem 3.1.3. If (17) holds for some $\beta > 0$ then for all $0 \leq \alpha \leq \beta$, the modified power divergences are well defined by (**??**) and finite, satisfying for all $P \in \mathcal{P}$, $Q \in \mathcal{P}^+$ the continuity relation

$$\lim_{\alpha \downarrow \mathbf{0}} \mathfrak{D}_\alpha(P, Q) = \mathfrak{D}_{\mathbf{0}}(P, Q). \tag{18}$$

Example 3.1.3: L_2-estimator revisited. By (**??**), the min $\mathfrak{D}_\alpha$-estimator of order $\alpha = 1$ is defined by

$$\theta_{1,n} = \text{argmin}_\theta \left[\int p_\theta^2 \, \mathrm{d}\lambda - \frac{2}{n} \sum_{i=1}^{n} p_\theta(X_i) \right]$$

so that it is nothing but the L_2-estimator θ_n from Example 3.1.2. The family of estimators $\theta_{n,\alpha}$ from (**??**) smoothly connects this robust estimator with the effi cient MLE$\theta_{n,\mathbf{0}}$ when the parameter α decreases from 1 to 0.

The special class of the min $\mathfrak{D}_\alpha$-estimators $\theta_{\alpha,n}$ given above was proposed by Basu et al. (1998) who confirmed their effi ciency for$\alpha \approx 0$ and their intuitively expected robustness for $\alpha > 0$. These authors called $\theta_{\alpha,n}$ *minimum density power divergence estimators* without actual clarification of the relation of the "density power divergences" $\mathfrak{D}_\alpha(P,Q)$ to the standard power divergences $D_\alpha(P,Q)$ studied in Liese and Vajda (1987) and Read and Cressie (1988).

$$\theta_{\alpha,n} = \mathrm{argmax}_\theta \begin{cases} \frac{1}{n}\sum_{i=1}^n \frac{1}{\alpha}\left(p_\theta^\alpha(X_i) - 1\right) - \frac{1}{1+\alpha}\int p_\theta^{1+\alpha}\,\mathrm{d}\lambda & \text{if } \alpha > 0 \\ \frac{1}{n}\sum_{i=1}^n \ln p_\theta(X_i) - 1 & \text{if } \alpha = 0. \end{cases} \tag{19}$$

This subclass of general min $\mathfrak{D}_\alpha$-estimators (19) was included in a wider family of generalized MLE's introduced and studied previously in Vajda (1984,1986). However, the whole class (19) was not introduced there.

If the statistical model $\langle(\mathcal{X},\mathcal{A}); \mathcal{P} = (P_\theta : \theta \in \Theta)\rangle$ is reparametrized by $\vartheta = \vartheta(\theta)$ then the new min $\mathcal{D}_\alpha$-estimates ϑ_{α_n} are related to the original $\theta_{\alpha,n}$ by $\vartheta_{\alpha,n} = \vartheta(\theta_{\alpha,n})$. If the observations $x \in \mathcal{X}$ are replaced by $y = T(x)$ where $T : (\mathcal{X},\mathcal{A}) \mapsto (\mathcal{Y},\mathcal{B})$ is a measurable statistic with the inverse T^{-1} then the densities

$$\tilde{p}_\theta = \frac{\mathrm{d}\tilde{P}_\theta}{\mathrm{d}\tilde{\lambda}}$$

in the transformed model $\langle(\mathcal{Y},\mathcal{B}); \tilde{\mathcal{P}} = (\tilde{P}_\theta = P_\theta T^{-1} : \theta \in \Theta)\rangle$ w.r.t. σ-finite dominating measure $\tilde{\lambda} = \lambda T^{-1}$ is related to the original densities p_θ by

$$\tilde{p}_\theta(y) = p_\theta(T^{-1}y)\,\mathcal{J}_T(y) \tag{20}$$

$\mathcal{J}_T(y)$ is the determinant

$$\mathcal{J}_T(y) = \left|\frac{\mathrm{d}}{\mathrm{d}y}H(y)\right|.$$

The min $\mathcal{D}_\alpha$-estimators are in general not equivariant w.r.t. invertible transformations of observations T, unless $\alpha = 0$. However

Theorem 10 *The* $\min \mathfrak{D}_\alpha$*-estimates* $\tilde{\theta}_{\alpha,n}$ *in the above considered transformed model coincide with the original* $\min \mathfrak{D}_\alpha$*-estimates* $\theta_{\alpha,n}$ *if the Jacobian* $\mathcal{J}_T$ *of transformation is a nonzero constant on the transformed observation space* $\mathcal{Y}$*. Thus if* $\mathcal{X}, \mathcal{Y}$ *are Euclidean spaces then the* $\min \mathfrak{D}_\alpha$*-estimators are equivariant under linear statistics* $Tx = ax + b$*.*

5 Bibliography

References

[1] D. F. Andrews, P.J. Bickel, F. R. Hampel, P. J. Huber, W. H. Rogers and J. W. Tukey (1972). *Robust Estimates of Location*. Princeton University Press, Princeton N. J.

[2] A. Basu, I. R. Harris, N.L. Hjort and M. C. Jones (1998). "Robust and effi cient estimation by minimizing a density power divergence," *Biometrika*, vol. 85, No. 3, pp. 549-559.

[3] M. Broniatowski and A. Keziou (2006). "Minimization of ϕ-diveregnces on sets of signed measures," *Studia Scientiarum Mathematica Hungarica*, vol. 43, pp. 403-442.

[4] M. Broniatowski and A. Keziou (2009). "Parametric estimation and tests through divergences and the duality technique," *Journal of Multivariate Analysis*, vol. 100, No. 1,pp. 16-31.

[5] M. Broniatowski and I. Vajda (2009). Several applications of divergence criteria in continuous families, arXiv:0911.0937v1.

[6] M. Cherfi (2010) Contribution à lětude des divergences, Doctorat de Mathématiques, Université Pierre et Marie Curie.

[7] F. R. Hampel, E. M. Ronchetti, P. J. Rousseuw and W. A. Stahel (1986). *Robust Statistics: The approach Based on Influence Functions*, New York: Willey.

[8] F. Liese and I. Vajda, (1987). *Convex Statistical Distances*, Leipzig: Teubner.

[9] F. Liese and I. Vajda, (2006). "On divergences and informations in statistics and information theory," *IEEE Trans.actions on Information Theory*, vol. 52, No. 10, pp. 4394-4412.

[10] C. Miescke and F. Liese (2008). *Statistical Decision Theory*, Berlin: Springer.

[11] M. R. C. Read and N. A. C. Cressie (1988). *Goodness-of-Fit Statistics for Discrete Multivariate Data*, Berlin: Springer.

[12] A. Rényi (1961). "On measures of entropy and information," *Proc. 4-th Berkeley Symp. on Probability and Statistics*, vol. 1, pp. 547-561. Berkeley: University of California Press.

[13] A. Toma, M. Broniatowski (2011). "Minimum divergence estimators

and tests: Robustness results," *Journal of Multivariate Analysis*, vol 102, No 1, pp. 20-36.

[14] I. Vajda, (1984). Minimum divergence principle in statistical estimation. *Statistics and Decisions. Suppl. Issue No.1*, pp. 239-261.

[15] I. Vajda, (1986). Effi ciency and robustness control via distorted maximum likelihood estimation. *Kybernetika*, vol. 22, pp. 47-67.

[16] I. Vajda, (1989a). Comparison of asymptotic variances for several estimators of location. *Problems of Control and Information Theory*, vol. 18, No. 2, pp. 79-89.

[17] I. Vajda, (1989b). Estimators asymptotically minimax in wide sense. *Biometrical Journal*, vol. 31, No. 7, pp. 803-810.

[18] I. Vajda, (2008). *Modifications od Divergence Criteria for Applications in Continuous Families.* Research Report No. 2230, Institute of Information Theory and Automation, Prague, November 2008.

[19] A. W. van der Vaart and J. A. Wellner (1996). *Weak Convergence and Empirical Processes,* Berlin: Springer.

[20] A. W. van der Vaart (1998). *Asymptotic Statistics.* Cambridge University Press, Cambridge.

RENDICONTI DEL CIRCOLO MATEMATICO DI PALERMO
Serie II, Suppl. 84 (2012), pp. 107-125

A Buffon-Laplace type problem for two Delone covex-concave octagonal lattices and obstacles

G. Caristi* and Marius Stoka**

Department SEA, University of Messina,
Via dei Verdi n.75, 98122 Messina, Italia.
E-mail:gcaristi@unime.it
**Accademia delle Scienze di Torino

Dedicated to Professor
August Florian

Abstract

In this paper we consider two Delone lattices with the cells represented in the figure 1 and in the figure 15 and we compute the probability that a segment of random position and costant length intersects a side of the lattice.

Keywords: Geometric Probability, stochastic geometry, random sets, random convex sets and integral geometry.

1 Obstacles isosceles triangles.

Let $\Re_1(a, \alpha, \beta; m)$ be Delone lattice with fundamental cell $C_0^{(1)}$ represented in the figure

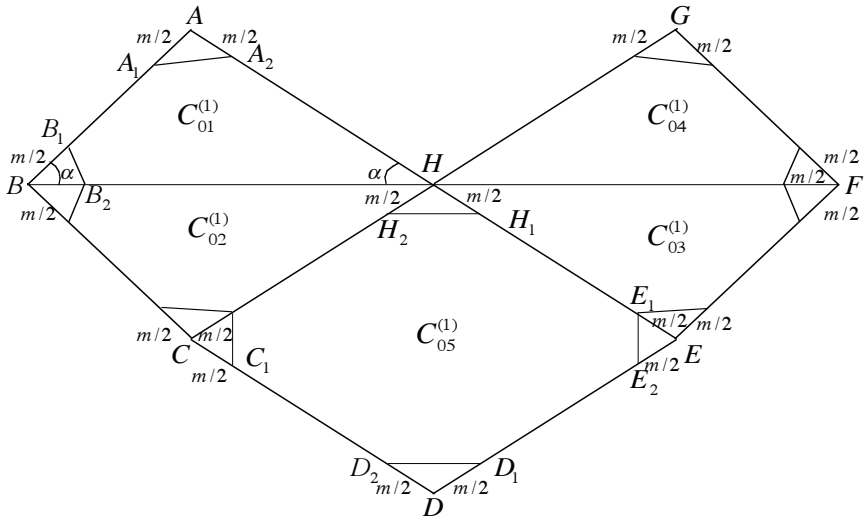


fig.1

where $\frac{\pi}{4} \leq \beta < \alpha \leq \frac{\pi}{3}$ and the 12 obstacles are isosceles triangles of sides $\frac{m}{2}$, $\frac{m}{2}$, with $m < a$.

From the figure 1 and considering the symmetries we have

$$|AB| = |BC| = |EF| = |FG| = a,$$

$$|AH| = |CH| = |CD| = |DE| = |EH| = |GH| = \frac{a \sin \alpha}{\sin \beta} > a,$$

$$|BH| = |FH| = \frac{a \sin(\alpha + \beta)}{\sin \beta}, \tag{1}$$

$$|A_1A_2| = m \cos \frac{\alpha + \beta}{2}, \quad |B_1B_2| = m \sin \frac{\alpha}{2},$$

$$|C_1C_2| = |E_1E_2| = m \sin \beta, \quad |D_1D_2| = |H_1H_2| = m \cos \beta, \tag{2}$$

$$areaAA_1A_2 = \frac{m^2}{8} \sin(\alpha + \beta), \quad areaCC_1C_2 = areaDD_1D_2 = areaEE_1E_2 =$$

$$areaHH_1H_2 = \frac{m^2}{8} \sin 2\beta, \quad areaBB_1B_2 = \frac{m^2}{8} \sin \alpha. \tag{3}$$

With these values we can write

$$areaC_{01}^{(1)} = areaC_{02}^{(1)} = areaC_{03}^{(1)} = areaC_{04}^{(1)} =$$

$$\frac{a^2 \sin \alpha \sin(\alpha + \beta)}{2 \sin \beta} - \frac{m^2}{8} [\sin(\alpha + \beta) - \sin \alpha],$$

$$areaC_{05}^{(1)} = \left(\frac{a^2 \sin^2 \alpha}{\sin^2 \beta} - \frac{m^2}{2}\right) \sin 2\beta. \tag{4}$$

We consider a segment s of random position and of constant length $l < \min\left(a - m,\ a(\cos\alpha + \cos\beta) - \frac{m}{2}\right)$ and we want to compute the probability that this segment intersects a side of lattice, therefore the probability $P_{int}^{(1)}$ that s intersects the side of the fundamental cell $C_0^{(1)}$.

The position of the segment s is determinated by his middle point O and by the angle φ that it forms with the side BF of the cell $C_0^{(1)}$.

To compute the probability $P_{int}^{(1)}$ we consider the limit positions of the segment s, for an assigned value of φ, situated in the cell $C_{0i}^{(1)}$, $(i = 1, 2, ..., 5)$, and we denote with $\widehat{C}_{0i}^{(1)}(\varphi)$ the polygon determined from these positions we have the figure

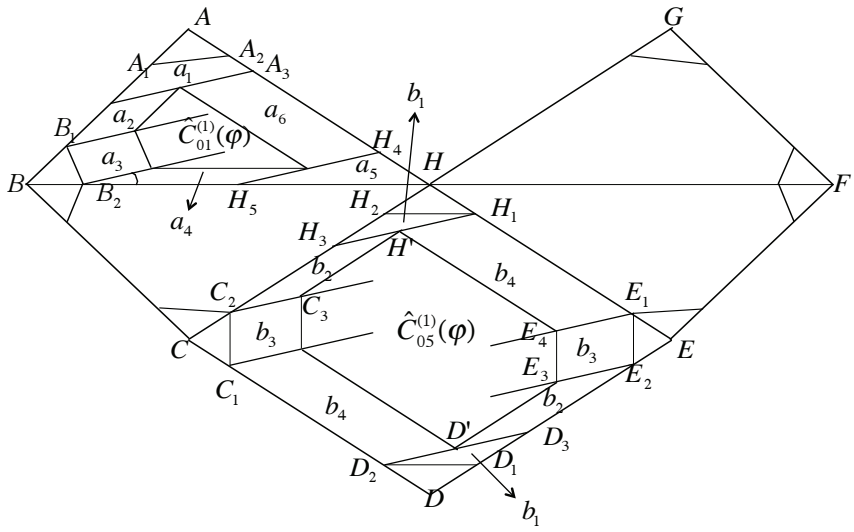


fig.2

From this figure follow

$$area\widehat{C}_{01}^{(1)}(\varphi) = area\widehat{C}_{02}^{(1)}(\varphi) = area\widehat{C}_{03}^{(1)}(\varphi) = area\widehat{C}_{04}^{(1)}(\varphi) =$$

$$areaC_{01}^{(1)} - [areaa_1(\varphi) + areaa_2(\varphi) + ... + areaa_6(\varphi)], \tag{5}$$

$$area\widehat{C}_{05}^{(1)}(\varphi) = areaC_{05}^{(1)}(\varphi) - 2[areab_1(\varphi) +$$

$$areab_2(\varphi) + areab_3(\varphi) + areab_4(\varphi)]. \tag{6}$$

The figure

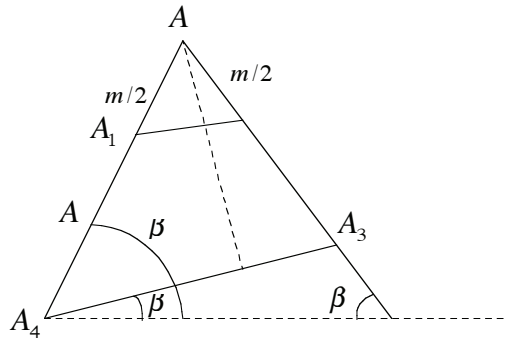


fig.3

.

give us

$$\widehat{A_3AA_4} = \pi - (\alpha + \beta), \qquad \widehat{A_3A_4A} = \alpha - \varphi,$$
$$\widehat{AA_3A_4} = \varphi + \beta. \tag{7}$$

From the triangle AA_3A_4 follow that:

$$\frac{l}{\sin(\alpha+\beta)} = \frac{|AA_3|}{\sin(\alpha-\varphi)} = \frac{|AA_4|}{\sin(\varphi+\beta)},$$

therefore

$$|AA_3| = \frac{l\sin(\alpha-\varphi)}{\sin(\alpha+\beta)}, \quad |AA_4| = \frac{l\sin(\varphi+\beta)}{\sin(\alpha+\beta)}. \tag{8}$$

Hence because

$$h_1 = |AA_4|\sin(\alpha-\varphi) = \frac{l\sin(\alpha-\varphi)\sin(\alpha+\beta)}{\sin(\alpha+\beta)},$$

we have

$$areaAA_3A_4 = \frac{l^2\sin(\alpha-\varphi)\sin(\alpha+\beta)}{2\sin(\alpha+\beta)},$$

therefore, considering the relation (3),

$$areaa_1(\varphi) = \frac{l^2\sin(\alpha-\varphi)\sin(\varphi+\beta)}{2\sin(\alpha+\beta)} - \frac{m^2}{8}\sin(\alpha+\beta). \tag{9}$$

Considering the figure

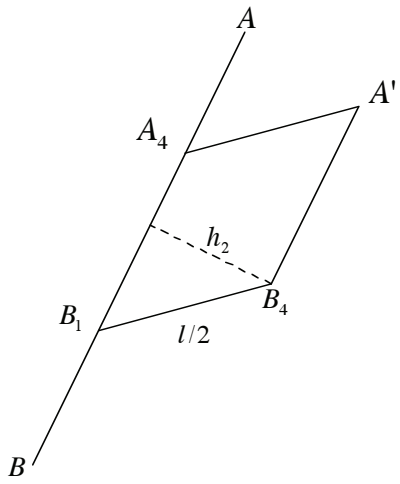


fig.4

With the relationes (7) and (8) we can write

$$\widehat{A_4B_1B_4} = \widehat{AA_4A'} = \alpha - \varphi,$$

$$h_2 = \frac{l}{2}\sin(\alpha - \varphi),$$

$$|A_4B_1| = a - \frac{m}{2} - |AA_4| = a - \frac{m}{2} - \frac{l\sin(\varphi + \beta)}{\sin(\alpha + \beta)}.$$

Therefore

$$areaa_2(\varphi) = \left[a - \frac{m}{2} - \frac{l\sin(\varphi + \beta)}{\sin(\alpha + \beta)}\right] \cdot \frac{l}{2}\sin(\alpha - \varphi). \tag{10}$$

The formulas (9) and (10) give us

$$areaa_1(\varphi) + areaa_2(\varphi) = (2a - m) \cdot \frac{l}{4}\sin(\alpha - \varphi) - \frac{m^2}{8}\sin(\alpha + \beta). \tag{11}$$

From the figure

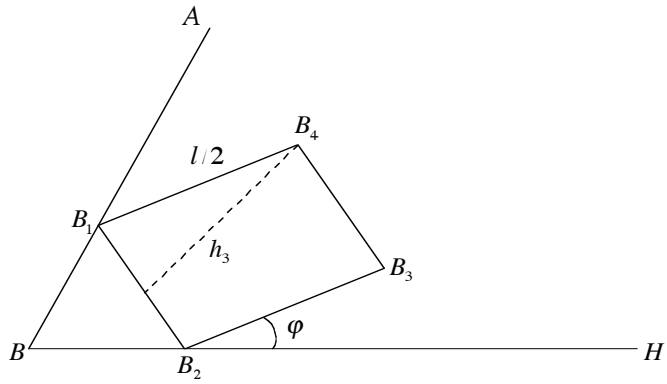


fig.5

follow

$$\widehat{B_2B_1B_4} = \pi - \widehat{B_1B_2B_3} =$$
$$\pi - \left(\pi - \varphi - \frac{\pi}{2} + \frac{\alpha}{2}\right) = \frac{\pi}{2} - \frac{\alpha}{2} + \varphi,$$
$$h_3 = \frac{l}{2}\sin\left(\frac{\pi}{2} - \frac{\alpha}{2} + \varphi\right) = \frac{l}{2}\cos\left(\varphi - \frac{\alpha}{2}\right),$$

therefore, considering the (2),

$$areaa_3(\varphi) = \frac{ml}{2}\sin\frac{\alpha}{2}\cos\left(\varphi - \frac{\alpha}{2}\right). \tag{12}$$

The figure

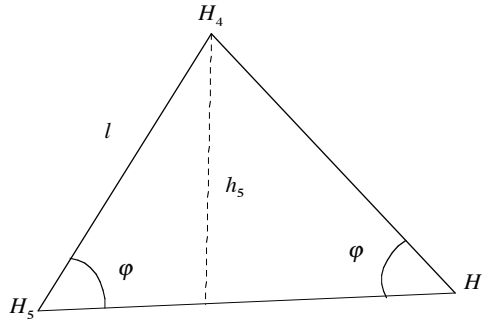


fig.6

give us

$$\widehat{HH_4H_5} = \pi - (\varphi + \beta),$$
$$h_5 = l\sin\varphi. \tag{13}$$

On the other hand, from the triangle HH_4H_5 follow

$$\frac{l}{\sin\beta} = \frac{|HH_4|}{\sin\varphi} = \frac{|HH_5|}{\sin(\varphi+\beta)},$$

hence

$$|HH_4| = \frac{l\sin\varphi}{\sin\beta}, \quad |HH_5| = \frac{l\sin(\varphi+\beta)}{\sin\beta}. \tag{14}$$

Therefore

$$areaa_5(\varphi) = \frac{l^2\sin\varphi\sin(\varphi+\beta)}{2\sin\beta}. \tag{15}$$

To compute $areaa_4(\varphi)$ we use the figure

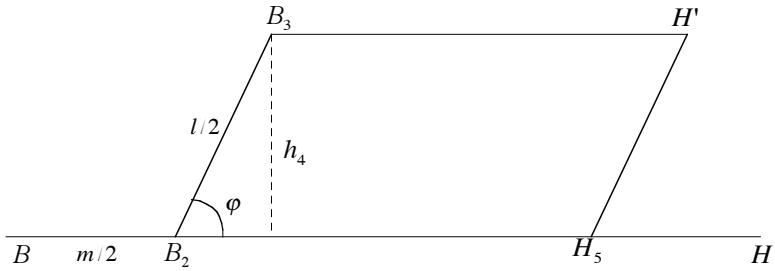


fig.7

From here and with the (14) we have

$$h_4 = \frac{l}{2}\sin\varphi, \quad |B_2H_5| = |BH| - \frac{m}{2} - |HH_5| =$$

$$\frac{a\sin(\alpha+\beta)}{\sin\beta} - \frac{m}{2} - \frac{l\sin(\varphi+\beta)}{\sin\beta}.$$

Therefore

$$areaa_4(\varphi) = \left[\frac{a\sin(\alpha+\beta)}{\sin\beta} - \frac{m}{2} - \frac{l\sin(\varphi+\beta)}{\sin\beta}\right]\cdot\frac{l}{2}\sin\varphi. \tag{16}$$

The relations (15) and (16) give us

$$areaa_4(\varphi) + areaa_5(\varphi) = \left[\frac{a\sin(\alpha+\beta)}{\sin\beta} - \frac{m}{2}\right]\cdot\frac{l}{2}\sin\varphi. \tag{17}$$

At the end, the figure

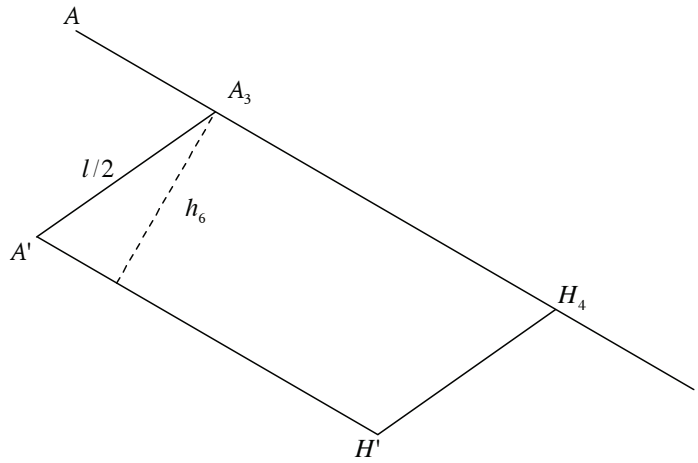


fig.8

and the relations (1), (8), (13) and (14) give us

$$\widehat{A_3A'H'} = \widehat{AA_3A_4} = \varphi + \beta,$$

$$h_6 = \frac{l}{2}\sin(\varphi+\beta),$$

$$|A_3H_4| = |AH| - |AA_3| - |HH_4| = \frac{a\sin\alpha}{\sin\beta} - \frac{l\sin(\alpha-\varphi)}{\sin(\varphi+\beta)} - \frac{l\sin\varphi}{\sin\beta}.$$

Consequently

$$areaa_6(\varphi) = \left[\frac{a\sin\alpha}{\sin\beta} - \frac{l\sin(\alpha-\varphi)}{\sin(\varphi+\beta)} - \frac{l\sin\varphi}{\sin\beta}\right]\cdot\frac{l}{2}\sin(\varphi+\beta). \qquad (18)$$

Replacing in the (5) the expressions (11), (12), (17) and (18) we obtain

$$area\widehat{C}_{01}^{(1)}(\varphi) = area\widehat{C}_{02}^{(1)}(\varphi) = area\widehat{C}_{03}^{(1)}(\varphi) = area\widehat{C}_{04}^{(1)}(\varphi) = areaC_{01}^{(1)} -$$

$$\frac{a\sin\alpha}{\sin\beta}\cdot l\sin(\varphi+\beta) + \frac{\sin\alpha}{4\sin\beta\sin(\alpha+\beta)}\cdot l^2\left[1-\cos 2(\varphi+\beta)\right] + \frac{m^2}{8}\sin(\alpha+\beta). \qquad (19)$$

Now we compute $area\widehat{C}_{05}^{(1)}(\varphi)$.

The figure

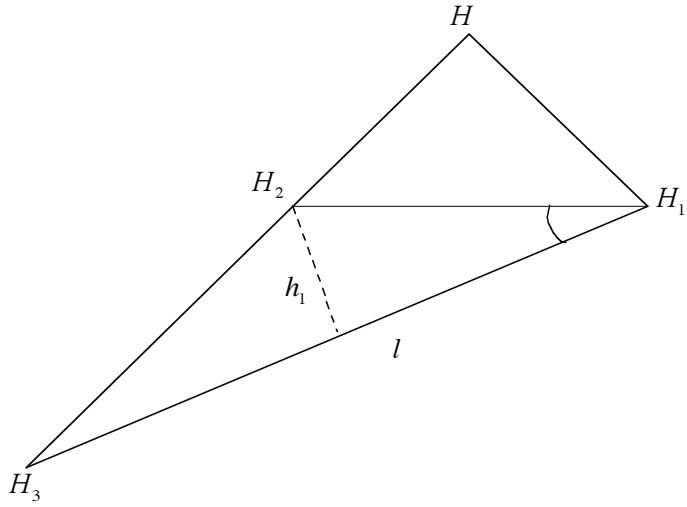


fig.9

give us

$$\widehat{H_1H_2H_3} = \pi - \widehat{HH_2H_1} = \pi - \beta,$$
$$\widehat{H_1H_3H_2} = \pi - (\pi - \beta + \varphi) = \beta - \varphi. \tag{20}$$

From the triangle $H_1H_2H_3$ follow

$$\frac{|H_2H_3|}{\sin\varphi} = \frac{l}{\sin\beta} = \frac{|H_1H_2|}{\sin(\beta-\varphi)},$$

therefore

$$|H_2H_3| = \frac{l\sin\varphi}{\sin\beta}. \tag{21}$$

Moreover, considering of the (2), we have the condition

$$2l\sin(\beta-\varphi) = m\sin 2\beta, \quad (m \neq 0).$$

Then, with the relations (20) and (21) we have

$$k_1 = |H_2H_3|\sin(\beta-\varphi) =$$
$$\frac{l\sin\varphi\sin(\beta-\varphi)}{\sin\beta}.$$

Therefore

$$areab_1(\varphi) = \frac{l^2\sin\varphi\sin(\beta-\varphi)}{2\sin\beta}. \tag{22}$$

Considering the figure

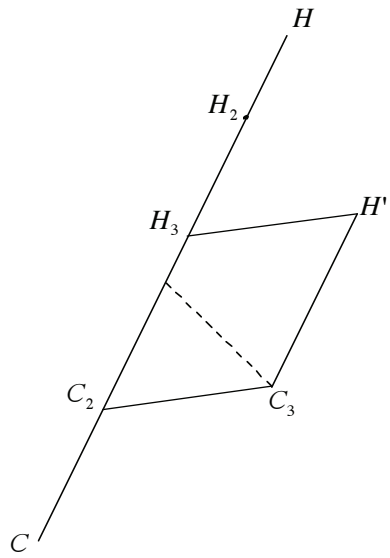


fig.10

and the relations (20) and (21), we can write

$$\widehat{H_3C_2C_3} = \widehat{H_1H_3H_2} = \beta - \varphi,$$

$$k_2 = \frac{l}{2}\sin(\beta - \varphi),$$

$$|C_2H_3| = |CH| - m - |H_2H_3| =$$

$$\frac{a\sin\alpha}{\sin\beta} - m - \frac{l\sin\varphi}{\sin\beta}.$$

Hence

$$areab_2(\varphi) = \left(\frac{a\sin\alpha}{\sin\beta} - m - \frac{l\sin\varphi}{\sin\beta}\right)\cdot\frac{l}{2}\sin(\beta - \varphi). \tag{23}$$

From the relations (22) and (23) we have

$$areab_1(\varphi) + areab_2(\varphi) = \left(\frac{a\sin\alpha}{\sin\beta} - m\right)\cdot\frac{l}{2}\sin(\beta - \varphi). \tag{24}$$

The figure

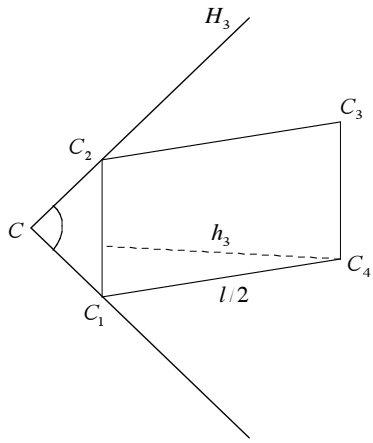


fig.11

give us

$$\widehat{C_1C_2C_3} = \pi - \left(\widehat{H_3C_2C_3} + \widehat{CC_2C_1}\right) =$$

$$\pi - \left(\beta - \varphi + \frac{\pi}{2} - \beta\right) = \frac{\pi}{2} + \varphi,$$

$$\widehat{C_2C_1C_4} = \frac{\pi}{2} - \varphi, \tag{25}$$

therefore

$$k_3 = \frac{l}{2}\sin\widehat{C_2C_1C_4} = \frac{l}{2}\cos\varphi$$

and, with the (2),

$$areab_3(\varphi) = \frac{ml\sin\beta}{2}\cos\varphi. \tag{26}$$

To compute $areab_4(\varphi)$ we consider the figure

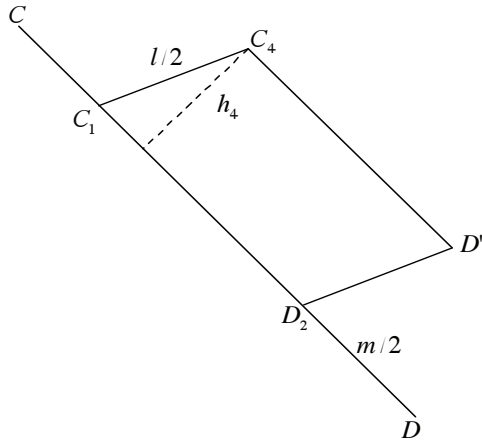


fig.12

The formula (25) give us

$$\widehat{C_4C_1D} = \pi - \left(\frac{\pi}{2} - \varphi + \frac{\pi}{2} - \beta\right) = \varphi + \beta,$$

$$k_4 = \frac{l}{2}\sin(\varphi + \beta).$$

Then, considering the relation (1), we have

$$|C_1D_2| = \frac{a\sin\alpha}{\sin\beta} - m,$$

therefore

$$areab_4(\varphi) = \left(\frac{a\sin\alpha}{\sin\beta} - m\right) \cdot \frac{l}{2}\sin(\varphi + \beta). \tag{27}$$

Replacing in the (6) the expressions (24), (26) and (27) we obtain

$$area\widehat{C}_{05}^{(1)}(\varphi) = areaC_{05}^{(1)}(\varphi) - 2(2a\sin\alpha - m\cos\alpha) \cdot l\cos\varphi. \tag{28}$$

Denoting with $M_i^{(1)}, (i = 1, 2, ..., 5)$, the set of segments s which have the middle point O in $C_{0i}^{(1)}$ and with $N_i^{(1)}$ the set of segments s completely contained in $C_{0i}^{(1)}$, we have [2]:

$$P_{int}^{(1)} = 1 - \frac{\mu\left(N_1^{(1)}\right) + \mu\left(N_2^{(1)}\right) + ... + \mu\left(N_5^{(1)}\right)}{\mu\left(M_1^{(1)}\right) + \mu\left(M_2^{(1)}\right) + ... + \mu\left(M_5^{(1)}\right)}, \tag{29}$$

where μ is the Lebesgue measure in Euclidean plane. To compute the measures we use the Poincaré kinematic measure [1]:

$$dK = dx \wedge dy \wedge d\varphi, \tag{30}$$

where x, y are the coordinates of the point O and φ the defined angle.

Considering the figure

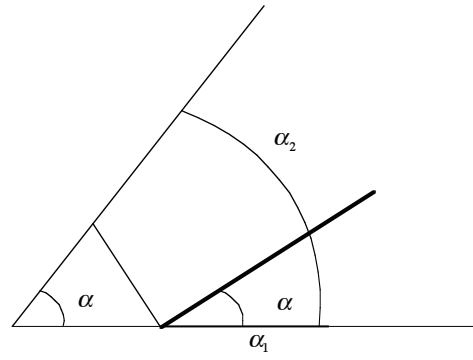


fig.13

From here follow

$$\varphi_1 = 0, \qquad \varphi_2 = \alpha.$$

Therefore, for the cell $C_{0j}^{(1)}$, $(j = 1, 2, 3, 4)$,we have

$$\varphi \in [0, \alpha] .$$

Then, the figure

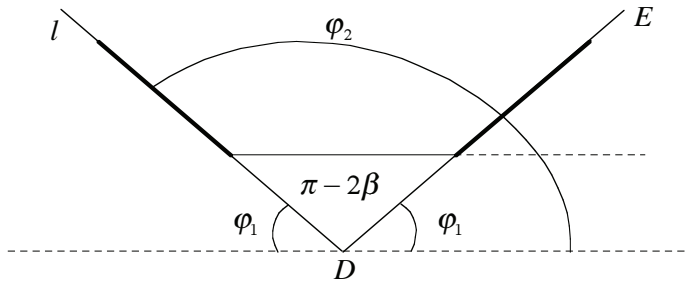


fig.14

give us

$$\varphi_2 = \pi - 2\beta + \varphi_1,$$
$$2\varphi_1 + \pi - 2\beta = \pi,$$

therefore

$$\varphi_1 = \beta, \quad \varphi_2 = \pi - \beta.$$

Consequently, for the cell $C_{05}^{(1)}$ we have

$$\varphi \in [\beta,\ \pi - \beta] .$$

With the formula (30) we have

$$\mu\left(M_1^{(1)}\right) = \mu\left(M_2^{(1)}\right) = \mu\left(M_3^{(1)}\right) = \mu\left(M_4^{(1)}\right) =$$

$$\int_0^{\alpha} d\varphi \iint_{\left\{(x,y)\in C_{01}^{(1)}\right\}} dxdy = \int_0^{\alpha} \left[area C_{01}^{(1)}\right] d\varphi = \alpha area C_{01}^{(1)}, \tag{31}$$

$$\mu\left(M_5^{(1)}\right) = \int_{\beta}^{\pi-\beta} d\varphi \iint_{\left\{(x,y)\in C_{05}^{(1)}\right\}} dxdy =$$

$$\int_{\beta}^{\pi-\beta} \left[area C_{05}^{(1)}\right] d\varphi = (\pi - 2\beta)\, area C_{05}^{(1)}. \tag{32}$$

Then, considering the formulas (19) and (28), we can write

$$\mu\left(N_1^{(1)}\right)=\mu\left(N_2^{(1)}\right)=\mu\left(N_3^{(1)}\right)=\mu\left(N_4^{(1)}\right)=$$

$$\int_0^{\alpha} d\varphi \iint\limits_{\left\{(x,y)\in \widehat{C}_{01}^{(1)}(\varphi)\right\}} dxdy=\int_0^{\alpha}\left[area\widehat{C}_{01}^{(1)}(\varphi)\right]d\varphi=$$

$$\alpha area C_{01}^{(1)}-\{\sin\alpha\left[\sin a+(1-\cos\alpha)\cot\beta\right]\cdot al-$$

$$\frac{\sin\alpha}{8\sin\beta\sin(\alpha+\beta)}\left[2\alpha+\sin 2\beta-\sin 2(\alpha+\beta)\right]\cdot l^2-\frac{m^2}{8}\alpha\sin(\alpha+\beta)\Big\}, \quad (33)$$

$$\mu\left(N_5^{(1)}\right)=\int_{\beta}^{\pi-\beta} d\varphi \iint\limits_{\left\{(x,y)\in \widehat{C}_{05}^{(1)}\right\}} dxdy=$$

$$\int_{\beta}^{\pi-\beta}\left[area\widehat{C}_{05}^{(1)}(\varphi)\right]d\varphi=(\pi-2\beta)\,area C_{05}^{(1)}+$$

$$4\cos\beta(2a\sin\alpha-m\sin\beta)\cdot l. \quad (34)$$

The formulas (29), (31), (32), (33) and (34) give us

$$P_{int}^{(1)}=\Big\{2\alpha\left[\frac{a^2\sin\alpha\sin(\alpha+\beta)}{\sin\beta}-\frac{m^2}{2}\sin\frac{\beta}{2}\cos\left(\alpha+\frac{\beta}{2}\right)\right]+$$

$$(\pi-2\beta)\left(\frac{a^2\sin^2\alpha}{\sin^2\beta}-\frac{m^2}{2}\right)\sin 2\beta\Big\}^{-1}\cdot\{4al\sin\alpha\cdot$$

$$[\sin\alpha-2\cos\beta+(1-\cos\alpha)\cot\beta]+ml\sin\beta\cos\beta-$$

$$\frac{\sin\alpha}{\sin\beta\sin(\alpha+\beta)}\left[\alpha-\sin\alpha\cos(\alpha+2\beta)\right]l^2-$$

$$\frac{m^2}{2}\alpha\sin(\alpha+\beta)\Big\}.$$

For $m=0,\ \beta=\frac{\pi}{4}$, $\alpha=\frac{\pi}{3}$, we obtain the probability

$$P=\frac{6}{\pi}\cdot\frac{l}{a}-\frac{\left(2-\sqrt{3}\right)(4\pi+9)}{2\pi}\cdot\left(\frac{l}{a}\right)^2. \quad (35)$$

2 Obstacles isosceles triangles and circolar sections

Let $\Re_2(a, \alpha, \beta; m)$ be the Delone lattice with fundamental cell $C_0^{(2)}$ represented in the figure

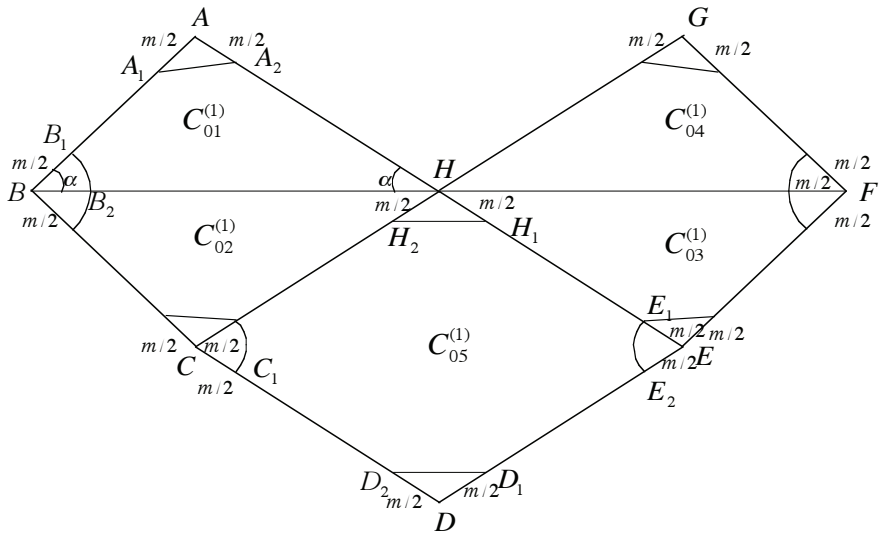


fig.15

where $\frac{\pi}{4} \leq \beta < \alpha \leq \frac{\pi}{3}$ and where six obstacles are isosceles triangles of sides $\frac{m}{2}$, $\frac{m}{2}$, and six are circolar sections with radius $\frac{m}{2}$, with $m < a$.

From the figure 1 and 15 we obtain that the formulas (1) and (2) are true also for the lattice R_2,while in the expressions (3) we have to take

$$areaBB_1B_2 = \frac{m^2\alpha}{8}, \qquad areaCC_1C_2 = areaEE_1E_2 = \frac{m^2\beta}{8}. \tag{36}$$

With these values we can write

$$areaC_{01}^{(2)} = areaC_{02}^{(2)} = areaC_{03}^{(2)} = areaC_{04}^{(2)} =$$

$$areaC_{01}^{(1)} - \frac{m^2}{8}(\alpha - \sin\alpha),$$

$$areaC_{05}^{(2)} = areaC_{05}^{(1)} - \frac{m^2}{4}(2\beta - \sin 2\beta). \tag{37}$$

As in the section 1 we want to compute the probability $P_{int}^{(2)}$ that the segment s of random position and of constant length $l < \min\left[a - m,\ a(\cos\alpha + \cos\beta) - \frac{m}{2}\right]$ intersects a side of the fundamental cell $C_0^{(2)}$.

With the notations of the section 1 we denote with $\widehat{C}_{0i}(\varphi)$, $(i = 1, 2, ..., 5)$ the polygon determined from the limit positions of the segment s situated in the cell $C_{0i}^{(2)}$ for an assigned value of φ. So we have the figure

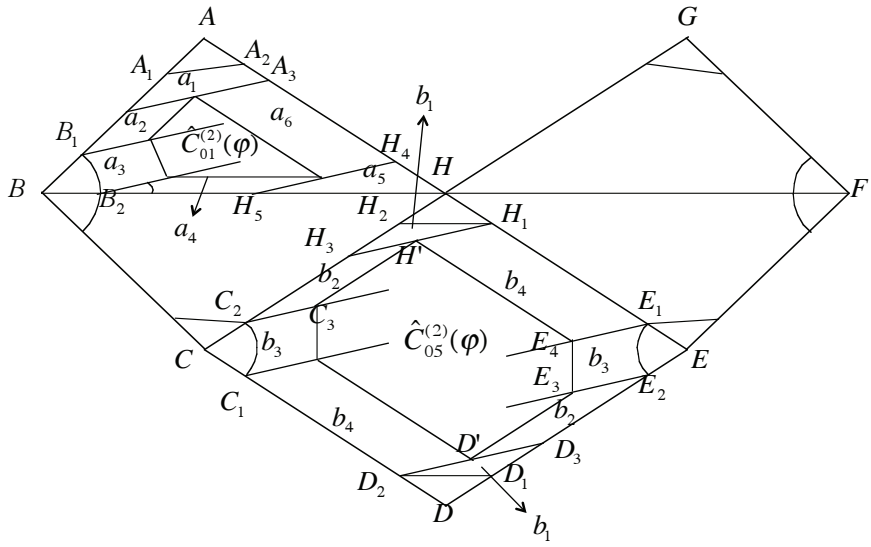


fig.16

From this figure we have

$$area\widehat{C}_{01}^{(2)}(\varphi) = area\widehat{C}_{02}^{(2)}(\varphi) = area\widehat{C}_{03}^{(2)}(\varphi) = area\widehat{C}_{04}^{(2)}(\varphi) =$$

$$areaC_{01}^{(2)} - [areac_1(\varphi) + areac_2(\varphi) + ... + areac_6(\varphi)], \tag{38}$$

$$area\widehat{C}_{05}^{(2)}(\varphi) = areaC_{05} - 2[aread_1(\varphi) +$$

$$aread_2(\varphi) + aread_3(\varphi) + aread_4(\varphi)]. \tag{39}$$

The figures 2 and 16 give us

$$areac_1(\varphi) = areaa_1(\varphi), \quad areac_2(\varphi) = areaa_2(\varphi),$$

$$areac_4(\varphi) = areaa_4(\varphi), \quad areac_5(\varphi) = areaa_5(\varphi),$$

$$areac_6(\varphi) = areaa_6(\varphi), \tag{40}$$

$$aread_1(\varphi) = areab_1(\varphi), \quad aread_2(\varphi) = areab_2(\varphi),$$

$$aread_4(\varphi) = areab_4(\varphi), \tag{41}$$

To compute $areac_3(\varphi)$ we consider the figure

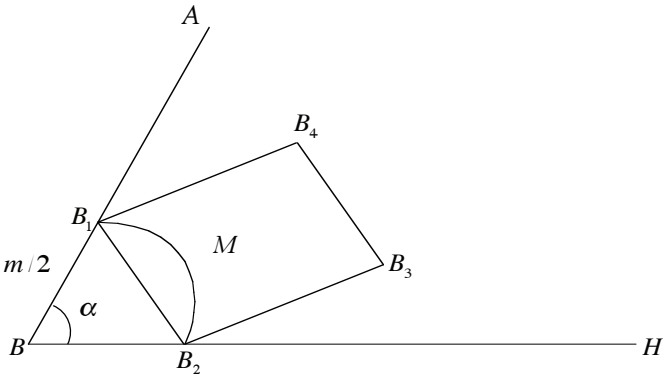


fig.17

From this figure and from the figure 5 follow

$$areac_3(\varphi) = areaa_3(\varphi) - area(circular\ segment\ B_1MB_2).$$

Considering the relations (36) and (3) we have

$$areac_3(\varphi) = areaa_3(\varphi) - \frac{m^2}{8}(\alpha - \sin\alpha). \tag{42}$$

In the same way, the figure

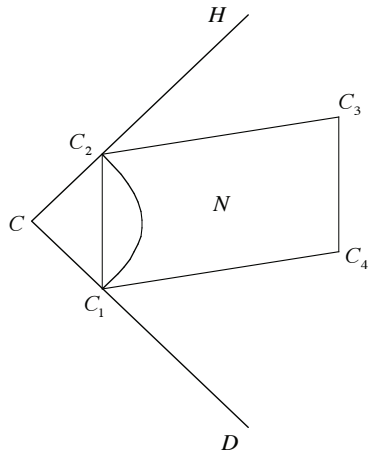


fig.18

and the figure 11 with the formulas (36) and (3) give us

$$aread_3(\varphi) = areab_3(\varphi) - \frac{m^2}{8}(2\beta - \sin 2\beta). \tag{43}$$

From the relations (19), (38), (40) and (42) we have

$$area\widehat{C}_{01}^{(2)}(\varphi) = area\widehat{C}_{01}^{(1)}(\varphi) - \frac{m^2}{8}(\alpha - \sin\alpha), \tag{44}$$

while the relationes (28), (39), (41) and (43) give us

$$area\widehat{C}_{05}^{(2)}(\varphi) = area\widehat{C}_{05}^{(1)}(\varphi) - \frac{m^2}{8}(2\beta - \sin 2\beta). \tag{45}$$

With the notations of the section 1, we have

$$P_{int}^{(2)} = 1 - \frac{\mu\left(N_1^{(2)}\right) + \mu\left(N_2^{(2)}\right) + ... + \mu\left(N_5^{(2)}\right)}{\mu\left(M_1^{(2)}\right) + \mu\left(M_2^{(2)}\right) + ... + \mu\left(M_5^{(2)}\right)}. \tag{46}$$

Considering of the relations (31) and (32) we can write

$$\mu\left(M_1^{(2)}\right) = \mu\left(M_2^{(2)}\right) = \mu\left(M_3^{(2)}\right) = \mu\left(M_4^{(2)}\right) =$$

$$\mu\left(M_1^{(1)}\right) - \frac{m^2}{8}\alpha(\alpha - \sin\alpha), \tag{47}$$

$$\mu\left(M_5^{(2)}\right) = \mu\left(M_5^{(1)}\right) - \frac{m^2}{8}(\pi - 2\beta)(2\beta - \sin 2\beta).$$

At the end the formulas (33), (34), (44) and (45) give us

$$\mu\left(N_1^{(2)}\right) = \mu\left(N_2^{(2)}\right) = \mu\left(N_3^{(2)}\right) = \mu\left(N_4^{(2)}\right) =$$

$$\mu\left(N_1^{(1)}\right) - \frac{m^2}{8}\alpha(\alpha - \sin\alpha), \tag{48}$$

$$\mu\left(N_5^{(2)}\right) = \mu\left(N_5^{(1)}\right) - \frac{m^2}{8}(2\beta - \sin 2\beta)$$

From the relations (46), (47) and (48) follow

$$P_{int}^{(2)} = 1 - \frac{4\mu\left(N_1^{(1)}\right) - \frac{m^2}{2}\alpha(\alpha - \sin\alpha) + \mu\left(N_5^{(1)}\right) - \frac{m^2}{8}(\pi - 2\beta)(2\beta - \sin 2\beta)}{4\mu\left(M_1^{(1)}\right) - \frac{m^2}{2}\alpha(\alpha - \sin\alpha) + \mu\left(M_5^{(1)}\right) - \frac{m^2}{8}(\pi - 2\beta)(2\beta - \sin 2\beta)}. \tag{49}$$

The formula (29) give us

$$4\mu\left(N_1^{(1)}\right) + \mu\left(N_5^{(1)}\right) = \left[4\mu\left(M_1^{(1)}\right) + \mu\left(M_5^{(1)}\right)\right]\left(1 - P_{int}^{(1)}\right).$$

Replacing this relation in the (49) we obtain

$$P_{int}^{(2)} = \frac{4\mu\left(N_1^{(1)}\right) + \mu\left(N_5^{(1)}\right)}{4\mu\left(M_1^{(1)}\right) + \mu\left(M_5^{(1)}\right) - \frac{m^2}{8}\left[4\alpha(\alpha - \sin\alpha) + (\pi - 2\beta)(2\beta - \sin 2\beta)\right]} \cdot P_{int}^{(1)},$$

therefore

$$P_{int}^{(2)} = \frac{\frac{2\sin\alpha}{\sin\beta}\left[\alpha\sin(\alpha+\beta)+(\pi-2\beta)\sin\alpha\cos\beta\right]a^2-}{\frac{2\sin\alpha}{\sin\beta}\left[\alpha\sin(\alpha+\beta)+(\pi-2\beta)\sin\alpha\cos\beta\right]a^2-}$$

$$\frac{\left[\alpha\sin(\alpha+\beta)-\alpha\sin\alpha+(\pi-2\beta)\sin 2\beta\right]m^2}{\left[\alpha\sin(\alpha+\beta)-\alpha^2+\left(\frac{\pi}{2}-\beta\right)(\beta+3\sin\beta\cos\beta)\right]\frac{m^2}{2}}\cdot P_{int}^{(1)}.$$

From here follow

$$P_{int}^{(2)} \leq P_{int}^{(1)}$$

and, for $m = 0$,

$$P_{int}^{(2)} = P_{int}^{(1)}$$

References

[1] Poincaré H., Calcul des probabilitiés, ed. 2, Carré, Paris, 1912.

[2] Stoka M., Probabilités géométriques de type Buffon dans le plan euclidien, Atti Acc. Sci. Torino, T. 110, pp. 53-59, 1975-1976.

RENDICONTI DEL CIRCOLO MATEMATICO DI PALERMO
Serie II, Suppl. 84 (2012), pp. 127-156

A Buffon-Laplace type problem for two lattices of Delone with obstacles

G. Caristi* and Marius Stoka**
*Department S.E.A.
University of Messina
**Accademia delle Scienze di Torino

Deditcated to Professor
P. M. Gruber
in occasion of his 70^{th} *birthday*

Abstract

In this paper we consider two lattice of Delone with the cell represented in the figure 1 and in the figure 16 and we compute the probability that a segment of random position and costant length intersects a side of lattice.

Keywords: Geometric Probability, stochastic geometry, random sets, random convex sets and integral geometry.

1 Triangle cell

Let $\Re_1(a, \alpha; m)$ be the irregular lattice of Delone with fundamental cell $C_0^{(1)}$ represented in the figure

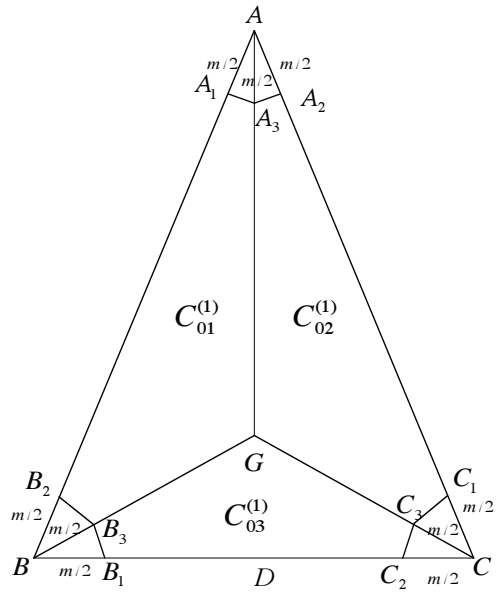


fig.1

where $\alpha \in \left]0, \frac{\pi}{2}\right[$ is an angle and $0 \leq m \leq \min(a, 2a\cos\alpha)$ and the lines AG, BG, and CG are the bisettrici of the respective angles.

From the figure 1 we have the follow relations

$$|BC| = 2a\cos\alpha, \qquad |AD| = a\sin\alpha$$

$$|AG| = a\tan\frac{\alpha}{2}, \qquad |DG| = a\cos\tan\frac{\alpha}{2}, \qquad |BG| = \frac{a\cos\alpha}{\cos\frac{\alpha}{2}}, \tag{1}$$

$$\widehat{ABC} = \alpha, \qquad \widehat{BAG} = \frac{\pi}{2} - \alpha,$$

$$\widehat{ABG} = \frac{\alpha}{2}, \qquad \widehat{AGB} = \frac{\pi}{2} + \frac{\alpha}{2}, \tag{2}$$

$$|A_1A_3| = |A_2A_3| = \frac{m\sqrt{2}}{2}(\cos\frac{\alpha}{2} - \sin\frac{\alpha}{2}),$$

$$|B_1B_3| = |B_2B_3| = |C_1C_3| = |C_2C_3| = m\sin\frac{\alpha}{4},$$

$$areaAA_1A_3 = areaAA_2A_3 = \frac{m^2}{8}\cos\alpha,$$

$$areaBB_1B_3 = areaBB_2B_3 =$$

$$areaCC_1C_3 = areaCC_2C_3 = \frac{m^2}{8}\sin\frac{\alpha}{2}. \tag{3}$$

From this relations we obtain

$$areaC_{01}^{(1)} = areaC_{02}^{(1)} = \frac{\alpha^2}{2}\tan\frac{\alpha}{2}\cos\alpha - \frac{m^2}{8}\left(\cos\alpha + \sin\frac{\alpha}{2}\right),$$

$$areaC_{03}^{(1)} = a^2\cos\alpha\left(\sin\alpha - \tan\frac{\alpha}{2}\right) - \frac{m^2}{4}\sin\frac{\alpha}{4},$$

$$areaC_{0}^{(1)} = \frac{a^2\sin 2\alpha}{2} - \frac{m^2}{4}\sin\frac{\alpha}{4}.$$

Now we consider a segment s of random position and constant length $l < \min(a-m,\ 2a\cos\alpha - m)$ and we want compute the probability that this segment intersects a side of lattice; therefore this probability is equal to the probability $P_{int}^{(1)}$ that the segment intersects the side of the fundamental cell $C_0^{(1)}$.

The position of the segment s is determinated by his middle point O and by the angle φ that it forms with the side BC of the fundamental cell $C_0^{(1)}$.

To compute this probability we consider the limit positions of the segment s, for an assigned value of φ, in the cell $C_{0i}^{(1)}$, $(i = 1, 2, 3)$; we indicate with $\widehat{C}_{0i}^{(1)}(\varphi)$ the polygon determined from these positions we obtain the figure:

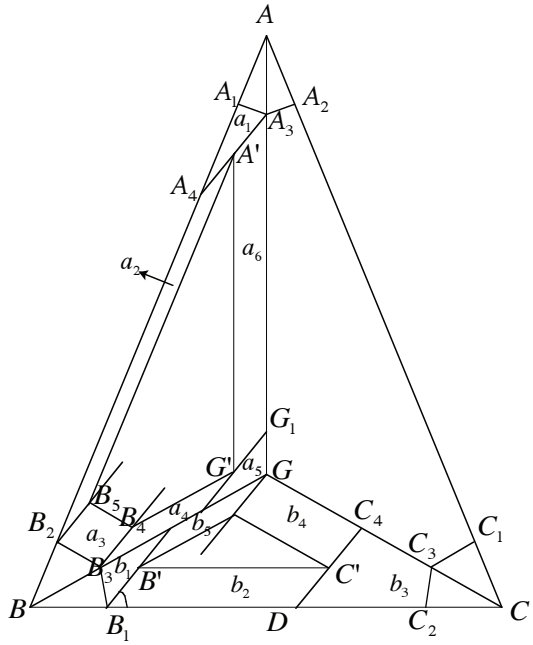


fig.2

Then considering the symmetry respect to the side AD of the cell $C_{01}^{(1)}$ and $C_{02}^{(1)}$, we can write

$$area\widehat{C}_{01}^{(1)}(\varphi) = area\widehat{C}_{02}^{(1)}(\varphi) =$$

$$areaC_{01}^{(1)} - [areaa_1(\varphi) + areaa_2(\varphi) + ... + areaa_6(\varphi)], \tag{4}$$

$$area\widehat{C}^{(1)}(\varphi) = areaC_{03}^{(1)}(\varphi) - [areab_1(\varphi) + areab_2(\varphi) + ... + areab_5(\varphi)]. \tag{5}$$

To compute $areaa_1(\varphi)$ we consider the figure

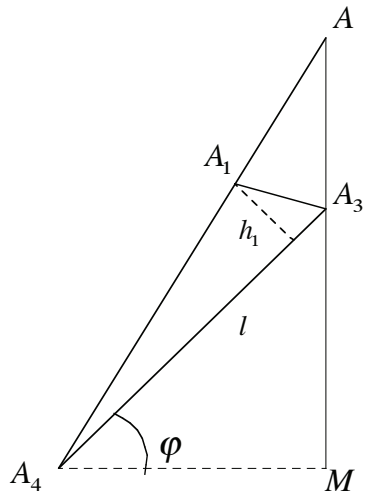


fig.3

We have

$$\widehat{A_3AA_4} = \frac{\pi}{2} - \alpha, \quad \widehat{AA_4A_3} = \widehat{AA_4M} - \widehat{A_3A_4M} = \alpha - \varphi,$$

$$\widehat{AA_3A_4} = \frac{\pi}{2} + \varphi. \tag{6}$$

The triangle AA_3A_4 follow that:

$$\frac{l}{\sin\left(\frac{\pi}{2} - \alpha\right)} = \frac{|AA_4|}{\sin\left(\frac{\pi}{2} + \varphi\right)} = \frac{|AA_3|}{\sin(\alpha - \varphi)},$$

therefore,

$$\frac{l}{\cos\alpha} = \frac{|AA_4|}{\cos\varphi} = \frac{m}{2\sin(\alpha - \varphi)}.$$

From here follow

$$|AA_4| = \frac{l\cos\varphi}{\cos\alpha} \tag{7}$$

and the condition

$$m\cos\alpha = 2l\sin(\alpha - \varphi). \tag{8}$$

With the (9) we have

$$|A_1A_4| = |AA_4| - \frac{m}{2} = \frac{l\cos\varphi}{\cos\alpha} - \frac{m}{2}$$

and consequently

$$h_1 = |A_1A_3| \cdot \sin(\alpha - \varphi) = \left(\frac{l\cos\varphi}{\cos\alpha} - \frac{m}{2}\right)\sin(\alpha - \varphi).$$

Then

$$areaa_1(\varphi) = \frac{lh_1}{2} - areaAA_1A_{3,}$$

therefore, considering the (4),

$$areaa_1(\varphi) = \left(\frac{l\cos\varphi}{\cos\alpha} - \frac{m}{2}\right) \cdot \frac{l}{2}\sin(\alpha - \varphi) - \frac{m^2}{8}\cos\alpha. \tag{9}$$

The figure

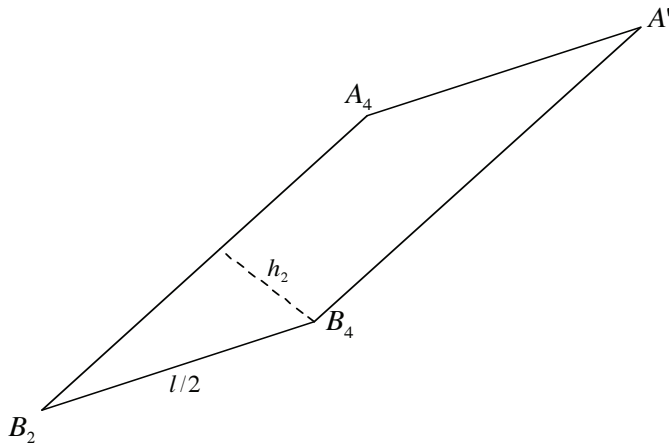


fig.4

and the relations (8) e (9), give us

$$|A_4B_2| = a - \frac{m}{2} - |AA_4| = a - \frac{m}{2} - \frac{l\cos\varphi}{\cos\alpha},$$

$$\widehat{A_4B_2B_4} = \widehat{AA_4A_3} = \alpha - \varphi,$$

$$h_2 = \frac{l}{2}\sin(\alpha - \varphi).$$

Therefore

$$areaa_2(\varphi) = \left(a - \frac{m}{2} - \frac{l\cos\varphi}{\cos\alpha}\right) \cdot \frac{l}{2}\sin(\alpha - \varphi). \tag{10}$$

From the relations (11) e (12) we obtain

$$areaa_1(\varphi) + areaa_2(\varphi) = (a-m)\frac{l}{2}\sin(\alpha-\varphi) - \frac{m^2}{8}\cos\alpha. \tag{11}$$

Now we consider the figure

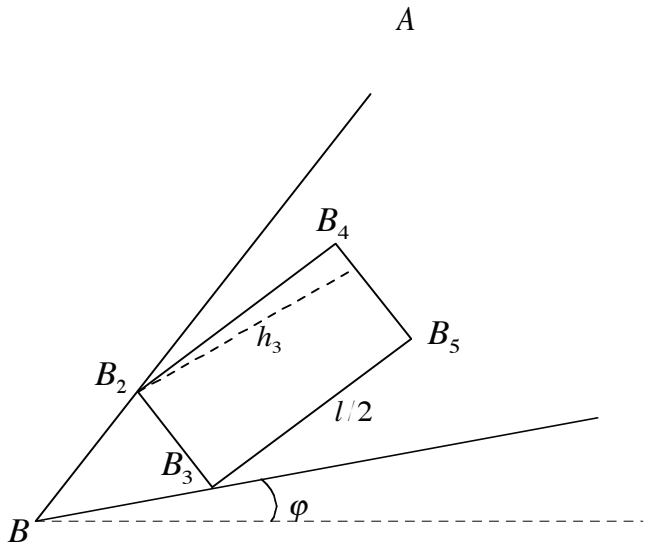


fig.5

We have

$$\widehat{AB_2B_4} = \alpha - \varphi, \quad \widehat{BB_2B_3} = \frac{\pi}{2} - \frac{\alpha}{4},$$

$$\widehat{B_3B_2B_4} = \pi - \left(\alpha - \varphi + \frac{\pi}{2} - \frac{\alpha}{4}\right) = \frac{\pi}{2} - \frac{3\alpha}{4} + \varphi,$$

$$\widehat{B_2B_4B_5} = \pi - \widehat{B_3B_2B_4} = \frac{\pi}{2} - \varphi + \frac{3\alpha}{4},$$

$$h_3 = \frac{l}{2}\sin\widehat{B_2B_4B_5} = \frac{l}{2}\cos\left(\varphi - \frac{3\alpha}{4}\right).$$

Then condidering the (3),

$$areaa_3(\varphi) = |B_2B_3| \cdot h_3 = m\sin\frac{\alpha}{4} \cdot \frac{l}{2}\cos\left(\varphi - \frac{3\alpha}{4}\right),$$

therefore

$$areaa_3(\varphi) = \frac{ml}{2}\left(\sin\frac{\alpha}{4}\cos\frac{3\alpha}{4}\cdot\cos\varphi + \sin\frac{\alpha}{4}\sin\frac{3\alpha}{4}\cdot\sin\varphi\right) \tag{12}$$

We compute $areaa_5(\varphi)$ using the figure:

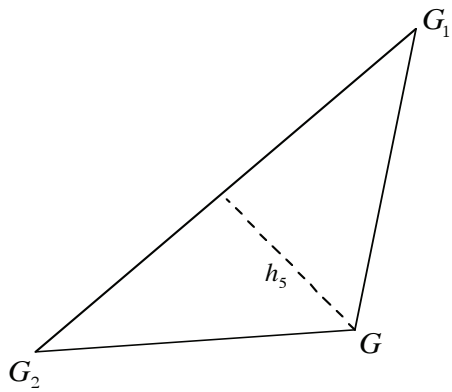


fig.6

$$\widehat{G_1GG_2} = \frac{\pi}{2} + \frac{\alpha}{2}$$

$$\widehat{GG_1G_2} = \frac{\pi}{2} - \varphi, \qquad \widehat{G_1G_2G} = \varphi - \frac{\alpha}{2}.$$

From the triangle GG_1G_2 follow

$$\frac{l}{\sin\left(\frac{\pi}{2}+\frac{\alpha}{2}\right)} = \frac{|GG_1|}{\sin\left(\varphi-\frac{\alpha}{2}\right)} = \frac{|GG_2|}{\sin\left(\frac{\pi}{2}-\varphi\right)}$$

therefore

$$|GG_1| = \frac{l\sin\left(\varphi-\frac{\alpha}{2}\right)}{\cos\frac{\alpha}{2}}, \qquad |GG_2| = \frac{l\cos\varphi}{\cos\frac{\alpha}{2}}. \tag{13}$$

From here we have:

$$h_5 = |GG_1|\sin\widehat{GG_1G_2} = \frac{l\sin\left(\varphi-\frac{\alpha}{2}\right)\cos\varphi}{\cos\frac{\alpha}{2}}. \tag{14}$$

Hence

$$areaa_5(\varphi) = \frac{lh_5}{2} = \frac{\sin\left(\varphi-\frac{\alpha}{2}\right)\cos\varphi}{\cos\frac{\alpha}{2}}\cdot\frac{l^2}{2} \tag{15}$$

The figure

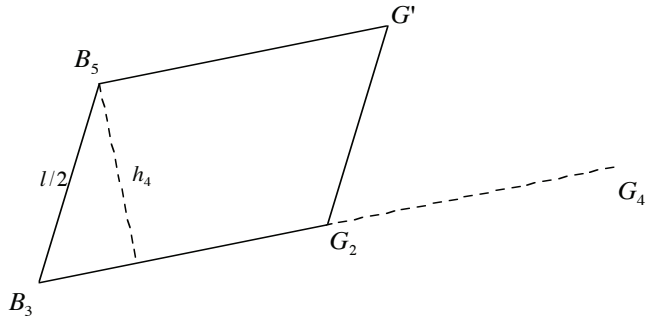


fig.7

give us

$$\widehat{B_5B_3B_2} = \widehat{G_1G_2G} = \varphi - \frac{\alpha}{2},$$

$$h_4 = \frac{l}{2}\sin\left(\varphi - \frac{\alpha}{2}\right)$$

and, with the (15)

$$|B_3G_2| = |BG| - \frac{m}{2} - |GG_2| = \frac{a\cos\alpha}{\cos\frac{\alpha}{2}} - \frac{m}{2} - \frac{l\cos\varphi}{\cos\frac{\alpha}{2}}.$$

Therefore

$$areaa_4(\varphi) = \left(\frac{a\cos\alpha}{\cos\frac{\alpha}{2}} - \frac{m}{2} - \frac{l\cos\varphi}{\cos\frac{\alpha}{2}}\right)\cdot\frac{l}{2}\sin\left(\varphi - \frac{\alpha}{2}\right). \tag{16}$$

The relations (15) and (16) give us

$$areaa_4(\varphi) + areaa_5(\varphi) = \left(\frac{a\cos\alpha}{\cos\frac{\alpha}{2}} - \frac{m}{2}\right)\cdot\frac{l}{2}\sin\left(\varphi - \frac{\alpha}{2}\right). \tag{17}$$

At the end, to compute $areaa_4(\varphi)$ we consider the figure

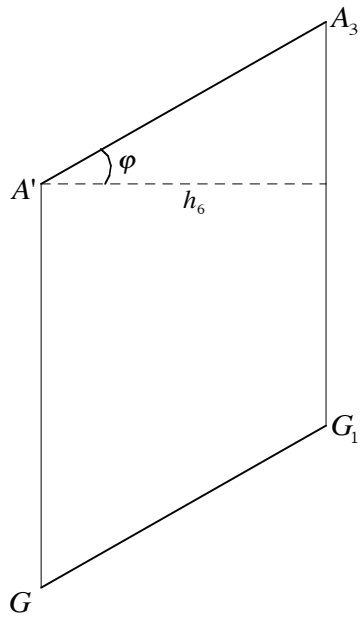


fig.8

We have

$$h_6 = \frac{l}{2}\cos\varphi$$

and, considering the (15),

$$|A_3G_1| = |AG| - \frac{m}{2} - |GG_1| = a\tan\frac{\alpha}{2} - \frac{m}{2} - \frac{l\sin\left(\varphi - \frac{\alpha}{2}\right)}{\cos\frac{\alpha}{2}}.$$

Consequently

$$area a_6(\varphi) = \left[a\cos\alpha\tan\frac{\alpha}{2} - \frac{m}{2} - \frac{l\sin\left(\varphi - \frac{\alpha}{2}\right)}{\cos\frac{\alpha}{2}}\right]\cdot\frac{l}{2}\cos\varphi. \qquad (18)$$

Replacing in the (6) the relations (11), (12), (17) and (18) and considering the (10) give us

$$area\widehat{C}_{01}^{(1)}(\varphi) = area\widehat{C}_{02}^{(1)}(\varphi) = areaC_{01}^{(1)} - \left\{\left[a\sin\alpha - \frac{m}{2}\left(\sin\alpha + \sin\frac{\alpha}{2} + 1\right)\right]\cdot\frac{\iota}{2}\cos\varphi +\right.$$

$$\frac{m}{2}\left(\cos\alpha + \cos\frac{\alpha}{2}\right)\cdot\frac{l}{2}\sin\varphi - \frac{l^2}{4\cos\alpha}\left[\left(\cos\alpha + \sin\frac{3\alpha}{2}\right)\cdot\sin 2\varphi +\right.$$

$$\left(\cos\frac{3\alpha}{2}-\cos\alpha\tan\frac{\alpha}{2}\right)\cdot\cos 2\varphi-\cos\alpha\tan\frac{\alpha}{2}-\cos\frac{\alpha}{2}\Big]-\frac{m^2}{8}\cos\alpha\Big\}. \quad (19)$$

To compute $areab_1(\varphi)$ we consider the figure

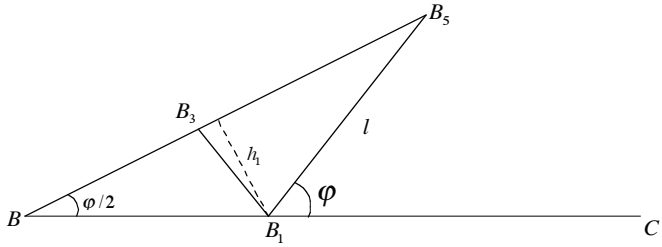


fig.9

We have

$$\widehat{BB_1B_3}=\widehat{BB_3B_1}=\frac{\pi}{2}-\frac{\alpha}{4},$$

$$\widehat{BB_5B_1}=\varphi-\frac{\alpha}{2},\qquad \widehat{BB_1B_5}=\pi-\varphi.$$

The triangle BB_1B_5 give us

$$\frac{|BB_5|}{\sin\varphi}=\frac{l}{\sin\frac{\alpha}{2}},$$

therefore

$$|BB_5|=\frac{l\sin\varphi}{\sin\frac{\alpha}{2}}. \quad (20)$$

Morover

$$h_1=l\sin\widehat{BB_5B_1}=l\sin\left(\varphi-\frac{\alpha}{2}\right)$$

and with the (21),

$$|B_3B_5|=|BB_5|-\frac{m}{2}=\frac{l\sin\varphi}{\sin\frac{\alpha}{2}}-\frac{m}{2}.$$

Hence

$$areab_1(\varphi)=\left(\frac{l\sin\varphi}{\sin\frac{\alpha}{2}}-\frac{m}{2}\right)\cdot\frac{l}{2}\sin\left(\varphi-\frac{\alpha}{2}\right) \quad (21)$$

The figure

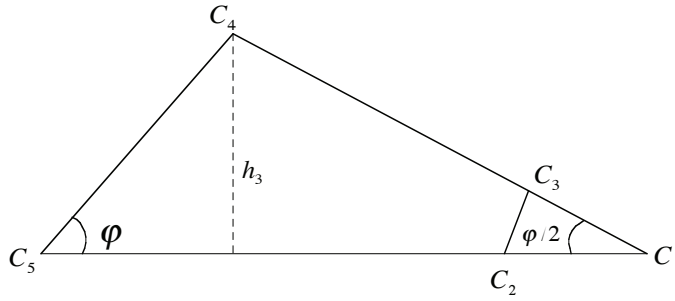


fig.10

give us

$$\widehat{C_5C_4C} = \pi - \left(\varphi + \frac{\alpha}{2}\right),$$

$$h_3 = l\sin\varphi,$$

while from the triangle CC_4C_5 follow

$$\frac{|CC_4|}{\sin\varphi} = \frac{|CC_5|}{\sin\left(\varphi + \frac{\alpha}{2}\right)} = \frac{l}{\sin\frac{\alpha}{2}}.$$

From here

$$|CC_4| = \frac{l\sin\varphi}{\sin\frac{\alpha}{2}}, \quad |CC_5| = \frac{l\sin\left(\varphi + \frac{\alpha}{2}\right)}{\sin\frac{\alpha}{2}}. \tag{22}$$

Hence, with the (4),

$$areab_3(\varphi) = \frac{|CC_5|\cdot k_3}{2} - \frac{m^2}{8}\sin\frac{\alpha}{2},$$

therefore

$$areab_3(\varphi) = \frac{l^2\sin\varphi\sin\left(\varphi + \frac{\alpha}{2}\right)}{2\sin\frac{\alpha}{2}} - \frac{m^2}{8}\sin\frac{\alpha}{2}. \tag{23}$$

To compute $areab_2(\varphi)$ considering the figure

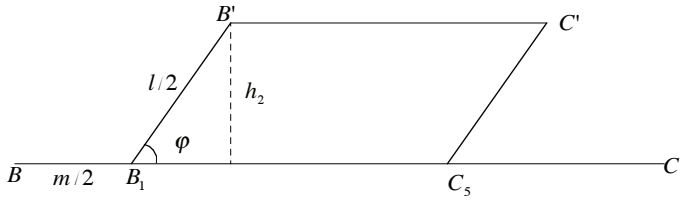


fig.11

This figure and the relations (1) and (22) give us

$$|B_1B_5| = |BC| - \frac{m}{2} - |CC_5| = 2\alpha\cos\alpha - \frac{m}{2} - \frac{l\sin\left(\varphi+\frac{\alpha}{2}\right)}{\sin\frac{\alpha}{2}}. \tag{24}$$

and

$$h_2 = \frac{l}{2}\sin\varphi.$$

Hence

$$areab_2(\varphi) = \left[2\alpha\cos\alpha - \frac{m}{2} - \frac{l\sin\left(\varphi+\frac{\alpha}{2}\right)}{\sin\frac{\alpha}{2}}\right]\cdot\frac{l}{2}\sin\varphi. \tag{25}$$

From the relations (23) and (25) follow

$$areab_2(\varphi) + areab_3(\varphi) = \left(2\alpha\cos\alpha - \frac{m}{2}\right)\cdot\frac{l}{2}\sin\varphi - -\frac{m^2}{8}\sin\frac{\alpha}{2}. \tag{26}$$

Now, we consider the figure

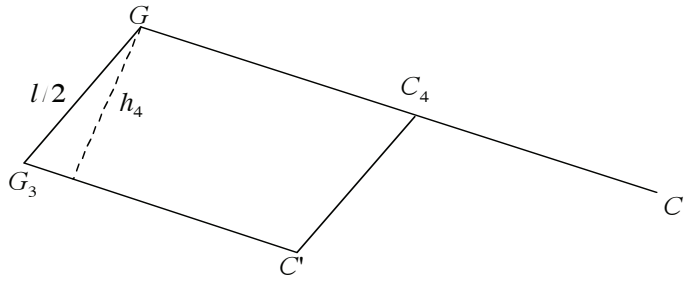


fig.12

The (23) give us

$$\widehat{C'C_4C} = \pi - \widehat{C_5C_4C} = \varphi + \frac{\alpha}{2},$$

therefore

$$h_4 = \frac{l}{2}\sin\widehat{C'C_4C} = \frac{l}{2}\sin\left(\varphi+\frac{\alpha}{2}\right).$$

$$|GC_4| = |CG| - |CC_4| = \frac{a\cos\alpha}{\cos\frac{\alpha}{2}} - \frac{l\sin\varphi}{\sin\frac{\alpha}{2}}.$$

Therefore

$$areab_4(\varphi) = \left(\frac{a\cos\alpha}{\cos\frac{\alpha}{2}} - \frac{l\sin\varphi}{\sin\frac{\alpha}{2}}\right)\cdot\frac{l}{2}\sin\left(\varphi+\frac{\alpha}{2}\right). \tag{27}$$

At the end we considering the figure

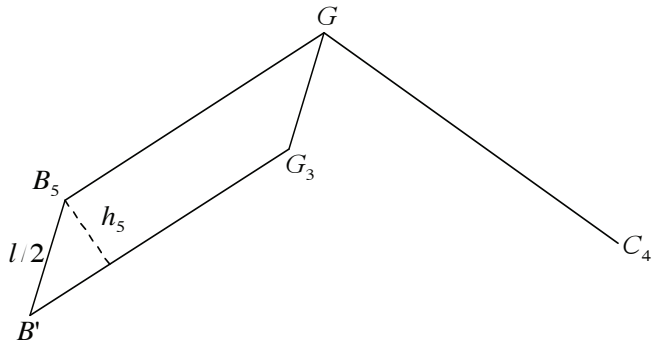


fig.13

We have

$$\widehat{B_5GG_3} = \widehat{BGC} - \widehat{G_3GC_4} = \pi - \alpha - \widehat{G_5C_4C} = \varphi - \frac{\alpha}{2},$$

therefore

$$h_5 = \frac{l}{2}\sin\left(\varphi - \frac{\alpha}{2}\right).$$

In the same way, with the (20) we have

$$|B_5G| = |BG| - |BB_5| = \frac{a\cos\alpha}{\cos\frac{\alpha}{2}} - \frac{l\sin\varphi}{\sin\frac{\alpha}{2}}$$

Hence

$$areab_5(\varphi) = \left(\frac{a\cos\alpha}{\cos\frac{\alpha}{2}} - \frac{l\sin\varphi}{\sin\frac{\alpha}{2}}\right)\cdot\frac{l}{2}\sin\left(\varphi - \frac{\alpha}{2}\right). \tag{28}$$

The relations (21) and (28) give us

$$areab_1(\varphi) + areab_5(\varphi) = \left(\frac{a\cos\alpha}{\cos\frac{\alpha}{2}} - \frac{m}{2}\right)\cdot\frac{l}{2}\sin\left(\varphi - \frac{\alpha}{2}\right). \tag{29}$$

Replacing in the (7) the expressions (26), (27), and (29) we obtain:

$$area\widehat{C}_{03}^{(1)}(\varphi) = areaC_{03}^{(1)} -$$

$$\left\{\frac{m\sin\frac{\alpha}{2}}{4}\cdot l\cos\varphi + \left[a\cos\alpha - \frac{m}{4}\left(1+\cos\frac{\alpha}{2}\right)\right]l\sin\varphi -\right.$$

$$\left.\frac{l^2}{4}\left(\sin 2\varphi - \cot\frac{\alpha}{2}\cdot\cos 2\varphi + \cot\frac{\alpha}{2}\right) - \frac{m^2}{8}\sin\frac{\alpha}{2}\right\}. \tag{30}$$

Denoting with $M_1^{(1)}$ the set of segments s which have the middle point in $C_{0i}^{(1)}$ and with $N_i^{(1)}$ the set of segments s completely contained in $C_{0i}^{(1)}$, $(i = 1, 2, 3)$, we have that [2]:

$$P_{int}^{(1)} = 1 - \frac{\mu\left(N_1^{(1)}\right) + \mu\left(N_2^{(1)}\right) + \mu\left(N_3^{(1)}\right)}{\mu\left(M_1^{(1)}\right) + \mu\left(M_2^{(1)}\right) + \mu\left(M_3^{(1)}\right)}, \tag{31}$$

where μ is the Lebesgue measure in Euclidean plane.

We compute the measures $\mu\left(M_i^{(1)}\right)$ and $\mu\left(N_i^{(1)}\right)$ using the Poincaré kinematic measure [1]

$$dK = dx \wedge dy \wedge d\varphi,$$

where x, y are the coordinates of the point O and φ the defined angle.

The figure

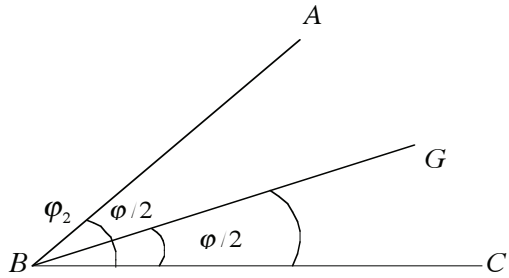


fig.14

give us

$$\varphi_1 = \frac{\alpha}{2}, \qquad \varphi_2 = \alpha$$

therefore, for the celles $C_{01}^{(1)}$ and $C_{02}^{(1)}$, we have

$$\varphi \in \left[\frac{\alpha}{2}, \alpha\right]. \tag{32}$$

The figure

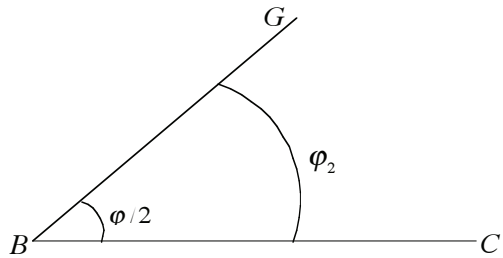


fig.15

give us

$$\varphi_1 = 0, \quad \varphi_2 = \frac{\alpha}{2},$$

therefore, for the celles C_{03}, we have

$$\varphi \in \left[0, \frac{\alpha}{2}\right]. \tag{33}$$

The relations (19), (30) and (32) give us

$$\mu\left(M_1^{(1)}\right) = \mu\left(M_2^{(1)}\right) = \int\limits_{\frac{\alpha}{2}}^{\alpha} d\varphi \iint\limits_{\left\{(x,y)\in C_{01}^{[1]}\right\}} dxdy = \int\limits_{\frac{\alpha}{2}}^{\alpha} \left(areaC_{01}^{(1)}\right) d\varphi = \frac{\alpha}{2} areaC_{01}^{(1)},$$

$$\mu\left(N_1^{(1)}\right) = \mu\left(N_2^{(1)}\right) = \int\limits_{\frac{\alpha}{2}}^{\alpha} d\varphi \iint\limits_{\left\{(x,y)\in \widehat{C}_{01}^{(1)}(\varphi)\right\}} dxdy = \int\limits_{\frac{\alpha}{2}}^{\alpha} \left[area\widehat{C}_{01}\left(\varphi\right)\right] d\varphi =$$

$$= \frac{\alpha}{2} areaC_{01}^{(1)} - \left\{\left(a\sin\alpha - \frac{m}{2}\right)\left(\sin\alpha - \sin\frac{\alpha}{2}\right)\cdot\frac{l}{2} -\right.$$

$$\frac{l^2}{8\cos\alpha}\left[2\sin\frac{\alpha}{2} - \cos\alpha\tan\frac{\alpha}{2}\left(\sin 2\alpha - \sin\alpha\right) -\right.$$

$$\left.\left.\cos\alpha\left(\cos 2\alpha - \cos\alpha\right) - \frac{\alpha}{2}\left(\cos\alpha\tan\frac{\alpha}{2} - \cos\frac{\alpha}{2}\right)\right] - \frac{\alpha m^2}{16}\sin\frac{\alpha}{2}\right\}. \tag{34}$$

The relations (30) and (33) give us

$$\mu\left(M_3^{(1)}\right) = \int\limits_{0}^{\frac{\alpha}{2}} d\varphi \iint\limits_{\left\{(x,y)\in \widehat{C}_{03}^{(1)}(\varphi)\right\}} dxdy = \int\limits_{0}^{\frac{\alpha}{2}} \left(areaC_{03}^{(1)}\left(\varphi\right)\right) d\varphi = \frac{\alpha}{2} area\widehat{C}_{03}^{(1)}$$

$$\mu\left(N_3^{(1)}\right) = \int\limits_{0}^{\frac{\alpha}{2}} d\varphi \iint\limits_{\left\{(x,y)\in \widehat{C}_{03}^{(1)}(\varphi)\right\}} dxdy = \int\limits_{0}^{\frac{\alpha}{2}} \left[area\widehat{C}_{03}^{(1)}\left(\varphi\right)\right] d\varphi = \frac{\alpha}{2} area\widehat{C}_{03}^{(1)} -$$

$$\left\{\left(a\sin\alpha - \frac{m}{2}\right)\left(\sin\alpha - \sin\frac{\alpha}{2}\right)\cdot\frac{l}{2} - \left[2\sin\frac{\alpha}{2} - \cos\alpha\tan\frac{\alpha}{2}\left(\sin 2\alpha - \sin\alpha\right) -\right.\right.$$

$$\left.\left.\cos\alpha\left(\cos 2\alpha - \cos\alpha\right) - \frac{\alpha}{2}\left(\cos\alpha\tan\frac{\alpha}{2} - \cos\frac{\alpha}{2}\right)\right]\frac{l^2}{8\cos\alpha} - \frac{\alpha m^2}{16}\sin\frac{\alpha}{2}\right\}. \tag{35}$$

Replacing in the (31) the relations (34) and (35) we obtain:

$$P_{int}^{(1)} = \frac{6}{\alpha\left(a^2\sin 2\alpha - \frac{m^2}{2}\sin\frac{\alpha}{2}\right)}\left\{\left(a\sin\alpha - \frac{m}{2}\right)\left(\sin\alpha - \sin\frac{\alpha}{2}\right)l - \right.$$

$$\left[2\sin\frac{\alpha}{2} - \cos\alpha\tan\frac{\alpha}{2}\left(\sin 2\alpha - \sin\alpha\right) - \cos\alpha\left(\cos 2\alpha - \cos\alpha\right) - \right.$$

$$\left.\left.\frac{\alpha}{2}\left(\cos\alpha\tan\frac{\alpha}{2} - \cos\frac{\alpha}{2}\right)\right]\frac{l^2}{4\cos\alpha} - \frac{\alpha m^2}{16}\sin\frac{\alpha}{2}\right\}.$$

When $m = 0$, this probability becomes:

$$P = \frac{6}{\alpha a^2\sin 2\alpha}\left\{a\sin\alpha\left(\sin\alpha - \sin\frac{\alpha}{2}\right)l - \right.$$

$$\left[2\sin\frac{\alpha}{2} - \cos\alpha\tan\frac{\alpha}{2}\left(\sin 2\alpha - \sin\alpha\right) - \cos\alpha\left(\cos 2\alpha - \cos\alpha\right) - \right.$$

$$\left.\left.\frac{\alpha}{2}\left(\cos\alpha\tan\frac{\alpha}{2} - \cos\frac{\alpha}{2}\right)\right]\frac{l^2}{4\cos\alpha}\right\}.$$

If here we take $\alpha = \frac{\pi}{3}$, (therefore the triangle ABC equilateral) we obtain

$$P = \frac{9\left(\sqrt{3}-1\right)}{\pi}\cdot\left(\frac{l}{a}\right) - \frac{\sqrt{3}}{3\pi}\left(18 + \sqrt{3}\pi\right)\cdot\left(\frac{l}{a}\right)^2.$$

2 Rectangle cell

Let $\Re_2(a, \alpha; m)$ be the lattice of Delone with fundamental cell $C_0^{(2)}$ represented in the figure

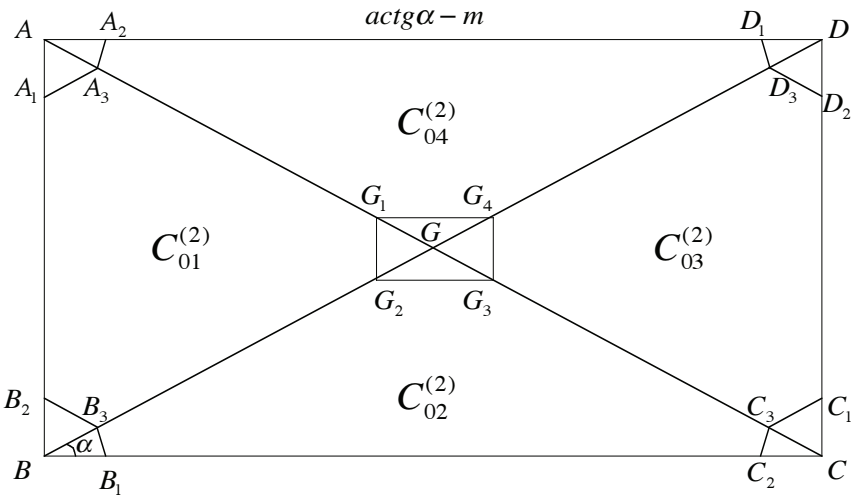


fig.16

where $\alpha \in \left]0, \frac{\pi}{4}\right[$ is an angle and $0 \leq m < (a, \frac{a}{2\sin\alpha})$.

From the figure 16 we have the follow relations

$$|BC| = a\cot\alpha, \qquad |BG| = \frac{a}{2\sin\alpha}, \tag{36}$$

$$\widehat{GBC} = \alpha, \quad \widehat{ABG} = \frac{\pi}{2} - \alpha, \quad \widehat{AGB} = 2\alpha, \tag{37}$$

$$|A_2A_3| = |B_1B_3| = |C_2C_3| = |D_1D_3| = m\sin\frac{\alpha}{2},$$

$$|A_1A_3| = |B_2B_3| = |C_1C_3| = |D_2D_3| = \frac{m\sqrt{2}}{2}\left(\cos\alpha - \sin\frac{\alpha}{2}\right),$$

$$|G_1G_2| = |G_3G_4| = m\sin\alpha, \qquad |G_2G_3| = |G_1G_4| = m\cos\alpha, \tag{38}$$

$$area AA_1A_3 = area BB_2B_3 = area CC_1C_3 = area DD_2D_3 = \frac{m^2}{8}\cos\alpha,$$

$$area AA_2A_3 = area BB_1B_3 = area CC_2C_3 = area DD_1D_3 = \frac{m^2}{8}\sin\alpha,$$

$$area GG_1G_2 = area GG_3G_4 = area GG_2G_4 = area GG_1G_4 = \frac{m^2}{8}\sin 2\alpha. \tag{39}$$

From this relations we obtain

$$area C_{01}^{(2)} = area C_{03}^{(2)} = \frac{\alpha^2}{4}\cot\alpha - \frac{m^2}{4}\cos\alpha\,(1+\sin\alpha)\,,$$

$$area C_{02}^{(2)} = area C_{04}^{(2)} = \frac{\alpha^2}{4}\cot\alpha - \frac{m^2}{4}\cos\alpha\,(1+\cos\alpha)\,,$$

$$areaC_0^{(2)} = a^2 \cot\alpha - \frac{m^2}{2}\left(\sin\alpha + \cos\alpha + \sin 2\alpha\right). \tag{40}$$

As in the point 1, we compute the probability $P_{int}^{(2)}$ that a segment of random position and of constant length $l < \min\left(a - m, \frac{a}{2\sin\alpha} - m\right)$ intersects a side of the fundamental cell $C_0^{(2)}$.

The position of the segment s is determinated by his middle point O and by the angle φ that it forms with the side BC of the fundamental cell $C_0^{(1)}$.

To compute this probability using the polygons $\widehat{C}_{0i}^{(2)}(\varphi)$, $(i = 1, 2, 3)$ we consider the limit positions of the segment situated in $C_{0i}^{(2)}$ for an assigned value of φ, (figure 17)

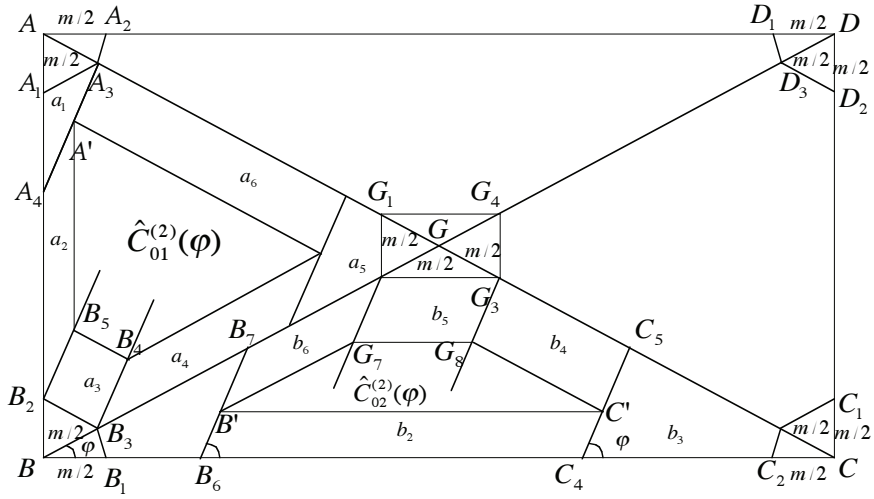


fig.17

From this figure and considering the central symmetry we can write

$$area\widehat{C}_{01}^{(2)}(\varphi) = area\widehat{C}_{03}^{(2)}(\varphi) =$$

$$areaC_{01}^{(2)} - \left[areaa_1(\varphi) + areaa_2(\varphi) + ... + areaa_6(\varphi)\right] \tag{41}$$

and

$$area\widehat{C}_{02}^{(2)}(\varphi) = area\widehat{C}_{04}^{(2)}(\varphi) - \left[areab_1(\varphi) + areab_2(\varphi) + ... + areab_6(\varphi)\right]. \tag{42}$$

We consider the figure

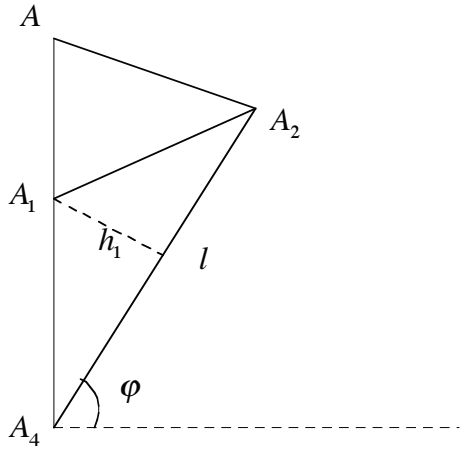


fig.18

We have

$$\widehat{AA_1A_2} = \widehat{AA_2A_1} = \frac{\pi}{4} + \frac{\alpha}{2}, \quad \widehat{A_4A_1A_3} = \frac{3\pi}{4} - \frac{\alpha}{2},$$
$$\widehat{A_1A_4A_3} = \frac{\pi}{2} - \varphi, \quad \widehat{A_1A_3A_4} = \varphi + \frac{\alpha}{2} - \frac{\pi}{4}. \tag{43}$$

The triangle $A_1A_3A_4$ give us

$$\frac{|A_1A_4|}{\sin\left(\varphi + \frac{\alpha}{2} - \frac{\pi}{2}\right)} = \frac{l}{\sin\left(\frac{\pi}{4} + \frac{\alpha}{2}\right)} = \frac{\frac{m\sqrt{2}}{2}\left(\cos\frac{\alpha}{2} - \sin\frac{\alpha}{2}\right)}{\cos\varphi}.$$

From here we have

$$|A_1A_4| = l\left(\sin\varphi - \frac{\cos\alpha}{1+\sin\alpha}\cos\varphi\right) \tag{44}$$

and the condition

$$m\sin\alpha\left(\sin\frac{\alpha}{2} + \cos\frac{\alpha}{2}\right) = \sqrt{2}l\cos\varphi, \qquad (m \neq 0). \tag{45}$$

With then (44) we have

$$h_1 = |A_1A_4| \cdot \sin\left(\frac{\pi}{2} - \varphi\right) = \left[\sin 2\varphi - \frac{\cos\alpha}{1+\sin\alpha}(1+\cos 2\varphi)\right] l.$$

Then

$$areaa_1(\varphi) = \left[\sin 2\varphi - \frac{\cos\alpha}{1+\sin\alpha}(1+\cos 2\varphi)\right]\frac{l^2}{4}. \tag{46}$$

The figure

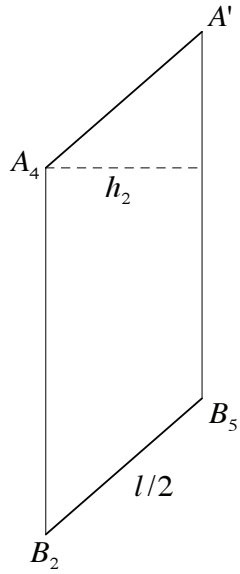


fig.19

and the (43) give us

$$\widehat{A_4B_2B_5} \;=\; \widehat{A_1A_4A_3} \;= \frac{\pi}{2} - \varphi.$$

Therefore

$$h_2 = \frac{l}{2} \sin \widehat{A_4B_2B_5} = \frac{l}{2} \cos \varphi,$$

and because, with the (47),

$$|A_4B_2| = a - m - \left(\sin \varphi - \frac{\cos \alpha}{1 + \sin \alpha} \cos \varphi \right) l,$$

we have

$$areaa_2 (\varphi) = \left[a - m - \left(\sin \varphi - \frac{\cos \alpha}{1 + \sin \alpha} \cos \varphi \right) l \right] \frac{l}{2} \cos \varphi,$$

hence

$$areaa_2 (\varphi) = \frac{(a-m)\, l}{2} \cos \varphi - \left[\sin 2\varphi - \frac{\cos \alpha}{1 + \sin \alpha} (1 + \cos \varphi) \right] \frac{l^2}{4}. \qquad (47)$$

The relations (46) and (47) we obtain

$$areaa_1 (\varphi) + areaa_2 (\varphi) = \frac{(a-m)\, l}{2} \cos \alpha. \qquad (48)$$

Now we consider the figure:

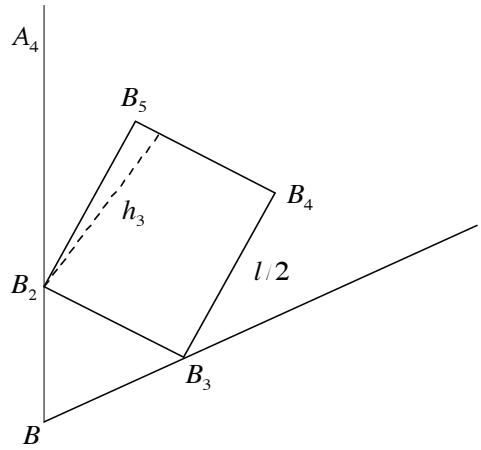


fig.20

we have

$$\widehat{B_2B_5B_4} = \pi - \widehat{B_5B_2B_3} = \widehat{A_4B_2B_5} + \widehat{BB_2B_3} = \frac{\pi}{2} - \varphi + \frac{\pi}{4} + \frac{\alpha}{2} = \frac{3\pi}{4} - \varphi + \frac{\alpha}{2},$$

therefore

$$h_3 = \frac{l}{2}\sin\left(\frac{3\pi}{4} - \varphi + \frac{\alpha}{2}\right) = \frac{l\sqrt{2}}{4}\left[\left(\cos\frac{\alpha}{2} - \sin\frac{\alpha}{2}\right)\cos\varphi + \left(\cos\frac{\alpha}{2} + \sin\frac{\alpha}{2}\right)\sin\varphi\right].$$

Then considering the (38) we obtain

$$areaa_3(\varphi) = \frac{ml}{4}\left[(1 - \sin\alpha)\cos\varphi + \cos\alpha\sin\varphi\right]. \tag{49}$$

To compute $areaa_5(\varphi)$ using the figure

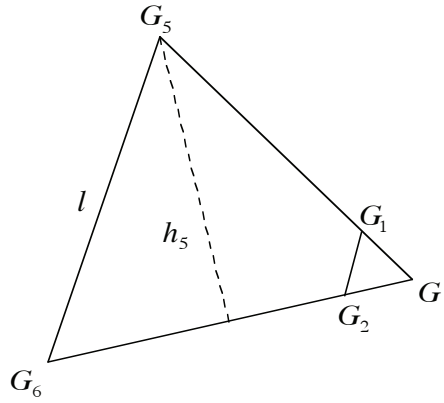


fig.21

we have

$$\widehat{G_5G_6G} = \widehat{B_4B_3G} = \widehat{BB_7B_4} = \varphi - \alpha,$$

therefore

$$h_5 = l \sin(\varphi - \alpha).$$

The triangle GG_5G_6 give us

$$\frac{|GG_5|}{\sin(\varphi - \alpha)} = \frac{l}{\sin 2\alpha} = \frac{|GG_6|}{\sin(\varphi + \alpha)},$$

hence

$$|GG_5| = \frac{l \sin(\varphi - \alpha)}{\sin 2\alpha}, \qquad |GG_6| = \frac{l \sin(\varphi + \alpha)}{\sin 2\alpha}. \tag{50}$$

Therefore

$$areaa_5(\varphi) = \frac{\sin(\varphi - \alpha)\sin(\varphi + \alpha)}{2 \sin 2\alpha} \cdot l^2 - \frac{m^2}{8} \sin 2\alpha. \tag{51}$$

The figure

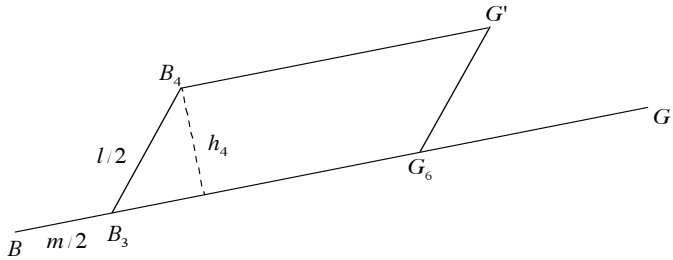


fig.22

give us

$$\widehat{B_4B_3G_6} = \widehat{G_5G_6G} = \varphi - \alpha,$$
$$h_4 = \frac{l}{2}\sin\left(\varphi - \frac{\alpha}{2}\right).$$

Then considering the (50), we have

$$|B_3G_6| = |BG| - \frac{m}{2} - |GG_6| = \frac{a}{2\sin\alpha} - \frac{m}{2} - \frac{l\sin(\varphi+\alpha)}{\sin 2\alpha}.$$

Consequently

$$areaa_4(\varphi) = \left[\frac{a}{\sin 2\alpha} - \frac{m}{2} - \frac{l\sin(\varphi+\alpha)}{\sin 2\alpha}\right]\cdot\frac{l}{2}\sin(\varphi-\alpha). \tag{52}$$

The relations (51) and (52) give us

$$areaa_4(\varphi) + areaa_5(\varphi) = \left(\frac{a}{\sin\alpha} - m\right)\frac{l}{4}\sin(\varphi-\alpha) - \frac{m^2}{8}\sin 2\alpha. \tag{53}$$

At the end, we consider the figure

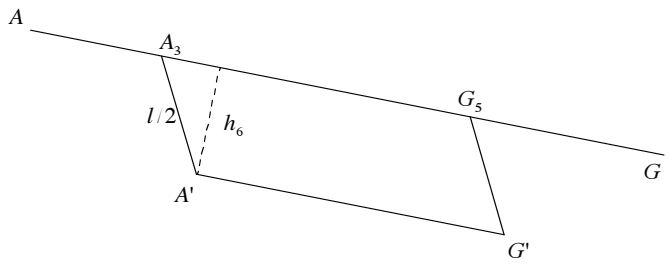


fig.23

From this figure and from (50) follow

$$|A_3G_5| = |AG| - \frac{m}{2} - |GG_5| = \frac{a}{2\sin\alpha} - \frac{m}{2} - \frac{l\sin(\varphi-\alpha)}{\sin 2\alpha}.$$

In the same way we have

$$\widehat{A'A_3G_5} = \widehat{G'G_5G} = \pi - (\varphi+\alpha),$$

therefore

$$h_6 = \frac{l}{2}\sin(\varphi+\alpha).$$

Hence

$$areaa_6(\varphi) = \left[\frac{a}{2\sin\alpha} - \frac{m}{2} - \frac{l\sin(\varphi-\alpha)}{\sin 2\alpha}\right]\cdot\frac{l}{2}\sin(\varphi+\alpha). \tag{54}$$

Replacing in the (41) the relations (48), (49), (53) and (54) we obtain

$$area\widehat{C}_{01}^{(2)}(\varphi) = area\widehat{C}_{03}^{(2)}(\varphi) = areaC_{01}^{(2)} - \left\{ \left[a - \frac{m(1+\sin\alpha)}{2} \right] \frac{l}{2} \cos\varphi + \right.$$

$$\left. \left(a\cot\alpha - \frac{m}{2}\cos\alpha \right) \cdot \frac{l}{2}\sin\varphi - \frac{l^2}{4\sin 2\alpha}(\cos 2\alpha - \cos 2\varphi) - \frac{m^2}{8}\sin 2\alpha \right\}. \quad (55)$$

To compute $areab_1(\varphi)$ we consider the figure

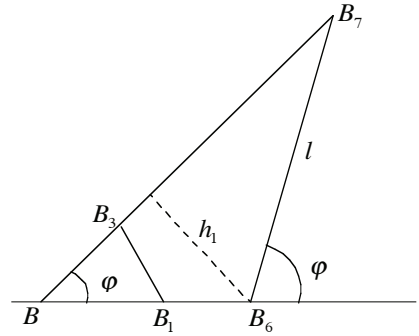


fig.24

We have

$$\widehat{BB_6B_7} = \pi - \varphi, \qquad \widehat{BB_7B_6} = \varphi - \alpha. \quad (56)$$

From the triangle BB_6B_7 follow

$$|BB_6| = \frac{l\sin(\varphi-\alpha)}{\sin\alpha}, \qquad |BB_7| = \frac{l\sin\varphi}{\sin\alpha}. \quad (57)$$

therefore, because

$$h_1 = l\sin(\varphi-\alpha),$$

we have

$$areaBB_6B_7 = \frac{|BB_7|\,h_1}{2} = \frac{l^2\sin\varphi\sin(\varphi-\alpha)}{2\sin\alpha}.$$

Consequently, considering the (39), we have

$$areab_1(\varphi) = \frac{l^2\sin\varphi\sin(\varphi-\alpha)}{2\sin\alpha} - \frac{m^2}{8}\sin\alpha. \quad (58)$$

From the figure

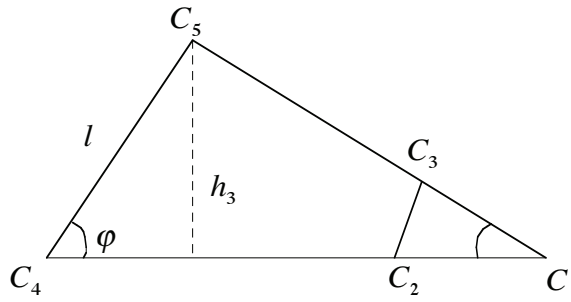


fig.25

follow

$$\widehat{C_4C_5C} = \pi - (\varphi + \alpha)\,.$$

$$h_3 = l \sin \varphi,$$

The triangle CC_4C_5 give us

$$\frac{|CC_4|}{\sin(\varphi+\alpha)} = \frac{|CC_5|}{\sin\varphi} = \frac{l}{\sin\alpha},$$

therefore

$$|CC_4| = \frac{l\sin(\varphi+\alpha)}{\sin\alpha}, \quad |CC_5| = \frac{l\sin\varphi}{\sin\alpha}. \tag{59}$$

Hence, because

$$h_3 = l\sin\varphi,$$

we have

$$areaCC_4C_5 = \frac{h_3 \cdot |CC_4|}{2} = \frac{l^2 \sin\varphi \sin(\varphi+\alpha)}{2\sin\alpha} \tag{60}$$

and considering the relations (39)

$$areab_{13} = \frac{l^2 \sin\varphi \sin(\varphi+\alpha)}{2\sin\alpha} - \frac{m^2}{8} \cdot \sin\alpha \tag{61}$$

Now we consider the figure

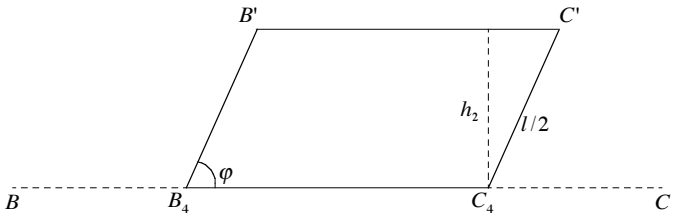


fig.26

From here follow

$$h_2 = \frac{l}{2}\sin\varphi,$$

and considering the relations (60) and (62)

$$|B_4C_4| = |BC| - |BB_4| - |CC_4| =$$
$$a\cot\alpha - \frac{l\sin(\varphi-\alpha)}{\sin\alpha} - \frac{l\sin(\varphi+\alpha)}{\sin\alpha}.$$

Hence

$$areab_2(\varphi) = \left[a\cot\alpha - \frac{l\sin(\varphi-\alpha)}{\sin\alpha} - \frac{l\sin(\varphi+\alpha)}{\sin\alpha}\right]\cdot\frac{l}{2}\sin\varphi. \qquad (62)$$

From the relations (58) (61) and (62) follow

$$areab_1(\varphi) + areab_2(\varphi) + areab_3(\varphi) = \frac{a\cot\alpha}{2}\cdot l\sin\varphi - \frac{m^2}{4}\sin\alpha. \qquad (63)$$

To compute $areab_4(\varphi)$ we consider the figure

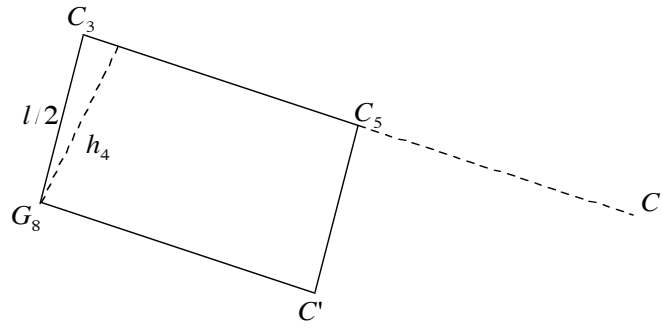


fig.27

We have

$$\widehat{G_8G_3C_5} = C'C_5C = \pi - (\varphi+\alpha),$$

therefore

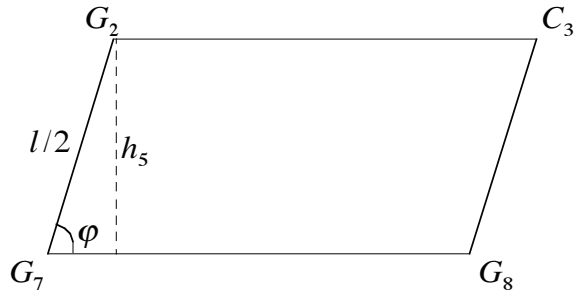
$$h_4 = \frac{l}{2}\sin(\varphi+\alpha).$$

Then, in the relations (36) and (59),

$$|G_3C_5| = |GC| - m - |CC_5| = \frac{a}{2\sin\alpha} - m - \frac{l\sin\varphi}{\sin\alpha},$$

hence

$$areab_4(\varphi) = \left(\frac{a}{2\sin\alpha} - m - \frac{l\sin\varphi}{\sin\alpha}\right)\cdot\frac{l}{2}\sin(\varphi+\alpha). \qquad (64)$$



This figure

fig.28

give us

$$h_5 = \frac{l}{2}\sin\varphi$$

and with the (41),

$$areab_5(\varphi) = \frac{m\cos\alpha}{2}\cdot l\sin\varphi. \tag{65}$$

At the end, we considering the figure

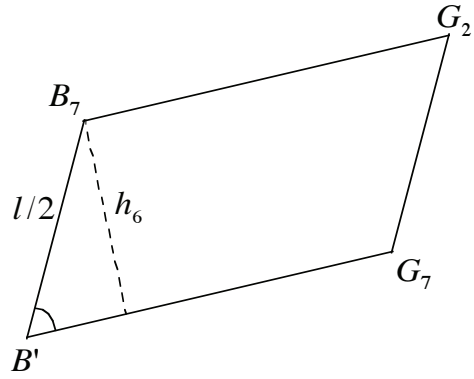


fig.29

and the relations (36), (56), (57), we have

$$|B_7G_2| = |BG| - m - |BB_7| = \frac{a}{2\sin\alpha} - m - \frac{l\sin\varphi}{\sin\alpha},$$

$$\widehat{B_7B'G_7} = \widehat{BB_7B_6} = \varphi - \alpha,$$

$$h_6 = \frac{l}{2}\sin(\varphi+\alpha).$$

Therefore

$$areab_6(\varphi) = \left(\frac{a}{2\sin\alpha} - m - \frac{l\sin\varphi}{\sin\alpha}\right)\cdot\frac{l}{2}\sin(\varphi-\alpha). \tag{66}$$

Replacing in the (42) the expressions (63), (64), (65) and (66) we obtain:

$$area\widehat{C}_{02}^{(2)}(\varphi) = area\widehat{C}_{04}(\varphi) = areaC_{02} -$$

$$\left\{\left[\frac{m}{4}\sin\alpha\cos\varphi + \frac{1}{2}(2a\cot\alpha - \frac{m}{2}\cos\alpha)\right] l -\right.$$

$$\left.\frac{l^2}{4}\cot\alpha\,(1-\cos 2\varphi) - \frac{m^2}{4}\sin\alpha\right\}. \tag{67}$$

With the notes of the point 1 (see the formula (31)), we have

$$P_{int}^{(2)} = 1 - \frac{\mu\left(N_1^{(2)}\right) + \mu\left(N_2^{(2)}\right) + \mu\left(N_3^{(2)}\right) + \mu\left(N_4^{(2)}\right)}{\mu\left(M_1^{(2)}\right) + \mu\left(M_2^{(2)}\right) + \mu\left(M_3^{(2)}\right) + \mu\left(M_4^{(2)}\right)}. \tag{68}$$

The figure

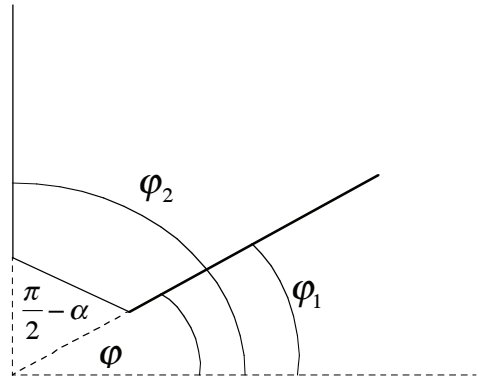


fig.30

give us

$$\varphi_1 = \alpha, \qquad \varphi_2 = \frac{\pi}{2},$$

therefore to compute the misure $\mu\left(M_1^{(2)}\right) = \mu\left(M_3^{(2)}\right)$ and $\mu\left(N_1^{(2)}\right) = \mu\left(N_3^{(2)}\right)$ we have

$$\varphi \in \left[\alpha, \frac{\pi}{2}\right].$$

The figure

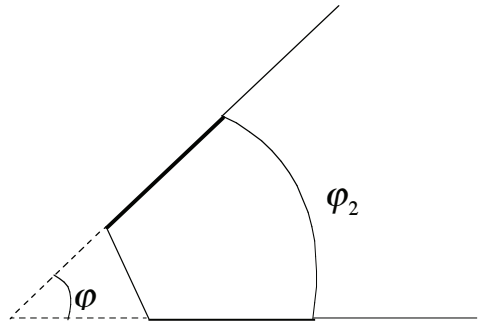


fig.31

give us

$$\varphi_1 = 0, \quad \varphi_2 = \alpha,$$

therefore, for the misure $\mu\left(M_2^{(2)}\right) = \mu\left(M_4^{(2)}\right)$ and $\mu\left(N_2^{(2)}\right) = \mu\left(N_4^{(2)}\right)$ we have

$$\varphi \in [0, \alpha].$$

We have

$$\mu\left(M_1^{(2)}\right) = \mu\left(M_3^{(2)}\right) = \int\limits_{\alpha}^{\frac{\pi}{2}} d\varphi \iint\limits_{\left\{(x,y)\in C_{02}^{[2]}\right\}} dxdy = \int\limits_{0}^{\alpha} \left[area C_{02}^{(2)}\right] d\varphi = \alpha area C_{02}^{(2)}.$$

Then, considering the formula (55) and (67), follow

$$\mu\left(N_1^{(2)}\right) = \mu\left(N_3^{(2)}\right) = \int\limits_{\alpha}^{\frac{\pi}{2}} d\varphi \iint\limits_{\left\{(x,y)\in \widehat{C}_{01}^{(2)}(\varphi)\right\}} dxdy = \int\limits_{\alpha}^{\frac{\pi}{2}} \left[area\widehat{C}_{01}(\varphi)\right] d\varphi =$$

$$= \left(\frac{\pi}{2} - \alpha\right) area C_{01}^{(2)} - \left\{\left(a + \frac{a\cos 2\alpha}{\sin\alpha} - m\cos^2\alpha\right)\frac{l}{2} -\right.$$

$$\left.\left|\frac{l^2}{4}\left[\left(\frac{\pi}{2} - \alpha\right)\cot 2\alpha - \frac{1}{2}\right] - \frac{m^2}{8}\left(\frac{\pi}{2} - \alpha\right)\sin 2\alpha\right\} \tag{69}$$

and

$$\mu\left(N_2^{(2)}\right) = \mu\left(N_4^{(2)}\right) = \int\limits_{\alpha}^{\frac{\pi}{2}} d\varphi \iint\limits_{\left\{(x,y)\in \widehat{C}_{02}^{(2)}(\varphi)\right\}} dxdy = \int\limits_{\alpha}^{\frac{\pi}{2}} \left[area\widehat{C^{(2)}}_{02}(\varphi)\right] d\varphi =$$

$$= \alpha area C_{02}^{(2)} - \left\{\left[a\cot\alpha\left(1 - \cos\alpha\right) + \frac{m}{4}\left(1 - 2\cos\alpha\right)\right] l -\right.$$

$$\left| \frac{l^2}{4} \cot \alpha \left(\alpha - \frac{\sin 2\alpha}{2} \right) - \frac{m^2}{4} \alpha \sin \alpha \right\}. \tag{70}$$

Replacing in the (68) the relation (69) and (70) we obtain:

$$P_{int}^{(2)} = \frac{8}{\pi \left[a^2 \cot \alpha - m^2 \cos \alpha \left(1 + \sin \alpha \right) \right] + 2\alpha m^2 \left(\cos \alpha - \sin \alpha \right)}$$

$$\left\{ \left[a \left(1 + \frac{2 \cos \alpha - 1}{\sin \alpha} \right) - m \left(\cos^2 \alpha + \cos \alpha - \frac{1}{2} \right) \right] l -$$

$$\left[(\pi - \sin 2\alpha) \cot \alpha - 1 \right] \frac{l^2}{4} - \frac{m^2}{4} \sin \alpha \left[2\alpha \left(1 - \cos \alpha \right) + \pi \cos \alpha \right] \right\}. \tag{71}$$

When $m = 0$ and $\alpha = \dfrac{\pi}{4}$ this probability (71) becomes:

$$P = \frac{8 \left(3 - \sqrt{2} \right)}{\pi} \cdot \frac{l}{a} - \frac{2 \left(\pi - 2 \right)}{\pi} \cdot \left(\frac{l}{a} \right)^2.$$

References

[1] Poincaré H., Calcul des probabilitiés, ed. 2, Carré, Paris, 1912.

[2] Stoka M., Probabilités géométriques de type Buffon dans le plan euclidien, Atti Acc. Sci. Torino, T. 110, pp. 53-59, 1975-1976.

RENDICONTI DEL CIRCOLO MATEMATICO DI PALERMO
Serie II, Suppl. 84 (2012), pp. 157-166

THE GLOBAL COMFORT CRITERIA AS A TOOL FOR THE OPTIMIZATION OF THE SAFETY, QUALITY AND EFFICIENCY IN THE RAILWAY TRACKS

CORRIERE F. - DI VINCENZO D.

Ferdinando Corriere*

Dario Di Vincenzo*

(*) Dipartimento di Architettura – Università degli Studi di Palermo

Il criterio del global comfort per l'ottimizzazione della sicurezza, della qualità e dell'efficienza nelle linee ferroviarie.

Riprendendo, gli esiti di alcune recenti memorie già presentate in occasione della VI International Conference of *"Stochastic Geometry, Convex Bodies, Empirical Measure & Applications To Mechanics And Engineering Of Train-Transport",* viene proposto un criterio, basato sull'analisi del global comfort, che consente di ottimizzare la sicurezza d'esercizio, la qualità di marcia dei convogli e l'efficienza economica degli interventi nell'ambito delle risorse disponibili.

The global comfort criteria as a tool for the optimization of the safety, quality and efficiency in the railway tracks

From the results of some memories already introduced in the VI International Conference of *"Stochastic Geometry, Convex Bodies, Empirical Measure & Applications To Mechanics And Engineering Of Train-Transport",* it's improved now a criteria, based on global comfort analyses , that allows to optimize the safety of the exercise, the quality and the economic efficiency into the available resources.

1. Experimental analysis with the global comfort theory.

The research for designing solutions suited to guarantee acceptable travelling safety and quality standards between two of any relationship origin-destination is one of the key-objectives which needs to be achieved whenever an intervention in a transport network is being carried out.

In fact, these particular configurations of the way, together with the peculiarities of the environment pertaining to the infrastructure under consideration and with the specific performance and efficiency properties of the vehicle produce specific "outputs" in the driver during the journey along the pre-established plan, yielding consequential travelling quality levels also for passengers.

The concept of "global comfort" implying the safety concept, can be therefore qualitatively formalized as a particular psychophysical condition in which a human being expresses his/her satisfactory relationship with the environment.

According to what has been said so far, the problem of investigating the conditions which can produce the comfort state for a user travelling at the speed V along a prearranged plan, with fixed operational configurations and a given vehicle, can be solved by researching the sets of the values which concern the elements of the system described above.

As a consequence, the group of the states of satisfaction towards the travelling quality standards expressed by a road or railway user can be seen as a particular subset of the states without discomfort. Thus, it follows that 'not to generate discomfort' is the necessary condition to experience a comfort state during the journey (Fig.1).

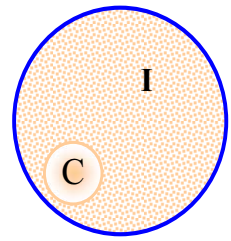


Fig. 1 - Set of the states without discomfort; C ⊂ I is the subset of the comfort configurations

According to such a definition, therefore, comfort can be seen as a subjective and logical value of the "human being system"; in *Boolean* terms, then, the value 1 or 0 can be given to the different configurations which take place in operation (the comfort state exists or it does not exist).[(2)]

If we then consider that in the present study several sensory organs are involved simultaneously, the condition of "global comfort" will be consequently obtained by means of a logical product and linked up to the concurrent presence of the comfort states concerning every single sector interested.

[(2)] For the abovementioned reasons, it is worth noting that, as regards comfort, only a scale of evaluation can be fixed, but not a unit.

In analytical terms, indicating the *global comfort* with C_g and the generic sensory class with the symbol j which defines the *relative comfort* indicator C_j among the d_s globally considered, it follows that

$$C_g = C_1 \wedge \ldots \wedge C_j \wedge \ldots \wedge C_d \qquad (1)$$

In order to fully define the problem, a human being can be considered as a system which continually interacts with the surrounding space if we look at the sensations s/he experiences by means of his/her own perceptive and sensory organs (seen as properties of the *boundary* of this set), while environment is meant to denote the set of natural or artificial elements with which a human being coexists and makes exchanges of different entity and typology (including, in such a broader meaning, the infrastructure and the vehicle).

A human being, then, may be assimilated to a system **S** which can be represented by means of appropriate coordinates in $\mathfrak{R}^d$; in such a system, however, the coexistence of the occurring balances (mechanical, chemical, thermal, etc..) is a necessary but inadequate condition to determine a state of global balance. Indeed, the observation of variables of the environment system **A**, as above defined, can induce in human beings such psychoemotional sensations to urge him/her to react and thus, in order to define the balance of the interactive relationship it is necessary to consider an appropriate interpretative model of the reality which is being examined here.

For this reason, let an appropriate variable U be considered which takes into due account the user's actions of adjustment and behavioural change following his/her interactions with the aforesaid system **A**.

Named $z_1,...z_h,...z_n$, then, the different sensations which play a role of independent variables of the system **S**, there will be a function so that

$$u = f(z_1, ..., z_h, ..., z_n); \qquad (2)$$

moreover, the achievement of the balance entails the existence of a particular function **φ** which satisfies the following relationship

$$u = \varphi(\alpha_1, ..., \alpha_k, ..., \alpha_m); \qquad (3)$$

being $\alpha_1, ..., \alpha_k, ..., \alpha_m$ the independent variables of the vehicle-infrastructure-environment system.

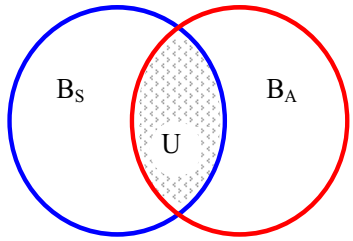


Fig. 2 - Set U of the values assumed by the variable u and obtained as an intersection of the sets of the values of the state indicators Bs in a human being with those BA concerning the vehicle-infrastructure-environment system.

From above, considering (2) and (3), it follows that

$$\Phi (z_1, ..., z_n, \alpha_1, ..., \alpha_m) = 0 \qquad (4)$$

(4) shows that the set $\mathbf{B_s}$ of the travelling user's state variables and the set $\mathbf{B_A}$ which characterizes the vehicle-infrastructure-environment trinomial, are composed of elements which lead to a subset intersection $\mathbf{U}$[(3)].

Now, let us observe the domains $Z = (z_1, ..., z_h, ..., z_n)$ and $= (\alpha_1, ..., \alpha_k, ..., \alpha_m)$ within which the above considered functions f and φ are defined[(4)], and the several interactions which take place in operation between the system **S**, i.e. road or railway user, and the system **A**, composed of all the elements which are external to the boundary of **S** and interfere with it, given

$$\mathbf{Z} = \mathbf{Z}_v \cup \mathbf{Z}_t \cup \mathbf{Z}_a \cup \mathbf{Z}_h \cup \ldots,$$

where the symbols, v, t, a, h, …, denote respectively the visual, thermal, acoustic, hygrometric, etc.. interactions, we obtain the following relation:

$$\mathbf{Z} \rightarrow \mathbf{U} \quad (5)$$

As a consequence, the set

$$A = \alpha_v \cup \alpha_t \cup \alpha_a \cup \alpha_h \cup \ldots,$$

in turn will result in a specific variable u characterizing the system **A,** with $u_i \subset \mathbf{U}$.

Operationally, the states of "Wellness" BS that the user faces the journey and those trio of BA-vehicle-environment and infrastructure belonging to the intersection subset U can be achieved with a series of management actions on security, efficiency and quality according to as shown in fig. follows.

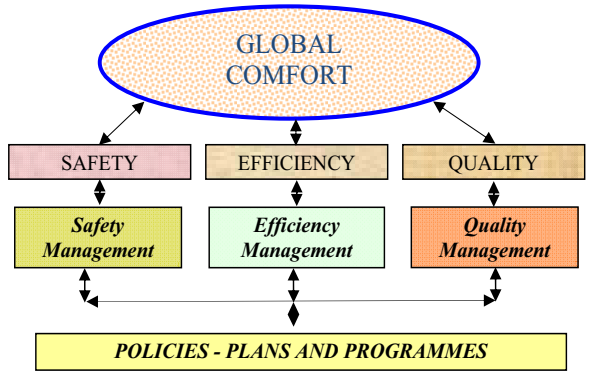


Fig. 3 - The attributes of the Global Comfort

Obviously, the actions described can be achieved through appropriate programs and action plans that enable the joint management of the three aspects mentioned.

---

(3) Similarly, it happens for instance to the temperature in the thermal equilibrium.

(4) If we consider, for example, the set of the values of the variables characterizing the interactions which take place in a moving condition (dynamic perspective vision [ ] [ ]), the relevant sensory duct enables the person concerned to have a one-way correspondence between the environmental values $\alpha_{1v}, ..., \alpha_{hv}, ..., \alpha_{nv}$ and the induced sensation $Z^{\tau}(v)$ which is registered at each moment $\tau \in [0,T]$, where T is the analysis period under consideration. Named $\mathbf{A_v}$, then, the set of values $\alpha_{1v}, ..., \alpha_{nv}$ and Z_v the set resulting from the values of the visual sensation, it follows that: $\mathbf{A_v \rightarrow Z_v \rightarrow U}$.

(5) Such one-way correspondence between the abovementioned values is given by the function f of (2).

2. *The maintenance planning of the railway superstructure as a tool for global comfort in railway management.*

By means of the instrumental measures carried out through diagnostic carriages or trains, it is possible to make an assessment of the state of a superstructure by comparing directly the threshold values which differentiate the warning level according to every geometrical parameter under consideration, with reference to the three above-described aspects of safety, efficiency and quality of travel with reference to the direct appreciation of the user.

The regulations on the survey of the track geometry, made by RFI, provide for three ***track quality levels*** according to which the 'full implementation of the line" is expected and a level which requires some operational restrictions on the railway in the form of slowing-down in the line and traffic block. More specifically, it is stated:

- ***1° quality level:*** in this field the geometry is to be considered in excellent conditions;
- ***2° quality level:*** in this field the geometry is to be monitored: it is indeed required to identify and assess the reasons why the deterioration has occurred, how the defect will evolve over time and finally, to plan maintenance works according to such a rate;
- ***3° quality level*** (or segment of intervention): in this field the implementation of the maintenance works is required within set times or on the basis of the value assumed by the Track Geometry Quality Index;
- ***level involving operational restrictions***: in this case some traffic slowing down or block is required.

The defects which are included in the last level as well as those in the 3rd level calling for immediate intervention (within 48 hours) are defined as relevant defects of the track geometry. These defects are highly dangerous to the railway traffic and therefore must be repaired in the shortest possible time. Should it prove impossible, operational restrictions must be imposed proportionate to the type of the parameter and to the value assumed by the parameter itself. Such restrictions may be traffic slowing down or block.

Such track quality indexes (TQI) then allow to assess the "effectiveness of the line", and its evolution over time, so as to plan adequate *"on condition"* maintenance works, optimizing human and economical resources and avoiding proceeding with a more expensive "logic of 24-hour repair service" to be performed urgently whenever the relevant defects arise.

In order to calculate the quality indexes, RFI regulations on track maintenance specify the following defectiveness indexes:

- *defectiveness index of the longitudinal level*, equal to the standard deviation on a 200m plane of the longitudinal level;
- *defectiveness index of the alignment*, equal to the standard deviation on a 200m plane of the alignment;
- *defectiveness index of the transversal level*, equal to the standard deviation on a 200m plane of the transversal level;
- *wedging index*, equal to the highest on a 200m plane, and therefore to the worst of the above-mentioned defectiveness indexes.

As regards the track quality indexes (IQB), they are defined as follows:

❖ **Track geometry quality index in a section IQBT** is the mean value of the wedging indexes (one at every 200 m) concerning the section considered. It is assessed at a full line, so the tracks at stations and the other places comprising points are excluded.

❖ **Track geometry quality index in a station IQBS** is the mean value of the defectiveness indexes of the longitudinal level (one at every 200 m) at the place considered.

The index values must of course be contained within specific threshold values that define the type of line, the time within which the maintenance operations must be planned, designed to restore levels of comfort, safety and ride quality you want.

If Xt is the state of the system defined by the parameters evaluated on the geometric characteristics and wear of the superstructure such as the railway as *the Gauge, the Alignment, the Longitudinal Level, the Transversal Level, the Skew*, and *the Wear of a 45° Rail*. For each of them the regulations specify the following levels and thresholds:

- 1st Quality Level (optimal)
- 2nd Quality Level (warning)
- 3rd Quality Level (short-term or medium-term intervention)
- 4th Quality Level (operational restrictions: slowing down or block)

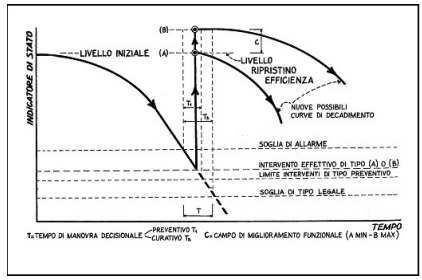
Each state of the system previously defined can be associated to the undertaken action A_t. The action can be an operational restriction, the implementation of maintenance works or can consist in keeping the superstructure without any intervention up to the next inspection period. In any case, if $X_t=i$ and $A_t=k$, P_{ij} (k) denotes the probability for the system to be in the state j, at the time t+1, by undertaking action k. Moreover, for each state i and the subsequent action k there will be an estimated cost $C(i, k)$.

The characteristics of the superstructure contribute, as a whole, to the definition of the *decay function of each parameter:*

$$F = (P, U, R)$$

As a matter of fact, since railway headquarters also play a leading role, it is clear that every single parameter must be within the limitations provided for by the regulations.

The functional form F will express the decay speed of the structural and functional track characteristics up to the achievement of a minimum threshold $F_{\min}$ which corresponds to loss of functionality of the superstructure.



Any maintenance strategy involves, therefore, the preventive knowledge of the state $X_t=i$ of the system, which is known to be defined by the values assumed by the diverse geometric and wear parameters observed.

The high-performance means of measurements allow nowadays to determine the value of such parameters and finally through data post-processing, to define the value of a synthetic

indicator of the state of the system under analysis IQB. The IQB levels can define, however, the operational timing of "on condition" maintenance as they are situations which require maintenance works all the same, even if depending on different time limits of intervention.

3. *Theoretical observations on Markovian stochastic decision processes*

A Markov chain is a stochastic process at such finite states (with values in X) $\{X_t\}$(t=1,2...) that, being X_t and A_t the state of the system and the subsequent action in the time t respectively, if $Xt = i$ and $A_t = a$, then denoting with $P_{ij}(a)$ the probability that the system, at the state i at first, will be, in the time $t+1$, at the state j after action a has been undertaken, it follows that:

$$P\{X_{t+1} = j \mid H_t, X_t = i, A_t = a\} = P\{X_{t+1} = j \mid X_t = i, A_t = a\} = P_{ij}(a).$$

This expresses Markov chain's property assuming that the conditional probability $P_{ij}(a)$ of any future 'event', given each past 'event' and the present state $X_t = i$, is independent from the past "event" and from the time sequence $H(t)$ of states and actions of the system $H(t) = \{X_0, A_0, X_1, A_1, ..., X_{t-1}, A_{t-1}\}$, whereas it is only dependent on the present state of the process.

For each $X_t = i$ and $A_t = a$, there will be also an estimated cost $C(i, a)$, which is assumed to be limited (i.e. we decide to operate in the presence of budgetary constraints), then there will be a number M such that:

$$|C(i, a)| < M \quad per\ ogni\ i \in I\ e\ a \in K$$

The conditions of deterioration of the superstructure are known to be expressed by means of the values assumed by such strategic variables as load-carrying capacity, regularity and wrinkling which, in function of the time, define the state of the superstructure in terms of efficiency or degree of deterioration.

The determination of the state of the system will be followed by an action (decision) selected from a finite set of possible actions. A rule applied for the choice of an action at each instant is defined *Policy* and is denoted by π. In general, the action specified by a policy in the time t, may be dependent not only on the present state X_t, but also on the history H_t and on t itself. A policy can be also randomized in the sense that a probability distribution is assigned to possible actions.

An important subset of the set containing all the policies is that of the stationary policies. A policy (or scenario of coordinate activities) is stationary if the action which specifies in the time t is only dependent on the present state X_t and if it is non-randomized (deterministic). In other words, a stationary policy is a function f which traces the state space in the action space by expressing that for each state i, $f(i)$ denotes the action chosen by the policy when the state i occurs. It follows that, if a stationary policy is adopted, then the state sequence $\{X_n, n = 0, 1, 2, \ldots\}$ forms a Markov chain with a transition probability $P_{ij} = P_{ij(f(i))}$. Therefore the process will be referred to as Markov decision process.

In order to determine the most effective actions of intervention above the ***Global comfort*** criteria, it is necessary to establish a criterion for optimality. Standing in the best conditions, above the point of view of operational ***safety*** and ***quality*** for the user expressed by functional levels described, it can be defined as "optimal" the maintenance policy that obtains the minimum average cost per time unit (maximum **economic *efficiency***) in optimal conditions with regard to the economical resource employment. Such a solution can be obtained by solving a problem of linear programming through the Simplex Method, in which the objective function to minimize is as follows:

Remaining in the optimality conditions from the point of view of best economic efficiency and riding quality expressed by the functional levels described above, can be considered that good maintenance policy that minimizes the average cost per unit of time and that also realizes the condition of maximum economic efficiency, the 'identification of such a solution can be obtained by

solving a linear programming problem, through the use of the Simplex Method, using the following objective function to minimize:

$$\Phi = \sum_{j=0}^{m}\sum_{k=1}^{K} x_{jk} c_{jk} \qquad (1)$$

Where, x_{jk} stands for the stationary probability to take a decision k when the system is at the state j, and $c_{jk}(t) \geq 0$ the average cost covered when the system is at the state j in the time t and the decision k is taken. It is assumed that $c_{ik}(t)=c_{ik}$, independent of t.

$$\sum_{k=1}^{K} x_{jk} = \sum_{i \in I}\sum_{k=1}^{K} x_{jk} q_{jk}(k) \qquad \text{for each } j \in I \quad (2a)$$

$$\sum_{j \in I}\sum_{k=1}^{K} x_{jk} = 1 \qquad (2b)$$

$$x_{jk} \geq 0 \qquad (2c)$$

in which $q_{ij}(k)$ express the transition probability of a system, being in the state i, to change to the state j in the following step when action k is taken. For each type of action k the sum of all the probabilities that the system, being in the state i, has to change to each state $j = 0,1\ldots m$:

$$\sum_{j=0}^{m} q_{ij}(k) = 1 \qquad \text{and} \qquad qij(k) \geq 0 \qquad \text{For each i and k set.}$$

As previously shown [21], the optimum solution of (2) is unique for $\sum_{k} x_{jk} > 0$, $j \in I$, and it satisfies the optimum non-randomized choice to take action k in the state j, then it follows:

$$D_{jk} = \frac{x_{jk}}{\pi_j} = \frac{x_{jk}}{\sum_{k=1}^{K} x_{jk}};$$

in which there is, $x_{jk} = \pi_j D_{jk}$ and $\pi_j = \sum_{k} x_{jk}$, with πj as equilibrium probability distribution.

4. *Application of markovian decision process to maintenance problems of railway superstructures*

In order to fully describe the real possibility to use the mathematical model suggested and closely follow the application steps of the method, the case of a system characterized by possible states for each geometrical parameter above mentioned, by possible actions to be undertaken and by actions consistent with every state and every action, has been reported as an exemplification.

Considering the state indicators suggested by RFI, let us examine, for the sake of simplicity, the following four states so as to classify the qualitative characteristics of the infrastructure:

State	Deterioration threshold
0	Optimal Level
1	Warning Threshold
2	Intervention Threshold
3	Safety Threshold

Table 3 – Costs and transition probability for each state and action

where:

- *optimal level*: characteristic value equal to that of a new or efficiently restored superstructure;
- *warning threshold*: characteristic value such as to induce monitoring of the section in order to assess the defect evolution over time;
- *intervention threshold*: conditions of deterioration of the superstructure such as to require implementation of maintenance works within times set in advance;
- *safety threshold*: characteristic values which definitely compromise the safety to such an extent that they require the implementation of traffic slowing down or block.

Let us suppose that at each initial period t the infrastructure is inspected by means of high-performance diagnostic carriages and classified according to one of the four states above considered. After the observation of the qualitative state of the superstructure a decision needs to be taken, either to still utilize it without any intervention up to the following inspection period (action c) or to carry out maintenance works in order to restore the best structural and functional conditions (action m). Let us suppose, moreover, that action c is allowed only at the state 0 while action m is permitted only at the state 3.

For each parameter, from every state to the others, the transition probability may be calculated by knowing its decay function F and by carrying out a statistical analysis of the data obtained from the measurements of the structural and functional characteristics (monitoring and survey of the quality indicators).

5. Conclusions

The fundamental objective of a railway maintenance plan is to guarantee, by means of suitable mathematical models for optimizing the effectiveness of the interventions, a support system for the decisions which are required to perform upgrading actions so as to ensure the necessary degree of reliability of the structure and at the same time to optimize the resource allocation.

Therefore, the optimization of the maintenance processes and of other aspects related to environmental quality and organization of the exercise, allows a general improvement of the "Global Comfort", which includes within it the "security", "efficiency" and "quality", and can be formalized as a particular psycho-physical condition in which the man expresses satisfaction in the her relationship with the trinomial vehicle-infrastructure-environment.

Methodologically, the proposed model uses the stochastic dynamic programming and in particular Markov's decision processes applied to the Index of Quality of Binary (IQB), thus allowing to define, through the integrated analysis of the classes of variables which characterize the overall quality of service (in terms of comfort and safety), to find the solutions of the decisional process in function of the probability of decline over the time of the variables state of the infrastructure and of the flow of available resources.

It is thus possible develops the most suitable intervention policies, at out light of ***global comfort*** with regard to speed ***quality*** for the user and operational ***safety*** at the minimum average cost per time unit (maximum ***efficiency***) in optimal conditions with regard to the economical resource employment.

6. BIBLIOGRAPHY

[1] Dantzig G. B., Wolfe P. (1962), *Linear Programming in a Markov Chain*., Operations Research, 10, 702-710,

[2] Derman C. (1962), *On Sequential Decision and Markov Chains*. Management Science, 9, 16-24, 1962.

[3] Klein M. (1962), *Inspection-Maintenance-Replacement Schedules Under Markovian Deterioration*. Management Science, 9, 25-32,.

[4] Barlow E.R., Proschan F. (1965), *Mathematical Theory of Reliability*, Wiley & Sons, Inc. New York

[5] Kolesar P. (1966), *Minimum Cost Replacement Under Markovian Deterioration*. Management Science, 12, 9, 694-706,.

[6] Jorgenson D.W., Mc Call J.J., Radner R. (1967), *Optimal Replacement Policy*. The RAND Corporation, Santa Monica, California. North-Holland Publishing Company. Amsterdam.

[7] Kalymon B. A (1972), *Machine Replacement with Stochastic Costs*. Management Science, 18, 5, 288-298,.

[8] Corriere F. (1992), *Affidabilità, efficienza e vulnerabilità del sistema dei trasporti: criteri e metodi per la programmazione degli interventi*, Selezione tecnica - Aprile.

[9] Stoka M. (1994), *Calcolo delle probabilità e statistica,* Ed. Cedam.

[10] Corriere F, Lo Bosco D (2001), *Global comfort and operational security in linear transportation infrastructures: A mathematical model for interdependency's analysis of "man – vehicle – infrastructure – environment" quadrinomial* - Seminarberichte aus dem Fachbereich Matematik und informatik, Fernuniversitat Hagen , Deutschland – Band 72.

[11] Corriere F, Russo R. (2003), *I piani manutentivi per la sicurezza d'esercizio delle infrastrutture viarie:un modello matematico per la ottimizzazione della efficacia degli interventi* - Atti del XIII Convegno Nazionale della SIIV – 30-31/10/2003 Padova.

[12] D. Di Vincenzo e M. Guerrieri (2005), *Gestione e Diagnostica della Sovrastruttura Ferroviaria. Un caso studio: la linea "Palermo–Messina*" – Argomenti 07/2005 – Rivista quadrimestrale di RFI;

[13] Corriere F, Di Vincenzo D. (2006), *Applicazione di processi decisionali per l'ottimizzazione degli interventi manutentivi sulle infrastrutture viarie* - Atti del XVI Convegno Nazionale della SIIV – 20-22/09/2006 Cosenza.

[14] Corriere F, Di Vincenzo D. (2007), "A markovian model as a tool for optimisation of maintenance interventions on railway lines" *VI International Conference stochastic geometry, convex bodies, empirical measure & applications to engineering of traintransport - Milazzo (Messina), 27 May – 03 June 2007*.

[15] Corriere F, Di Vincenzo D. (2007), "A markovian model as a tool for optimisation of maintenance interventions on railway lines" *VI International Conference stochastic geometry, convex bodies, empirical measure & applications to engineering of traintransport - Milazzo (Messina), 27 May – 03 June 2007*.

[16] Corriere F., Di Vincenzo D. (2010), "L'ottimizzazione degli interventi manutentivi sulle linee ferroviarie con l'utilizzo di un modello markoviano: analisi di un caso studio." In: *Rendiconti del Circolo Matematico di Palermo - I° summer school quantitative methods for economic agricultural-food and enviromental sciences. Castiglione di Sicilia, 22-24 September 2010.*

RENDICONTI DEL CIRCOLO MATEMATICO DI PALERMO
Serie II, Suppl. 84 (2012), pp. 167-175

Empirical Analysis of Married Women's Working Time and Paid-Work EquationEstimation in Italy

Antonino Di Pino and Maria Gabriella Campolo

Abstract Empirical studies show that married women's labour supply in Italy is sensitive to variations in individual wage, but misspecification of labour supply equation may result in inefficient wage-elasticity estimates. Consequently, several problems arise in evaluating the influence of small children on female labour supply and wage-elasticity. In order to reduce the variability of the estimates, we suggest a structural form specification of both paid work and unpaid work equations and an instrumental variables based estimation procedure. A new type of instruments are introduced to improve the estimation performance. The empirical application to Istat data (Time Use Survey, in Italy) produces apparently reasonable results.
Keywords: Labor statistics, Econometrics, Fertility and family

1 Introduction

The estimation of the labour supply function and wage-elasticity of women represents a topic of great interest for analysts, especially in Italy where women are an underutilized contingent of labour force. Several methods for estimating labour supply function and wage-elasticity have been adopted, but estimation results prove generally unsatisfactory, because they are extremely sensitive to model specification and to the utilized estimation procedure. A detailed survey of the most important studies on wage-elasticity of female labour supply

[1]Antonino Di Pino, Dipartimento D.E.S.Ma.S. "V. Pareto" - Università degli Studi di Messina; dipino@unime.it

Maria Gabriella Campolo, Dipartimento D.E.S.Ma.S. "V. Pareto" - Università degli Studi di Messina; mgcampolo@unime.it

estimation can be found in Killingsworth and Heckman, (1986); Blundell and Macurdy, (1999) and, more recently, Evers, De Mooij and Van Vuuren, (2008).

Our purpose is to estimate a female labour supply model that takes into account the decisions on time allocation of both partners and uses time use data collected with the diary method (Klevmarken, (2005); Bloemen and Stancanelli, (2008); Kalenkowski, Ribar and Stratton, (2009); *inter alia*). In this way, a simultaneous equation model of paid and unpaid work supply may be estimated.

However, labour supply models specified with a simultaneous equation approach typically suffer from inferential problems. In particular, the risk of endogeneity in the estimates discourages the analysts from specifying the structural form of the equations. For this reason, non-market working activities are generally not included as explanatory variables in the paid work equation. But the incomplete specification of the equation of paid work leads to an increase in the variability of the results and in particular of wage-elasticity.

In order to circumvent this difficulty, we specify a "complete structural form" of both labour supply and home-production equations, and we correct our estimates for endogeneity by adopting an instrumental variables approach. Empirical measures of the economic value of the time spent by the partners in non-market (or domestic) activity and an empirical measure of individual non-working activity (leisure time and physiological activities) are utilized as instrumental variables. In this way, the variability in the estimated elasticity coefficient should decrease.

We use a cross sectional dataset selected from the 2002-2003 ISTAT Survey on Time Use in Italy. Unfortunately, this survey contains no information on income: this forced us to resort to a matching procedure in order to "import" income data from the Bank of Italy Survey on Household Income and Wealth (*SHIW* 2002). The matching procedure we adopted gives apparently satisfactory results for the assignment of individual labour income, but not for the assignment of household income and consumption data. This makes it impossible for us to introduce taxation effects in the model of labour supply.

Our model estimates a wage-elasticity coefficient of paid work close to 0.30 if small children live in the family[1]. The results of simulations based on model estimates show that if the wage level increases, women work more for the market, but, at the same time, about 65% of their additional market working time is subtracted to their domestic working time.

Theoretical and methodological aspects regarding the economic evaluation of domestic work utilized as instrumental variable will be discussed in the next section. In Section 3 we show the characteristics of the dataset and the results of both matching procedure and model estimation. Then, the fourth section reports the final observations and remarks.

[1] The cross-sectional nature of the survey and the absence of information on the dynamic relationship between fertility and participation in the labor market of the partners forced us to treat the presence and the number of small children in the family as an exogenous factor.

2 Model Specification and Estimation

How valuable are non-market working activities? A tentative answer comes from measuring the time devoted to unpaid work and "pricing" it. To this end, two criteria have been proposed in the literature: i) the "market price" criterion and ii) the "opportunity cost" criterion. With the former, the market price is the average market hourly wage of an outside collaborator recruited from the labour market. With the latter, the opportunity cost is given by the potential hourly wage of the subject assumed as a unit of evaluation (shadow price) for the time spent on his/her household duties (Gronau, 1986). There are several studies about the consequences in economic and statistical analysis that derive from the adoption of both the evaluation methods[1]. In this analysis, we adopt a solution which, in part, represents a synthesis of both evaluation criteria[2]. In practice, the evaluation here attributed to the domestic activity and child care corresponds to the greater of the two hourly costs given, respectively, by the average price of the outside service and by the potential (estimated) wage of the subject: $\max(p_d T_h; \hat{w} T_h)$, where T_h are the hours of domestic work, p_d the average hourly price of the outside service for domestic activities, $\hat{w}$ the potential predicted hourly wage of the subject[3].

Following this line, we propose to include in the right side of the labour supply equation, as an explanatory variable, the computed economic values of domestic work and child-care of the woman and of her partner. However, a methodological problem arises with this procedure. Wage and empirical measures of time devoted to domestic duty and child-care may be potentially endogenous with respect to the market working time. We try to solve this problem by substituting potentially endogenous regressors with instrumental variables obtained from reduced-form regressions estimated at a first stage. For this reason we must specify the simultaneous equation model including several reduced-form specified equations. Therefore the structural form specified equations of the model are given by the equations 6) and 9) of the following model:

[1] See, *inter alia*, Bonke, (1992), and De Santis, (2004).
[2] See Di Pino, (2004).
[3] This solution for the computation of shadow price of the home production is based on the consideration that if the subject entrusts all household duties (including child care) to outside collaborators, he/she will pay the service at an hourly price equal to p_h, and will not sustain any opportunity cost. *Vice versa*, if he/she prefers to personally attend to household duties, renouncing alternative payment of his/her own time equal to $\hat{w}$, he/she evidently considers direct involvement in household activity and child care not qualitatively replaceable by outside services. In this case, $\hat{w}$ can be assumed as a proxy of the measurement of the home production opportunity cost.

1) $L^* = a_0 + a_1 age + a_2 age^2 + a_3 sex + a_4 health + a_5 edufather + a_6 labfather + a_7 regwage + a_8 edupart + u_1$

2) $H_L = L - \left[L^*\right] \qquad \left(L = 1 \; if \; L^* > 0;\; L = 0 \; otherwise\right)$

3) $lnW = a_9 + a_{10} age_m + a_{11} age^2{}_m + + a_{12} age_f + a_{13} age^2{}_f + a_{14} dlabour + a_{15} partfull + a_{16} edufather_m + a_{17} edufather_f + a_{18} regGNP + a_{19} regwage + a_{20}\left[H_L\right] u_3$

4) $lnNW = a_{21} + a_{22} age + a_{23} age^2 + a_{24} sex + a_{25} nchild + a_{26} dday + u_4$

5) $lnCH_f = a_{27} + a_{28} age + a_{29} edufather + a_{30} nchild + a_{31} sitting + a_{32} sitting^2 + a_{33} dday + u_5$

6) $lnDOM_f = a_{34} + a_{35} age + a_{36} age^2 + a_{37} darea + a_{38}\left[H_L\right] + a_{39} ln\left[W\right] + a_{40} nchild + a_{41} dday + a_{42} colf + a_{43} edu + a_{44} edupartner + a_{45} ln\left[NW\right] + u_6$

7) $CHCOST_f = \left[CH_f\right] * \max\left\{\left[W / \left[WORK_f\right]\right];\; p_d\right\}$

8) $DOMCOST_f = \left[DOM_f\right] * \max\left\{\left[W / \left[WORK_f\right]\right];\; p_d\right\}$

9) $lnWORK_f = a_{46} + a_{47} age + a_{48} age^2 + a_{49} darea + a_{50}\left[H_L\right] + a_{51} ln\left[W\right] + a_{52} edu + a_{53} edupartner + a_{54} ln\left[CHCOST_f\right] + a_{55} ln\left[DOMCOST_f\right] + a_{56} ln\left[NW\right] + a_{57} dday + u_9$

There are nine endogenous variables (in brackets when they appear in the right side of the equation):
L^*= Labour participation (L = dummy variable: 0 if the subject works; 1 if doesn't work); H_L = Heckman correction factor; lnW = Log of Individual Wage; $lnNW$ = Log of Non-working time (leisure and physiological time); $CHCOST_f$ = Economic value of individual childcare activity (women only); $DOMCOST_f$ = Economic value of individual domestic work (childcare excluded); $lnCH_f$ = Log of Time spent for childcare (women only); $lnDOM_f$ = Log of Time dedicated to domestic work (women only) $lnWORK_f$ = Log of Time dedicated to external work (women only)
and 20 exogenous variables:
intercept; age, age_m, age_f = Age (and fixed effect male/female); age^2, $age^2{}_m$, $age^2{}_f$ = Square of age (and fixed effect male/female); *sex* = Dummy variable (male=0; female=1); *health* = Health status satisfaction (Dummy variable: not satisfied=0; satisfied=1); *edufather*, $edufather_m$, $edufather_f$ = Father education (years of schooling) (fixed effect male/female); *labfather* = Father working status when the subject was 14 years old (Dummy: not work=0; work=1); *regwage* = Regional wage increase propensity (fixed effect); *edu* = Education level of the subject (years of schooling); *edupartner* = Partner's education (years of schooling); *dlabour* = Type of work (dummy variable : occasional=0;

habitual=1); *partfull* = Dummy: if the subject works part-time=0 if he/she works full time=1; *regGNP* = Regional GNP pro capite (fixed effect); *darea* = Regional area (dummy variable: North-centre=0; South-Islands=1); *dday* = Reference day activities of the diary (Dummy variable: weekend = 0; Monday - Friday=1); *colf* = Home help service time (minutes in a week); *nchild* = Number of children (0-13 years); *sitting* = *B*aby sitter time (minutes in a week); $sitting^2$ = Square of baby sitter time; p_d = average market hourly price of the outside service for domestic activities and child-caring; Error terms u_1;... u_8 ;u_9 are assumed i.i.d. with zero mean.

Note that equations 5), 6), 7), 8), and 9) are estimated only on the sub-sample of the female partners, while equations 1), 2), 3) and 4) are estimated on the full sample, including male and female partners. Adopting exclusion-restriction rules, we can identify both equation 6) (unpaid work equation) and equation 9) (paid work equation). Equation 1) (participation function) specifies the selection criterion of both the log-Wage function (Eq. 3) and the labour supply function (in Eq. 9) where the dependent variables are observable on working people only. The coefficients a_{39} in the equation 6) (unpaid work supply) and a_{51} in the equation 9) (paid work supply) measure the uncompensated wage-elasticity, respectively, of female domestic work and female paid work. To specify both market and non-market work equations we cannot directly use household income, not asked in the Istat Time Use Survey. Equation 7) and 8) give the reduced form estimates of the economic value of, respectively, childcare and domestic work.

In order to estimate equations 6) and 9) we adopt different procedures, all based on the use of the instrumental variables obtained from the estimation at a first stage of equations 1), 2), 3), 4) and 5), 7) and 8). We apply as alternative estimators : i) *IV* and OLS with Heckman correction for selectivity[1]; ii) *IV* and *Tobit* standard; iv) *IV* and *Censoring Least Absolute Deviation Estimator* (*CLAD*)[2].

3 Sample Selection and Estimation Results

The subjects interviewed in the Istat Time Use Survey provide detailed information on their own daily time allocation through the compilation of a diary in which they register all of their daily activities. These can be classified in four categories: i) paid work or market working time; ii) domestic work or

[1] Estimation of the log-wage equation implies the adoption of the Heckman correction for selectivity, given by the inclusion as regressor of the residuals (*H*) obtained from the *Probit* reduced form estimation of the participation equation 1).
[2] Cf. Powell, (1984).

unpaid work; iii) child-care; iv) non working time[1]. The selected sample is composed by 8 026 couples of Italian partners (16 052 subjects in all); equitably distributed by area of residence, age, and employment status[2]. The results of the descriptive analysis, not reported here, show that men work more for the market than women do (8.4 hours per day, against 3.4). Conversely, women spend more time in domestic work and child-care (respectively, 5.7 and 1.2 hours) than men (1.0 and 0.4 hours). Furthermore, with more children in the family, women spend more hours working indoors, but fewer in paid work.

Istat Time Use dataset does not report information on income, of any kind. For this reason we draw individual labour incomes from the Bank of Italy *SHIW* dataset (3 640 cases) in year 2002 by applying a matching procedure. The "Conditional Propensity Score" estimation is utilized as matching method. We impose to the matching procedure that the variables conditioning the Propensity Score estimation be independent of the outcome variables[3]. The variables, common to both the dataset, used to estimate the Propensity Score (by *Probit*) are: age, sex, education, father's working status when the subject was fourteen, economic regional fixed effects, status of the subject within his/her family and geographical area of residence. In order to avoid the risk of importing data characterized by self-selection, we adopt a sensitivity test to verify if the assignment to the treatment (Istat Time Use dataset) depends on the outcome variables (labour income). To this purpose a Cochran-Mantel-Haenszel (*CMH*) test is applied by computing a Chi Square statistics (Becker and Caliendo, 2007). Furthermore, so as to verify if latent factors affect the assignment to the treatment, a sensitivity testing procedure based on the simulation of confounding variables affecting propensity score estimation is applied[4].

As for the model estimation, we report here only the estimation results, at the second stage, of female's paid work equation (Table 1)[5]. The estimated coefficients of log Wage are similar in different estimation procedures. The estimated coefficient of the *IV* representing domestic activity economic cost ($DOMCOST_f$) is characterized by a high significativity.

[1] The variable "non working time" is the result of the sum of time dedicated to leisure-activities and time spent in physiological and personal activities.
[2] Self-employed are included in the sample.
[3] This condition is known as Conditional Independence Assumption (*CIA*).
[4] Cfr. Rosembaum and Rubin, (1983) and Ichino, Mealli and Nannicini, (2008).
[5] The results of reduced form estimates at a first stage and of structural form estimates of Eq. 6 (domestic work), not reported here, are disposable on request.

Table 1: Logarithm of Paid Work "structural-form" estimation (Eq. 9 – Women only)

Dependent variable: $lnWORK_f$	**OLS**		**CLAD**		**TOBIT (i)**		**TOBIT (ii)**	
regressors:	**Coeff.**	**p**	**Coeff.**	**p**	**Coeff.**	**p**	**Coeff.**	**p**
Intercept	6.9082	*	3.0020	*	2.5540	*	-2.3259	*
age	0.0879	*	0.0115	*	0.0125	*	0.2978	*
age^2	-0.0009	*					-0.0035	*
darea	-0.2589	*	-1.3956	*	-1.4857	*	-1.51107	*
dday	-0.4955	*	-0.4281	*	-0.4169	*	-0.5021	*
H – (*Heckman correction)*	-0.0848	**	8.7589 **(iii)**	*	9.3741 **(iii)**	*	9.3011 **(iii)**	*
$\boldsymbol{ln\hat{W}}$	**0.3078**	*	**0.3072**	*	**0.2984**	*	**0.2489**	*
edu	-0.0081	*	0.0420	*	0.0548	*	0.0502	*
edupartner	-0,0053	*	0.2035	*	0.2153	*	0.2135	*
$CHCOST_f$	-0.0024	#	0.0184	*	0.0121	**	-0.0081	*
$DOMCOST_f$	-0.8073	*	-0.6002	*	-0.5956	*	-0.7995	#
$lnN\hat{W}$	-0.1076	*	-0.3308	*	-0.3440	*	-0.2525	*
Cases (Women)	4506 (working women only)		8026		8026		8026	

p-value: * < 1%; ** <5%; # > 5%; **(i)** estimated without including age^2 as regressor; **(ii)** estimated by including age^2 as regressor; **(iii)** correction for endogeneity

By estimating the market labour supply equation for different sub-samples characterized by a varying number of children (aged 0-13) in the family, we can observe (Table 2) how the estimated wage-elasticity of female's paid work is lower in the families without children, but becomes higher when the number of children increases. This result could appear inconsistent with the descriptive statistics mentioned above, showing that female's working time decreases when the number of children increases. Nevertheless, we must consider that the estimated coefficient of wage-elasticity represents an estimate of an "uncompensated" elasticity given by the joint and indistinct influence of a "substitution effect" and an "income effect" of wage. Consequently, the estimated wage-elasticity coefficient could increase if the presence of small children in the family is accompanied (and dominated by) an income effect of wage on paid work supply. The estimation results of the female domestic work equation (not reported here) show little differences in the estimated coefficient of domestic work wage-elasticity when the estimation procedure changes (respectively -0,27 for *OLS* estimate and -0,22 for *Tobit*). in both cases, female domestic work supply diminishes if the wage rises. We also estimated the domestic work wage-elasticities in different sub-samples with different number of children in the family, and found no relevant difference with coefficients estimated on the full sample.

Table 2: Estimated wage-elasticity of female's paid work for number of children *0-13* in the family

Children 0-13	**OLS**		**CLAD**		**TOBIT**	
	coeff	***s.e.***	**coeff**	***s.e.***	**coeff**	***s.e.***
0	0.2100	*0.0458*	0.1716	*0.0726*	0.1882	*0.0594*
1	0.3162	*0.0531*	0.2676	*0.0825*	0.3224	*0.0715*
>1	0.3524	*0.0604*	0.3243	*0.0983*	0.3865	*0.0791*

Simulating the effects of the estimation results we can observe that a theoretical positive variation in the wage level of 10% involves makes a woman's paid work supply increase by about 7 days per year but, contextually, woman's domestic unpaid work diminishes by about 6 days per year. If small children are present in the family, a percentage of 62-63% of the increase in working time (due to a higher wage) is "subtracted" from domestic activity. However this result does not take into account the different availability of public and/or private service of childcaring in the Italian regions.

4 Final Remarks

The inclusion of the cost of unpaid work as an instrumental variable in female's labour supply estimation allows us to obtain an apparently sound estimate of female's paid work. The estimated coefficients of wage elasticity seem to be characterized by high significativity and robustness. The unavailability of data about both household consumption and income limits our analysis to the estimation of uncompensated elasticities. If we had this information, we could include in the model a utility function equation, and a wage compensated elasticity could be computed for any given, "predicted", level of utility. With this model, a consistent empirical relationship between individual wage and both paid and unpaid work supply emerges, even if important variables such as taxes and public childcare services are absent from the analysis. Without considering taxes and public services, the effects of an increase of woman's wage level involves a positive influence on female labour supply in the market but also a negative effect on unpaid domestic work supply. This implies that important consequences at the macro level can occur in terms of quality of family life if a potential domestic time reduction (due to an increase in wage level) is not adequately compensated by the utilization of external services, parental aid or, at least, by a redistribution of the domestic duties within the family.

References

1. Bank of Italy: Survey on Household Income and Wealth in Italy in 2002. (2004)
2. Becker S.O., Caliendo M.: Mhbounds-Sensitivity Analysis for Average Treatment Effects, IZA Discussion Papers 2542, (2007)
3. Bloemen H.G., Stancanelli E.G.F.: How Do Parents Allocate Time: the Effects of Wages and Income. IZA Discussion Papers 3679, (2008)
4. Blundell R., Macurdy T.: Labor Supply: A Review of Alternative Approaches. In: Ashenfelter O., Card D. (eds.) Handbook of Labor Econ. (1999) doi:10.1016/S1573-4463(99)03008-4
5. Bonke J.: Distribution of Economic Resources: Implications of Including Household Production. Rev. Income Wealth (1992) doi:10.1111/j.1475-4991.1992.tb00426.x
6. De Mooij R., Evers M., Van Vuuren D.: The Wage Elasticity of Labour Supply: A Synthesis of Empirical Estimates. De Economist (2008) doi:10.1007/s10645-007-9080-z
7. De Santis G.: The Monetary Cost of Children, Theory and Empirical Estimates for Italy. GENUS \textbf{LX,1}, 161--183 (2004)
8. Di Pino A.: Economic estimation of the time devoted to household chores and childcare in Italy. GENUS \textbf{LX,1}, 139--159 (2004)
9. Gronau R.: Home Production – A Survey. In: O. Aschenfelter, Layard R. (eds.) Handbook of Labor Econ. (1986) doi:10.1016/S1573-4463(86)01007-6
10. Ichino A, Mealli F., Nannicini T.: From Temporary Help Jobs to Permanent Employment: What Can We Learn from Matching Estimators and their Sensitivity?. J. Appl. Econometrics (2008) doi: 10.1002/jae.998
11. ISTAT: Survey on Time Use in Italy 2002-2003. (2004)
12. Kalenkosky G.M., Ribar D.C., Stratton L.S.: The Influence of Wages on Parents' Allocation of Time to Child Care and Market Work in the United Kingdom. J. Popul. Econ. (2009) doi:10.1007/s00148-008-0192-9
13. Killingsworth M.R., Heckman J.J.: Female Labor Supply: A Survey. In O.Aschenfelter, Layard R. (eds.), Handbook of Labor Econ. (1986) doi:10.1016/S1573-4463(86)01005-2
14. Klevmarken N.A.: Estimates of a Labour Supply Function Using Alternative Measures of Hours of Work. Eur. Econ. Rev. (2005) doi:10.1016/j.euroecorev.2004.02.002
15. Powell J.L.: Least Absolute Deviations Estimation for the Censored Regression Model. J. Econometrics (1984) doi:10.1016/0304-4076(84)90004-6
16. Rosembaum P.R., Rubin D.B.: Assessing Sensitivity to an Unobserved Binary Covariate in an Observational Study with Binary Outcome. *J. R. Stat Soc. Ser. B* \textbf{45}, 212--218 (1983)

RENDICONTI DEL CIRCOLO MATEMATICO DI PALERMO
Serie II, Suppl. 84 (2012), pp. 177-186

The creditworthiness of construction companies

Antonio F. Forgione

University di Messina, Department SEA, 98122 Messina, Italia

fabio.forgione@unime.it

Abstract: Construction companies have peculiar characteristics that distinguish them from manufacturing firms and, in general, from standardized production companies. Their specific features need to be appropriately considered when evaluating the credit risk involved in financing them. Companies operating in the area of public works contracts, in particular, expose their financiers to lower levels of credit risk on average because of the complex administrative regulations in place for awarding public contracts and for containing the phenomenon of tax payment avoidance.

Keywords: credit risk; construction companies; economic value.

1 Introduction

The management of Italian banks, over recent years, have neglected the topic of evaluating the creditworthiness of firms obtaining funding, also because of the important and unfamiliar issues raised by the adoption of new intermediation models, known by the term *originate to distribute*, with regard to the traditional *originate to hold* and by the implementation of *credit risk management*, widely imposed by regulatory bodies.

The crisis of the new credit intermediation framework, essentially due to incapacity to correctly measure and communicate the credit risk transferred onto the market through *originations* operations, has led many expert observers to call for a return to a more traditional form of intermediation, appropriately adapted to recent changes, above all in the field of risk measurement (Cesarini, 2010; Bongini, Di Battista, Nieri, 2009).

The Basel 2 regulations underline that *rating* models must incorporate all available information, including qualitative elements, as well as requiring a certain degree of autonomy to be left to subjective judgements (the so-called *judgmental* component) and lend themselves to being effectively implemented even in a changed operational context.

With regard to the aim of improving understanding of the credit risk taken on by banks through financing operations, a particularly useful possibility is that of discretionally modifying, following adequate justification explained by

customer service representatives, the automatic scores attributed by the *rating* model, by means of the *override* procedure. Indeed, variation of the *rating* demands detailed knowledge of the receiver of funds and of his *business*, requisites for appreciating the qualitative aspects and for evaluating income prospects beyond the short term and risk.
In this context, this paper proposes to describe the processes characteristic of construction companies operating in the area of public works contracts, in order to highlight their financial cycle and underline the critical points. It is observed that the conceptual models applied for analysis of these companies and used for evaluating their creditworthiness assume that they are manufacturing firms, with the result that indicators taken from the company accounts may not be immediately applicable when the firm analysed operates in other sectors of production, in the sense that they need to be interpreted in the light of the charateristics of said companies.
Some of the observations that will be made should be taken into consideration by those responsible for granting credit when evaluating the reliability of these companies if, as is often the case, they operate principally as public contractors. This customer base means that construction companies, in order to participate in the awarding of contracts, possess certificates with an intrinsic value, which does not show up (and cannot be included) in company accounts. Moreover, these companies have a more limited capacity to activate the mechanism of turnover of sources of finance and this, contrary to appearances, should make them less of a risk at the end of the day.

2 Characteristics of companies performing public works

Traditional evaluations of financial equilibrium, based on the anaysis of accounts and aimed at highlighting indicators such as structural margin, net circulating capital, treasury margin, used in practice for expressing judgements on the reliability of manufacturing firms, may turn out to be inadequate evaluation tools when surveying enterprises that operate in the service sector (Canale, 2000) or, as in the case of construction companies, perform an economic activity characterised by a long production cycle. In fact, analysis of financial requirements presumes correct evaluation of the management dynamics that generate them and this does not happen if the evaluation is carried out using conceptual models that do not adequately explain these dynamics.
The distinctive features of construction companies, from the production point of view, can be found in the fact that the constructions are unique, since they are carried out in accordance with the commissioned project. Moreover, work is largely carried out on the site where these constructions must be built and

placed on the market, making it necessary to organise an "on site" production structure (Rossignoli, 2000).

The financial effects of this peculiarity, in contrast with standardised production companies, which produce for the warehouse, regard the variability of the monetary cycle, caused by the technical charateristics of the works commissioned and the relative completion times. In other words, the production cycle is not predetermined, but heavily dependent on customer base requirements and, consequently, the duration of the borrowing requirements, understood as the time necessary for the disinvestment of the factors used to this end, is equally variable. Moreover, it is affected by the overlapping of the various production cycles of the works in progress.

These characteristics of the production process are of importance to those evaluating the creditworthiness of construction companies also from another point of view. The absolute uniqueness of the product, moreover always constructed in different places, means a fundamental contribution to the achievement of corporate objectives comes from the intangible elements of the company's assets, such as the experience and the accomplishment capacity of the personnel, to a much greater degree than in other sectors. The exploitation of the relevant economies, heightened by these production peculiarities, carries great weight in the achievement of corporate objectives of economic equlibrium.

One indicator, albeit a very indirect one, of possessing adequate experience in the performance of public works, for companies operating in the European Union, is constituted by the certificates needed in order to be awarded contracts[1]. Moreover, as a result of the administrative procedure regulating their issue and the requirement for firms to possess them in order to participate in the award of public contracts, these contracts have an intrinsic value which can be transferred to third parties, if this is done in observance of the relevant legal provisions.

A further peculiar characteristic of companies that perform public works contracts is the substantial absence of market risk associated with the sale of the products made. Indeed, once the contract has been awarded, the principal task of corporate management is to supervise production, since sale to the customer is certain.

These companies are, however, wholly exposed to the financial risk of serious delay in payment by the customer for the work carried out. This risk may be higher than that to which other kinds of companies are exposed, since the law, as is currently the case in Italy, may be more favourable to the debtor because the functions performed by contracting bodies are considered to be of public interest.

The absence of market risk must obviously be observed on an overall corporate level, taking into consideration all the works in progress and not individual or partial combinations. The borrowing requirements are created as a result of the need to bear costs before obtaining revenue, but the amount of the latter is

given. However, the time needed to collect debts can only be estimated, and more inaccurately than in other sectors, because of the smaller number of customers and their nature.
The uniqueness of the production carried out by company management, moreover, makes historical information, obtained through traditional balance sheet analysis, less significant than that obtained for companies operating in other sectors; greater importance can be attached, especially in the case of smaller firms operating on few sites, to information regrading contracts currently being performed or already awarded. We know that such a contract includes prices and the quantity of work to be carried out and, thus, allows us to estimate the amount of revenue that will be generated in the future as a result of said contract and, with the addition of other information, the costs to be borne.
The circulating assets of construction companies include values, such as works in progress, which, if the conditions provided for by the accounting principles are met, add to the price of the factors of production used to build the part of the construction already completed, the margin achieved by the company as a result of the public contract awarded[2].

3 The value of certificates

In Italy, some of the requisites for obtaining the issue of certificates needed to compete for the award of public contracts can be transferred to third parties if they are transferred along with the whole company or a "branch of a company". This is a fairly large market, as can easily be seen by reading the press specialising in this sector, which publishes numerous advertisements offering their sale or rental.
The examination of 60 offers for sale in various regions of Italy this year has invariably shown that the offers exclusively regard the certificates, as the text of the advertisements refers only to the certificates for the respective category and value size class. This immediately leads us to deduce that the value to be transferred onto the market is exclusively the certificates needed to compete for the award of public contracts.
Access to the public works market for those interested in competing for the award of contracts, throughout the member states of the European Union, depends on possession of particular requisites making them suitable contractors for public authorities. In Italy, in accordance with the European directive, for work of a value above €150,000, they have to demonstrate that they possess specific general qualities and special qualities relating to their economic-financial and technical-organisational capacities. The aim of this regulation is to achieve an improvement in the quality of work and constructions.
In order to facilitate the task of selecting those subjects able to compete for each single contract there is provision for a certificate, issued by private subjects,

specifically authorised and subject to the control of an independent administrative authority, attesting to the suitability of a competitor to obtain the award of a contract. In this way, both contracting parties are freed from the onus of demonstrating or verifying possession of the necessary requisites. It is, therefore, sufficient (and necessary) to present a copy of the document, called a "certificate of qualification", issued by authorised bodies, in order to allow a company to compete for a contract for the assignment of work up to the value of €20,658,276, in place of all the documents needed to demonstrate possession of the special requisites outlined above.

The bodies authorised to issue certificates, known as *società organismo di attestazione* (s.o.a.) are, therefore, private bodies that exercise a public function, since the certificates are of a public nature and binding. In the past, this function was performed by a public body, the national association of constructors.

An *s.o.a.* issues a certificate (by value size or category of work) after verifying that the company has adequate experience of undertaking work of a similar kind with satisfactory results; it has the material, human and managerial resources to complete the jobs assigned to it; it is in a secure financial position; it possesses other characteristics that are verified as the result of an inquest.

Some of the requisites for the issue of certificates coincide with those needed for business goodwill.

Possession of these certificates, consequently, indicates that the company's management has (obviously) borne direct and, above all, indirect costs (for the recruitment and training of personnel, etc.), and that it has earned lower revenue (discounts offered to customers in order to win contracts and to make a name for itself, renewal of employment contracts, etc.). Indirect costs are not detected autonomously by the company's accounting system, in accordance with its functions. In particular, these costs, as we know, are entirely defrayed to the revenue account, together with all other expenses for the acquisition of fattori produttivi di esercizio, thus not being capitalised. They are seen, on the other hand, as contributing greater value to the economic capital, whch is determined for particuar aims, such as sale of whole company or the entrance of new partners, by carrying out complex and laborious calculations.

These are typical intangible assets, capable of contributing to the generation of future income and which, in the event of bankruptcy, can rarely be liquidated in favour of creditors and, thus, do not increase the bankruptcy assets.

Although the certificates in question are subject to modification by administrative procedures, are valid only in a predetermined geographical and temporal context and can be transferred to third parties, allowing them to compete for the award of public contracts, they can still contribute to limiting credit risk, as a component of *loss given default* borne by a bank.

This circumstance, with appropriate caution, can be adequately considered when evaluaitng companies' creditworthiness. There is no doubt that, if these certificates have an autonomous value, even when they are transferred to third parties together with other corporate activities, they consequently involve an

increase of the recoverable value in the event of a debtor's insolvency and/or liquidation of assets. From this viewpoint, it can be said that these certificates increase the size of guarantees for creditors.
In reference to creditworthiness, doctrine has proposed a logical model, known as "*two barriers*" (De Laurentis, 2000), which allows us to understand credit risk as a whole, also fully defined by banking doctrine (Dell'Amore, 1965). This model sets the final objective of the evaluation process as the verification of the probability of pathology of credit (the first barrier) and of the degree of coercive recovery (the second barrier). The analysis of income prospects (pathology probability) of construction companies is substantially no different from that of other kinds of company, except for necessary consideration of the peculiarity of the production process and the relative effects on borrowing requirements. However, with specific regard to the possibility of recovering sums lent by banks, possession of *s.o.a.* certificates and the fact that these have an intrinsic value determines an increased possibility of coercive recovery.
The importance of the correlation between the value of credit and the value of the guarantees that accommodate it has long been highlighted by doctrine, which underlines how banks share in corporate risk, without enjoying the benefits of any positive results, as repayment of the loan granted is predetermined (Bianchi, 1977).
Construction companies in possession of *s.o.a.* certificates expose their financiers to a lower credit risk than those operating in sectors of production in which economic initiative is not subject to authorisations and public control.
In order to determine the contribution made by these certificates to the lowering of credit risk, however, it would be necessary to estimate their value analytically. Literature has offered various contributions to the measurement of the value of certificates for the awarding of public works contracts, based on empirical estimates of the investments (particularly for promotional costs) that a company must make in order to highlight its market presence, capitalising the relative costs (Zanda, Lacchini, 1991).
In fact, rather than using empirical methods that implicitly consider certificates as being susceptible to autonomous evaluation, it would be more correct to consider them within the framework of the whole company and estimate how much they contribute to the company's income and, thus, will contribute in the future. For this reason it is held that, in order to proceed rationally in measuring the aforementioned value, it is necessary to estimate the value of the economic capital of the company to which the certificates belong and attribute a value to them expressed as a fraction of said capital.
The goodwill value of a healthy business possessing *s.o.a.* certificates should be higher than the current market value of the latter, which, however, as a result of administrative rules, maintain their value also when in a company crisis phase, right up until insolvency. The administrative regulations lead to intangible assets of construction companies gaining a market value. The real value of these assets, in healthy companies, should be higher than the current market value of

the relative certificates, which maintain their value when transferred to third parties, even when the company is insolvent.
This minimal value, however, being transferrable to third parties, increases the value of a company's assets.

4 Turnover of sources of finance

Construction companies, in particular those of small and medium size, offer banks a more limited opportunity to recover sums of money lent by exploiting the turnover of sources of finance. Consequently, it could superficially and, indeed as we will see, erroneously be said that banks expose themselves to greater risk when lending to companies operating in this sector of production rather than in other sectors.
Doctrine has explained that, in order to consider banking operations as short term, it is necessary to examine not only the formal characteristics, such as the expiry clauses of contracts, but also substantial ones, meaning the existence of the conditions for respecting the repayment terms of contracts in the future. In this sense, short term loans are considered to be those granted when the routine management of the borrower will be able to generate, before expiry, a monetary flow sufficient to repay the loan. More generally, it is held that operations can be described as short term also when a company is able to fulfil its undertakings without the contribution of routine management, by selling part of the company's activities or by securing other loans.
In the case of construction companies, banks cannot exploit the substitutability of sources of finance in order to recover loans to the same extent as they can in other sectors. In fact, this presupposes that the indication times, or the degree of perception of the pathology of credit, differ from one financier to another and/or between borrower and lender (De Laurentis, 2000) and that the bank succeeds in taking appropriate action to recover the sums lent.
Leaving aside the complex problems connected to the voidability of voluntary conveyances to defraud creditors, which makes the use of recovery strategies undertaken in proximity to the start of coercive liquidation critical, it can be observed that construction companies have fewer opportunities for finding resources to repay bank loans by putting off payment of taxes and national insurance contributions.
In general, the availability throughout the banking system of centralised information on risks means that it is impractical for borrowers to their debt by borrowing from other banks. Typically, therefore, substitution of sources can be achieved either by increasing trade credit, if conditions allow it, or, in particular in the case of small or medium sized firms, by delaying the payment of taxes and national insurance contributions, which are reverse charged and paid by deadlines laid down by law. The pressure exerted by the tax and social security

authorities is certainly less stringent than that concretely used by a company's other financiers. It is, thus, easy to understand why financial resources are normally found by omitting to pay these debts on time.
In many countries, including Italy, public contractors cannot use this method as a solution without risking the paralysis of their business because, in order to enter into a contract and to obtain payment for the work carried out, they have to demonstrate that they are up to date with the payment of taxes and national insurance contributions.
The impossibility for a company of using this method may, however, be a source a reduced risk for the company's creditors. Companies decide to turnover the sources of finance, also by resorting to the non-payment of taxes and national insurance contributions, in order to avert definitive bankruptcy, resulting from an already existing serious corporate crisis.
This source of finance is normally very onerous, because it leads to further costs being incurred and is usually associated with the adoption of high risk readjustment strategies, since these are the only ones able to generate enough resources to repay all debts and weather the crisis[3].
Borrowers adopt risky strategies, which normally destroy economic value, maing their creditors bear the relative risk.
The whole risk of readjustment strategies, by definition a very high risk, is however borne entirely by the company's other financiers, who will see the value of their credit reduced, since tax and social security authorities have legal privileges for credit recovery in the event of bankruptcy, thus reducing the bankruptcy assets available for other creditors[4].
Consequently, construction companies are less of a risk and, in the abstract, financing them should be less onerous. Indeed, significant damage may be caused to a financier in the event of delayed ascertainment of an insolvency risk.

5 Conclusions

Financial analysts responsible for expressing an evaluation of companies' creditworthiness cannot ignore the specific features of the sector in which these companies operate. This is necessary in order to understand the relationships existing between the management peculiarites of the relevant sector and the obvious consequences for the company's borrowing requirements, as well as to correctly estimate the possibility of coercive recovery of debts in the event of the receiver of funds having solvency problems.
In this paper certain specific features of the construction sector have been described, with particular reference to public works contracts. After a brief description of the processes characterising companies operating in this sector, it was highlighted how the certificates needed in order to obtain the award of

public works contracts, though constituting a very important part of companies' intangible assets, are not represented in company accounts.
Moreover, these certificates, which can be transferred together with the company, or one of its "branches", have an intrinsic value and should, therefore, be appropriately considered when evaluating creditworthiness.
Consdering the fact that companies operating in the public works sector offer their financiers fewer opportunities for the coercive recovery of debts through the substitutability of sources of finance, appear, in the abstract, to be riskier. Indeed, it is observed that customers, when assigning contracts and paying credit accrued must request certification of up to date payment of tax and national insurance contributions from creditors.
This does not allow the company, in the event of a solvency crisis, to adopt highly risky and potentially profitable strategies, which in any case reduce the value of the credit.

Bibliography

[1] BONGINI P., DI BATTISTA M.L., NIERI L., *Relationship banking: una soluzione antica contro la crisi recente?*, in Bancaria, Roma, n. 5/2009.
[2] BIANCHI T., *I fidi bancari*, Utet, Torino, 1977.
[3] CANALE M., *Il finanziamento delle imprese non manifatturiere: analisi dei fabbisogni e valutazione di affidabilità,* in C. CACCIAMANI, (a cura di), *La valutazione di affidabilità delle imprese non manifatturiere,* Egea, Milano, 2000.
[4] CAPRARA U., *La banca. Principi di economia delle aziende di credito*, Giuffrè, Milano, 1986.
[5] DE LAURENTIS G., *Il rischio di credito. I fidi bancari nel nuovo contesto teorico, normativo e di mercato*, Egea, Milano, 2000.
[6] DELL'AMORE G., *Economia delle aziende di credito. I prestiti bancari*, Giuffrè, Milano, 1965.
[7] GUATRI L., *La valutazione delle aziende. Teoria e pratica a confronto*, Egea, Milano, 1990.
[8] MAINO R., DE LAURENTIS G., *I rating interni durante e dopo la crisi:rapport banca-imrpesa, vincoli regolamentari e modelli di business*, Bancaria Abi n. 1/2010.
[9] MOTTURA P., *Condizioni di equilibrio della strategia d'impresa*, in Finanza Marketing e Produzione, n. 1, 1987.
[10] ROSSIGNOLI B., *L'analisi di affidabilità delle imprese di costruzione*, in C. CACCIAMANI, (a cura di), *La valutazione di affidabilità delle imprese non manifatturiere,* Egea, Milano, 2000.
[11] RUOZI R., *Luci e ombre nell'evoluzione dell'attività bancaria,* Bancaria, Roma, n. 3/2008.

[12] TAGLIAVINI G., *Costo del capital, analisi finanziaria e corporate banking*, Egea.

[13] ZANDA G., LACCHINI M., *La valutazione delle iscrizioni all'Albo Nazionale dei Costruttori ai fini del calcolo del capitale economico delle imprese edili*, in Rivista italiana di ragioneria ed economia aziendale, mag.-giu. 1991.

[14] ZANDA G., LACCHINI M., ORICCHIO G., *La valutazione del capitale umano d'impresa. Modelli qualitativi e quantitativi di logica economico-aziendali,* Giappichelli, Torino, 1993.

[1] National regulations originate from EC Directive n. 2004/18/CE of 31/03/2004

[2] See IAS 11.

[3] The resources obtained from non-payment of taxes and national insurance contributions are often invested in the company without having developed particual readjustment startegies, but simply in order to delay the emergence of a solvency crisis, which is not perceived as such.

[4] This represents an authentic moral risk regarding non privileged creditors since, in the event of a debtor suffering a solvency crisis, they entirely bear the risk that the latter will "finance" risky strategies with resources that are ultimately deducted from credit guarantees.

RENDICONTI DEL CIRCOLO MATEMATICO DI PALERMO
Serie II, Suppl. 84 (2012), pp. 187-194

SQUARE IN EULER TRIPLES FROM PELL AND PELL-LUCAS NUMBERS

ZVONKO ČERIN e GIAN MARIO GIANELLA

Abstract. *In this paper we continue from* [7]*, for* $k = -4$ *and* $k = 8$*, to study the infinite sequences of triples* $A = (P_{2n+1},\ 2\,P_{2n+1},\ P_{2n+3})$*,* $B = (P_{2n+1},\ P_{2n+3},\ 2\,P_{2n+3})$ *and* $C = (Q_{2n+1},\ 2\,Q_{2n+1},\ Q_{2n+3})$*,* $D = (Q_{2n+1},\ Q_{2n+3},\ 2\,Q_{2n+3})$ *with the property that the product of any two different components of them increased by* k *are squares. The sequences* A *and* B *are built from the Pell numbers* P_n *while the sequences* C *and* D *from the Pell-Lucas numbers* Q_n*. We show some interesting properties of these sequences that give various methods how to get squares from them.*

Keywords: property $D(n)$, Pell numbers, Pell-Lucas numbers, square, components, symmetric sums, products.

1. Introduction

For integers a, b and c, let us write $a \overset{b}{\sim} c$ provided $a + b = c^2$. For the triples $A = (a, b, c)$, $D = (d, e, f)$ and $\widetilde{A} = (\widetilde{a}, \widetilde{b}, \widetilde{c})$ the notation $A \overset{D}{\sim} \widetilde{A}$ means that $b\,c \overset{d}{\sim} \widetilde{a}$, $c\,a \overset{e}{\sim} \widetilde{b}$ and $a\,b \overset{f}{\sim} \widetilde{c}$. When $D = (k, k, k)$, let us write $A \overset{k}{\sim} \widetilde{A}$ for $A \overset{D}{\sim} \widetilde{A}$. Hence, A is the $D(k)$-triple (see [1]) if and only if there is a triple $\widetilde{A}$ such that $A \overset{k}{\sim} \widetilde{A}$.

In the paper [7] we constructed infinite sequences $\alpha = \{\alpha(n)\}_{n=0}^{\infty}$ and $\beta = \{\beta(n)\}_{n=0}^{\infty}$ of $D(-4)$-triples and $\gamma = \{\gamma(n)\}_{n=0}^{\infty}$ and $\delta = \{\delta(n)\}_{n=0}^{\infty}$ of $D(8)$-triples. Here, $\alpha(n) = A = (P_{2n+1},\, 2\,P_{2n+1},\, P_{2n+3})$, $\beta(n) = B = (P_{2n+1},\, P_{2n+3},\, 2\,P_{2n+3})$ and $\gamma(n) = C = (Q_{2n+1},\, 2\,Q_{2n+1},\, Q_{2n+3})$, $\delta(n) = D = (Q_{2n+1},\, Q_{2n+3},\, 2\,Q_{2n+3})$, where the Pell and Pell-Lucas sequences of natural numbers P_n and Q_n are defined by the recurrence relations $P_0 = 0$, $P_1 = 2$, $P_n = 2\,P_{n-1} + P_{n-2}$ for $n \geqslant 2$ and $Q_0 = 2$, $Q_1 = 2$, $Q_n = 2\,Q_{n-1} + Q_{n-2}$ for $n \geqslant 2$.

The numbers Q_k make the integer sequence $A002203$ from [9] while the numbers $\frac{1}{2}\,P_k$ make $A000129$. The authors studied some sums of these numbers in the recent articles [4], [5] and [6].

The goal of this article is to further explore the properties of the sequences α, β, γ and δ. Each member of these sequences is an Euler $D(-4)$- or $D(8)$-triple (see [2] and [3]) so that many of their properties follow from the properties of the general (pencils of) Euler triples. It is therefore interesting to look for those properties in which at least two of the sequences appear. This paper presents several results of this kind giving many squares from the components, various sums and products of the sequences α, β, γ and δ. Most of our theorems have also versions for the associated sequences $\widetilde{\alpha}$, $\widetilde{\beta}$, $\widetilde{\gamma}$ and $\widetilde{\delta}$, where $\widetilde{\alpha}(n) = \widetilde{A} = (Q_{2n+2}, P_{2n+2}, Q_{2n+1})$,

$\widetilde{\beta}(n) = \widetilde{B} = (Q_{2n+3}, Q_{2n+2}, P_{2n+2})$, $\widetilde{\gamma}(n) = \widetilde{C} = (2\,P_{2n+2}, Q_{2n+2}, 2\,P_{2n+1})$ and $\widetilde{\delta}(n) = \widetilde{D} = (2\,P_{2n+3}, 2\,P_{2n+2},\ Q_{2n+2})$ satisfy $A \overset{-4}{\sim} \widetilde{A}$, $B \overset{-4}{\sim} \widetilde{B}$, $C \overset{8}{\sim} \widetilde{C}$ and $D \overset{8}{\sim} \widetilde{D}$.

2. Squares from products of components

The relations $A \overset{-4}{\sim} \widetilde{A}$ and $C \overset{8}{\sim} \widetilde{C}$ imply that the components of A and C satisfy $A_2A_3 \overset{-4}{\sim} \widetilde{A}_1$ and $C_2C_3 \overset{8}{\sim} \widetilde{C}_1$. Our first theorem shows that the product $A_2A_3C_2C_2$ is in a similar relation with respect to 64. Of course, the other products $A_3A_1C_3C_1$, $A_1A_2C_1C_2$ as well as $B_2B_3D_2D_3$, $B_3B_1D_3D_1$ and $B_1B_2D_1D_2$ exhibit a similar property.

Theorem 1. *The following hold for the products of components:*

$$A_2\,A_3\,C_2\,C_3 \overset{64}{\sim} 2\,P_{4n+4}, \qquad B_2\,B_3\,D_2\,D_3 \overset{0}{\sim} 2\,P_{4n+6},$$

$$A_3\,A_1\,C_3\,C_1 \overset{16}{\sim} P_{4n+4}, \qquad B_3\,B_1\,D_3\,D_1 \overset{64}{\sim} 2\,P_{4n+4},$$

$$A_1\,A_2\,C_1\,C_2 \overset{0}{\sim} 2\,P_{4n+2}, \qquad B_1\,B_2\,D_1\,D_2 \overset{16}{\sim} P_{4n+4}.$$

Proof. Let $\varphi = 1 + \sqrt{2}$ and $\psi = 1\sqrt{2} = -\frac{1}{\varphi}$. Since $P_j = \frac{\varphi^j - \psi^j}{\sqrt{2}}$ and $Q_j = \varphi^j + \psi^j$, it follows that $A_2 = \frac{4(\varphi^{2\,n+1} - \psi^{2\,n+1})}{\varphi - \psi}$, $A_3 = \frac{2(\varphi^{2\,n+3} - \psi^{2\,n+3})}{\varphi - \psi}$, $C_2 = 2(\varphi^{2\,n+1} + \psi^{2\,n+1})$ and $C_3 = \varphi^{2\,n+3} + \psi^{2\,n+3}$.

After the substitutions $\psi = -\frac{1}{\varphi}$ and $M = \varphi^n$, the sum of $A_2A_3C_2C_3$ and 64 becomes $\frac{2\,\varphi^8(M^2-\psi^2)^6(M^2+\psi^2)^2}{M^8}$. However, this is precisely the square of $2\,P_{4n+4}$. This shows the first relation. The other relations have similar proofs. □

The version of the previous theorem for the sequences $\widetilde{\alpha}$, $\widetilde{\beta}$, $\widetilde{\gamma}$ and $\widetilde{\delta}$ is the following result.

Theorem 2. *The products of components of $\widetilde{A}$, $\widetilde{B}$, $\widetilde{C}$ and $\widetilde{D}$ satisfy:*

$$\widetilde{A}_2\widetilde{A}_3\widetilde{C}_2\widetilde{C}_3 \overset{4}{\sim} Q_{4n+3}, \qquad \widetilde{B}_2\widetilde{B}_3\widetilde{D}_2\widetilde{D}_3 \overset{4}{\sim} Q_{4n+4},$$

$$\widetilde{A}_3\widetilde{A}_1\widetilde{C}_3\widetilde{C}_1 \overset{16}{\sim} 2\,P_{4n+3}, \qquad \widetilde{B}_3\widetilde{B}_1\widetilde{D}_3\widetilde{D}_1 \overset{4}{\sim} Q_{4n+5},$$

$$\widetilde{A}_1\widetilde{A}_2\widetilde{C}_1\widetilde{C}_2 \overset{4}{\sim} Q_{4n+4}, \qquad \widetilde{B}_1\widetilde{B}_2\widetilde{D}_1\widetilde{D}_2 \overset{16}{\sim} 2\,P_{4n+5}.$$

Proof. Since $\widetilde{A}_2 = \frac{2(\varphi^{2\,n+2} - \psi^{2\,n+2})}{\varphi - \psi}$, $\widetilde{A}_3 = \varphi^{2,n+1} + \psi^{2,n+1}$, $\widetilde{C}_2 = \varphi^{2,n+2} + \psi^{2,n+2}$ and $\widetilde{C}_3 = \frac{4(\varphi^{2,n+1} - \psi^{2,n+1})}{\varphi - \psi}$, the sum of $\widetilde{A}_2\widetilde{A}_3\widetilde{C}_2\widetilde{C}_3$ and 4, after the substitutions $\psi = -\frac{1}{\varphi}$ and $M = \varphi^n$, becomes $\frac{\varphi^6(M^8 - \psi^6)^2}{M^8}$. However, the square of Q_{4n+3} has the same value. This proves the first relation $\widetilde{A}_2\widetilde{A}_3\widetilde{C}_2\widetilde{C}_3 \overset{4}{\sim} Q_{4n+3}$. The remaining five relations in this theorem have similar proofs. □

The same kind of relations hold also for the products of components from all four sequences α, β, γ and δ.

Theorem 3. *The following relations for products of components hold:*

$$A_2B_3C_2D_3 \overset{256}{\sim} 4\,P_{4n+4}, \qquad A_3B_2C_3D_2 \overset{0}{\sim} P_{4n+6},$$
$$A_3B_1C_3D_1 \overset{16}{\sim} P_{4n+4}, \qquad A_1B_3C_1D_3 \overset{64}{\sim} 2\,P_{4n+4},$$
$$A_1B_2C_1D_2 \overset{16}{\sim} P_{4n+4}, \qquad A_2B_1C_2D_1 \overset{0}{\sim} 2\,P_{4n+2}.$$

Proof. Notice that the components A_2, B_3, C_2 and D_3 are $\frac{4(\varphi^{2\,n+1}-\psi^{2\,n+1})}{\varphi-\psi}$, $\frac{4(\varphi^{2\,n+3}-\psi^{2\,n+3})}{\varphi-\psi}$, $2(\varphi^{2\,n+1}+\psi^{2\,n+1})$ and $2(\varphi^{2\,n+3}+\psi^{2\,n+3})$. Since B_3 and D_3 are $2\,A_3$ and $2\,C_3$, it is now clear from the proof of Theorem 1 that after the substitutions $\psi=-\frac{1}{\varphi}$ and $M=\varphi^n$, the sum of $A_2B_3C_2D_3$ (i. e., four times $A_2A_3C_2C_3$) and 256 (i. e., four times 64) is the square of twice $2\,P_{4n+4}$ (i. e., of $4\,P_{4n+4}$). This shows the first relation $A_2B_3C_2D_3 \overset{256}{\sim} 4\,P_{4n+4}$. The other relations in this theorem have similar proofs. □

There is again the version of the previous theorem for the products of components from all four sequences $\widetilde{\alpha}$, $\widetilde{\beta}$, $\widetilde{\gamma}$ and $\widetilde{\delta}$.

Theorem 4. *The products of components of $\widetilde{A}$, $\widetilde{B}$, $\widetilde{C}$ and $\widetilde{D}$ satisfy:*

$$\widetilde{A}_2\widetilde{B}_3\widetilde{C}_2\widetilde{D}_3 \overset{0}{\sim} P_{4n+4}, \qquad \widetilde{A}_3\widetilde{B}_2\widetilde{C}_3\widetilde{D}_2 \overset{16}{\sim} 2\,P_{4n+3},$$
$$\widetilde{A}_3\widetilde{B}_1\widetilde{C}_3\widetilde{D}_1 \overset{64}{\sim} 2\,P_{4n+4}, \qquad \widetilde{A}_1\widetilde{B}_3\widetilde{C}_1\widetilde{D}_3 \overset{4}{\sim} Q_{4n+4},$$
$$\widetilde{A}_1\widetilde{B}_2\widetilde{C}_1\widetilde{D}_2 \overset{0}{\sim} 2\,P_{4n+4}, \qquad \widetilde{A}_2\widetilde{B}_1\widetilde{C}_2\widetilde{D}_1 \overset{4}{\sim} Q_{4n+5}.$$

Proof. The components $\widetilde{A}_3$, $\widetilde{B}_1$ and $\widetilde{C}_3$, $\widetilde{D}_1$ are the sums $\varphi^{2n+1}+\psi^{2n+1}$, $\varphi^{2n+3}+\psi^{2n+3}$ and the quotients $\frac{4(\varphi^{2\,n+1}-\psi^{2\,n+1})}{\varphi-\psi}$ and $\frac{4(\varphi^{2\,n+3}-\psi^{2\,n+3})}{\varphi-\psi}$. It is now clear from the proof of Theorem 1 that the sum of $\widetilde{A}_3\widetilde{B}_1\widetilde{C}_3\widetilde{D}_1$ and 64 is precisely the square of $2\,P_{4n+4}$.

This shows the third relation $\widetilde{A}_3\widetilde{B}_1\widetilde{C}_3\widetilde{D}_1 \overset{64}{\sim} 2\,P_{4n+4}$. The other five relations in this theorem have similar proofs. □

It is interesting (as the next two theorems show) that we can even mix components of the triples A, B, C, D and $\widetilde{A}$, $\widetilde{B}$, $\widetilde{C}$, $\widetilde{D}$.

Theorem 5. *The products of components of A, B, C, D and $\widetilde{A}$, $\widetilde{B}$, $\widetilde{C}$, $\widetilde{D}$ satisfy:*

$$\widetilde{A}_2B_3C_2\widetilde{D}_3 \overset{16}{\sim} 2(P_{4n+4}-2), \qquad A_2\widetilde{B}_3\widetilde{C}_2D_3 \overset{16}{\sim} 2(P_{4n+4}+2),$$
$$\widetilde{A}_3B_1C_3\widetilde{D}_1 \overset{36}{\sim} 8\,P_{4n+2}+Q_{4n}, \qquad A_3\widetilde{B}_1\widetilde{C}_3D_1 \overset{36}{\sim} 8\,P_{4n+2}+Q_{4n},$$
$$\widetilde{A}_1B_1C_2\widetilde{D}_2 \overset{16}{\sim} 2\,P_{4n+3}, \qquad A_2\widetilde{B}_2\widetilde{C}_1D_1 \overset{16}{\sim} 2\,P_{4n+3}.$$

Proof. The parts C_2, $\widetilde{D}_3$ and $\widetilde{A}_2$, B_3 are the sums $2(\varphi^{2n+1}+\psi^{2n+1})$, $\varphi^{2n+3}+\psi^{2n+3}$ and the quotients $\frac{2(\varphi^{2\,n+2}-\psi^{2\,n+2})}{\varphi-\psi}$, $\frac{4(\varphi^{2\,n+3}-\psi^{2\,n+3})}{\varphi-\psi}$.

It is now clear from the proof of Theorem 1 that the sum of $\widetilde{A}_2B_3C_2\widetilde{D}_3$ and 16 is equal $\frac{2\,\varphi^8(M^8-2\sqrt{2}\psi^4\,M^4-\psi^8)^2}{M^8}$ (i. e., the square of $2(P_{4n+4}-2)$).

This shows the first relation $\widetilde{A}_2B_3C_2\widetilde{D}_3 \overset{16}{\sim} 2(P_{4n+4}-2)$. The other five relations in this theorem have similar proofs. □

Theorem 6. *The products of components of A, B, C, D and $\widetilde{A}$, $\widetilde{B}$, $\widetilde{C}$, $\widetilde{D}$ satisfy:*

$$\widetilde{A}_3B_2\widetilde{C}_3D_2 \overset{36}{\sim} 8P_{4n+2}+Q_{4n}, \qquad A_3\widetilde{B}_2C_3\widetilde{D}_2 \overset{4}{\sim} Q_{4n+5},$$
$$\widetilde{A}_1B_3\widetilde{C}_1D_3 \overset{16}{\sim} 2\,Q_{4n+5}, \qquad A_1\widetilde{B}_3C_1\widetilde{D}_3 \overset{4}{\sim} P_{4n+3},$$
$$\widetilde{A}_2B_1\widetilde{C}_2D_1 \overset{4}{\sim} P_{4n+3}, \qquad A_2\widetilde{B}_1C_2\widetilde{D}_1 \overset{144}{\sim} 8\,P_{4n+2}+Q_{4n}.$$

Proof. The parts $\widetilde{A}_3$, D_2 and B_2, $\widetilde{C}_3$ are the sums $\varphi^{2n+1}+\psi^{2n+1}$, $\varphi^{2n+3}+\psi^{2n+3}$ and the quotients $\frac{2(\varphi^{2\,n+3}-\psi^{2\,n+3})}{\varphi-\psi}$, $\frac{8(\varphi^{2\,n+1}-\psi^{2\,n+1})}{\varphi-\psi}$. It is now clear that the sum of $\widetilde{A}_3B_2\widetilde{C}_3D_2$ and 36 is equal

$$\frac{\varphi^8[(M^4+\psi^4)^2-\psi^2(1+\psi)^2\,M^4]^2}{M^8}$$

(i. e., to the square of $8P_{4n+2}+Q_{4n}$).

This shows the first relation $\widetilde{A}_3B_2\widetilde{C}_3D_2 \overset{36}{\sim} 8P_{4n+2}+Q_{4n}$. The other five relations in this theorem have similar proofs. □

3. Squares from symmetric sums

Let $\sigma_1,\ ,\sigma_2,\ ,\sigma_3 : \mathbb{Z}^3 \to \mathbb{Z}$ be the basic symmetric functions defined for $x=(a,\,b,\,c)$ by $x_{\sigma_1}=a+b+c$, $x_{\sigma_2}=bc+ca+ab$, $x_{\sigma_3}=a\,b\,c$. Let σ_2^*, $\sigma_1^* : \mathbb{Z}^3 \to \mathbb{Z}$ be defined by $x_{\sigma_2^*}=b\,c-c\,a+a\,b$ and $x_{\sigma_1^*}=a-b+c$. Note that $x_{\sigma_1^*}$ is the determinant of the 1×3 matrix $[a,b,c]$ (see [8]).

Let us note the identities $A_{\sigma_1^*}\,D_{\sigma_1^*}+16=B_{\sigma_1^*}\,C_{\sigma_1^*}=(2\,Q_{2n+2})^2$. In fact, since $A_{\sigma_1^*}=2\,P_{2n+2}$ and $D_{\sigma_1^*}=4\,P_{2n+2}$, it follows that

$$A_{\sigma_1^*}\,D_{\sigma_1^*}+16=8\,P_{2n+2}^2+16=(2\,Q_{2n+2})^2.$$

On the other hand, the identity $B_{\sigma_1^*}\,C_{\sigma_1^*}=(2\,Q_{2n+2})^2$ is obvious since $B_{\sigma_1^*}=C_{\sigma_1^*}=2\,Q_{2n+2}$.

For the sums σ_2 and σ_2^* of the components analogous relations are true.

Theorem 7. *The following is true for the sums σ_2 of the components:*

$$A_{\sigma_2}C_{\sigma_2} \overset{144}{\sim} 8\,P_{4n+3}+P_{4n}, \qquad B_{\sigma_2}D_{\sigma_2} \overset{144}{\sim} 88\,P_{4n+2}-15\,P_{4n},$$
$$\widetilde{A}_{\sigma_2}\widetilde{C}_{\sigma_2} \overset{48}{\sim} 2\,Q_{4n+4}, \qquad \widetilde{B}_{\sigma_2}\widetilde{D}_{\sigma_2} \overset{32}{\sim} 4\,P_{4n+5}.$$

Proof. Since $A_{\sigma_2} = \frac{1}{2}P_{2n+1}(23Q_{2n+1} + 11Q_{2n})$ and $C_{\sigma_2} = Q_{2n+1}(2P_{2n+4} - Q_{2n})$, the sum $A_{\sigma_2}C_{\sigma_2} + 144$ is the square of $\frac{\xi(49\,M^8-\zeta^2)}{M^4}$, where ξ and ζ are $\frac{57+80\sqrt{2}}{98}$ and $57 - 40\sqrt{2}$. It is now easy to check that $\frac{\xi(49\,M^8-\zeta^2)}{M^4}$ is equal to the sum $8\,P_{4n+3} + P_{4n}$. This proves the first relation $A_{\sigma_2}C_{\sigma_2} \overset{144}{\sim} 8\,P_{4n+3} + P_{4n}$. The other relations in this theorem have similar proofs. □

Theorem 8. *The following is true for the sums σ_2^* of the components:*

$$A_{\sigma_2^*}C_{\sigma_2^*} \overset{16}{\sim} 8\,P_{4n+2} - P_{4n}, \qquad B_{\sigma_2^*}D_{\sigma_2^*} \overset{16}{\sim} 64\,P_{4n+2} - 11\,P_{4n},$$
$$\widetilde{A}_{\sigma_2^*}\widetilde{C}_{\sigma_2^*} \overset{-16}{\sim} 2\,Q_{4n+3}, \qquad \widetilde{B}_{\sigma_2^*}\widetilde{D}_{\sigma_2^*} \overset{48}{\sim} 2\,Q_{4n+4}.$$

Proof. Since $B_{\sigma_2^*} = \frac{1}{2}P_{2n+3}(13Q_{2n+1} + 5Q_{2n})$ and $D_{\sigma_2^*} = Q_{2n+3}(9Q_{2n+1} + 4Q_{2n})$, the sum $B_{\sigma_2^*}D_{\sigma_2^*} + 16$ is the quotient $\frac{\xi_+(7\,M^8+\xi_-)^2}{98\,M^8}$, where $\xi_\pm$ is $65529 \pm 46336\sqrt{2}$. It is now easy to check that this is the square of $64P_{4n+2} - 11P_{4n}$. This proves the second relation $B_{\sigma_2^*}C_{\sigma_2} \overset{16}{\sim} 64\,P_{4n+2} - 11\,P_{4n}$. The other relations in this theorem have similar proofs. □

In the next result we consider the products of the same components of the triples A, B, C and D and the product of their components.

Theorem 9. *The following relations and the identity hold:*

$$A_1B_1C_1D_1 \overset{0}{\sim} P_{4n+2}, \qquad A_2B_2C_2D_2 \overset{64}{\sim} 2\,P_{4n+4},$$
$$A_3B_3C_3D_3 \overset{0}{\sim} P_{4n+6}, \qquad 4\,A_{\sigma_3}B_{\sigma_3}C_{\sigma_3}D_{\sigma_3} = (4\,P_{4n+2}\,P_{4n+6})^3.$$

Proof. Since $A_3 = P_{2n+3}$, $B_3 = 2\,P_{2n+3}$, $C_3 = Q_{2n+3}$ and $D_3 = 2\,Q_{2n+3}$, it follows that $A_3B_3C_3D_3 = (2\,P_{2n+3}\,Q_{2n+3})^2 = (2\,P_{4n+6})^2$. This proves the third relation. The other relations have similar proofs. □

The products of the same components of the triples $\widetilde{A}$, $\widetilde{B}$, $\widetilde{C}$ and $\widetilde{D}$ and the product of their components appear in the following result.

Theorem 10. *The following relations and the identity hold:*

$$2\,\widetilde{A}_1\widetilde{B}_1\widetilde{C}_1\widetilde{D}_1 \overset{16}{\sim} 2\,Q_{4n+5}, \qquad \widetilde{A}_3\widetilde{B}_3\widetilde{C}_3\widetilde{D}_3 \overset{4}{\sim} Q_{4n+3},$$
$$2\,\widetilde{A}_2\widetilde{B}_2\widetilde{C}_2\widetilde{D}_2 \overset{0}{\sim} 2\,P_{4n+4}, \qquad \widetilde{A}_{\sigma_3}\widetilde{B}_{\sigma_3}\widetilde{C}_{\sigma_3}\widetilde{D}_{\sigma_3} = (2\,P_{4n+4})^4\,P_{4n+6}\,P_{4n+2}.$$

Proof. Since $\widetilde{A}_3 = Q_{2n+1}$, $\widetilde{B}_3 = P_{2n+2}$, $\widetilde{C}_3 = 2\,P_{2n+1}$ and $\widetilde{D}_3 = Q_{2n+2}$, it follows that the sum of $\widetilde{A}_3\widetilde{B}_3\widetilde{C}_3\widetilde{D}_3$ and 4 is the square of $\frac{\varphi^3(M^8-\psi^6)}{M^4}$ that we recognize as Q_{4n+3}. This proves the second relation. The other relations in this theorem and the identity have similar proofs. □

The products of the sums σ_1 and σ^* of the components of the triples A, B, C and D show the same kind of relations. This is also true for the associated triples $\widetilde{A}$, $\widetilde{B}$, $\widetilde{C}$ and $\widetilde{D}$.

Theorem 11. *The following relations hold for the sums σ_1 and σ_1^*:*

$$A_{\sigma_1}B_{\sigma_1}C_{\sigma_1}D_{\sigma_1} \overset{1024}{\sim} 28P_{4n+4}, \qquad \widetilde{A}_{\sigma_1}\widetilde{B}_{\sigma_1}\widetilde{C}_{\sigma_1}\widetilde{D}_{\sigma_1} \overset{144}{\sim} 3\,P_{4n+6},$$

$$A_{\sigma_1^*}B_{\sigma_1^*}C_{\sigma_1^*}D_{\sigma_1^*} \overset{64}{\sim} 4Q_{4n+4}, \qquad \widetilde{A}_{\sigma_1^*}\widetilde{B}_{\sigma_1^*}\widetilde{C}_{\sigma_1^*}\widetilde{D}_{\sigma_1^*} \overset{0}{\sim} 3P_{4n+4}.$$

Proof. The sums of the components A_{σ_1}, B_{σ_1}, C_{σ_1} and D_{σ_1} are equal $Q_{2n+3}+Q_{2n}$, $2(4\,P_{2n+2}-P_{2n})$, $2(P_{2n+3}+P_{2n})$ and $2(4\,Q_{2n+2}-Q_{2n})$. Hence, the sum of $A_{\sigma_1}B_{\sigma_1}C_{\sigma_1}D_{\sigma_1}$ and 1024 is the quotient

$$\frac{392\,\varphi^8(M^4-\psi^4)^2[(M^2+\psi^2)^2-(1+\psi)^2M^2]^2}{M^8}$$

that we recognize as the square of $28P_{4n+4}$. This proves the above first relation. The other relations in this theorem have similar proofs. □

4. Squares from the sums of squares

For a natural number $k>1$, let the sums ν_k, $\nu_k^*:\mathbb{Z}^3\to\mathbb{Z}$ of powers be defined for $x=(a,b,c)$ by $x_{\nu_k}=a^k+b^k+c^k$ and $x_{\nu_k^*}=a^k-b^k+c^k$.

We proceed with the version of the Theorem 7 for the sums ν_2 of the squares of components.

Theorem 12. *The following relations are true for the sums ν_2:*

$$A_{\nu_2}C_{\nu_2} \overset{-320}{\sim} 16\,P_{4n+3}+2\,P_{4n}, \qquad B_{\nu_2}D_{\nu_2} \overset{-320}{\sim} 176\,P_{4n+2}-30\,P_{4n},$$

$$\widetilde{A}_{\nu_2}\widetilde{C}_{\nu_2} \overset{-96}{\sim} 8\,P_{4n+3}+P_{4n}, \qquad \widetilde{B}_{\nu_2}\widetilde{D}_{\nu_2} \overset{-96}{\sim} 88\,P_{4n+2}-15\,P_{4n}.$$

Proof. Since $A_{\nu_2}=8Q_{4n+3}+Q_{4n}+6$ and $C_{\nu_2}=2(8Q_{4n+3}+Q_{4n}-6)$, the difference of $A_{\nu_2}C_{\nu_2}$ and 320 is equal to the quotient

$$\frac{2\,\xi_+^2(49\,M^8-\xi_-^2)^2}{(49\,M^4)^2},$$

where $\xi_\pm=57\pm40\sqrt{2}$. But, one can easily check that this quotient is the square of $16\,P_{4n+3}+2\,P_{4n}$. This concludes the proof of the first relation. The other relations in this theorem have similar proofs. □

The next is the version of the Theorem 8 for the alternating sums ν_2^* of the squares of components.

Theorem 13. *The following relations are true for the sums ν_2^*:*

$$A_{\nu_2^*}C_{\nu_2^*} \overset{192}{\sim} 9\,Q_{4n+3}+Q_{4n}, \qquad B_{\nu_2^*}D_{\nu_2^*} \overset{-192}{\sim} 30\,Q_{4n+3}+2\,Q_{4n},$$

$$\widetilde{A}_{\nu_2^*}\widetilde{C}_{\nu_2^*} \overset{-32}{\sim} 8\,P_{4n+2}-P_{4n}, \qquad \widetilde{B}_{\nu_2^*}\widetilde{D}_{\nu_2^*} \overset{64}{\sim} 64\,P_{4n+2}-11\,P_{4n}.$$

Proof. Note that the alternating sums of squares of components $A_{\nu_2^*}$ and $C_{\nu_2^*}$ are $16Q_{4n+2} - 3Q_{4n} - 2$ and $2(16Q_{4n+3} - 3Q_{4n} + 2)$. Hence, the sum of $A_{\nu_2^*}C_{\nu_2^*}$ and 192 is equal to the quotient $\frac{2\,\xi_+(23\,M^8+\xi_-)^2}{(23\,M^4)^2}$, where $\xi_\pm = 4073 \pm 2880\sqrt{2}$. This quotient is in fact the square of $9\,Q_{4n+3} + Q_{4n}$. This proves the first relation. The other relations in this theorem have similar proofs. □

5. Squares from the products $\odot$, $\triangleright$ and $\triangleleft$

Let us introduce three binary operations $\odot$, $\triangleright$ and $\triangleleft$ on the set $\mathbb{Z}^3$ of triples of integers by the rules $(a,\,b,\,c)\odot(u,\,v,\,w) = (a\,u,\,b\,v,\,c\,w)$, $(a,\,b,\,c)\triangleright(u,\,v,\,w) = (a\,v,\,b\,w,\,c\,u)$, and

$$(a,\,b,\,c)\triangleleft(u,\,v,\,w) = (a\,w,\,b\,u,\,c\,v).$$

This section contains four theorems which show that the operations $\odot$, $\triangleright$ and $\triangleleft$ are also the source of squares from components of the eight sequences.

Theorem 14. *The following relations for the sequences A, B, C and D hold:* $(A\odot B)_{\sigma_1}(C\odot D)_{\sigma_1} \overset{-64}{\sim} 83\,P_{4n+2} - 14\,P_{4n}$,

$$(A\triangleright B)_{\sigma_1}(C\triangleright D)_{\sigma_1} \overset{576}{\sim} 6\,P_{4n+4},$$

$$(A\triangleleft B)_{\sigma_1}(C\triangleleft D)_{\sigma_1} \overset{-64}{\sim} 49\,P_{4n+2} - 8\,P_{4n}.$$

Proof. Since $(A\triangleright B)_{\sigma_1} = 6\,P_{2n+3}\,P_{2n+1}$ and $(C\triangleright D)_{\sigma_1} = 6\,Q_{2n+3}\,Q_{2n+1}$, it follows that the sum of $(A\triangleright B)_{\sigma_1}(C\triangleright D)_{\sigma_1}$ and 576 is the square of $6\,P_{4n+4}$. This proves the second relation. The first and the third could be established similarly. □

Theorem 15. *The following relations for the sequences A, B, C and D hold:* $(A\odot B)_{\sigma_1^*}(C\odot D)_{\sigma_1^*} \overset{-64}{\sim} 59\,P_{4n+2} - 10\,P_{4n}$,

$$(A\triangleright B)_{\sigma_1^*}(C\triangleright D)_{\sigma_1^*} \overset{64}{\sim} 2\,P_{4n+4},$$

$$(A\triangleleft B)_{\sigma_1^*}(C\triangleleft D)_{\sigma_1^*} \overset{192}{\sim} 18\,P_{4n+3} + P_{4n}.$$

Proof. Since the alternating sums $(A\triangleright B)_{\sigma_1^*}$ and $(C\triangleright D)_{\sigma_1^*}$ are $-2\,P_{2n+3}\,P_{2n+1}$ and $-2\,Q_{2n+3}\,Q_{2n+1}$, it follows that the sum of $(A\triangleright B)_{\sigma_1^*}(C\triangleright D)_{\sigma_1^*}$ and 64 is the square of $2\,P_{4n+4}$. This is the outline of the proof of the second relation. The similar proofs of the first and the third relation are left to the reader. □

Theorem 16. *The following relations for the triples $\widetilde{A}$, $\widetilde{B}$, $\widetilde{C}$ and $\widetilde{D}$ hold:* $(\widetilde{A}\odot\widetilde{B})_{\sigma_1}(\widetilde{C}\odot\widetilde{D})_{\sigma_1} \overset{-16}{\sim} 2\,Q_{4n+5}$, $(\widetilde{A}\triangleright\widetilde{B})_{\sigma_1}(\widetilde{C}\triangleright\widetilde{D})_{\sigma_1} \overset{0}{\sim} 5\,P_{4n+4}$, *and* $(\widetilde{A}\triangleleft\widetilde{B})_{\sigma_1}(\widetilde{C}\triangleleft\widetilde{D})_{\sigma_1} \overset{96}{\sim} 4\,Q_{4n+4}$.

Proof. Since the sums $(\widetilde{A} \triangleleft \widetilde{B})_{\sigma_1}$ and $(\widetilde{C} \triangleleft \widetilde{D})_{\sigma_1}$ are $4(P_{4n+4} - 1)$ and $8(P_{4n+4} + 1)$, it follows that the sum of $(\widetilde{A} \triangleleft \widetilde{B})_{\sigma_1}(\widetilde{C} \triangleleft \widetilde{D})_{\sigma_1}$ and 96 is the square of $4\,Q_{4n+4}$. This is the outline of the proof of the third relation. The similar proofs of the first and the second relation are left to the reader. □

Theorem 17. *The following relations hold for the triples $\widetilde{A}$, $\widetilde{B}$, $\widetilde{C}$ and $\widetilde{D}$:* $(\widetilde{A} \odot \widetilde{B})_{\sigma_1^*}(\widetilde{C} \odot \widetilde{D})_{\sigma_1^*} \overset{-32}{\sim} 4\,P_{4n+4}$, $(\widetilde{A} \triangleright \widetilde{B})_{\sigma_1^*}(\widetilde{C} \triangleright \widetilde{D})_{\sigma_1^*} \overset{0}{\sim} 3\,P_{4n+4}$, *and* $(\widetilde{A} \triangleleft \widetilde{B})_{\sigma_1^*}(\widetilde{C} \triangleleft \widetilde{D})_{\sigma_1^*} \overset{-16}{\sim} 2\,Q_{4n+3}$.

Proof. Since the alternating sums $(\widetilde{A} \triangleleft \widetilde{B})_{\sigma_1^*}$ and $(\widetilde{C} \triangleleft \widetilde{D})_{\sigma_1^*}$ are $-2\,P_{4n+3}$ and $-4\,P_{4n+3}$, it follows that the difference of $(\widetilde{A} \triangleleft \widetilde{B})_{\sigma_1^*}(\widetilde{C} \triangleleft \widetilde{D})_{\sigma_1^*}$ and 16 is the square of $2\,Q_{4n+3}$. This is the outline of the proof of the third relation. The similar proofs of the first and the second relation are left to the reader. □

References

[1] E. Brown, *Sets in which $x\,y + k$ is always a square*, Mathematics of Computation, **45** (1985), 613-620.

[2] Z. Čerin, *On pencils of Euler triples, I*, (to appear).

[3] Z. Čerin, *On pencils of Euler triples, II*, (to appear).

[4] Z. Čerin and G. M. Gianella, *On sums of squares of Pell-Lucas numbers*, INTEGERS: Electronic Journal of Combinatorial Number Theory, **6** (2006), A15.

[5] Z. Čerin and G. M. Gianella, *Formulas for sums of squares and products of Pell numbers*, Acc. Sc. Torino - Atti Sci. Fis. 140 (2006), 113-122.

[6] Z. Čerin and G. M. Gianella, *On sums of Pell numbers*, Acc. Sc. Torino - Atti Sci. Fis. 141 (2007), 23-31.

[7] Z. Čerin and G. M. Gianella, *On Diophantine triples from Pell and Pell-Lucas numbers*, Acc. Sc. Torino - Atti Sci. Fis. **143** (2009), 83-94.

[8] M. Radić, *A definition of determinant of rectangular matrix*, Glasnik Mat. 1 (21) (1966), 17-22.

[9] N. Sloane, *On-Line Encyclopedia of Integer Sequences*, `http://www.research. att.com/~njas/sequences/`.

ZVONKO ČERIN
Kopernikova 7,
10010 Zagreb, Croatia.
`cerin@math.hr`

GIAN MARIO GIANELLA
Dipartimento di Matematica, Università di Torino,
via C. Alberto 10, 10123 Torino,Italy.
`gianmario.gianella @unito.it`

RENDICONTI DEL CIRCOLO MATEMATICO DI PALERMO
Serie II, Suppl. 84 (2012), pp. 195-205

Some New Results on Second-Order Chord Power Integrals of Convex Quadrangles

LOTHAR HEINRICH

Dedicated to Univ.-Prof. Dr.phil. Dr.h.c.mult. Peter M. Gruber on the occasion of his 70th birthday

Abstract

We study some geometric inequalities for second-order chord power integrals $I_2(K)$ of convex quadrangles K with positive area $A(K)$ and boundary length $L(\partial K)$. Based on different representations of $I_2(K)$ for convex quadrangles K we derive lower and upper bounds and give explicit formulas for $I_2(K)$ in case of parallelograms and rhombs. Further, an elementary proof of the isoperimetric inequality and a Carleman-type inequality for quadrangles is given. At the end of the paper we state two conjectures on sharp upper and lower bounds of $I_2(K)$ for convex polygons and their extensions to parallelotopes in higher dimensions.

Keywords : Poisson strip process, isoperimetric inequality, Carleman-type inequality, Steiner symmetrization, kite, parallelogram, rhomb, parallelotope

MSC 2000: Primary 52A40 60G05 Secondary 52A07 52A22

1 CLT for Motion-Invariant Poisson Strip Processes and Chord Power Integrals of Star-Shaped Discs

To motivate our study of *chord power integrals* (CPI's) we state a central limit theorem for the total area of the union of stationary and isotropic Poisson strips contained in an expanding planar region ϱK as $\varrho \uparrow \infty$, where K has positive area $A(K)$ and is star-shaped w.r.t. the origin $\mathbf{o}$. Let

$$g(p,\varphi) = \{\, (x,y) \in \mathbb{R}^2 : x\cos\varphi + y\sin\varphi = p \,\} \;\;,\;\; \varphi \in [0,\pi)\;,\; p \in \mathbb{R}\,,$$

be an unoriented line in a xy-coordinate system with normal unit vector $(\cos\varphi, \sin\varphi)$ directed in the upper half-plane and signed perpendicular

distance $p \in \mathbb{R}$ from $\mathbf{o}$. We define the Poisson strips as dilated Poisson lines and its union set by

$$\Xi_{\lambda,F} = \bigcup_{i\in\mathbb{Z}} g(P_i, \Phi_i) \oplus B_2(R_i)$$

with $B_2(r) = \{\mathbf{x} \in \mathbb{R}^2 : \|\mathbf{x}\| \le r\}$, see Figure 1. Further, $\{P_i, i \in \mathbb{Z}\}$ forms a stationary Poisson process on $\mathbb{R}$ with intensity λ, $\{\Phi_i, i \in \mathbb{Z}\}$ are independent equidistributed angles in $[0, \pi]$, and $\{R_i, i \in \mathbb{Z}\}$ are independent radii with common distribution F such that $\mathbb{E}R_0^2 < \infty$. see e.g. [7],[4] for the definition of general stationary (Poisson) cylinder processes.

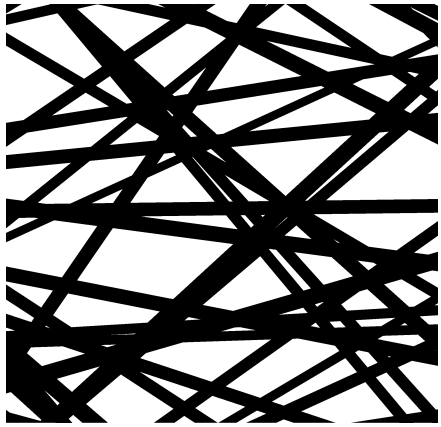


Figure 1: Isotropic Poisson strips

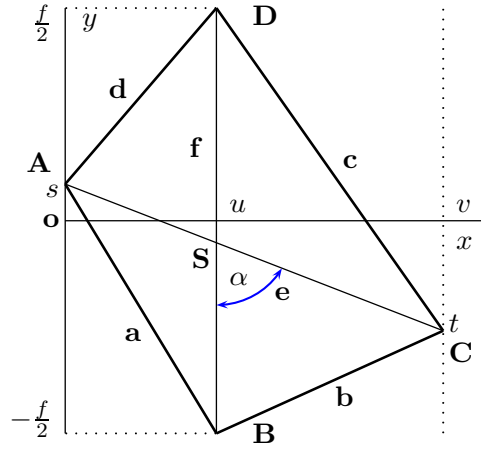


Figure 2: Convex quadrangle

As special case of a result proved in [4] we get the convergence in distribution

$$\sqrt{\varrho}\,\Big(\frac{A(\Xi_{\lambda,F}\cap\varrho\,K)}{A(\varrho\,K)} - \mu\Big) \xrightarrow[\varrho\to\infty]{\mathrm{d}} \mathcal{N}\Big(0\,,\,\tau^2\,\frac{I_2(K)}{A^2(K)}\Big)\,, \tag{1}$$

where $\mu = 1 - \exp\{-2\,\lambda\,\mathbb{E}R_0\}$ and $\tau^2 = 4\,\lambda\,\mathbb{E}R_0^2\,\exp\{-4\,\lambda\,\mathbb{E}R_0\}/\pi$. Here, $\mathcal{N}(0,\sigma^2)$ is a zero mean Gaussian random variable with variance $\sigma^2 > 0$ and $I_2(K)$ denotes the second-order CPI of $K \subset \mathbb{R}^2$ defined by

$$I_2(K) = \int_0^\pi \int_{\mathbb{R}} L^2(K \cap g(p,\varphi))\,\mathrm{d}p\,\mathrm{d}\varphi = \int_K \int_K \frac{\mathrm{d}\mathbf{x}\,\mathrm{d}\mathbf{y}}{\|\mathbf{x}-\mathbf{y}\|} \tag{2}$$

with length measure $L(\cdot)$, see [2] and [7] for more on CPI's in convex and integral geometry. From the view point of *optimal experimental design* it is

an aim to minimize the ratio $I_2(K)/A^2(K)$ in (1) given the perimeter $L(\partial K)$ of K. In convex geometry, see [1], [6], it is also of interest to maximize $I_2(K)$ when $A(K)$ is fixed, at least within certain families of convex discs.

In Section 2 and 4 we derive integral representations of $I_2(K)$ in case of general quadrangles K and evaluate them expclitly for parallelograms and rhombs. From these expressions we deduce some inequalities between their second-order CPI's. But before doing this, we discuss the comparatively simple case of triangles $\triangle = \triangle(a,b,c)$ with sides a,b,c and half-perimeter $s=(a+b+c)/2$. In [3] we could show that

$$\frac{I_2(\triangle)}{A^2(\triangle)} = \frac{4}{3}\Big[\,\frac{1}{a}\log\Big(\frac{s}{s-a}\Big)+\frac{1}{b}\log\Big(\frac{s}{s-b}\Big)+\frac{1}{c}\log\Big(\frac{s}{s-c}\Big)\,\Big]\,, \qquad (3)$$

whence together with Heron's formula $A(\triangle)=\sqrt{s(s-a)(s-b)(s-c)}$ and by substituting $x=(s-a)/s$, $y=(s-b)/s$ so that $x+y=c/s$, it follows that the ratio $I_2(\triangle)/A^{3/2}(\triangle)$ is bounded from above by

$$\begin{aligned}
&\frac{4}{3}\max_{\substack{0\le x,y\le 1\\ x+y\le 1}}\left[\sqrt[4]{x\,y\,(1-x-y)}\left(\frac{\log\left(\frac{1}{x}\right)}{1-x}+\frac{\log\left(\frac{1}{y}\right)}{1-y}+\frac{\log\left(\frac{1}{1-x-y}\right)}{x+y}\right)\right]\\
=\;&\frac{4}{3}\max_{\substack{0\le x\le a\\ 0\le a\le 1}}\left[\sqrt[4]{x\,(a-x)\,(1-a)}\left(\frac{\log\left(\frac{1}{x}\right)}{1-x}+\frac{\log\left(\frac{1}{a-x}\right)}{1-a+x}+\frac{\log\left(\frac{1}{1-a}\right)}{a}\right)\right]\\
=\;&\frac{4}{3}\max_{0\le a\le 1}\left[\sqrt[4]{\frac{a^2}{4}\,(1-a)}\,\Big(\,\frac{4\,\log\frac{2}{a}}{2-a}+\frac{\log\frac{1}{1-a}}{a}\,\Big)\right] = 2\,\sqrt[4]{3}\,\log 3\approx 2.8917\,,
\end{aligned}$$

where in the second line the maximum is attained at $x=a/2$ and in the third line at $a=2/3$. This estimate combined with the lower bound of $I_2(\triangle)/A^2(\triangle)$ obtained in [3] yields the inclusion

$$\frac{c_3}{L(\partial\triangle)}\le\frac{I_2(\triangle)}{A^2(\triangle)}\le\frac{\sqrt[4]{3}\,c_3}{6\,\sqrt{A(\triangle)}}\quad\text{with}\quad c_3=12\,\log 3 \qquad (4)$$

and "=" holds on both sides iff $a=b=c$ (so that $c_3=16\,I_2(\triangle(1,1,1))$).

2 Second-Order CPI of Convex Quadrangles

We consider a convex quadrangle $\square ABCD$ embedded in the $xy-$coordinate system as in Figure 2 with diagonal $\mathbf{f}=\overline{BD}$ chosen parallel to the $y-$axis

and bisected by the point $(u,0)$ on the $x-$axis with varying $u \in [0,v]$. For the moment let $f = \|\overline{BD}\|$ and $v > 0$ be fixed whereas the vertices $A = (0,s))$ and $C = (v,t)$ may vary on and parallel to the $y-$axis, respectively, as long as the convexity of $\Box ABCD$ is not hurt. We shortly write $\Box_{f,v}(s,t,u)$ for this quadrangle which has area $A(\Box_{f,v}(s,t,u)) = \frac{1}{2}\, f\, v$ not depending on $s,t \in \mathbb{R}$ and $u \in (0,v]$. Another parametrization arises from parallel shifts of both diagonals $\mathbf{f}$ and $\mathbf{e} = \overline{AC}$ (with length $e = \|\overline{AC}\|$) which intersect in $\mathbf{S}$ at a fixed angle $\alpha \in [0,\pi/2]$, see Fig. 2. Put $p = \|\overline{AS}\|/\|\overline{AC}\| \in [0,1]$ and $q = \|\overline{BS}\|/\|\overline{BD}\| \in [0,1]$ and, for fixed e,f,α, let $\Box_{e,f,\alpha}(p,q)$ denote the corresponding quadrangle $\Box ABCD$. By the obvious relations

$$v = e\,\sin\alpha\ ,\ u = p\,e\,\sin\alpha\ ,\ s = (q-\frac{1}{2})\,f + p\,e\,\cos\alpha\ ,\ t = s - e\,\cos\alpha$$

we get the area $A(\Box_{e,f,\alpha}(p,q)) = \frac{1}{2}\,e\,f\,\sin\alpha$ for any $0 \le p,q \le 1$.

We introduce linear functions $f_i(\cdot)$ and $g_i(\cdot)$ which describe the lower line segments $\overline{AB}, \overline{BC}$ (for $i=1$) and the upper line segments $\overline{AD}, \overline{DC}$ (for $i=2$). They are given by

$$f_1(x) = -\Big(s + \frac{f}{2}\Big)\,\frac{x}{u} + s \qquad , \quad f_2(x) = -\Big(s - \frac{f}{2}\Big)\,\frac{x}{u} + s \ \ , \ \ 0 \le x \le u$$

$$g_1(x) = \Big(t + \frac{f}{2}\Big)\,\frac{x-v}{v-u} + t \quad , \quad g_2(x) = \Big(t - \frac{f}{2}\Big)\,\frac{x-v}{v-u} + t \ \ , \ \ u \le x \le v\,.$$

Making use of the triangles $\triangle_1 = \triangle_1(s,u) = \triangle ABD$ and $\triangle_2 = \triangle_2(t,w) = \triangle BCD$ (with $w := v-u$) we may write $\Box := \Box_{f,v}(s,t,u) = \triangle_1 \cup \triangle_2$ and, therefore, from (2) it follows the representation

$$I_2(\Box) = I_2(\triangle_1) + I_2(\triangle_2) + 2\,I_2(\triangle_1,\triangle_2) \ \text{ with } \ I_2(\triangle_1,\triangle_2) = \int\limits_{\triangle_1}\int\limits_{\triangle_2} \frac{\mathrm{d}\mathbf{x}\,\mathrm{d}\mathbf{y}}{\|\mathbf{x}-\mathbf{y}\|}\,.$$

By means of (3) and $a^2/d^2 = (\frac{f}{2} \pm s)^2 + u^2$, $b^2/c^2 = (\frac{f}{2} \pm s)^2 + w^2$ we get closed-term formulas for $I_2(\triangle_1)$ und $I_2(\triangle_2)$. Next, we rewrite the two-fold integration in $I_2(\triangle_1,\triangle_2)$ over $\mathbf{x} = (x_1,y_1) \in \triangle_1$ and $\mathbf{y} = (x_2,y_2) \in \triangle_2$ leading to the four-fold integral

$$\int\limits_0^u \int\limits_{f_1(x_1)}^{f_2(x_1)} \int\limits_u^v \int\limits_{g_1(x_2)}^{g_2(x_2)} \frac{\mathrm{d}y_2\,\mathrm{d}x_2\,\mathrm{d}y_1\,\mathrm{d}x_1}{\sqrt{(x_2-x_1)^2+(y_2-y_1)^2}} \ = \ \int\limits_0^u \int\limits_u^v H(x_1,x_2,s,t)\,\mathrm{d}x_2\,\mathrm{d}x_1\,,$$

where

$$H(x_1,x_2,s,t) = \int\limits_{f_1(x_1)}^{f_2(x_1)} \int\limits_{g_1(x_2)}^{g_2(x_2)} \frac{\mathrm{d}y_2\,\mathrm{d}y_1}{\sqrt{(x_2-x_1)^2+(y_2-y_1)^2}}\,.$$

To calculate $H(x_1, x_2, s, t)$ (for $x_1 < x_2$) we need the integral functions

$$F(z) := \int_0^z \frac{\mathrm{d}y}{\sqrt{1+y^2}} = \log(z + \sqrt{z^2+1}) = -F(-z)$$

$$G(z) := \int_0^z F(x)\,\mathrm{d}x = z\,\log(z + \sqrt{z^2+1}) - \sqrt{z^2+1} + 1 = G(-z)$$

defined for all $z \in \mathbb{R}$, where the odd function $F(\cdot)$ is strictly increasing (convex for $z \geq 0$) and the even function $G(\cdot)$ is strictly convex since $G''(z) = F'(z) = (z^2+1)^{-1/2} > 0$. From the inner integral of $H(x_1, x_2, s, t)$

$$\int_{g_1(x_2)}^{g_2(x_2)} \frac{\mathrm{d}y_2}{\sqrt{(x_2-x_1)^2 + (y_2-y_1)^2}} = F\Big(\frac{y_1 - g_1(x_2)}{x_2 - x_1}\Big) - F\Big(\frac{y_1 - g_2(x_2)}{x_2 - x_1}\Big),$$

it follows after a short calculation that

$$\frac{H(x_1, x_2, s, t)}{x_2 - x_1} = \sum_{i=1}^{2} (-1)^{i-1} \Big(G\Big(\frac{f_2(x_1) - g_i(x_2)}{x_2 - x_1}\Big) - G\Big(\frac{f_1(x_1) - g_i(x_2)}{x_2 - x_1}\Big) \Big).$$

In summary after some rearrangements we arrive at

$$I_2(\triangle_1, \triangle_2) = u\,w \int_0^1 \int_0^1 (u\,x + w\,y) \sum_{i=0}^{1} \Big[G\Big(\frac{s\,x - t\,y}{u\,x + w\,y} + (-1)^i \frac{f\,(2 - x - y)}{2\,(u\,x + w\,y)}\Big) - G\Big(\frac{s\,x - t\,y}{u\,x + w\,y} + (-1)^i \frac{f\,(x - y)}{2\,(u\,x + w\,y)}\Big)\Big] \mathrm{d}y \mathrm{d}x$$

and, by setting $t = w = 0$ resp. $s = u = 0$ and integrating over y resp. x,

$$I_2(\triangle_1) = \frac{2\,u^3}{3} \int_0^1 x \sum_{i=0}^{1} \Big[G\Big(\frac{s}{u} + \frac{(-1)^i\,f}{2\,u}\big(\frac{2}{x} - 1\big)\Big) - G\Big(\frac{s}{u} - \frac{(-1)^i\,f}{2\,u}\Big)\Big] \mathrm{d}x\,,$$

$$I_2(\triangle_2) = \frac{2\,w^3}{3} \int_0^1 y \sum_{i=0}^{1} \Big[G\Big(\frac{t}{w} + \frac{(-1)^i\,f}{2\,w}\big(\frac{2}{y} - 1\big)\Big) - G\Big(\frac{t}{w} - \frac{(-1)^i\,f}{2\,w}\Big)\Big] \mathrm{d}y\,.$$

Now, we are ready to prove two inequalities concerning the behaviour of the CPI $I_2(\square_{f,v}(s, t, u)$ when s and t are shifted.

Theorem 1. For any fixed $f, v > 0$ and $0 \le u \le v$,

$$I_2(\Box_{f,v}(s,t,u)) \le I_2(\Box_{f,v}(0,0,u) \le I_2(\Box_{f,v}(0,0,v/2) \tag{5}$$

and, if $s \le 0 \le t$ or $t \le 0 \le s$,

$$I_2(\Box_{f,v}(s,t,u)) \le I_2(\Box_{f,v}(-s,t,u) = I_2(\Box_{f,v}(s,-t,u)\,. \tag{6}$$

Corollary. For any $s \in \mathbb{R}$, $I_2(\Box_{f,v}(s,-s,v/2) \le I_2(\Box_{f,v}(s,s,v/2))$ and $I_2(\triangle_1(s,u)) \le I_2(\triangle_1(0,u))$, $I_2(\triangle_2(t,w)) \le I_2(\triangle_2(0,w))$, where the latter inequality means that, among all triangles with fixed altitude and base, the corresponding isosceles triangle has the greatest second-order CPI.

Proof of Theorem 1. We only need to prove (5) and (6) for the mixed CPI $I_2(\triangle_1(s,u), \triangle_2(t,w))$ since $I_2(\triangle_1(s,u)) \le I_2(\triangle_1(0,u))$ and $I_2(\triangle_2(t,w)) \le I_2(\triangle_2(0,w))$ follow by direct computation from (3). Without loss of generality let $s \le 0 \le t$. It suffices to verify the inequalities $H(x_1,x_2,s,t) \le H(x_1,x_2,-s,t) \le H(x_1,x_2,0,t)$ for fixed $x_1 \in [0,u], x_2 \in (u,v]$. For brevity, introduce $a_i(x) = (f_i(x) - g_1(x_2))/(x_2 - x_1)$ and $b_i(x) = (f_i(x) - g_2(x_2))/(x_2 - x_1)$ for $i = 1,2$. Write $a_i^0(x), b_i^0(x)$ resp. $a_i^+(x), b_i^+(x)$ if $f_i(x)$ is defined with s replaced by 0 resp. $-s$. By definition of $f_i(\cdot)$, the relations $f_i(x_1) \le f_i^0(x_1) \le f_i^+(x_1)$ for $i = 1,2$ and $f_2(x_1) - f_1(x_1) = f_2^0(x_1) - f_1^0(x_1) = f_2^+(x_1) - f_1^+(x_1)$ (being valid also for a_i and b_i instead of f_i) hold and imply, by exploiting the convexity of the function $G(\cdot)$, that

$$G(a_2(x_1)) - G(a_1(x_1)) = G\Big(\frac{f_2(x_1) - f_1(x_1)}{x_2 - x_1} + a_1(x_1)\Big) - G(a_1(x_1))$$

$$\le G\Big(\frac{f_2^+(x_1) - f_1^+(x_1)}{x_2 - x_1} + a_1^+(x_1)\Big) - G(a_1^+(x_1)) = G(a_2^+(x_1)) - G(a_1^+(x_1))$$

since $a_1(x_1) \le a_1^+(x_1)$, and, by $f_1(x_1) - f_1^+(x_1) = f_2(x_1) - f_2^+(x_1) \le 0$, we get that

$$G(b_1(x_1)) - G(b_2(x_1)) = G\Big(\frac{f_2(x_1) - f_2^+(x_1)}{x_2 - x_1} + b_1^+(x_1)\Big)$$
$$-G\Big(\frac{f_2(x_1) - f_2^+(x_1)}{x_2 - x_1} + b_2^+(x_1)\Big) \le G(b_1^+(x_1)) - G(b_2^+(x_1))\,.$$

Notice that the convexity of $G(\cdot)$ means that $G(b) - G(a) \le G(b+h) - G(a+h)$ for any $h \ge 0$ and $a \le b$. By addition of the previous inequalities it follows $H(x_1,x_2,s,t) \le H(x_1,x_2,-s,t)$ proving (6). Likewise, together with $G(-x) = G(x)$ for $x \in \mathbb{R}$, we find that $G(a_2^+(x_1)) - G(a_1^+(x_1)) \le G(a_2^0(x_1)) - G(a_1^0(x_1))$ and $G(b_1^+(x_1)) - G(b_2^+(x_1)) \le G(b_1^0(x_1)) - G(b_2^0(x_1))$

and , thus, $H(x_1, x_2, -s, t) \leq H(x_1, x_2, 0, t)$ proving the left part of (5). Finally, we rotate the kite $\square_{f,v}(0, 0, u)$ by a right angle and apply the last step once more showing that the rhomb $\square_{f,v}(0, 0, v/2)$ has a greater (mixed) second-order CPI. This completes the proof of Theorem 1. $\square$

Remark. The transformation $\square_{f,v}(s, t, u) \mapsto \square_{f,v}(0, 0, u)$ coincides with the well-known Steiner-symmetrization, see [2]. It turns out that $(s, t) \mapsto I_2(\triangle_1(s, u), \triangle_2(t, w))$ is a strictly concave function. The mixed second-order CPI of the kite $\square_{f,e}(0, 0, p\,e)$ for $0 < p < 1$ can be expressed in terms involving the *area sinus hyberbolicus* function $F(\cdot)$.

3 Isoperimetric Inequality for Quadrangles

We return to the quadrangle $\square_{e,f,\alpha}(p, q)$ as defined in Sect.2 with fixed e, f, acute angle $\angle ASD = \alpha \in [0, \pi/2]$ and varying $p, q \in [0, 1]$. By a little trigonometry we get the following formula for the perimeter $L_\alpha(p, q) = L(\partial\square_{e,f,\alpha}(p, q)) = P(p, q) + P(1 - p, 1 - q)$, where $P(p, q) = a + d =$

$$\sqrt{p^2\,e^2 + q^2\,f^2 + 2\,p\,q\,e\,f\,\cos\alpha} + \sqrt{p^2\,e^2 + (1-q)^2\,f^2 - 2\,p\,(1-q)\,e\,f\,\cos\alpha}\,.$$

Lemma. Among all convex quadrangles $\square_{e,f,\alpha}(p, q)$ the parallelogram $\square_{e,f,\alpha}(\frac{1}{2}, \frac{1}{2})$ has the least perimeter, i.e.

$$L_\alpha(p, q) \geq L_\alpha(\frac{1}{2}, \frac{1}{2}) = \sum_{i=0}^{1} \sqrt{e^2 + f^2 + (-1)^i\,2\,e\,f\,\cos\alpha} \tag{7}$$

for all $p, q \in [0, 1]$ with "=" iff $p = q = \frac{1}{2}$.

Proof of Lemma. For fixed $p, q \in [0, 1]$, the function $[0, 1] \ni s \mapsto Q(s) := P(\,(1-s)p + s(1-p)\,,\ (1-s)q + s(1-q)\,)$ turns out to be (strictly) convex. To show this, define $a(s, p) := (1-s)\,p + s\,(1-p) \in [0, 1]$. Since $1 - a(s, q) = a(s, 1-q)$ we may write

$$\begin{aligned} Q(s) &= \sqrt{a^2(s,p)\,e^2 + a^2(s,q)\,f^2 + 2\,a(s,p)\,a(s,q)\,e\,f\,\cos\alpha} \\ &+ \sqrt{a^2(s,p)\,e^2 + a^2(s,1-q)\,f^2 - 2\,a(s,p)\,a(s,1-q)\,e\,f\,\cos\alpha}\,. \end{aligned}$$

A rather lengthy calculation (for details see Appendix in [5]) shows that

$$\begin{aligned} Q''(s) &= \frac{e^2\,f^2\,\sin^2\alpha\,[\,(1-2p)\,a(s,q) - (1-2q)\,a(s,p)\,]^2}{[\,a^2(s,p)\,e^2 + a^2(s,q)\,f^2 + 2\,a(s,p)\,a(s,q)\,e\,f\,\cos\alpha\,]^{3/2}} \\ &+ \frac{e^2\,f^2\,\sin^2\alpha\,[\,(1-2p)\,a(s,1-q) + (1-2q)\,a(s,p)\,]^2}{[\,a^2(s,p)\,e^2 + a^2(s,1-q)\,f^2 - 2\,a(s,p)\,a(s,1-q)\,e\,f\,\cos\alpha\,]^{3/2}} > 0 \end{aligned}$$

–

for $p, q \neq 1/2$. Hence, applying Jensen's inequality reveals that

$$P\big(\frac{1}{2},\frac{1}{2}\big) = Q\big(\frac{1}{2}\big) \leq \frac{1}{2}\,Q(0) + \frac{1}{2}\,Q(1) = \frac{1}{2}\,P(p,q) + \frac{1}{2}\,P(1-p,1-q)\,,$$

which coincides with (7). □

From (7) we can easily derive the isoperimetric inequality for quadrangles.

Theorem 2. For any quadrangle $\square_{e,f,\alpha}(p,q)$ with area $A_\alpha(p,q)$ we have

$$\frac{L^2_\alpha(p,q))}{A_\alpha(p,q))} \geq \frac{L^2_\alpha(\frac{1}{2},\frac{1}{2})}{A_\alpha(\frac{1}{2},\frac{1}{2})} \geq \frac{L^2_{\pi/2}(\frac{1}{2},\frac{1}{2})}{A_{\pi/2}(\frac{1}{2},\frac{1}{2})} = \frac{8\,(e^2+f^2)}{e\,f} \geq 16$$

with "=" iff $e = f$ and $\alpha = \pi/2$.

4 Lower and Upper Bounds for Second-Order CPI of Parallelograms

We consider a parallelogram $\square_\alpha(a,b) = \{\lambda_1\,(b,0) + \lambda_2\,(a\,\cos\alpha, h) : 0 \leq \lambda_1, \lambda_2 \leq 1\}$ with altitude $h = a\,\sin\alpha$ and base $b = \|\overline{AB}\|$ $(a = \|\overline{AC}\|\,,\ \alpha = \angle(CAB) \in (0,\pi/2]\,,\ A(\square_\alpha(a,b)) = b\,h = a\,b\,\sin\alpha)$ which yields

$$I_2(\square_\alpha(a,b)) = \int\limits_{[0,1]^4} \frac{b^2\,h^2\,\mathrm{d}(\lambda_1\,,\,\lambda_2\,,\,\mu_1\,,\,\mu_2)}{\sqrt{[(\lambda_1-\mu_1)b + (\lambda_2-\mu_2)a\,\cos\alpha]^2 + [(\lambda_2-\mu_2)\,h]^2}}$$

$$= \int\limits_0^1\int\limits_0^1\int\limits_0^1\int\limits_0^1 \frac{a^2\,b^2\,\sin^2\alpha\,\mathrm{d}\lambda_1\,\mathrm{d}\lambda_2\,\mathrm{d}\mu_1\,\mathrm{d}\mu_2}{\sqrt{b^2(\lambda_1-\mu_1)^2 + 2\,a\,b\cos\alpha\,(\lambda_1-\mu_1)(\lambda_2-\mu_2) + a^2(\lambda_2-\mu_2)^2}}$$

$$\begin{aligned}
\frac{I_2(\square_\alpha(a,b))}{A^2(\square_\alpha(a,b))} &= 2\sum_{i=0}^{1}\int_0^1\int_0^1 \frac{(1-x)\,(1-y)\,\mathrm{d}x\,\mathrm{d}y}{\sqrt{a^2\,x^2 + (-1)^i\,2\,a\,b\,\cos\alpha\,x\,y + b^2\,y^2}} \\
&= \frac{1}{3}\sum_{i=0}^{1}\int_0^1 \frac{(3-z)\,\mathrm{d}z}{\sqrt{a^2 + (-1)^i\,2\,a\,b\,z\,\cos\alpha + b^2\,z^2}} \\
&+ \frac{1}{3}\sum_{i=0}^{1}\int_0^1 \frac{(3-z)\,\mathrm{d}z}{\sqrt{a^2\,z^2 + (-1)^i\,2\,a\,b\,z\,\cos\alpha + b^2}} \qquad (8)
\end{aligned}$$

Theorem 3. For any parallelogram $\square_\alpha(a,b)$ with altitude $h = a\,\sin\alpha$ and perimeter $L(\square_\alpha(a,b)) = 2\,(a+b)$ the following inequalities are valid:

$$\frac{c_4}{2\,(a+b)} \le \frac{I_2(\square_{\pi/2}(a,b))}{A^2(\square_{\pi/2}(a,b))} \le \frac{I_2(\square_\alpha(a,b))}{A^2(\square_\alpha(a,b))} \le \frac{I_2(\square_{\pi/2}(h,b))}{A^2(\square_{\pi/2}(h,b))} \le \frac{c_4}{4\sqrt{a\,b\,\sin\alpha}}$$

with "=" left and right iff $a = b$, $\alpha = \pi/2$, where $c_4 = 4\,I_2(\square_{\pi/2}(1,1))$ and

$$I_2(\square_{\pi/2}(1,1)) = 4\int\limits_0^1\int\limits_0^1 \frac{(1-x)(1-y)}{\sqrt{x^2+y^2}}\mathrm{d}x\mathrm{d}y = \frac{4}{3}\Big[3\log(1+\sqrt{2}) + 1 - \sqrt{2}\Big]\,.$$

Proof of Theorem 3. We only sketch the essential steps. The above integral transformations are more or less straightforward and they are left to the reader. Next, using the elementary inequality $(x+c)^{-1/2} + (x-c)^{-1/2} \ge 2\,x^{-1/2}$ for $x > 0$, $-x < c < x$, it follows that

$$\frac{1}{\sqrt{a^2 - 2\,a\,b\,z\,\cos\alpha + b^2\,z^2}} + \frac{1}{\sqrt{a^2 + 2\,a\,b\,z\,\cos\alpha + b^2\,z^2}} \ge \frac{2}{\sqrt{a^2 + b^2\,z^2}}$$

and, by interchanging a and b and using (8) we get the first lower bound in Theorem 3. To verify the first upper bound it suffices to prove with $c := a\,\cos\alpha$ that

$$\int_0^1 \frac{(3-z)\,\mathrm{d}z}{\sqrt{(b\,z+c)^2+h^2}} + \int_0^1 \frac{(3-z)\,\mathrm{d}z}{\sqrt{(b\,z-c)^2+h^2}} \le 2\int_0^1 \frac{(3-z)\,\mathrm{d}z}{\sqrt{b^2\,z^2+h^2}} \qquad (9)$$

and the corresponding inequality with $(b\,z \pm c)^2 + h^2$ and $b^2\,z^2 + h^2$ replaced by $(b \pm c\,z)^2 + h^2\,z^2$ and $b^2 + h^2\,z^2$, respectively. Note that the left-hand side of (9) is decreasing in $c \ge 0$. The remaining bounds left and right are obtained by direct evaluation of the integrals and determining their extreme values. For details we refer to the Appendix in [5]. □

The four integrals on the right-hand side of (8) can be taken from a usual table of integrals. Putting $H(z) = F(z) + z\,\sqrt{z^2+1}$ and

$$J_\alpha(a,b) = \sum_{i=0}^{1} \big(3\,b + (-1)^i\,a\,\cos\alpha\big)\,H\Big(\frac{b + (-1)^i a\,\cos\alpha}{a\,\sin\alpha}\Big) - 2\,a\,\cos\alpha\,H\big(\cot\alpha\big)$$

we may write together with the diagonals $e/f = \sqrt{a^2+b^2 \pm 2\,a\,b\,\cos\alpha}$:

$$\frac{I_2(\square_\alpha(a,b))}{A^2(\square_\alpha(a,b))} = \frac{2\,(a^3+b^3) - 4\,(e^3+f^3)}{3\,a^2\,b^2\,\sin^2\alpha} + \frac{J_\alpha(a,b)}{3\,b^2} + \frac{J_\alpha(b,a)}{3\,a^2}\,.$$

In the special case of a rhomb $\square_\alpha(a,a)$ with diagonals $e/f = a\sqrt{2\,(1 \pm \cos\alpha)}$ we obtain

$$\frac{4\,a\,I_2(\square_\alpha(a,a))}{A^2(\square_\alpha(a,a))} = \frac{16}{3}\,T(\alpha) \;\text{ and }\; \frac{I_2(\square_\alpha(a,a))}{(A(\square_\alpha(a,a))^{3/2}} = \frac{4}{3}\,T(\alpha)\,\sqrt{\sin\alpha}\,, \quad (10)$$

where the function $T(\alpha)$ takes the form

$$1-\sin\frac{\alpha}{2}-\cos\frac{\alpha}{2}+\Big(1+\sin^2\frac{\alpha}{2}\Big)\log\Big(1+\frac{1}{\sin\frac{\alpha}{2}}\Big)+\Big(1+\cos^2\frac{\alpha}{2}\Big)\log\Big(1+\frac{1}{\cos\frac{\alpha}{2}}\Big)\,.$$

It is easily verified that the left/right-hand ratio in (10) decreases/increases in $\alpha \in [0,\pi/2]$ with minimum/maximum at $\alpha = \pi/2$. In summary, this result combined with (5) proves

Theorem 4. Among all convex quadrangles $\square ABCD$ with fixed $A = A(\square ABCD)$ the square $\square_{\pi/2}(\sqrt{A},\sqrt{A})$ has the greatest second-order CPI, more precisely:

$$\frac{I_2(\square ABCD)}{(A(\square ABCD))^{3/2}} \le \frac{4}{3}\,T\Big(\frac{\pi}{2}\Big) = \frac{c_4}{4} \approx 2.97321 < \frac{16}{3\sqrt{\pi}} \approx 3.00901\,.$$

We remark that Carleman's inequality, see [1], says that the ratio in Theorem 4 attains its maximum (taken over all convex discs) for circles giving the right-hand value, see also [6].

5 Conjectures for Convex Polygons and Parallelotopes in Higher Dimensions

To conclude this paper we formulate two conjectures which have been proved only for special cases so far.

Conjecture I. For any convex n-gon K_n the inequality

$$\frac{c_n}{L(\partial K_n)} \le \frac{I_2(K_n)}{A^2(K_n)} \le \frac{c_n}{\sqrt{4\,n\,\tan\big(\frac{\pi}{n}\big)\,A(K_n)}} \;\text{ with }\; c_n = \frac{16}{n}\,\tan\big(\frac{\pi}{n}\big)\,I_2(K_n^*)$$

holds with "=" on both sides iff K_n is a regular n-gon. Here, K_n^* denotes the regular n-gon with edges of length 1, see [3] for explicit values of c_n.

Let $\mathbf{a}_i = (a_i^{(1)},...,a_i^{(d)})$, $i = 1,...,d$, be linearly independent vectors in $\mathbb{R}^d$ which define a so-called *$d-$parallelotope* $P(\mathbf{a}_1,...,\mathbf{a}_d) = \{\sum_{i=1}^d \lambda_i\,\mathbf{a}_i : 0 \le$

$\lambda_1, ..., \lambda_d \le 1\}$. Without loss of generalty, we may assume that $a_i^{(1)}, ..., a_i^{(i-1)} \ge 0$, $a_i^{(i+1)} = ... = a_i^{(d)} = 0$ and put $a_i := a_i^{(i)} > 0$ for $i = 1, ..., d$. Further, let $I_d(K)$ denote the rigth-hand double integral of (2) for some convex body K in $\mathbb{R}^d$ with $d-$volume $V_d(K) > 0$ and *mean breadth* $b_d(K)$, see [2], [7].

Conjecture II. For any positive $a_1, ..., a_d \in \mathbb{R}$ the inequality

$$\frac{d\, I_d([0,1]^d)}{\|\mathbf{a}_1\| + \cdots + \|\mathbf{a}_d\|} \le \frac{I_d(P(\mathbf{a}_1, ..., \mathbf{a}_d))}{(\,a_1 \cdots a_d\,)^2} \le \frac{I_d([0,1]^d)}{(\,a_1 \cdots a_d\,)^{1/d}}$$

holds with "=" on each side iff $a_1 = \|\mathbf{a}_1\| = \cdots = a_d = \|\mathbf{a}_d\|$.

Note that the lower bound could be verified by the author, see [5]. Further, one can show that $V_d(P(\mathbf{a}_1, ..., \mathbf{a}_d)) = a_1 \cdots a_d$, $b_d(P(\mathbf{a}_1, ..., \mathbf{a}_d))\, d\, \kappa_d / 2\, \kappa_{d-1} = \|\mathbf{a}_1\| + \cdots + \|\mathbf{a}_d\|$ (where $\kappa_d = d-$volume of the unit ball in $\mathbb{R}^d$) and

$$I_d([0,1]^d) = 2^d \int_0^1 \cdots \int_0^1 \prod_{i=1}^d (1 - x_i) \Big(\sum_{i=1}^d x_i^2 \Big)^{-1/2} \mathrm{d}x_1 \cdots \mathrm{d}x_d\,.$$

References

[1] Carleman, T. (1919). Über eine isoperimetrische Aufgabe und ihre physikalischen Anwendungen. *Math. Z.*, **3**, 1–7.

[2] Gruber, P. M. (2007). *Convex and Discrete Geometry*. Springer, Berlin.

[3] Heinrich, L. (2009). On lower bounds of second-order chord power integrals convex discs. *Rend. Circ. Mat. Palermo*, Serie II, Suppl. **81**, 213–222.

[4] Heinrich, L. and Spiess, M. (2011). CLT for for the volume of stationary Poisson cylinder processes in expanding domains. submitted.

[5] Heinrich, L. (2011). Some new results on second-order chord power integrals of convex quadrangles. Institut für Mathematik, Universität Augsburg, Preprint 21/2011 (http://www.math.uni-augsburg.de/)

[6] Pfiefer, R. E. (1990). Maximum and minimum sets for some geometric mean values. *J. Theoret. Probab.* **3**, 169–179.

[7] Schneider, R. and Weil, W. (2008). *Stochastic and Integral Geometry*. Springer, Berlin.

Postal address: Universität Augsburg, 86135 Augsburg, Germany
E-mail address: heinrich@math.uni-augsburg.de

RENDICONTI DEL CIRCOLO MATEMATICO DI PALERMO
Serie II, Suppl. 84 (2012), pp. 207-218

The Gap model applied to rural tourism – a theoretical approach*

Maurizio Lanfranchi[1,*], Carlo Gianetto[2], Maria Luiza Souca[3,]**

[1]University of Messina, Department Sefisast, Faculty of Economics Messina, Italy
[2]University of Messina, Department Sefisast, Faculty of Economics Messina, Italy
[2]Babeş-Bolyai University, Faculty of Economics and Business Administration, Marketing Department, Cluj-Napoca, Romania

* mlanfranchi@unime.it

Abstract: Tourism, as an industry, is dynamic and has an incredible growth rate as the latest statistics show (913 millions international tourists in 2008, 877 millions in 2009 and 935 millions in 2010, (World Tourism Organization, 2011)) This growth has been experienced in some geographical areas even in 2009, the worst year of the crisis, which makes tourism in general, and one of its forms: rural tourism, in particular, the possible solution to sustainable economic development, as long as healthy managerial practices are followed. And one of these practices is creating, measuring and maintaining customer satisfaction through a careful monitoring of the perceived quality of the accommodation services, as both customer satisfaction and perceived service quality are key factors used to gain competitive advantage and customer retention (Lopez-Toro *et al.*, 2010). This is an especially stringent problem as most of the entrepreneurs that have turned to rural tourism to supplement their agricultural income lack the necessary managerial skills and customer orientation. The objective of this paper is to show the link between the concept of customer satisfaction and perceived service quality with a succinct literature review of previous research on the subject, to present the benefits customer satisfaction can bring to a developing rural tourism industry, to propose a simple model of evaluating the customer satisfaction for rural tourism by reviewing and modifying the existing Gap model, and to present some work hypothesis for subsequent research in the realm of rural tourism by highlighting the current problems this particular brand of tourism encounters in Romania.

Keywords: Gap model, service quality, customer satisfaction, rural tourism.

---

* The work is the result of a complete cooperation and it is, therefore, of responsability of both the authors. The material drawing up of paraghraphs 3, 4 and 5 are attribuiting to Maurizio Lanfranchi, paragraph 1 to Carlo Giannetto and paraghraphs 2 and 3.1,3.2. 3.3. 3.4 to Maria Luiza Souca.

** ***Investing in people!*** Ph.D. scholarship, Project co-financed by the SECTORAL OPERATIONAL PROGRAM FOR HUMAN RESOURCES DEVELOPMENT 2007 - 2013
Priority Axis 1. "Education and training in support for growth and development of a knowledge based society" **Key area of intervention 1.5:** Doctoral and post-doctoral programs in support of research.
Contract no.: **POSDRU/88/1.5/S/60185 –** "INNOVATIVE DOCTORAL STUDIES IN A KNOWLEDGE BASED SOCIETY"
Babeş-Bolyai University, Cluj-Napoca, Romania

1. The concept of "customer satisfaction" versus "perceived service quality"

Customer satisfaction, "an attitude-like judgment following a purchase act or based on a series of consumer product interactions" (Fournier&Mick,1999, p. 5), is a central and powerful construct in marketing (Oliver,1997). As many researches show, customer satisfaction influences loyalty (Anderson & Sullivan, 1993; Matzler, Füller & Faullant,2007), recommendations to others, or word-of-mouth marketing (Cronin & Taylor, 1992; Hui *et al.*, 2007), and profitability (Anderson, Fornell, & Lehmann, 1994), all economical results that for better or for worse are depending on the fact whether customer satisfaction has been achieved or not. These economical effects are especially desirable for small businesses who struggle for survival while they are developing in a highly competitive field such as tourism, one of the most dynamic service industries. The point hits home especially with rural tourism, a fertile ground for developing new businesses, as most of the accommodations here are enterprises with the following characteristics: they are a potential source of economic and social benefits; they globally belong to the indigenous population; are family run and their owner-managers preserve the smallest of physical, employee and market size economically viable solution (Page *et al.*, 1999; Morrison *et al.*, 1999; Getz and Carlsen, 2000; Morrison and Teixeira, 2004; Hwang and Lockwood, 2006; Morrison, 2006).

So how do small rural tourism enterprises develop, maintain and control customer satisfaction? According to the literature, if customer satisfaction depends largely on the client, there is a component that is under the control of the entrepreneur: the quality of the services he provides and how this is presented to the customer in order to create certain perceptions.

The two concepts, customer satisfaction and perceived service quality have been debated in many studies as some researchers used them as distinct items (Oliver, 1997; Taylor & Baker, 1994), but sharing a direct connection (Cronin & Taylor, 1992; Gotlieb et al., 1994; Spreng & Mackoy, 1996), while others gave them the same meaning (Iacobuci et al., 1994; Parasuraman et al., 1994; Taylor and Baker, 1994; Oliver, 1997; Mittal et al., 1998).

Generally, it can be said that both perceived service quality and customer satisfaction are both evaluations of a number of variables that the customer takes into account when he or she judges a finished product or a delivered service. However, while the perceived quality is a cognitive action, set by a number of specific attributes, customer satisfaction is an affective and emotional response to the global view of the service. (Oliver, 1997). If we are to introduce also a time constraint, then it can be said that perceived quality of a product is a long term cognitive evaluation of the delivered service, while customer

satisfaction is a short-term emotional evaluation. (Lovelock & Wright, 1999). The argument for this delimitation is that fact that customer satisfaction renews itself every time a service is delivered, the emotional positive or negative result modifying the customer's view on the perceived quality of the service. However, it must be pointed that the customer's view and attitude towards a service is not the sole product of experimenting said service – advertising certainly plays an important part here – therefore it can be said that the existence of customer satisfaction decides whether a service was high-quality or not. From this hypothesis Oliver (1997) stated that the causal relationship between customer satisfaction and perceived quality of the product depends on the moment when the measurement is made:

- When there is only one transaction is a strong direct relationship between the concepts as perceived quality influences satisfaction.
- When more than one transaction is evaluated, the relationship changes: satisfaction influences the perceived quality as the service evaluation is the result of an overview impression of the delivered service.

Taking this into consideration Parasuraman et al (1994) has answered the challenge issued by Oliver by creating two models for evaluating customer satisfaction: one model is based on a single transaction while the other is global, as it differentiates between past and present deliveries of the same service. However Parasuraman initiated his models on the premise that the concept of customer satisfaction includes the one of perceived quality of the product, as satisfaction is influenced by perception, a point of view that was support by the majority of the researchers. (Cronin & Taylor, 1992; Anderson & Sullivan, 1993; Anderson et al., 1994; Gotlieb et al., 1994; Taylor & Baker, 1994; Taylor & Cronin, 1994; Spreng & Mackoy, 1996; Meleg & Tar, 1997; Kasper et al., 1999). However the 1994 models weren't the first to be developed by Parasuraman and his team, as in 1988 they developed SERVQUAL, the best known instrument for evaluating the perceived quality of the delivered service and implicit the customer satisfaction. And the base for that was nothing else but the Gap model.

2. The Gap model and customer satisfaction in tourism

In 1982 Gronroos showed that the perceived quality of a service is the result of an evaluation process through which the customers compares their perceptions on how the services was delivered, the final result and their initial expectations of said service – which were the benchmark for the firm's delivery performance (Lovelock, 2001). Starting from this point of view, the team of researchers led by Parasuraman et al. (1985) proposed creating an evaluation model for the service quality in which the customer's expectations and the customer's perceptions are compared. To be more exact, the model states that each customer is evaluating not only the final result, but also the delivery in itself, and the expectation's based on which the evaluation is made, are

the result of individual needs, past experience, word-of-mouth and the service provider's promotion strategy.

Another aspect that Parasuraman's research has highlighted is the existence of gaps – which are under the direct control of the service provider, but they also directly influence the customer's satisfaction:

1. The gap between actual customer's expectations and how the management perceives said expectations;
2. The gap between the management's perceptions of customer's expectations and the way service quality specifications are hashed out;
3. The gap between the service quality specifications and the service delivery;
4. The gap between service delivery and external communication to customers;
5. The last gap between the customers' expectations and the way they perceived the actual delivery of the service they have purchased.

The goal of any service organization is to minimize as much as possible the final gap and eventually overcome the expected levels for the service and so creating satisfaction, by eliminating as much as possible of the other four gaps. This model's strong point is that is can be used for any kind of services, from financial, tourism and health to sports and public services. The weak point of the model is that is not particular to any kind of service, so each industry must come with their adapted version of it.

So, is the Gap model and the instrument it inspired – SERVQUAL, suitable to be used for tourism services, especially accommodation. Previous studies point to a definite yes. Since hotel managers have realized that high quality services mean a higher market share and profitability (Oh & Parks, 1997), there have been numerous studies successfully applying the SERVQUAL instrument in its original or adapted form. (Fick &Ritchie, 1991 ; Akan, 1995 ; Armstrong *et al* , 1997 ; Mei *et al* , 1999 ; Akbaba, 2006 ; Ekinci *et al* , 2003 ; Juwaheer, 2004, Nadiri & Hussain, 2005). Most of these studies were focused on the hotel offer of accommodation services, a big part of the tourism services a destination has to provide, and it can be argued that their findings can also be extended to rural tourism accommodations services and facilities. However, lately studies regarding the customer's satisfaction related to rural tourism have also started to emerge, and their findings show that not only the rural accommodation services have several characteristics that set them apart from their hotel counterparts, but also a different instrument is needed when considering the needs and expectations of the customers that chose this type of service. (Albacete-Saez, 2007)

3. The Gap model and rural tourism: Romania and Italy case study

The original Gap model, as it was proposed by Parasuraman et al (1985) has five gaps, or differences, that cumulated threaten the achievement of customer's satisfaction. These gaps can be summarized as follows (Parasuraman, 2005): market information gap, service's standards gap, service's performance gap, internal communication gap and service quality gap. Each of these gaps can be eliminated with a dedicated effort

from the part of the rural tourism entrepreneur, as long as the causes that created them are transformed from weak points to strengths and there's a continuous evaluation of the customer's expectations and perceptions.

The rural tourism as a form of sustainable tourism, can be counted among the so-called no traditional tourism, is extremely interrelated with the territory. The attempt to adapt the model developed by Parasuman based on the calculation of the gaps related to customer satisfaction compared to expectations is particularly interesting.

In fact, the Gap model is based on two fundamental principles: the first argues that the success of a proposal depends on the attitude taken by all tourism stakeholders in the initiative, the second principle says that the level of satisfaction that the tourist product originates a tourist, can be measured by the attitude he takes towards the product. Therefore the attitude of tourists towards the person making the tourism product, can be understood as the sum of its attitudes towards the individual attributes of which the product is formed. Each attribute that makes the product is susceptible to evaluation. Based on these considerations, it has Gap when there is not convergence of opinion between the various stakeholder (value gap), when there is not convergence on the assessment of the degree of presence of individual attributes (perception gap) .

The analysis of the causes of differences (gaps) between the actors of the territory is particularly important because it provides practical guidelines for the design of the development of a rural area by promoting local tourism. The construction of a tourism product that enhances the rural area, requires the ability to implement the following conditions which may allow the socioeconomic development of rural areas in Romania.

The first condition is the differentiation of the territory, this is only possible if there are elements that distinguish an area from the nearest well, represented by cultural social and economic values. The second condition is the ability to create a system or create a tourist product that is the result of a network services that meet common standards and strong connotations for their typicality. Another essential condition is to focus on quality not an individual, the individual firm, but overall the whole area. Therefore the success of rural tourism in Romania can only advance through research of all the elements of differentiation that characterize each region and distinguish it from other geographically nearby. It is clear that differentiation does not mean search for items common to many other places, such as hotels, shops, etc. To differentiate it should enhance the features present in a specific local area.

The only way to differentiate is represented by the value of what it characterizes not only a local community from another, but what, within the same local community, features a small area compared to another which is also a few kilometers away.

3.1. Market information gap

Or the gap between the actual customer's expectations and the management's perceptions on said expectations has the following key factors: insufficient market research, inadequate use of marketing research, lack of interaction between management and customers and insufficient between contact employees and manager. In the case of rural tourism, with most of the businesses being small sized family owned and staffed

(Morrison *et al.,* 2010), the lack of interaction between the management and the customers is not such a big an issue, the manager often being set also in the role of contact personnel. The biggest problem here is the insufficient marketing research in the field. There are almost no studies regarding the profile of the client requiring Romanian rural tourism services, which also means a lack of a profile of possible expectations that can be used to evaluate the service quality. And while the research from other countries with developing rural tourism industries can be extrapolated to a certain point to Romanian's rural tourism industry in creating a customer's profile – population between 25 and 45 years old, with high sociocultural level, medium-high purchasing power, and living in the urban area, with a proactive attitude towards tytpical rural activities (including sports and agriculture related labors) and landscape viewing; such tourist also take advance of the existing resources, which include accommodations to small „charming" guesthouses, and small living spaces in local farms, while spending more than the traditional tourist on cultural and natural resources. (Perales, 2002) – this profile doesn't take into account the particularities of those tourists that specifically chose Romania as a rural tourism destination, nor does it show their level of expectation. This lack of marketing research has led to some unfortunate effects such as „kitch" arhitecture with a complete disregard for authenticity for a number of pensions (Ilies *et. al*, 2008) their owners ignoring that one of the selling points of rural tourism is preserving the local patrimony and showing traditions. Until sound marketing research is done in the field, the industry has an obvious weakness that can threathen its development in the long run.

3.2. Service's standards gap

The service's standard gap occurs when there is a difference between the manager's perceptions on customer's expectations and the service quality specifications. The key factors that influence this gap are: inadequate management commitment to service quality, the absence of formal processes in setting service quality goals, the inadequate standardization of tasks and the perception of unfeasibility – that customer expectations can't be met.

To be able to create adequate quality specifications, there is a need for both managerial studies and skill and a customer orientation, something that many rural tourism entrepreneurs lack (Reichel *et al.,*2000; Zhang *et al.,*2008). In the case of Romania, there still a significant percent of rural boardinghouses that lack an official classification (Popa, 2008). Also the fact that not all of them are members of ANTREC (Romanian National Association for Rural, Cultural and Ecological Tourism), that also means that their managers-owners have no or little access to specialized managerial courses in pension and quality control management.

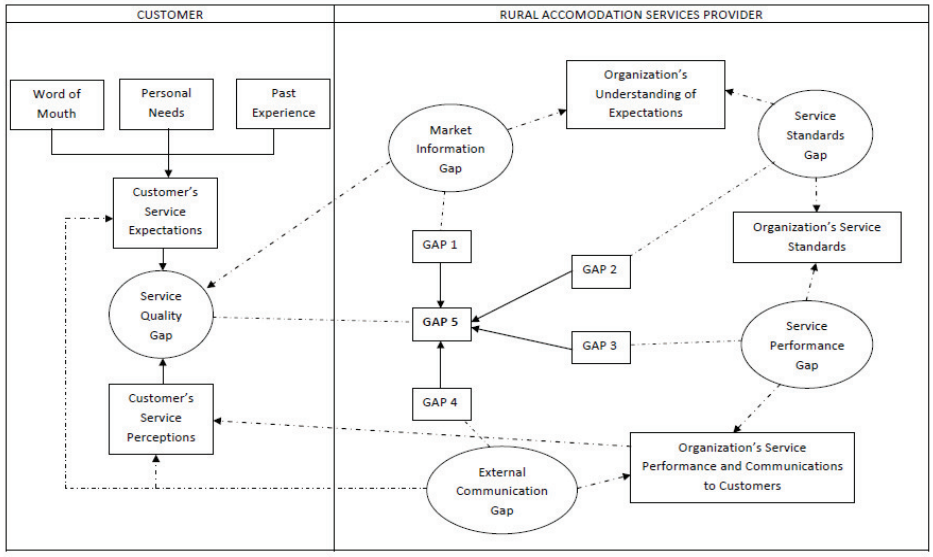
3.3. Service's performance gap

The service's performance gap occurs when there's a difference between the service quality specifications and the service delivery because of the following key factors: the lack of teamwork, poor personnel and technology fit for the job, the lack of perceived control, inappropriate evaluation/compensation system and role conflict and role ambiguity between contact personnel.
The fact that most rural tourism service providers run a small sized family business means that most of the roles that the employees play are interconnected and sometimes overlapping: the matron of the house will double as the cook and the cleaning lady. While traditionally these are seen as woman's natural responsibilities, there's still the danger of not rising to the tourist expectations. Still both Romanians and Italians have a reputation of hospitality, welcoming their guests with good food and drinks (Stroia & Chiru, 2010), which makes this gap not as threatening as the first two.

3.4. Internal communication gap

The last gap that is under the direct control of the manager, the difference between service delivery and external communication to customers is the result of the following key factors: inadequate communications between sales people and operations, inadequate communications between advertising and operations, differences in policies between branches and departments, puffery in advertising and personal selling.
When taking into account small size of most of the providers for accommodation services in rural tourism in both Romania and Italy, this gap seems the least applicable to rural tourism. However we must take into account the fact that most of the advertising is made by either tour operators that what to promote a certain rural circuit, so there's still the danger of creating unreasonable expectations. A possible solution would be taking advantage of the tools provided by the Internet: website, access to social networks, listing in specialized directories, however in the case of Romania there's a worrying lack of good quality websites advertising rural tourism, while those that currently exist have outdated information, also the case of ANTREC's website. The best advertising currently is that made at the point of sale, as the communication with the clients is strongly linked with the service delivery : the experience creating possible good memories that will call back the tourist for another visit. Because of this element, we believe that the current Gap model can be remade as shown in Figure 1, the main difference being that is links the service delivery with external communication to clients, while eliminating most of the unnecessary internal communication gap.

Figure 1: The Gap Model applied to Rural Accomodation Services Provider



(Source: Authors' adaptation after Parasuraman, 1994)

4. Methodology and future avenues for research

The authors are currently involved in a research project with the main objective of developing the Gap model as a necessary instrument for planning the rural tourism development in a rural area.

The rural space in Romania accounts for almost 89% from the entire territory and 45% of the population lives in the rural area. However, while agriculture dominates the rural economy, its predominant feature is the high share of subsistence farms, mainly producing for their own consumption and only marginally for the market. Because of this, the rural economy remains poorly integrated into the market economy, creating the need for alternative solutions that can help capitalize the rural area and achieve regional development. And one of those solutions was developing the rural tourism industry.

Among the Romanian regions that are known for their potential for rural tourism and also by great investments in the area, best known is the Maramureş County. Located in a mountain area, the Maramureş County has a rich and complex history. Known from ancient times for its natural resources: salt, wood and hunting, the county is now visited for its vast cultural heritage: eight wood made churches under the UNESCO patronage, a unique cemetery at Săpânţa renowned for its humoristic eulogies, the traditional house gate that retained its design since the Middle Ages, the numerous traditional celebrations and festivities and lastly, but not the least important: the traditional

Maramureş household. Boasting a reputation for hospitality, good food and traditional drinks, the chance to stay and relax as a guest to a traditional household is an unforgettable experience that has the guests coming back for more.

The research main objective will be to identify and describe the characteristics that differentiate one territory from another, by conducting a questionnaire based survey among the tourists that have traveled to the area and the operators involved in the rural tourism sector. The final result should point out the convergence level between the different actors of the local community, by highlighting which are the elements that create links and which are those that separate them, with the added purpose of finding way for smoothing the differences (weak points) and increasing the value of the strong points that define the territory - subject of the research.

5. Conclusions

Rural tourism accommodation services, although similar in many aspects with the hotel offer for accommodation, has some characteristics that set it apart, making the findings related to customer satisfaction studies not completely applicable in this case. The smaller size of the business, the fact that most of them are family owned and staffed and that rural tourism is a second vocation and means of supplementing the income coming from agriculture, especially in the case of Italy, shows some important weaknesses that if not addressed can put the future development of rural tourism in danger. However if the research regarding the customer satisfaction in rural tourism should develop further, both the customers and the entrepreneurs would have something important to gain.

A study and an adapted instrument regarding the relevance of the modifications proposed for the Gap model applied to rural tourism accommodation services has yet to be made, a limit to our research so far, but as customer satisfaction in the field of rural tourism is still at the beginning, we consider this article as a starting point for the future avenues of research.

References

1. Asociaţia Naţională de Turism Rural, Ecologic şi Cultural din România: http://www.antrec.ro, Retrieved 25.04.2011
2. Akan, P. (1995). Dimensions of service quality: A study in Istanbul. *Managing Service Quality, vol. 5 (6)* , 39-43.
3. Akbaba, A. (2006). Measuring service quality in the hotel industry: A study in a business hotel in Turkey. *International Journal of Hospitality Management, vol. 25, no. 2* , 170-192.

4. Albacete-Saez, C. A., Fuentes-Fuentes, M. M., & Llorens-Montes, F. J. (2007). Service Quality Measurement in Rural Accommodation. *Annals of Tourism Research, Vol. 34, No. 1* , 45–65.
5. Anderson, E. W., & Sullivan, M. W. (1993). The Antecedents and Consequences of Customer Satisfaction for Firms. *Marketing Science, Vol. 12, No. 2* , 125-142.
6. Anderson, E. W., Fornell, C., & Lehmann, D. R. (1994). Customer Satisfaction, Market Share, and Profitabilty: Findings from Sweden. *Journal of Marketing, Vol. 58, No. 3* , 53-66.
7. Armstrong, R. W., Mok, C., Go, F. M., & Chan, A. (1997). The importance of cross-cultural expectations in the measurement of service quality perceptions in the hotel industry. *International Journal of Hospitality Management, vol. 16, no.2* , 181-190.
8. Cronin, J., & Taylor, S. (1992). Measuring service quality: a re-examination and extension. *Journal of Marketing, No. 56* , 55-68.
9. Ekinci, Y., Prokopaki, P., & Cobanoglu, C. (2003). Service quality in Cretan accommodations: Marketing strategies for the UK holiday market. *Hospitality Management, no. 22* , 47-56.
10. Faullant, R., Matzler, K., & Fuller, J. (2008). The impact of satisfaction and image on loyalty: The case of alpine ski resorts. *Managing Service Quality, vol. 18, no. 2* , 163–178.
11. Fick, G. R., & Ritchie, J. R. (1991). Measuring service quality in the travel and tourism industry. *Journal of Travel Research, vol. 30* , 2-9.
12. Fournier, S., & Mick, D. G. (1999). Rediscovering satisfaction. *Journal of Marketing, no. 63* , 5-23.
13. Getz, D., & Carlsen, J. (2000). Characteristics and goals of family and owner-operated businesses in the rural tourism and hospitality sectors. *Tourism Management, no. 21* , 547–560.
14. Gotlieb, J., Grewal, D., & Brown, S. (1994). Consumer Satisfaction and Perceived Quality: Complementary or Divergent Constructs? *Journal of Applied Psychology* , 875-885.
15. Hui, T., Wan, D., & Ho, A. 2. (2007). Tourists' satisfaction recommendation and revisiting Singapore. *Tourism Management,vol. 28, no.4* , 965–975.
16. Hwang, L., & Lockwood, A. (2006). Understanding the challenges of implementing best practices in hospitality and tourism SMEs. *Benchmarking: An International Journal, vol.13, no. 3* , 337–354.
17. Iacobuci, D., Grayson, K., & Ostrom, A. (1994). The Calculus of Service Quality and Customer Satisfaction: Theoretical and Empirical Differentiation and Integration. *Advances in Services Marketing and Management: Research and Practice.*
18. Ilieş, A., Ilieş, D. C., Josan, I., Grama, V., & Gozner, M. (2008). Romanian rural tourism between authentic/traditional and modern/contemporary. The

case of Crişana and Maramureş areas. *GeoJournal of Tourism and Geosites, vol. 2, no.2,* , pp. 140-148.

19. Juwaheer, T. D. (2004). Exploring International tourists ' perceptions of hotel operations by using a modifi ed SERVQUAL approach-a case study of Mauritius. *Managing Service Quality, vol. 14, no.5* , 350-364.
20. Kasper, H., Van Helsdingen, P., & Vries, W. J. (1999). *Services Marketing Management. An International Perspective.* . Chichester: John Wiley & Sons.
21. Lopez-Toro, A. A., Dıaz-Munoza, R., & Perez-Moreno, S. (2010). An assessment of the quality of a tourist destination: The case of Nerja, Spain. *Total Quality Management vol. 21, No. 3* , 269–289.
22. Lovelock, C. (2001). *Services Marketing, 3rd ed.* Upper Saddle River, NJ.: Prentice-Hall.
23. Lovelock, C., & Wright, L. (1999). *Principles of Service Marketing and Management.* Englewood Cliffs: Prentice Hall.
24. Mei, A. W., Dean, A. M., & White, C. J. (1999). Analyzing service quality in the hospitality industry. *Managing Service Quality, vol. 9, no. 2* , 136-143.
25. Meleg, A., & J., &. T. (1997). Our Future is the Satisfied Customer. Five Years of Customer Satisfaction Measurement at DUNAFERR. *Proceedings of the 41st Congress of the European Organization for Quality, 1. European Organization for Quality* .
26. Mittal, V., Ross, W., & P.M., B. (1998). The Asymmetric Impact of Negative and Positive Attribute-Level Performance on Overall Satisfaction and Repurchase Intentions. *Journal of Marketing, no. 1* , 33-47.
27. Morrison, A. (2006). A contextualisation of entrepreneurship. *International Journal of Entrepreneurial Behaviour and Research, vol. 12, no. 4* , 192–209.
28. Morrison, A., & Teixeira, R. (2004). Small business performance:a tourism sector focus. *Journal of Small Business and Enterprise Development, vol 11, no.2* , 166–173.
29. Morrison, A., Carlsen, J., & Weber, P. (2010). Small Tourism Business Research Change and Evolution. *International Journal of Tourism Research, no. 12* , 739–749.
30. Nadiri, H., & Hussain, K. (2005). Diagnosing the zone of tolerance for hotel services. *Managing Service Quality, vol. 15, no. 2* , 259-277.
31. Oh, H., & Parks, S. C. (1997). Customer satisfaction and service quality: A critical review of the literature and research implications for the hospitality industry. *Hospitality Research Journal, vol. 20, no. 3* , 35-64.
32. Oliver, R. (1997). *Satisfaction: A behavioral perspective on the consumer.* New-York: McGraw-Hill.
33. Page, S., Forer, P., & Lawton, G. (1999). Small business development and tourism: terra incognita? *Tourism Management, no. 20* , 435–459.
34. Parasuraman, A. (2005). New Ways of Listening to Library Users: New Tools for Measuring Service Quality. *University of Miami course* .

35. Parasuraman, A., Berry, L. L., & Zeithaml, V. A. (1988). SERVQUAL: A multiple-item scale for measuring customer perceptions of service quality . *Journal of retailing No. 64* , 12-40.
36. Parasuraman, A., Zeithaml, V. A., & Berry, L. L. (1985). A conceptual model of service quality and its implications for future research. *Journal of Marketing, no. 49* , 41-50.
37. Parasuraman, A., Zeithaml, V., & & Berry, L. (1994). Reassessment of Expectations as a Comparison Standard in Measuring Service Quality: Implications for Further Research. *Journal of Marketing, no. 1* , 111-124.
38. Perales, R. M. (2002). Rural Tourism in Spain. *Annals of Tourism Research, vol 29, no. 4* , 1101-1110.
39. Popa, V. (2008). Quality management and the evolution of rural touristic pensions in Alba County during the period 2000-2007 according to categories of comfort. *Bulletin UASVM, Horticulture vol. 65, no. 2* , 299-301.
40. Reichel, A., Lowengart, O., & Milman, A. (2000). Rural tourism in Israel: service quality and orientation. *Tourism Management* , 451-459.
41. Spreng, R., & Mackoy, R. (1996). An Empirical Examination of a Model of Perceived Service Quality and Satisfaction. *Journal of Retailing* , 201-214.
42. Stroia, A., & Chiru, C. (2010). Traditionalism and Functionality in the Romanian Cuisine. *Quality - Access to Success, no.116* , 1234.
43. Taylor, S., & Baker, T. (1994). An Assessment of the Relationship Between Service Quality and Customer Satisfaction in the Formation of Consumer's Purchase Intentions. *Journal of Retailing, no. 2* , 163-178.
44. World Tourism Organization. (2011, February). *UNWTO World Tourism Barometer*. Retrieved April 10, 2011, from World Tourism Organization Web site: http://www.unwto.org
45. Zhang, J., Shi, Y., Mu, W., Wang, X., & Zhang, X. (2008). Measuring Customer Satisfaction Based on Gap Model and Structured Equation Model in Agro Tourism Industry in Shandong, China. *Wireless Communications, Networking and Mobile Computing, 2008. WiCOM '08. 4th International Conference on* , 1-4.

RENDICONTI DEL CIRCOLO MATEMATICO DI PALERMO
Serie II, Suppl. 84 (2012), pp. 219-230

An analysis of the agricultural activity in EU-27 using the multiple regression*

Associate Professor Maurizio Lanfranchi
Department SEFISAST Faculty of Economics University of Messina (Italy)
mlanfranchi@unime.it

Teaching Assistant *Pirnea Ionela Carmen*
Constantin Brancovean University, Valcea, Romania

Abstract

Purpose: This article aims to analyze how much index of income from agricultural activity and output at producer prices agricultural can influence GDP.
Methodology: To apply multiple regression model, we used data available on the Eurostat website. We selected data for the 27 European Union member states, namely GDP per capita in Purchasing Power Standards (PPS), 2008, income from agricultural activity Index of 2008, agricultural output at producer prices (EUR million) in 2008.
Findings: In applying multiple regression model were used data from EU-27. Data are genuine and were taken from Eurostat website. Generating Summary Output using the Excel, it can be noticed that the value of Multiple R (correlation ratio, which shows how the intensity of the connection takes values between 0 and 1) is equal to 0.36. This value indicates relationship between the income from agricultural activity, output at producer prices agricultural and GDP. Also, the value of R Square (shown as percent of variation explained turnover factors and assets) is 0.133. This value indicates that 13,3% of GDP is explained by the income from agricultural activity and output at producer prices agricultural
Limitations: Available data are for the period 2008.
Value: The purpose of this article is to highlight the importance of multiple regression model in assessing the influence that the index of income from agricultural activity and output at producer prices agricultural have on GDP for the EU-27.

Keywords: multiple regression model, agriculture, GDP, EU.

* The work is the result of a complete cooperation and it is, therefore, of responsability of both the authors. The material drawing up of paraghraphs 1, 2 and 3 are attribuiting to Maurizio Lanfranchi, paragraphs 4 and 5 to Pirnea Ionela Carmen.

JEL Classification: C34, Q1

1 Introduction

Agriculture was one of the first sectors of the economy (following coal and steel) to receive the attention of EU policymakers. Article 39 of the Treaty of Rome on the EEC (1957) set out the objectives for the first common agricultural policy (CAP); these were focused on increasing agricultural productivity as a way to ensure a fair standard of living for the agricultural community, stabilizing markets, and ensuring security of supply at affordable prices to consumers.

As the primary objective of producing more food was made, food surpluses accrued, distorting trade and raising environmental concerns. These were the principal drivers for changes in the CAP, a process that started in the early 1990s and which resulted in a change from support for production towards a market-oriented and a more environment-friendly and sustainable form of agriculture. These reforms have focused mainly on increasing the competitiveness of agriculture by reducing support prices and compensating farmers by the introduction of direct aid payments. A decisive step came in the 2003/04 CAP reforms with the decoupling of direct aids from production and a move to try to realign the CAP with consumer concerns.

The scope of this latest reform of the CAP was widened with the introduction of a comprehensive rural development policy. Together these policies aim to encourage entrepreneurial behaviour so that farm managers can respond better to market signals, introduce new techniques and promote diversified activities such as rural crafts, food processing facilities on farms, tourism, or afforestation, as well as promoting sustainable farming practices and various other rural development measures.

In November 2007, the European Commission adopted a Communication ‘preparing the health check of the CAP reform’ with the objective of assessing the implementation of the 2003 CAP reforms, and to introduce those adjustments to the reform process that were deemed necessary.

Notably, these proposals included a shift in funding from direct payments to greater rural development support.

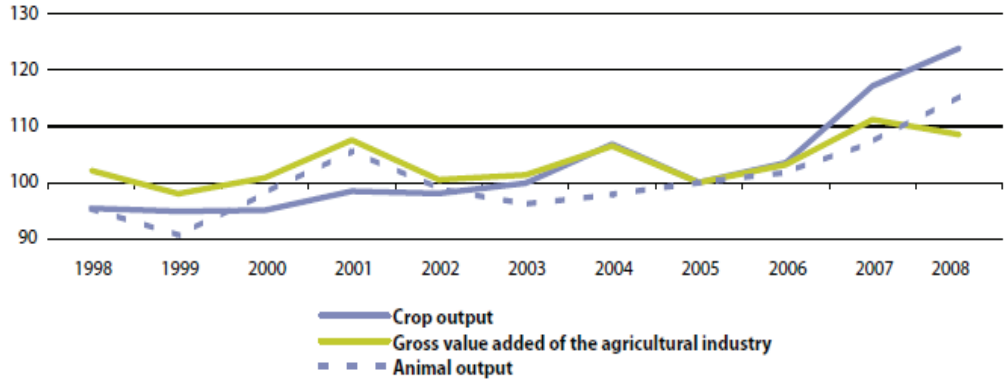
2 Agricultural output, price indices and income Index of income from agricultural activity

One of the principal objectives of the CAP remains providing farmers with a reasonable standard of living. Although this concept is not defined explicitly, one of the measures tracked is the development of incomes from farming activities; economic accounts for agriculture (EAA) are one data source that provides such income measures. This macro-economic set of data is used to analyse the production process of the agricultural activity and the primary income generated by it. The EAA provide key insights into the economic viability of agriculture, its contribution to a Member State's wealth, the structure and composition of agricultural production and inputs, the remuneration of factors of production, relationships between prices and quantities of both inputs and outputs, and responds to the need to have internationally comparable information.

The EAA comprise a production account, a generation of income account, an entrepreneurial income account, some elements of a capital account and agricultural labour input. For the output items of agricultural, hunting and related service activities, Member States transmit to Eurostat values at basic prices, as well as their components (the value at producer prices, subsidies on products and taxes on products). For the items of intermediate consumption, values at purchaser prices are transmitted.

The agricultural industry of the EU-27 generated EUR 141 200 million of gross value added at producer prices in 2008, which represented a modest reduction of 2.4 % in relation to the previous year. Strong increases in both the value of crop output (up 5.7 % to a relative high of EUR 195 700 million in 2008) and animal output (up 7.6 % to a relative high of EUR 148 900 million) were countered by a larger increase in the value of intermediate consumption of goods and services (12.7 % higher in 2008).

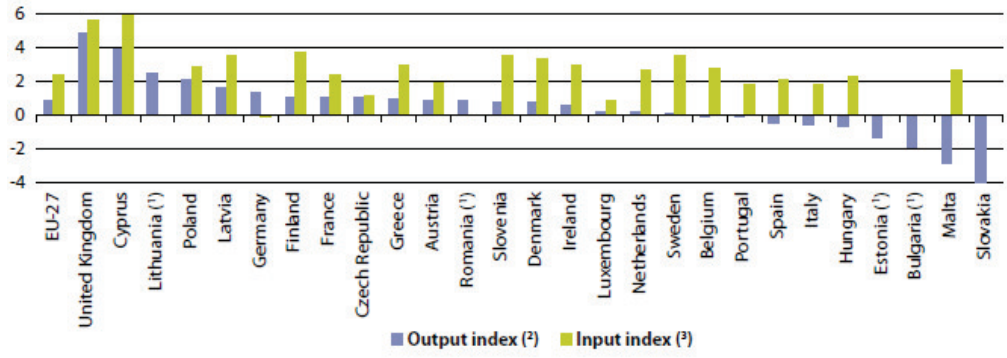
Figure 1: Agricultural output and gross value added at producer prices, EU-27 (2005=100)



Source: Eurostat (aact_eaa01) Europe in figures — Eurostat yearbook 2010, pp.423-460

Values comprise a volume and price component. One important strand of recent agricultural policy has been the move away from price support, so that prices more accurately reflect market forces and changes in supply and demand. Among the Member States, there were sharp contrasts in the development of deflated agricultural output prices during the period between 2002 and 2008; there were rises in the majority of Member States, the strongest increases being recorded for Malta (average growth of 3.9 % per annum) and the United Kingdom (4.8 % per annum), while reductions were posted in eight of the Member States, the largest of which was in Slovakia (-3.9 % per annum).

Figure 2: Evolution of deflated price indices of agricultural output and means of agricultural production, 2002-2008 (average annual growth rate, %)



Source: Eurostat (aact_eaa01) Europe in figures — Eurostat yearbook 2010, pp.423-460

Across the EU-27, deflated agricultural output prices rose by an average of 0.9 % per annum in the six-year period through until 2008, although this was far less than the average rate of increase in deflated input prices for the means of agricultural production during the same period (2.4 % per annum). This characteristic was widespread among the Member States: indeed, Germany was the only Member State for whom the deflated price of the means of agricultural production was relatively unchanged over the period in question (an average rate of decline of 0.1 % per annum).

Real net value added at factor cost of agriculture per unit of full-time labour (measured in annual work units), also termed as agricultural income indicator A, declined by an average 3.7 % across the EU-27 in 2008, compared with a relative peak in 2007. There were stark contrasts among the Member States, with increases of between 15 % and 20 % in the United Kingdom and Hungary, and closer to 30 % in Romania and Bulgaria, contrasting with declines of around 20 % to 25 % in Latvia, Belgium, Estonia and Denmark.

3 Research methodology

Linear regression by least squares method is most common modeling method used. Method is called "regression", "linear regression", "multiple regression" or "the

most squares when constructing a model. Order multiple regression (term used by Pearson, 1908) is to highlight the relationship between a dependent variable (explained endogenous outcome) and a host of independent variables (explanatory factors, exogenous predictors). By using multiple regression to attempt, often getting the response to a question: "what is the best prediction for ...?", "Who is the best predictor for ...?". Note that multiple regression is generalized theory of general linear model", which allow multiple dependent variables simultaneously and also variable factors are not linearly independent [Andrei, Bourbonnais, 2008]. Based on data collected by the Eurostat website, a multiple regression model was generated.

Applying multiple regression model we intend to follow the extent of the index of income from agricultural activity and output at producer prices agricultural can influence GDP. For this we used Excel and Eviews 4.1 programs.

The data series consists of EU-27, index of income from agricultural activity, output at producer prices agricultural and GDP.

List of variables including: continuously variable dependent - GDP per capita in purchasing power standards (PPS), 2008 and two independent variables: index of income from agricultural activity (note: IAA) and output at producer prices agricultural (note: AOPP). Data are available online on the website of the Eurostat.

The proposed multiple regression model the following equation:

$GDP = a + b*IAA + c*AOPP + \varepsilon$, where:

GDP = GDP per capita in purchasing power standards (PPS), 2008

IAA = index of income from agricultural activity

AOPP = output at producer prices agricultural

a, b, c = model parameters to be estimated.

Agricultural income indicators (in the EAA) are presented in the form of an index of real income of factors in agricultural activity per annual work unit (indicator A).

Eurostat also collects annual agricultural prices (in principle net of VAT) to compare agricultural price levels between Member States and study sales channels. Price indices for agricultural products and the means of agricultural production, on the other hand, are used principally to analyse price developments and their effect on

agricultural income. EU agricultural price indices are obtained by a base-weighted Laspeyres calculation (2000=100), and are expressed both in nominal terms and deflated using an implicit HICP deflator.

4 Analysis and interpretation of research results

Data series were used exactly as they were taken from the Eurostat website without having any change. Regression model estimation results in Excel can be seen down:

Figure 3: Regression model estimation results in Excel

SUMMARY OUTPUT

Regression Statistics	
Multiple R	0,364890301
R Square	0,133144932
Adjusted R Square	0,06090701
Standard Error	42,90062446
Observations	27

ANOVA

	df	*SS*	*MS*	*F*	*Significance F*
Regression	2	6784,480779	3392,24039	1,843144537	0,180035402
Residual	24	44171,12589	1840,463579		
Total	26	50955,60667			

	Coefficients	*Standard Error*	*t Stat*	*P-value*	*Lower 95%*	*Upper 95%*	*Lower 95,0%*	*Upper 95,0%*
Intercept	195,3292241	52,5012094	3,720470944	0,001064392	86,9720543	303,6863939	86,9720543	303,686394
IAA	-0,884482972	0,463511997	-1,908220234	0,068394847	-1,84112471	0,072158766	-1,84112471	0,07215877
AOPP	-4,14809E-05	0,001134049	-0,036577679	0,971124285	-0,002382043	0,002299082	-0,00238204	0,00229908

Significance of F value is 0.180035402, so it is lower than 5%, therefore we can say that the model is valid.

The value of Multiple R (the correlation ratio, which shows how the intensity of the connection takes values between 0 and 1) is equal to 0.36. This value indicates that between the GDP, IAA and AOPP there is a weak link.

Value of R square (shown as percent of variation factors explaining turnover assets and fixed assets), is 0.133. This value indicates that 13.3% of GDP is explained by index of income from agricultural activity and by the output at producer prices agricultural.

Calculating the descriptive indicators in EViews we have obtained the following data, which it can be seen in the figure 4.

In summary table presented above, it is noted that the average value of the output at producer prices agricultural is 10394.32 and median value of 1973,141. The data series is relatively heterogeneous view of standard deviation showed a higher value (27183.92) 10394.32 than average. Residual values are normally distributed through increased value of the indicator recorded Jarque Bera. Asymmetry coefficient value of 4.35 recorded series is therefore oriented asymmetric positive. Flattening coefficient shows a value of 21.43, which means that the series is leptokurtotic positive oriented.

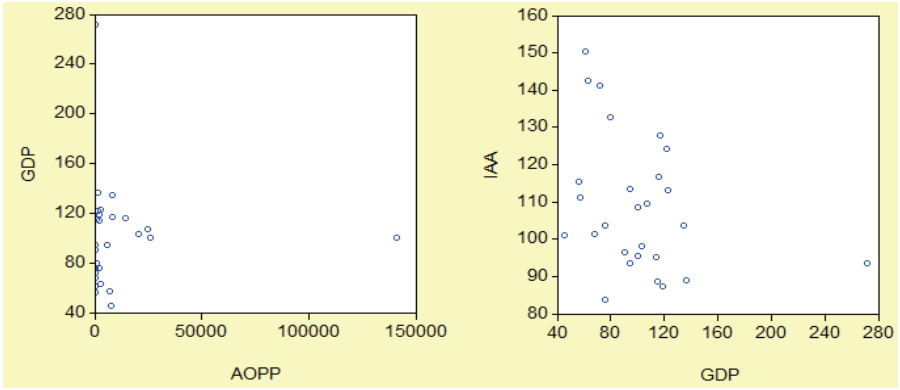
In summary table presented above, it appears that the index of income from agricultural activity analyzed is 108.7963 and median value of 103.8000. The data series is relatively heterogeneous view of standard deviation showed a higher value (17.96767) 108.7963 average for. Residual values are normally distributed through increased value of the indicator recorded Jarque Bera. Asymmetry coefficient value of 0.75 recorded series is therefore oriented asymmetric positive. Flattening coefficient shows a value of 2.71, which means that the series is leptokurtotic positive oriented.

Figure 4: Descriptive indices

	GDP	AOPP	IAA
Mean	100.4926	10394.32	108.7963
Median	100.0000	1973.141	103.8000
Maximum	271.4000	141207.0	150.5000
Minimum	45.80000	43.85630	83.60000
Std. Dev.	42.72141	27183.92	17.96767
Skewness	2.300575	4.354188	0.755510
Kurtosis	10.55822	21.43524	2.714488
Jarque-Bera	88.08445	467.6554	2.660285
Probability	0.000000	0.000000	0.264440
Sum	2713.300	280646.7	2937.500
Sum Sq. Dev.	47453.10	1.92E+10	8393.770
Observations	27	27	27

A series is normally distributed if it has average 0, variance 1, skewness 0 and kurtotica site 3. Analysis of variance conclude that average is not normally distributed, kurtotica is smaller than 3.

Figure 5: Chart "cloud point"



Seen from the chart (chart "cloud point") that includes the points of coordinates (Y, X1) and (Y, X1), a positive linear dependence between the two pairs of variables: the level of GDP is large, the index level of income from agricultural activity and agricultural output at producer prices is lower.

It is estimated multiple regression model parameters:

$GDP = a + b * IAA + c * AOPP + \varepsilon$, the method of least squares.

Figure 6: Results EViews estimate the parameters

Dependent Variable: GDP
Method: Least Squares
Date: 07/24/11 Time: 17:07
Sample: 1 27
Included observations: 27

Variable	Coefficient	Std. Error	t-Statistic	Prob.
AOPP	-1.43E-05	0.000303	-0.047262	0.9627
IAA	-0.790633	0.458029	-1.726163	0.0972
C	186.6592	50.68604	3.682655	0.0012

R-squared	0.110445	Mean dependent var	100.4926
Adjusted R-squared	0.036316	S.D. dependent var	42.72141
S.E. of regression	41.93851	Akaike info criterion	10.41473
Sum squared resid	42212.13	Schwarz criterion	10.55871
Log likelihood	-137.5988	F-statistic	1.489894
Durbin-Watson stat	1.282003	Prob(F-statistic)	0.245512

Now the new model is:

*GDP = -1.430834568e-05 *AOPP - 0.7906325545 *IAA + 186.6592118*

Durbin-Watson test value is around 2, exactly 1.28. This indicates no autocorrelation errors. Durbin-Watson statistics measured serial correlation between

residues. Mean dependent variable (100.4926) and S.D. lime-dependent (42.72141) is the average, respectively, the standard deviation of dependent variable. Akaike info criterion (10.41473), Akaike criterion is a criterion for model selection. We want the minimum. Scwartz criterion (10.55871), Schwartz criterion is analogous to the Akaike criterion. Difference is that impose a greater penalty for additional factors.

Prob (F-statistic) is the threshold marginal statistical significance of F. Its value, of 1.489894, high materiality of 5% or 1% immediately leads us to accept null hypothesis.

Statistical test is the decision taken after comparing the calculated statistics above (t_{calc}) with that of t-Student distribution for materiality stated that:

- null hypothesis H_0: b differ significantly from one

- for a materiality threshold of 5%, respectively 0.05 and 27-5 degrees of freedom we have $t_{0,\,05\,(22)} = 1.717$

$t_{calc} = (186.6592\text{-}1) / 50.68604 = 3.66295$

The value obtained is compared with that of student statistics determined materiality threshold of 5% and 27 to 5 degrees of freedom, which is equal to 1,717. It is accepted that free time value significantly different from the value indicated. Note that the value of F statistics determined from observed data is 1.489894, which has marginal significance level of 0.245512. It is accepted that the constant term value not significantly different from the value indicated.

5 Conclusion

As conclusions, we can propose Wald Test to estimate parameters. According to Eviews we have the following data:

Figure 7: Estimation using Wald Test, based on statistics F.

Wald Test:
Equation: Untitled

Test Statistic	Value	df	Probability
F-statistic	0.000803	(1, 24)	0.9776
Chi-square	0.000803	1	0.9774

Null Hypothesis Summary:

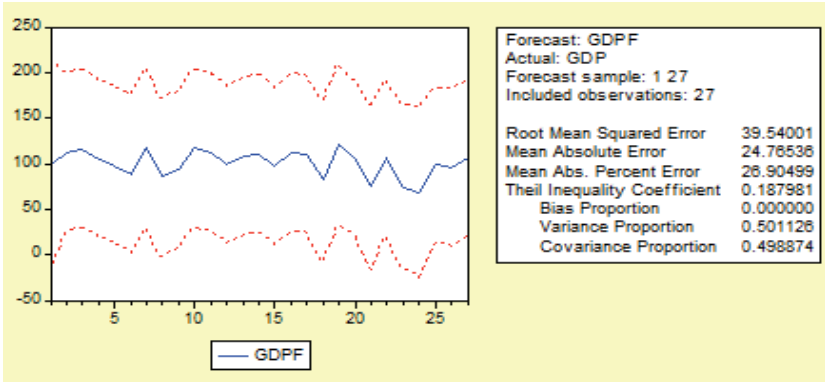
Normalized Restriction (= 0)	Value	Std. Err.
-AOPP*C(1) - C(3) + GDP - ...	1.144859	40.41222

Restrictions are linear in coefficients.
Restrictions evaluated at observation (t = 1)

The results highlight the acceptance of the null hypothesis of linear relationship between the two parameters of the regression model. For both tests are obtained threshold values significantly higher than 0.1.

We made a forecast for the next observation (year). We predicted that the value of index of income from agricultural activity and output at producer prices agricultural will increase next year, wanting to predict the evolution of GDP for the same next year.

Figure 8: Forecast for the next year



Graph and statistics calculated reveals the following findings: Theil's indicator is 0.18, Bias proportioned is 0.00, variance prop is 0.50 and covariance prop is 0.49, which is a situation for prediction validation. The value close to 0 for other indicators, it shows the quality acceptable prediction.

6 Aknowledgements

This article is a result of the project "Doctoral Program in Economics at standards of knowledge Europe (DoEsEC)" ("Doctorat în economie la standardele Europei cunoaşterii (DoEsEC)"), co funded by European Social Fund through The Sectorial Operational Programme for Human Resources Development 2007-2013, coordinated by The Bucharest Academy of Economic Studies.

7 Bibliography

1. Pecican Eugen - *Econometria pentru ... economişti*, Economic Publishing House, Bucharest, 2003, pp. 58-84, pp. 179-233.
2. Stiglitz E. Joseph, Walsh E.Carl - *Economie* Economic Publishing House, Bucharest, 2005, pp.426-441.
3. Tudorel Andrei, Stancu Stelian, Iacob Andreea, Tuşa Erika - *Introducere în econometrie utilizând Eviews*, Economic Publishing House, Bucharest, 2008, pp.49-70.
4. Tudorel Andrei, Spircu Liliana - *Aplicaţii în econometrie*, Economic Publishing House, Bucharest, 2009, pp. 35-48.
5. Tudorel Andrei, Regis Bourbonnais - *Econometrie*, Economic Publishing House mică, 2008, pp. 37-76.
6. ****Agriculture, forestry and fisheries,* Eurostat (aact_eaa01) Europe in figures — Eurostat yearbook 2010, pp.423-460, available on-line at http://epp.eurostat.ec.europa.eu/portal, accesed on July 21, 2011.
7. ****Eurostatistics. Data for short-term economic analysis*, Issue number 07, 2011 edition, Luxembourg: Publications Office of the European Union, ISSN 1831-3221, available on-line at http://epp.eurostat.ec.europa.eu/portal, accesed on July 21, 2011.
8. ****In the spotlight – national accounts: key macro-economic indicators for monitoring the economic and financial crisis,* Europe in figures, Eurostat yearbook 2010, pp.29-85, available on-line at http://epp.eurostat.ec.europa.eu/portal, accesed on July 21, 2011.
9. ***http://epp.eurostat.ec.europa.eu/portal
10. ***www.insse.ro

Authors data:

Maurizio Lanfranchi
Associate Professor
Department SEFISAST- Faculty of Economics University of Messina; Italy
Rizea (Pirnea) Ionela Carmen
Teaching Assistant[1], PhD. Candidate[2]
[1]"Constantin Brancoveanu" University, Valcea; [2] Bucharest Academy of Economic Studies, Romania

RENDICONTI DEL CIRCOLO MATEMATICO DI PALERMO
Serie II, Suppl. 84 (2012), pp. 231-239

A modified density-based algorithm for clustering[1]

Silvestro Montrone[2], Paola Perchinunno[3]

Liliana De Blasi[4], Samuela L'Abbate[5]

Abstract: The aim of this paper is to compare two different clustering methods We consider DBSCAN before in terms of reachability and after in terms of ordering (OPTICS algorithm); the other based on the use of *Seg*-DBSCAN our new version of DBSCAN that limits the arbitrariness of the choice of input parameters. As an application we use a meaningful data set and we compare the described methods.

Keywords: clustering, DBSCAN, *Seg*-DBSCAN, OPTICS.

1. Introduction

The goal of a clustering algorithm is to group the objects of a database into a set of meaningful subclasses. Our clustering approach is based on density. The density-based notion of clustering states that within each cluster, the density of the points is significantly higher than the density of points outside the cluster. We compare two different clustering methods: DBSCAN and Seg-DBSCAN, our modified version of DBSCAN.

2. DBSCAN method

DBSCAN (Density Based Spatial Clustering of Application with Noise) was the first density-based spatial clustering method proposed [1]. The key idea is that to define a new cluster or extend an existing cluster, a neighborhood around a point of a given radius ε must contain at least a minimum number of points *MinPts*, i.e. the density in the neighborhood is determined by the choice of a distance function for two points p and q, denoted by $dist(p,q)$.
There are two different kinds of points in a clustering: core points and non-core points. A point is a *core point* if it has more than a specified number of points (*MinPts*) within ε. These are points that are at the interior of a cluster. The non-core points in turn are either border or noise points. A *border point* has fewer

[1] This contribution is the result of joint reflections by the authors, with the following contributions attributed to: S. Montrone (paragraphs 1-4), to P. Perchinunno (paragraphs 5-6), to L. De Blasi (paragraph 3) and to S. L'Abbate (paragraph 2).
[2] Department of Statistics, University of Bari, s.montrone@dss.uniba.it
[3] Department of Statistics, University of Bari, p.perchinunno@dss.uniba.it
[4] Department of Statistics, University of Bari, liliana.deblasi@dss.uniba.it
[5] Department of Statistics, University of Bari, samuela.labbate@dss.uniba.it

than *MinPts* within ε, but is in the neighborhood of a core point. A *noise point* is any point that is not a core point or a border point.
So any two core points that are close enough - within a distance ε of one another - are put in the same cluster; any border point that is close enough to a core point is put in the same cluster as the core point; instead noise points are discarded.
The formal definitions for this notion of a clustering are shortly introduced in the following. For a detailed presentation see [1].

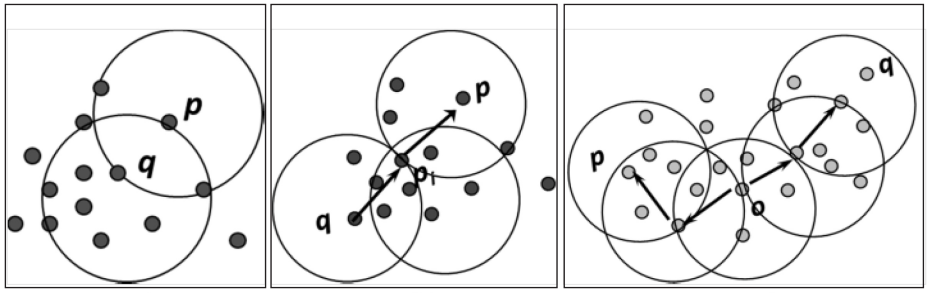
***Definition 1*:** (directly density-reachable)
A point p is *directly density-reachable* from point q with respect to ε and *MinPts* in a set of points D if

1) $N_\varepsilon(q)$, where $N_\varepsilon(q)$ is the subset of D contained in the ε-neighborhood of q, i.e. $N_\varepsilon(q) = \{p \in D | dist(p,q) \leq \varepsilon\}$.
2) $|N_\varepsilon(q)| \geq MinPts$.

The second represents the condition that q is a *core point*. Only from core points, other points can be directly density-reachable. (See Figure 1a)).

***Definition 2*:** (density-reachable)
A point p is *density-reachable* from a point q with respect to ε and *MinPts* in the set of points D if there is a chain of objects $p_1, \ldots, p_n$ with $p_1 = q$ and $p_n = p$, such that $p_i \in D$ and p_{i+1} is directly density-reachable from p_i with respect toε and *MinPts*.
Density-reachability is the transitive hull of direct density reachability and this relation is not symmetric in general; only core points can be mutually density-reachable. (See Figure 1b)).

***Definition 3*:** (density-connected)
A point p is *density-connected* to point q with respect to ε and *MinPts* in the set of points D if there is a point $o \in D$ such that both p and q are density-reachable from o with respect to ε and *MinPts* in D. (See Figure 1c)).
A density-based *cluster* is now defined as a set of density-connected points which is maximal with respect to density-reachability and the *noise* is the set of points not contained in any cluster.



a) **b)** **c)**

Figure 1

***Definition 4*:** (cluster and noise)
Let *D* be a set of points. A *cluster C* with respect to ε and *MinPts* in *D* is a non-empty subset of *D* satisfying the following conditions:
1) Maximality: $\forall p, q \in D$: if $p \in C$ and q is density-reachable from p with respect to ε and *MinPts*, then also $q \in C$.
2) Connectivity: $\forall p, q \in C$: p is density-connected to q with respect to ε and *MinPts in D*.
Every point not contained in any cluster is *noise*.

Note that a cluster contains not only core points but also points that do not satisfy the core point condition: border points. These points of the cluster are, however, directly density-reachable from at least one core point of the cluster (in contrast to noise points).
The algorithm DBSCAN [1], which discovers the clusters and the noise in a database according to the above definitions, is based on the fact that a cluster is equivalent to the set of all points in *D* which are density-reachable from an arbitrary core point in the cluster. The retrieval of density-reachable points is performed by iteratively collecting directly density-reachable points. DBSCAN checks the ε -neighborhood of each point in the database. If the ε -neighborhood $N_\varepsilon(p)$ of a point p has more than *MinPts* points, a new cluster *C* containing the objects in $N_\varepsilon(p)$ is created. Then, the ε -neighborhood of all points q in *C* which have not yet been processed is checked. If $N_\varepsilon(q)$ contains more than *MinPts* points, the neighbors of q which are not already contained in *C* are added to the cluster and their ε-neighborhood is checked in the next step. This procedure is repeated until no new point can be added to the current cluster *C*.
The greatest advantages of DBSCAN are that it can follow the shape of the clusters and that it requires only one distance function and two input parameters. Their choice is crucial because they determine whether a group is a cluster of points or a simple noise.

3. OPTICS method

The algorithm OPTICS (Ordering Points To Identify the Clustering Structure) [2] produces a special order of the dataset with respect to its density-based clustering structure: the points of the dataset are ordered such that points which are spatially closest become neighbors in the ordering.
The formal definitions for this notion of a clustering are shortly introduced in the following. For a detailed presentation see [2].

***Definition 5*:** (core-distance)
The *core-distance* of a point p, denoted by *core(p)*, is the smallest distance such that the *core(p)-neighborhood* of p contains *MinPts* points exactly. Otherwise, if p is not initially a core point with respect to ε then the value of *core (p)* is undefined.

***Definition 6*:** (reachability-distance)
The reachability-distance of a point p, relative to another point o, denoted by *reach (o, p)* is the smallest distance such that p is inside the *reach (o, p)-neighborhood* of o, and o continues to be a core point with respect to *reach (o, p)*. Otherwise, if o is not initially a core point with respect to ε then the value of *reach (o, p)* is undefined.

In the Figure 2 we can see o that is a core point with respect to ε and *MinPts*=5 and *reach (o, p_1)* and *reach (o, p_2)* are the reachability-distances of points p_1 and p_2 with respect to o.

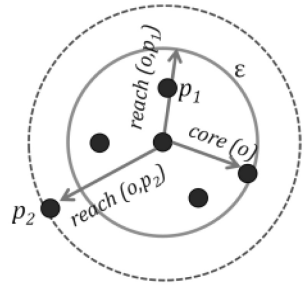


Figure 2

OPTICS algorithm creates an ordering of a data set, additionally storing the *core-distance* and a suitable *reachability-distance* for each point.
This information is sufficient to extract all density-based clusters with respect to *MinPts* and any distance ε' which is smaller than the generating distance ε from this order.
The *reachability-plot* (i.e. the reachability distances of all points plotted in the OPTICS ordering) yields an easy to understand visualization of the clustering structure of the dataset (see Figure 3). A low reachability-distance indicates a point within a cluster, and a high reachability-distance indicates a noise point or a jump from one cluster to another cluster. ε influences the number of clustering

levels which can be seen in the reachability-plot. The smaller we choose the value of ε , the more points may have an undefined reachability-distance, the value of ε have just to be "large" enough to yield a good result. The optimal value for ε is the smallest value so that a density based clustering of the data set with respect to ε and *MinPts* consists of only one cluster containing almost all points of the dataset.
There is a large range of values around this optimal value for which the appearance of the reachability-plot will not change significantly.

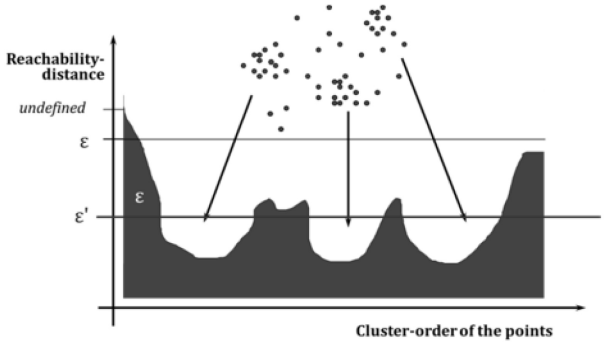


Figure 3: Reachability plot

Like DBSCAN, OPTICS requires two parameters: ε and *MinPts*. As DBSCAN we can use a heuristic procedure to determine the value of ε; we only need to guarantee that this value of ε is not be too small.

4. *Seg*-DBSCAN method

In order to limit the arbitrariness of the choice of a value to assign to ε, usually detected by a heuristic procedure, in this work we develop a new algorithm: *Segmented* DBSCAN (*Seg*-DBSCAN), a modified version of DBSCAN, in which the clusters are aggregated considering multiple levels of value of ε.
Therefore, to define levels of ε, a value of *MinPts* is fixed and we analyze the distribution of the maximum radius of the cores that are groups formed by *MinPts* points. In this algorithm we use a "Manhattan distance" rather than Euclidean:

$$d_{ij} = \sum_{k=1}^{p} |x_{ik} - x_{jk}| \qquad (1).$$

The choice of levels of ε is based on peaks of the distribution histogram of distances with lower variance inside class. We can fix the value of *MinPts* to a number corresponding at our perception of cluster (a core adequately dense).

The final phase of the algorithm is to merge the clusters obtained. The merging of two clusters C_1 and C_2 characterized by different levels of density ε_1 and ε_2 is obtained if

$$d(C_1, C_2) < \max(\varepsilon_1, \varepsilon_2) \quad (2).$$

With this new algorithm, parameter ε is no longer established a priori.

5. Application

As an application we have taken a meaningful data set[6] shown in Figure 4 in which points have great density, variable or constant.

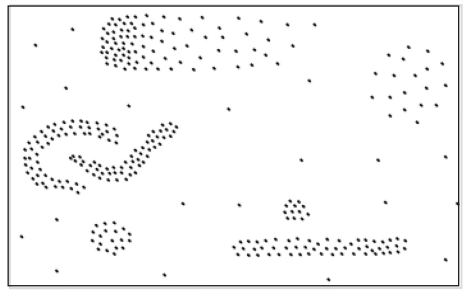


Figure 4: Data set

In this data set we applied described algorithms: classic DBSCAN, OPTICS and the new algorithm Seg-DBSCAN.
When we applied the DBSCAN, we started to consider the value of ε, as suggested in the literature [1]. But with the suggested value of ε equal to 0,002, the algorithm fails to identify meaningful clusters for our data set. So, proceeding by trial and error, we increase the value of ε, until we get an optimal value: 0,007, as shown in Figure 5.
If we try to further increasing the value of ε, we risk introducing noise points, like for ε equal to 0,008 or equal to 0,009,as shown in Figure 6.
When we applied OPTICS algorithm, if ε is too small the algorithm fails to identify meaningful clusters for our data set, as ε equal to 0,002. With a value of ε a little higher, like equal to 0,003, we get a good clustering, as shown in Figure 7.
Finally when we apply the our new algorithm Seg-DBSCAN we not need to establish ε a priori, immediately we obtain an optimal clustering.

[6] http://ubicomp.algoritmi.uminho.pt

Furthermore, we can require that the algorithm makes a merging between clusters and between clusters and border points, the application of Seg-DBSCAN algorithm is shown in Figure 8.

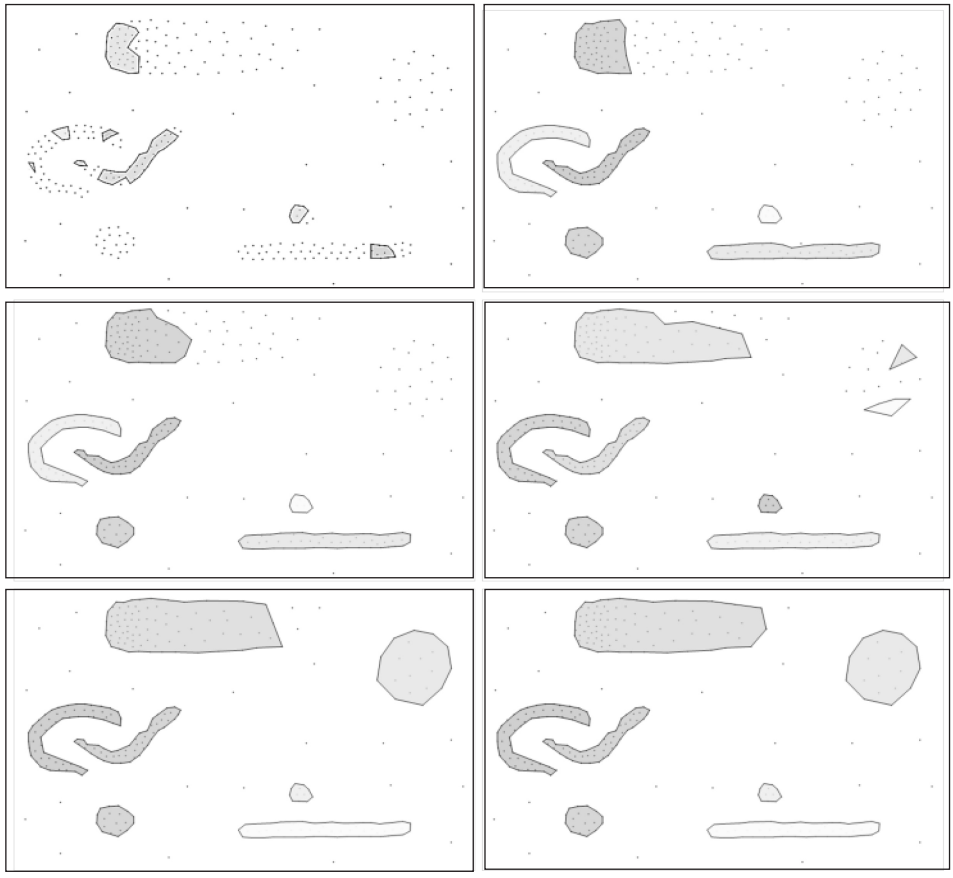


Figure 5: DBSCAN algorithm for ε=0,002; 0,003; 0,004; 0,005; 0,006; 0,007.

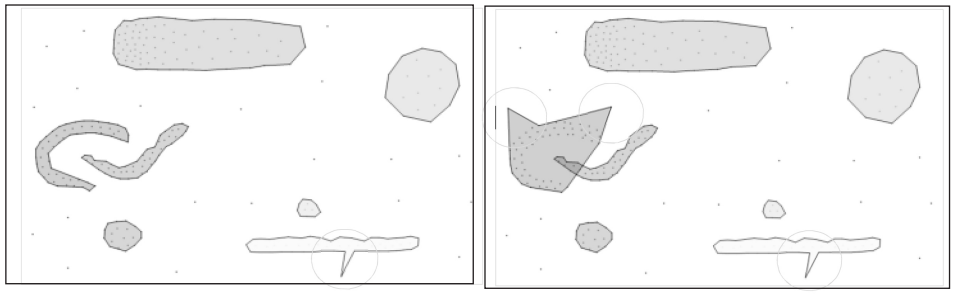


Figure 6: DBSCAN algorithm for ε=0,008; 0,009.

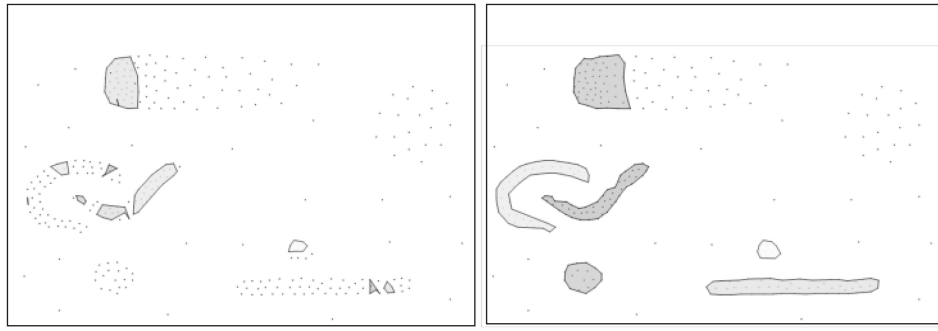


Figure 7: OPTICS algorithm for ε= 0,002 and 0,003.

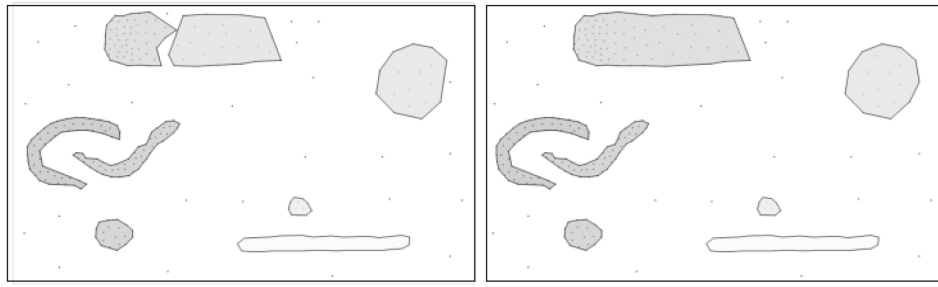


Figure 8: *Seg*-DBSCAN algorithm without and with merging of cluster.

6. Conclusions and future advancements

The presented methods can discover clusters of arbitrary shape and handle noise but need input density parameters; Seg-DBSCAN method not need input parameter ε.
Further advancements are the identification of territorial areas in terms of intensity w.r.t a particular phenomenon, so we implement a weighted *Seg*-DBSCAN to identify areas "at risk" to be monitored in various fields such as medicine or social security.

References

[1] M. Ester, H.-P. Kriegel, J. Sander, Xu X. (1996) *A Density-Based Algorithm for Discovering Clusters in Large Spatial Databases with Noise*. Proc. 2nd Int. Conf. on Knowledge Discovery and Data Mining, Portland.

[2] M. Ankerst, M. M. Breunig, H.-P. Kriegel, J. Sander (1999) *OPTICS: Ordering Points To Identify the Clustering Structure*. Proc. ACM SIGMOD'99 Int. Conf. on Management of Data, Philadelphia.

[3] M. M. Breunig, H.-P. Kriegel, T. Ng Raymond, J. Sander (1999) *OPTICS-OF: Identifying Local Outliers.* Proc. 3rd Eur. Conf. on Principles and Practice of Knowledge, Discovery in Databases (PKDD'99), Prague.

[4] S. Montrone, P. Perchinunno, S. L'Abbate, C. Ligorio (2011) *Comparing SaTScan and Seg-DBSCAN methods in spatial phenomena.* Proc. 2nd European Regional Conf. on Spatial Data Methods for Environmental and Ecological Processes, Italy.

RENDICONTI DEL CIRCOLO MATEMATICO DI PALERMO
Serie II, Suppl. 84 (2012), pp. 241-250

THE CHORD LENGTH DISTRIBUTION FUNCTION FOR A NON CONVEX POLYGON

LOREDANA SORRENTI

Abstract: Let $\mathfrak{R}_D$ be the lattice of Buffon. For a small non convex body $\mathcal{C}$ (a "Greek cross") placed with random position in the Euclidean plane E_2, we give formulas for the probability $p(s)$ that $\mathcal{C}$ intercepts a line segment of length at least equal to s on a line of the lattice $\mathfrak{R}_D$. As an application, we obtain the distribution of secants in $\mathcal{C}$, i.e. we determine the function F, which assigns to each real number s, the probability that any secants in $\mathcal{C}$ has a length less or equal than s.

AMS 2000 Subject Classifications: Geometric probability, stochastic geometry, random sets and random convex sets.
AMS Classification: 60D05, 52A22.

1. Introduction

We denote by $\mathfrak{R}_D$ the Buffon grid consisting of parallel lines with constant distance D. In recent years many authors have studied the geometric probability of the length of a chord, determined by a straight line of the Buffon grid on a polygon. In [2] the problem is studied for a regular hexagon, in [5] for a rectangle, in [3] for a non regular triangle, in [6] for a regular pentagon. In [7] a generalization for an arbitrary regular polygon is given. In [4] and in [8] the chord length distribution function is computed for a rectangular trapezium and an isosceles trapezium, respectively. In [1] the authors give a computation for a non convex polygon.
A fundamental problem in the papers [4], [3], [8], [1] is the large number of cases that must be considered, because there are a lot of different situations arising from the relations between the sides and the diagonals of the polygon. In this paper we consider the non-convex polygon of Figure 1 and we solve the following problem.

Problem 1. *Determining the distribution function F of secants in $\mathcal{C}$, i.e. the function F which assigns to every real number s the probability that any secant in $\mathcal{C}$ has a length less or equal than s.*

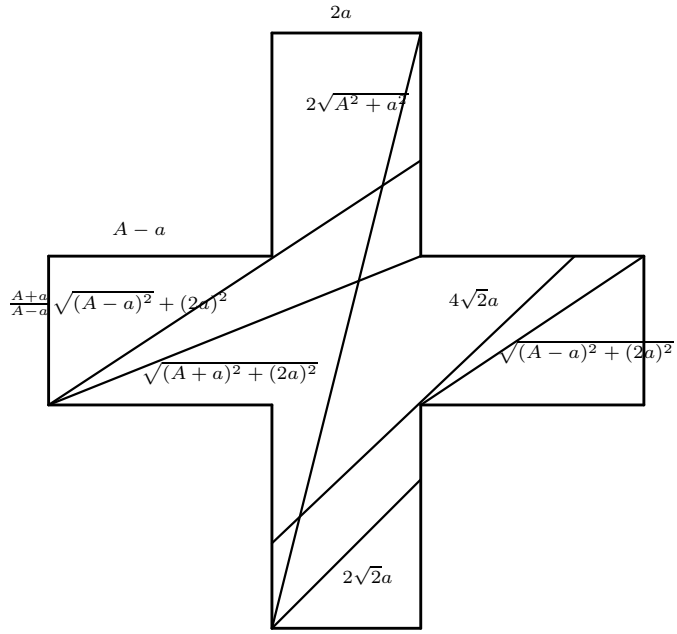


FIGURE 1. The test body $\mathcal{C}$

We denote by $p(s)$ the probability that $\mathcal{C}$ intercepts a line segment of length at least equal to s on a line of the lattice $\mathfrak{R}_D$. As we will see, the computation of $p(s)$ is fundamental to obtain a solution to Problem 1.

2. General considerations

We denote by $\operatorname{diam}(\mathcal{C})$ the diameter of $\mathcal{C}$. We may assume $3a \leq A$ and $D > \operatorname{diam}(\mathcal{C})$, that is, $\mathcal{C}$ is small compared with $\mathfrak{R}_D$. In order to compute $p(s)$ we have to distinguish a large number of different possible relations between the following sides and diagonals of $\mathcal{C}$:

$$2a,\ 2\sqrt{2}a,\ 4\sqrt{2}a,\ A-a,\ A+a,\ \sqrt{(A-a)^2+(2a)^2},\ \sqrt{(A+a)^2+(2a)^2},$$
$$\frac{A+a}{A-a}\sqrt{(A-a)^2+(2a)^2},\ 2\sqrt{A^2+a^2} = \operatorname{diam}(\mathcal{C}).$$

The following relations between the dimensions of $\mathcal{C}$ must be considered:

- $2a < 2\sqrt{2}a < 4\sqrt{2}a \leq \sqrt{(A-a)^2+(2a)^2} < A+a$;
- $\frac{A+a}{A-a} < 2A < 2\sqrt{A^2+a^2}$;
- $2a \leq A-a < \sqrt{(A-a)^2+(2a)^2} < A+a < \sqrt{(A+a)^2+(2a)^2} < \frac{A+a}{A-a}\sqrt{(A-a)^2+(2a)^2}$;
- $2a \leq 2\sqrt{2}a < \sqrt{(A-a)^2+(2a)^2} < A+a < \sqrt{(A+a)^2+(2a)^2}$;
- $2a < 2\sqrt{2}a < 4\sqrt{2}a$.

The other relations depend on the quotient $\frac{A}{a}$. The equivalences

$$2\sqrt{2}a \leq A - a \Leftrightarrow (2\sqrt{2}+1)a \leq A,$$
$$4\sqrt{2}a \leq A - a \Leftrightarrow (4\sqrt{2}+1)a \leq A,$$
$$4\sqrt{2}a \leq A + a \Leftrightarrow (4\sqrt{2}-1)a \leq A,$$
$$4\sqrt{2}a \leq \sqrt{(A+a)^2+(2a)^2} \Leftrightarrow (2\sqrt{7}-1)a \leq A,$$
$$4\sqrt{2}a \leq \sqrt{(A-a)^2+(2a)^2} \Leftrightarrow (2\sqrt{7}+1)a \leq A.$$

give us the values for the quotient $\frac{A}{a}$. In particular, we have to consider the quotient $\frac{A}{a}$ in the following intervals: $]3, 2\sqrt{2}+1], [2\sqrt{2}+1, 2\sqrt{7}-1], [2\sqrt{7}-1, 4\sqrt{2}-1], [4\sqrt{2}-1, 2\sqrt{7}+1], [2\sqrt{7}+1, 4\sqrt{2}+1], [4\sqrt{2}+1, +\infty[$. We consider as fundamental tile $\mathcal{F}$ of $\mathfrak{R}_D$, a boundless strip of width D and we denote by φ the angle between the direction of the straight lines of $\mathcal{F}$ and the oriented side $2a$. Because of the symmetries we may assume $\varphi \in \left[0; \frac{\pi}{4}\right]$. We denote by $d_s(\varphi)$ the maximum distance between two parallel segments with length s intersecting $\mathcal{C}$ and we put $d_s(\varphi) = 0$ if such two segments do not exist. In order to compute the desired probability $p(s)$, we will use the expressions of $x_s(\varphi)$, $y_s(\varphi)$, $z_s(\varphi)$ (see Figure 2) and the well known Stoka's formula [10]:

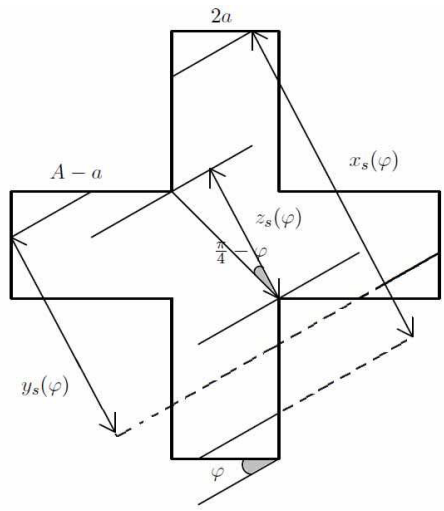


FIGURE 2

$$x_s(\varphi) = 2A\cos\varphi + 2a\sin\varphi - s\sin 2\varphi,\ y_s(\varphi) = 2A\sin\varphi + 2a\cos\varphi - s\sin 2\varphi,$$
$$z_s(\varphi) = 2(\cos\varphi + \sin\varphi)a,$$
$$p(s) = \frac{\int_0^{\frac{\pi}{4}} d_s(\varphi)d\varphi}{\int_0^{\frac{\pi}{4}} D d\varphi} = \frac{4}{\pi D}\int_0^{\frac{\pi}{4}} d_s(\varphi)d\varphi.$$

3. The possible subcases for $d_s(\varphi)$

In order to compute $d_s(\varphi)$ we have to consider the following angles: $\varphi_0, \varphi_1, \varphi_2, \tilde{\varphi}_2, \varphi_3, \varphi_4, \varphi_5$ (see Figure 3). These angles are useful to determine

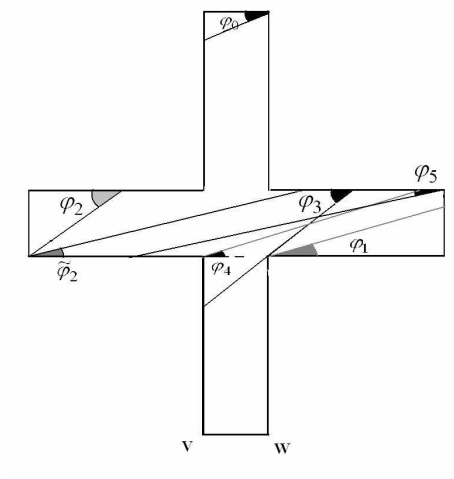


Figure 3

the maximum distance $d_s(\varphi)$ between the secants with length s, where φ is the angle between VW and the secant. All these angles are determined in the interval $\left[0, \frac{\pi}{4}\right]$ by the following equalities:

$$\cos\varphi_0 = \tfrac{2a}{s},\ \cos\varphi_1 = \tfrac{A-a}{s},\ \tfrac{1}{\sin\varphi_3} + \tfrac{1}{\cos\varphi_3} = \tfrac{s}{2a},\ \cos\varphi_4 = \tfrac{A+a}{s},\ \cos\varphi_5 = \tfrac{2A}{s}.$$

$$\tfrac{2a}{s} = \begin{cases} \sin\varphi_2, & \text{if } s \le \sqrt{(A-a)^2 + (2a)^2}; \\ \sin\tilde{\varphi}_2, & \text{if } s \ge \sqrt{(A+a)^2 + (2a)^2}. \end{cases}$$

There exist the following relations:

$$\varphi_1 \le \varphi_0, \varphi_0 < \varphi_2, \varphi_1 < \varphi_2, \varphi_1 < \varphi_3, \varphi_0 < \varphi_3, \varphi_3 < \varphi_2, \tilde{\varphi}_2 < \varphi_3.$$

Note that if the angle φ_4 exists, then $\varphi_0, \varphi_1, \varphi_2$ do not exist; if the angle φ_5 exists, then the other angles do not exist.
Taking into account these preliminary considerations, we have 16 different situations to consider, as the main result shows, in the next section.

4. Main result

Theorem 2. *The probability $p(s)$, that the test body $\mathcal{C}$, uniformly distributed in a bounded region of the plane intersects on a straight line of the Buffon grid $\mathfrak{R}_D$ a line segment with length greater or equal than s is*

computed with one of the following formulas:

$$p(s) = \frac{4}{\pi D}\left[\sqrt{2}A + (2-\sqrt{2})a - \frac{s}{2}\right], \text{ if } 0 \le s \le 2a. \tag{1}$$

$$p(s) = \frac{4}{\pi D}\left[(2+\sqrt{2}-2\sin\varphi_0-2\cos\varphi_0)A + (2\sin\varphi_0+2\cos\varphi_0-\sqrt{2})a + \right. \tag{2}$$
$$\left. -\frac{s}{2}\right], \text{ if } 2a \le s \le \min(A-a, 2\sqrt{2}a)$$

$$p(s) = \frac{4}{\pi D}\left[(\sqrt{2}-2\cos\varphi_0-2\sin\varphi_0+2\cos\varphi_1)A + \left(2-\sqrt{2}+2\cos\varphi_0+\right.\right. \tag{3}$$
$$\left.\left. +2\sin\varphi_0-2\cos\varphi_1\right)a - \frac{s}{2}\cos 2\varphi_1\right], \text{ if } 2a \le A-a \le s \le 2\sqrt{2}a.$$

$$p(s) = \frac{4}{\pi D}\left[(2-2\cos\varphi_2)A + 2a\cos\varphi_2 - \frac{1}{2}(1-2\cos 2\varphi_2)s\right], \tag{4}$$
$$\text{if } 2\sqrt{2}a \le s \le \min(A-a, 4\sqrt{2}a)$$

$$p(s) = \frac{4}{\pi D}\left[(2\cos\varphi_1-2\cos\varphi_2)A + (2-2\cos\varphi_1+2\cos\varphi_2)a - \frac{1}{2}(\cos 2\varphi_1\right. \tag{5}$$
$$\left. -\cos 2\varphi_2)\, s\right],$$
$$\text{if } \max(A-a, 2\sqrt{2}a) \le s \le \min(4\sqrt{2}a, \sqrt{(A-a)^2+(2a)^2});$$

$$p(s) = \frac{4}{\pi D}\left[(2-2\cos\varphi_2)A + (2\cos\varphi_2+2\sin\varphi_3-2\cos\varphi_3)a - \frac{1}{2}(1+\right. \tag{6}$$
$$\left. -\cos 2\varphi_2)\, s\right], \text{ if } 4\sqrt{2}a \le s \le A-a;$$

$$p(s) = \frac{4}{\pi D}\left[(2\cos\varphi_1-2\cos\varphi_2)A + (2-2\cos\varphi_1+2\cos\varphi_2+2\sin\varphi_3+\right. \tag{7}$$
$$\left. -2\cos\varphi_3)\, a - \frac{1}{2}(\cos 2\varphi_1-\cos 2\varphi_2)s\right],$$
$$\text{if } \max(A-a, 4\sqrt{2}a) \le s \le \sqrt{(A-a)^2+(2a)^2};$$

$$p(s) = \frac{4}{\pi D}[2a], \text{ if } \sqrt{(A-a)^2+(2a)^2} \le s \le \min(4\sqrt{2}a, A+a); \tag{8}$$

$$p(s) = \frac{4}{\pi D}\left[(2-2\cos\varphi_4)A + 2a\cos\varphi_4 - \frac{1}{2}(1-\cos 2\varphi_4)s\right], \tag{9}$$
$$\text{if } A+a \le s \le \min(4\sqrt{2}a, \sqrt{(A+a)^2+(2a)^2});$$

$$p(s) = \frac{4}{\pi D}\left[\left((2-2\cos\varphi_4)A + (2\sin\varphi_3-2\cos\varphi_3+2\cos\varphi_4)\, a - \frac{1}{2}(1+\right.\right. \tag{10}$$
$$\left.\left. -2\cos\varphi_4)\, s\right], \text{ if } \max(A+a, 4\sqrt{2}a) \le s \le \sqrt{(A+a)^2+(2a)^2};$$

$$p(s) = \frac{4}{\pi D}\left[(2-2\cos\tilde{\varphi}_2) + (2\sin\tilde{\varphi}_2+2\cos\varphi_4-2\sin\varphi_4)a + \right. \tag{11}$$
$$\left. -\frac{1}{2}(1-\cos 2\tilde{\varphi}_2)s\right], \text{ if } \sqrt{(A+a)^2+(2a)^2} \le s \le 4\sqrt{2}a;$$

$$p(s) = \frac{4}{\pi D}\left[(2+2\sin\varphi_3-2\cos\varphi_3)a\right], \quad (12)$$
$$\text{if } \max(\sqrt{(\mathrm{A}-\mathrm{a})^2+(2\mathrm{a})^2}, 4\sqrt{2}\mathrm{a}) \le \mathrm{s} \le \mathrm{A}+\mathrm{a};$$

$$p(s) = \frac{4}{\pi D}\left[(2\cos\varphi_1-2\cos\varphi_2)A+(2+2\sin\varphi_3-2\cos\varphi_1+2\cos\varphi_2+\right. \quad (13)$$
$$\left.-2\cos\varphi_3)\,a-\frac{1}{2}(\cos 2\varphi_1-\cos 2\varphi_2)s\right],$$
$$\text{if } \max(A-a, 4\sqrt{2}a) \le s \le \sqrt{(A-a)^2+(2a^2)};$$

$$p(s) = \frac{4}{\pi D}\left[(2-2\cos\tilde{\varphi}_2)A+(2\sin\tilde{\varphi}_2+2\sin\varphi_3-2\cos\varphi_3-2\sin\varphi_4+\right. \quad (14)$$
$$\left.+2\cos\varphi_4)\,a-\frac{1}{2}(1-\cos\tilde{\varphi}_2)s\right],$$
$$\text{if } \max(\sqrt{(A+a)^2+(2a)^2}, 4\sqrt{2}a) \le s \le \frac{A+a}{A-a}\sqrt{(A-a)^2+(2a)^2};$$

$$p(s) = \frac{4}{\pi D}\left[(2-2\cos\tilde{\varphi}_2)A+2a\sin\tilde{\varphi}_2-\frac{1}{2}(1-\cos\tilde{\varphi}_2)s\right], \quad (15)$$
$$\text{if } \frac{A+a}{A-a}\sqrt{(A-a)^2+(2a)^2} < s \le 2A;$$

$$p(s) = \frac{4}{\pi D}\left[(2\cos\varphi_5-2\cos\tilde{\varphi}_2)A+(2\sin\tilde{\varphi}_2-2\sin\varphi_5)a+\right. \quad (16)$$
$$\left.-\frac{1}{2}(\cos 2\varphi_5-\cos 2\tilde{\varphi}_2)s\right], \text{ if } 2A \le s \le 2\sqrt{A^2+a^2}.$$

Proof. 1. If $s \le 2a$, $\varphi \in \left[0, \frac{\pi}{4}\right]$, then $d_s(\varphi) = x_s(\varphi)$,

$$\int_0^{\frac{\pi}{4}} d_s(\varphi)\mathrm{d}\varphi = \sqrt{2}A + (2-\sqrt{2})a - \frac{s}{2}.$$

2. If $2a \le s \le \min(A-a, 2\sqrt{2}a)$, then $d_s(\varphi) = \begin{cases} y_s(\varphi), & 0 \le \varphi < \varphi_0; \\ x_s(\varphi), & \varphi_0 \le \varphi \le \frac{\pi}{4}. \end{cases}$

$$\int_0^{\frac{\pi}{4}} d_s(\varphi)\mathrm{d}\varphi = (2+\sqrt{2}-2\sin\varphi_0-2\cos\varphi_0)A +$$
$$+ (2\sin\varphi_0+2\cos\varphi_0-\sqrt{2})a - \frac{s}{2}.$$

3. If $2a \le A-a \le s \le 2\sqrt{2}a$, then $d_s(\varphi) = \begin{cases} z_s(\varphi), 0 \le \varphi < \varphi_1; \\ y_s(\varphi), \varphi_1 \le \varphi < \varphi_0; \\ x_s(\varphi), \varphi_0 \le \varphi \le \frac{\pi}{4}. \end{cases}$

$$\int_0^{\frac{\pi}{4}} d_s(\varphi)\mathrm{d}\varphi = (\sqrt{2}-2\cos\varphi_0-2\sin\varphi_0+2\cos\varphi_1)A +$$
$$+ (2-\sqrt{2}+2\cos\varphi_0+2\sin\varphi_0-2\cos\varphi_1)a - \frac{s}{2}\cos 2\varphi_1.$$

4. If $2\sqrt{2}a \leq s \leq \min(A-a, 4\sqrt{2}a)$, then $d_s(\varphi) = \begin{cases} y_s(\varphi), 0 \leq \varphi \leq \varphi_2; \\ z_s(\varphi), \varphi_2 < \varphi \leq \frac{\pi}{4}. \end{cases}$

$$\int_0^{\frac{\pi}{4}} d_s(\varphi)\mathrm{d}\varphi \quad = \quad (2-2\cos\varphi_2)A + 2a\cos\varphi_2 - \frac{1}{2}(1-2\cos\varphi_2)s.$$

5. If $\max(A-a, 2\sqrt{2}a) \leq s \leq \min(4\sqrt{2}a, \sqrt{(A-a)^2+(2a)^2})$, then
$d_s(\varphi) = \begin{cases} z_s(\varphi), 0 \leq \varphi \leq \varphi_1; \\ y_s(\varphi), \varphi_1 \leq \varphi \leq \varphi_2; \\ z_s(\varphi), \varphi_2 < \varphi \leq \frac{\pi}{4}. \end{cases}$

$$\begin{aligned} \int_0^{\frac{\pi}{4}} d_s(\varphi)\mathrm{d}\varphi \quad &= \quad (2\cos\varphi_1 - 2\cos\varphi_2)A + (2-2\cos\varphi_1+2\cos\varphi_2)a + \\ &\quad -\frac{1}{2}(\cos 2\varphi_1 - \cos 2\varphi_2)a. \end{aligned}$$

6. If $4\sqrt{2}a \leq s \leq A-a$, then $d_s(\varphi) = \begin{cases} y_s(\varphi), 0 \leq \varphi \leq \varphi_2; \\ z_s(\varphi), \varphi_2 < \varphi \leq \varphi_3; \\ 0, \varphi_3 < \varphi \leq \frac{\pi}{4}. \end{cases}$

$$\begin{aligned} \int_0^{\frac{\pi}{4}} d_s(\varphi)\mathrm{d}\varphi \quad &= \quad (2-2\cos\varphi_2)A + (2\cos\varphi_2 + 2\sin\varphi_3 - 2\cos\varphi_3)a + \\ &\quad -\frac{1}{2}(1-\cos 2\varphi_2)s. \end{aligned}$$

7. If $\max(A-a, 4\sqrt{2}a) \leq s \leq \sqrt{(A-a)^2+(2a)^2}$, then $d_s(\varphi) = \begin{cases} z_s(\varphi), 0 \leq \varphi \leq \varphi_1; \\ y_s(\varphi), \varphi_1 \leq \varphi \leq \varphi_2; \\ z_s(\varphi), \varphi_2 < \varphi \leq \varphi_3; \\ 0, \varphi_3 < \varphi \leq \frac{\pi}{4}. \end{cases}$

$$\begin{aligned} \int_0^{\frac{\pi}{4}} d_s(\varphi)\mathrm{d}\varphi \quad &= \quad (2\cos\varphi_1 - 2\cos\varphi_2)A + (2-2\cos\varphi_1+2\cos\varphi_2 + \\ &\quad +2\sin\varphi_3 - 2\cos\varphi_3)\,a - \frac{1}{2}(\cos 2\varphi_1 - \cos 2\varphi_2)s. \end{aligned}$$

8. If $\sqrt{(A-a)^2+(2a)^2} \leq s \leq \min(4\sqrt{2}a, A+a)$, then $d_s(\varphi) = z_s(\varphi)$, if $0 \leq \varphi \leq \frac{\pi}{4}$.

$$\int_0^{\frac{\pi}{4}} d_s(\varphi)\mathrm{d}\varphi = 2a.$$

9. If $A+a \leq s \leq \min(4\sqrt{2}a, \sqrt{(A+a)^2+(2a)^2})$, then $d_s(\varphi) = \begin{cases} y_s(\varphi), 0 \leq \varphi < \varphi_4; \\ z_s(\varphi), \varphi_4 \leq \varphi \leq \frac{\pi}{4}; \end{cases}$

$$\int_0^{\frac{\pi}{4}} (2-2\cos\varphi_4)A + 2a\cos\varphi_4 - \frac{1}{2}(1-\cos 2\varphi_4)s.$$

10. If $\max(A+a, 4\sqrt{2}a) \leq s \leq \sqrt{(A+a)^2+(2a)^2}$, then $d_s(\varphi) = \begin{cases} y_s(\varphi), 0 \leq \varphi < \varphi_4; \\ z_s(\varphi), \varphi_4 \leq \varphi \leq \varphi_3; \\ 0, \varphi_3 < \varphi \leq \frac{\pi}{4}; \end{cases}$

$$\int_0^{\frac{\pi}{4}} d_s(\varphi)\mathrm{d}\varphi \quad = \quad (2-2\cos\varphi_4)A + (2\sin\varphi_3 - 2\cos\varphi_3 + 2\cos\varphi_4)a - \frac{1}{2}(1-\cos 2\varphi_4)s.$$

11. If $\sqrt{(A+a)^2+(2a)^2} \le s \le 4\sqrt{2}a$, then $d_s(\varphi) = \begin{cases} y_s(\varphi), 0 \le \varphi \le \tilde{\varphi}_2; \\ 0, \tilde{\varphi}_2 < \varphi < \varphi_4; \\ z_s(\varphi), \varphi_4 \le \varphi \le \frac{\pi}{4}; \end{cases}$

$$\int_0^{\frac{\pi}{4}} d_s(\varphi)\mathrm{d}\varphi = (2-2\cos\tilde{\varphi}_2) + (2\sin\tilde{\varphi}_2 + 2\cos\varphi_4 - 2\sin\varphi_4)a + -\frac{1}{2}(1-\cos\tilde{\varphi}_2)s.$$

12. If $\max(\sqrt{(\mathrm{A}-\mathrm{a})^2+(2\mathrm{a})^2}, 4\sqrt{2}\mathrm{a}) \le \mathrm{s} \le \mathrm{A}+\mathrm{a}$, then $d_s(\varphi) = \begin{cases} z_s(\varphi), 0 \le \varphi \le \varphi_3; \\ 0, \varphi_3 < \varphi \le \frac{\pi}{4}; \end{cases}$

$$\int_0^{\frac{\pi}{4}} d_s(\varphi)\mathrm{d}\varphi = (2+2\sin\varphi_3 - 2\cos\varphi_3)a.$$

13. If $\max(A-a, 4\sqrt{2}a) \le s \le \sqrt{(A-a)^2+(2a)^2}$, then $d_s(\varphi)$ has the same value of case 7.

14. If $\max(\sqrt{(A+a)^2+(2a)^2}, 4\sqrt{2}a) \le s \le \frac{A+a}{A-a}\sqrt{(A-a)^2+(2a)^2}$, then $d_s(\varphi) = \begin{cases} y_s(\varphi), 0 \le \varphi \le \tilde{\varphi}_2; \\ 0, \tilde{\varphi}_2 < \varphi < \varphi_4; \\ z_s(\varphi), \varphi_4 \le \varphi \le \varphi_3; \\ 0, \varphi_3 < \varphi \le \frac{\pi}{4}. \end{cases}$

$$\int_0^{\frac{\pi}{4}} d_s(\varphi)\mathrm{d}\varphi = (2-2\cos\tilde{\varphi}_2)A + (2\sin\tilde{\varphi}_2 + 2\sin\varphi_3 - 2\cos\varphi_3 - 2\sin\varphi_4 + +2\cos\varphi_4)\,a - \frac{1}{2}(1-\cos\tilde{\varphi}_2)s.$$

15. If $\frac{A+a}{A-a}\sqrt{(A-a)^2+(2a)^2} < s \le 2A$, then $d_s(\varphi) = \begin{cases} y_s(\varphi), 0 \le \varphi \le \tilde{\varphi}_2; \\ 0, \tilde{\varphi}_2 < \varphi \le \frac{\pi}{4}; \end{cases}$

$$\int_0^{\frac{\pi}{4}} d_s(\varphi)\mathrm{d}\varphi = (2-2\cos\tilde{\varphi}_2)A + 2a\sin\tilde{\varphi}_2 - \frac{1}{2}(1-\cos\tilde{\varphi}_2)s.$$

16. If $2A \le s \le 2\sqrt{A^2+a^2}$, then $d_s(\varphi) = \begin{cases} 0, 0 \le \varphi < \varphi_5; \\ y_s(\varphi), \varphi_5 \le \varphi \le \tilde{\varphi}_2; \\ 0, \tilde{\varphi}_2 < \varphi \le \frac{\pi}{4}; \end{cases}$

$$\int_0^{\frac{\pi}{4}} d_s(\varphi)\mathrm{d}\varphi = (2\cos\varphi_5 - 2\cos\tilde{\varphi}_2)A + (2\sin\tilde{\varphi}_2 - 2\sin\varphi_5)a + -\frac{1}{2}(\cos 2\varphi_5 - \cos 2\tilde{\varphi}_2)s.$$

□

Remarks 3. (a) If $s = 2a$, then $\varphi_0 = 0$ and formulas (1) and (2) coincide.
(b) If $s = A - a$, then $\varphi_1 = 0$ and formulas (2) and (3) coincide.
(c) If $s = 2\sqrt{2}a$, then $\varphi_1 = 0$, $\varphi_0 = \varphi_2 = \frac{\pi}{4}$ and formulas (3) and (4) coincide.
(d) If $s = A - a \ge 2\sqrt{2}a$, then $\varphi_1 = 0$ and formulas (4) and (5) coincide.
(e) If $s = A - a = 4\sqrt{2}a$, then $\varphi_1 = 0$, $\varphi_3 = \frac{\pi}{4}$ and (5), (6), (7) coincide.
(f) If $A - a < 4\sqrt{2}a = s = \sqrt{(A-a)^2+(2a)^2}$, then $\varphi_3 = \frac{\pi}{4}$, $\varphi_1 = \varphi_2 = \arccos\left(\frac{2a}{\sqrt{(A-a)^2+(2a)^2}}\right)$ and formulas (7) and (8) coincide.

(g) If $s = A + a \leq 4\sqrt{2}a$, then $\varphi_4 = 0$ and formulas (8) and (9) coincide.
(h) If $A + a \leq s = 4\sqrt{2}a \leq \sqrt{(A+a)^2 + (2a)^2}$, then $\varphi_3 = \frac{\pi}{4}$ and formulas (9) and (10) coincide.
(i) If $\sqrt{(A+a)^2 + (2a)^2} = s = 4\sqrt{2}a \leq \sqrt{(A+a)^2 + (2a)^2}$, then $\varphi_3 = \frac{\pi}{4}$ and $\varphi_4 = \tilde{\varphi}_2$ and formulas (10) and (11) coincide.
(l) If $4\sqrt{2}a = s = \sqrt{(A-a)^2 + (2a)^2}$, then $\varphi_1 = \varphi_2$, $\varphi_3 = \frac{\pi}{4}$ and formulas (11) and (14) coincide.
(m) If $s = 4\sqrt{2}a$ then $\varphi_3 = \frac{\pi}{4}$ and formulas (11) and (14) coincide.
(n) If $s = 2A$, then $\varphi_5 = 0$ and formulas (15) and (16) coincide.

Remark 4. If $s = 0$ formula (1) returns

$$p(0) = \frac{4}{\pi D}\left[\sqrt{2}A + (2 - \sqrt{2})a\right]. \tag{17}$$

Note that the convex hull of $\mathcal{C}$, denoted by $co(\mathcal{C})$ (see Figure 4), has the

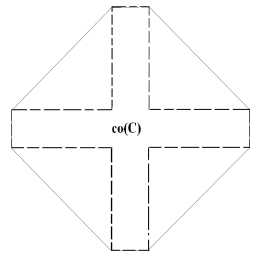


FIGURE 4

following perimeter:

$$\text{per}(co(\mathcal{C})) = 4\sqrt{2}A + 4(2 - \sqrt{2})a.$$

Then formula (17) coincides with the Cauchy's formula:

$$p(0) = \frac{\text{per}(co(\mathcal{C}))}{\pi D}. \tag{18}$$

5. The distribution of the chord in $\mathcal{C}$

Let us consider the function $F : [0, 2\sqrt{A^2 + a^2}] \to [0, +1]$, which assigns to each s, $s \in [0, 2\sqrt{A^2 + a^2}]$ the conditioned probability that a straight line intersecting $\mathcal{C}$, determines on $\mathcal{C}$ a chord with length less or equal than s. This function is called *distribution function of the chord in* $\mathcal{C}$. In order to compute F we consider a lattice $\mathfrak{R}_D$, with $D > 2\sqrt{A^2 + a^2} = \text{diam}(\mathcal{C})$ and we use the following formula:

$$F(s) = 1 - \frac{p(s)}{p(0)}.$$

In particular, in cases 1 and 8, we obtain

- $F(s) = 2s$, if $s \leq 2a$ (Case 1);
- $F(s) = \frac{A-a}{A+(\sqrt{2}-1)a}$, if $\sqrt{(A-a)^2+(2a)^2} \leq s \leq \min(4\sqrt{2}a, A+a)$ (Case 8).

Note that in these two cases F is a linear function of s. In all the other cases F is not a linear function of s. The density f of the distribution of the chord in $\mathcal{C}$ is the derivative of F, therefore $F' = f$. Since the function F is continuous and piecewise differentiable, then the density f is defined on $]0, 2a[\cup]2a, \min(A-a, 2\sqrt{2}a)[\cup]A-a, 2\sqrt{2}a[\cup]\ldots]2A, 2\sqrt{A^2+a^2}[$. In particular, in cases 1 and 8, f is a constant function:

- $f(s) = 2$, if $0 < s < 2a$ (Case 1);
- $f(s) = 0$, if $\sqrt{(A-a)^2+(2a)^2} < s < \min(4\sqrt{2}a, A+a)$ (Case 8).

References

[1] D. Barilla, A. Duma and A. Puglisi, *The distributions function of a chord in a non-convex polygon*, Suppl. Rend. Circ. Mat. Palermo, Serie II, 83, 2011, pp. 23-40.

[2] V. Conserva and A. Duma, *Schnitte eines regulären hexagons in Buffon-und Laplace-Gitter*, in Hagen, Band 78, 2007, pp. 29-36.

[3] A. Duma and S. Rizzo, *Chord lenght distribution functions for an arbitrary triangle*, Suppl. Rend. Circ. Mat. Palermo, Serie II, 81, 2009, pp. 141-158.

[4] A. Duma and S. Rizzo, *La funzione di distribuzione di una corda su un trapezio rettangolo*, Suppl. Rend. Circ. Mat. Palermo, Serie II, 83, 2011, pp. 147-160.

[5] M. Pettineo, *Geometric probability problems for Buffon and Laplace grid*, Suppl. Rend. Circ. Mat. Palermo, Serie II, 81, 2009, 267-274.

[6] L. Sorrenti, *On some geometric and algebraic models for image analysis*, Communications in Applied and Industrial Mathematics, Perspective on Applied Mathematics in Italy 2009, 2010.

[7] L. Sorrenti, *Geometric probability of the lenght of a chord for an arbitrary regular polygon*, Suppl. Rend. Circ. Mat. Palermo, Serie II, 83, 2011, pp. 249-257.

[8] L. Sorrenti, *Chord length distribution functions for an isosceles trapezium*, preprint 2010.

[9] M. Stoka, *Probabilitá e Geometria*, Herbita Editrice, Palermo, 1982.

[10] M. Stoka, *Probabilités géometriqués de type "Buffon" dans le plan euclidien*, Atti Acc. Sci. Torino, 110, pp. 53-59, 1975-76.

Università degli Studi Mediterranea di Reggio Calabria, DIMET, Facoltà di Ingegneria Via Graziella, Feo di Vito, 89100, Reggio Calabria, Italy, loredana.sorrenti@unirc.it

RENDICONTI DEL CIRCOLO MATEMATICO DI PALERMO
Serie II, Suppl. 84 (2012), pp. 251-257

On score tests devised to discover late registration of events of point processes

Franz Streit
Section de Mathématiques, Université de Genève
streit@unige.ch

Abstract

It happens frequently that due to imperfections of the recording device or some other problems some or all events of a point process are registered with delay. Locally most powerful tests are proposed which are useful to discover modifications of incoming point processes caused by such delay mechanisms. It is explained how to simulate point processes relevant in this context and the implementation of the test procedures on the resulting data sets is shown.

Keywords: Score tests, point processes, random delays of events.

1. Introduction

An important task of the statistical inference for point processes consists in developing statistical tests helpful to distinguish between different classes of point processes. Usually the null hypothesis for such tests is formed by a standard class of point processes, often homogeneous Poisson point processes. It is desired to find out whether this class contains a stochastic model appropriate for the description of the observed point process or if it is preferable to take into consideration a more complicated point process, which is a member of the alternative hypothesis. In the statistical literature for instance inhomogeneous Poisson point processes, renewal point processes, point processes with independent locations, Wold point processes and cluster point processes have been chosen as alternatives. Instead of taking such well-known subfamilies of point processes, we can however also consider classes of point processes, which are modified before observation due to the influence of problems arising when handling them. In

this contribution I shall be concerned with point processes which have undergone delayed registration of some or all of its point events. Such situations present themselves due to imperfectations of the recording device or practical problems (e.g. traffic jams, strikes, delivery problems) causing late registration of events. It is thus useful to discover modifications of the incoming point process due to the presence of delay mechanisms.

We suppose that the point process is started at time $t = 0$ and we designate by $T(i)$ the time of registration of the ith point event after $t = 0$. Random variables are represented by capital letters and their realized values by the corresponding lower case letters. By $N(t)$ we denote the number of recorded point events in $(0, t]$, $R_{(0,b]}$ stands for the uniform distribution with support $(0, b]\,[b > 0]$ and $N^*(a, g)$ for the normal distribution with mean a and variance g.

Depending on the knowledge of the statistician about the experimental situation and depending on the type of data collected the above described general problem admits different interpretations which may lead to different proposed solutions. I shall however work with the version of the problem based on the following assumptions:

We suppose that the input point process is a homogeneous Poisson point process with global intensity rate μ. Any individual point event arriving at some time x within the observation period $(0, t]$ of the point process is delayed with the same constant probability δ and the delay times for different point events are independent realizations from a distribution function F with $F(0) = 0$; alternatively the point event is recorded at arrival time with probability $1 - \delta$.

A point event recorded at time $t = y$ in this set up has thus intensity $\mu_d(y) = (1-\delta)\mu+\delta \int_0^y dF(y-x)\mu dx = ((1-\delta)\mu+\delta\mu F(y)\,[0 < y \leq t]$. Thus allowing delays to occur as indicated amounts to replace the homogeneous Poisson point process with global intensity rate μ by the inhomogemeous Poisson point process with intensity function μ_d as relevant stochastic model. It is well known that in this set-up the likelihood of observing exactly $N(t) = n$ recorded point events at the instants $t_1, \ldots, t_n$ within $(0, t]$ is equal to the local Janossi density, which takes the form

$j_n(t_1, \ldots, t_n|(0, t] : \delta) =$
$\prod_1^n((1 - \delta)\mu + \mu\delta F(t_i)) \cdot \exp[-(1 - \delta)\mu t - \mu\delta \int_0^t F(\tau)d\tau]$ [3,p.213].

A justification of this formula neglecting higher order δ-terms, which are not relevant in the following, is obtained by stating that exactly

n recorded point events arise in $(0,t]$ if either exactly n point events arrive which are non-delayed or if exactly n-1 such non-delayed and one delayed point event are recorded within $(0,t]$ or if n non-delayed events present themselves in $(0,t]$ and one delayed point event arriving in $(0,t]$ is recorded after time t and thus not observed, this leading to the alternative equivalent expression
$j_n(t_1,\ldots,t_n|(0,t]:\delta) =$
$\mu^n e^{-\mu t}(1-\delta)^n + \mu^n e^{-\mu t}(1-\delta)^{n-1}\delta\sum_1^n F(t_i) +$
$\mu^{n+1}e^{-\mu t}(1-\delta)^n\delta\int_0^t\int_t^\infty dF(y-x)dx + o(\delta).$
Statistically the problem to decide whether delays actually occur for the observed point process amounts to test the hypotheses $H_0:\delta=0$ versus $H_{\delta_0}:\delta=\delta_0$ for δ_0 with $0<\delta_0\leq 1$. Here we are faced with the difficulty that the exact value of the distortion probability δ_0 is usually not known even if complete knowledge of F is available. An examination of the likelihood shows that no uniformly most powerful test can exist: In fact the optimal statistic of H_0 versus H_{δ_0} depends on δ_0. Since only the first factor in the first formula for j_n involves the observed data, it is alone relevant. For $\delta_0=1$ an equivalent version of the test statistic is thus $\sum_{i=1}^{N(t)}\ln(F(T(i))$ and for $\delta_0=1/2$ $\sum_{i=1}^{N(t)}(\ln(1/2+F(T(i))/2))$ and these two expressions treat the observed data in general differently because the sets of realizations leading to equal given values are not the same.
Two methods may be used to deal with such a situation:
Either one incorporates an a-priori distribution for the unknown δ_0 and adoptes a Bayesian point of view, assuming that reliable information on the possible values of δ_0 and the chances to encounter them is available. On the other hand one can also determine a locally most powerful test for δ_0 positive but near 0, searching thus a test sensitive to typical deviations from the null hypothesis in the direction of the alternatives. Having already treated the former method in a recent paper [6], I shall discuss here the second approach.

2. Locally most powerful tests

The score statistic yielding a locally most powerful test is obtained as follows:
$T_{F,\mu}(0) = \partial\ln(j_{N(t)}(T(1),\ldots,T(N(t))|(0,t]:\delta)/\partial\delta|_{\delta=0} =$
$\sum_{i=1}^{N(t)}(F(T(i))-1) + \mu t - \mu\int_0^t F(\tau)d\tau.$

Since under $H_0\,(T(1),\ldots,T(N(t)))|N(t)=n$ is the order statistic of a random sample of size n $R_{[0,t]}(1),\ldots,R_{(0,t]}(n)$ from $R\sim R_{(0,t]}$ we have under H_0 the alternative representation
$T_{F,\mu}(0)=\sum_{i=1}^{N(t)}F(R_{(0,t]}(i))-1)+\mu t-\mu\int_0^t F(\tau)d\tau$,
which shows that the equivalent statistic
$\tilde{T}_{F,\mu}(0)=\sum_{i=1}^{N(t)}(F(R_{(0,t]}(i))-1)$, is a sum of a random number of independent identically distributed random variables. This suggest to apply the central limit theorem of Anscombe and Rényi [4,p.70 & 71] after the preliminary result
$\tilde{T}_{F,\mu}(0)/\sqrt{N(t)}|N(t)=n\sim N^*(n^{1/2}((\int_0^t((F(\tau)d\tau/t)-1),(\int_0^t F^2(\tau)d\tau/t)-[(\int_0^t F(\tau)d\tau/t]^2)$
under $H(0)$ for $n\to\infty$. Since
$E[T_{F,\mu}(0):\delta=0]=\mu t\int_0^t F(\tau)d\tau/t-\mu t+\mu t-\mu\int_0^t F(\tau d\tau=0$ and
$Var[T_{F,\mu}(0):\delta=0]=$
$Var[\sum_{i=1}^{N(t)}(F(R_{(0,t]}(i)-1):\delta=0]=$
$\mu tE[(F(R)-1)]^2+\mu tVar[(F(R)-1)]=\mu tE[(F(R)-1)^2]=$
$\mu t\int_0^t F^2(\tau)d\tau/t-2\mu t\int_0^t F(\tau)d\tau/t+\mu t.$
Thus under H_0 and for $t\to\infty$
$T_{F,\mu}(0)\sim N^*(0,\mu t(\int_0^t F^2(\tau)d\tau/t-2\int_0^t F(\tau)d\tau/t+1))$,
taking into account that $(N(t)/t)\to\mu$ in probability.
The critical region of size α of a locally most powerful test for H_0 versus H_1 has thus for large t the form
$T_{F,\mu}(0)/\sqrt{\mu t(\int_0^t F^2(\tau)d\tau/t-2\int_0^t F(\tau)d\tau/t+1)}>z(1-\alpha)$,
with $\Phi(z(1-\alpha))=1-\alpha$ and Φ the distribution function of the standard normal distribution.
In the special case where $F=R_{(0,t]}$, thus $F(\tau)=\tau/t\,[0<\tau\leq t]$ we find
$\int_0^t F(\tau)d\tau/t=\int_0^t\tau/t^2d\tau=1/2$ and therefore
$T_{R_{(0,t]},\mu}=\sum_{i=1}^{N(t)}(R_{(0,t]}(i)-1)+\mu t/2$ and
$\int_0^t F^2(\tau)d\tau/t=\int_0^t\tau^2/t^3d\tau=1/3$, leading to
$Var[T_{R_{(0,t]},\mu}:\delta=0]=\mu t/3-2\mu t/2+\mu t=\mu t/3.$

3. Numerical implementation

In order to illustrate the implementation of the test we choose $\mu=1$ and $t=100$ and construct first a typical realization of a homogeneous Poisson point process with global rate $\mu=1$. To obtain the

values t_i we add successively the terms of a sequence of independent, identically standard exponentially distributed random variables, stopping after reaching $t = 100$. Using the data published in the book of Cox and Miller [2, p.377] we get 87 point events in the observation period (Table I, column (2)). For the alternative with $\delta = 1$ the intensity function of the modified point process is $F(t) = t/100$ instead of the constant 1. Applying the simulation method for processes with bounded conditional intensities of Lewis and Shedler [5;3 p.270] we compare the values $F(t_i)$ (column (4)) with independent realizations v_i (column (5)) of a standard uniform distribution as published in Abramowitz and Stegun [1,p.991] and retain the point event only if $F(t_i) \geq v_i$ is satisfied. We end up with a modified point process with 38 observed point events in $(0, 100]$ (column (3)). If we calculate for these retained point events the contributions $F(t_i^*) - 1$ to the test statistic (column (6)) and sum them we get a realized value of $7,00$ for the standardized test statistic, whose observed asymptotic level of significance is only $1,3 \cdot 10^{-12}$. This extremly small value prompts us to accept H_1. On the other hand calculating the contributions to the test statistic for all the 87 point events of the original process results in the value 1,54 of the standardized test statistic with observed asymptotic level of significance $\alpha_{obs} = 0,06$. This is not a exceptionally small value and we accept thus H_0. In both cases the test arrives to the correct conclusions. Furthermore for $\delta = 1/4$ we obtain a standardized test statistic of $3,30$ with $\alpha_{obs} = 5 \cdot 10^{-4}$, which leads to acceptance of H_1. This indicates that the test recognizes even occasional delays if they are not too rare.

Table I gives some details of the evaluation for the alternative with $\delta = 1$.

Table 1

i	t_i	i^*	$F(t_i)$	v_i	$(F(t_{i^*})-1)$
(1)	(2)	(3)	(4)	(5)	(6)
1	0,22		0,00	0,53	
2	2,75		0,03	0,81	
3	3,91		0,04	0,98	
4	4,46		0,04	0,12	
5	4,60		0,05	0,60	
6	4,79		0,05	0,40	
7	5,71		0.06	0,41	
8	6,65		0,07	0,39	
9	9,11		0,09	0,43	
10	9,31		0,09	0,69	
11	10,50		0,11	0,97	
12	10,69		0,11	0,70	
13	10,81		0,11	0,58	
14	11,06		0,11	0,92	
15	11,97		0,12	0,26	
16	13,37		0,13	0,45	
17	13.93		0,14	0,83	
18	16,24		0,16	0,97	
19	17,22		0,17	0,93	
20	17,73		0,18	0,78	
21	19,22		0,19	0,66	
22	21,62		0,22	0,38	
23	27,22		0,27	0,75	
24	28,23		0,28	0,71	
25	29,24		0,29	0,85	
26	29,60	1	0,30	0,14	–0,70
27	32,71		0.33	0,99	
28	32,72		0,33	0,92	
29	33,44		0,33	0,66	
30	34,01		0,34	0,60	
31	35,83		0,36	1,00	
32	37,36		0,37	0,76	
33	38,09	2	0,38	0,32	–0,62
34	39,26		0,39	0,43	
35	41,91		0,42	0,83	
36	45,71		0,46	0,82	
37	45,78	3	0,46	0,15	–0,54
38	46,67	4	0,47	0,26	–0,53
39	48,73	5	0,49	0,25	–0,51
40	48,85	6	0,49	0,21	–0,51
41	48,86	7	0,49	0,30	–0,51
42	50,38	8	0,50	0,49	–0,50
43	55,79		0,56	0,92	
44	56,40	9	0,56	0,38	–0,44
45	57,42	10	0,57	0,43	–0,43
46	60,67	11	0,61	0,27	–0,39
47	60,74		0,61	0,84	
48	61,13	12	0,61	0,45	–0,39
49	61,38		0,61	0,69	
50	67,16		0,67	0,69	
51	67,33		0,67	0,82	
52	68,67		0,69	0,83	
53	69,36	13	0,69	0,15	–0,31
54	69,40		0,69	1,00	
55	71,80	14	0,72	0,13	–0,28
56	72,85	15	0,73	0,30	–0,27
57	73,43	16	0,73	0.48	–0,27
58	73,60		0,74	0,94	
59	75,58		0,76	0,87	
60	76,35		0,76	0.99	
61	76,60	17	0,77	0,20	–0,23
62	78.75		0,79	0,91	
63	80,23	18	0,80	0,72	–0,20
64	80,59		0,81	0,95	
65	80,68	19	0,81	0,56	–0,19
66	82,39	20	0,82	0,61	–0,18
67	82,91		0,83	0,84	
68	83,20	21	0,83	0,55	–0,17
69	84,35	22	0,84	0,48	–0,16
70	84,60	23	0,85	0,64	–0,15
71	85,24	24	0,85	0,09	–0,15
72	85,46	25	0,85	0,33	–0,15
73	86,77	26	0,87	0,54	–0,13
74	86,93	27	0,87	0,53	–0,13
75	88,54	28	0,89	0,19	–0,11
76	88,71	29	0,89	0,26	–0,11
77	89,22		0,89	0,96	
78	91,02	30	0,91	0,67	–0,09
79	92,99	31	0,93	0,78	–0,07
80	95,39		0,95	0,97	
81	95,70	32	0,96	0,31	–0.04
82	95,77	33	0,96	0,58	–0,04
83	96,03	34	0,96	0,41	–0,04
84	96,45	35	0,96	0,41	–0,04
85	98,66	36	0,99	0,21	–0,01
86	98,67	37	0,99	0,94	–0,01
87	99,52	38	1,00	0,49	–0,00

References

[1] Abramowitz,M. & Stegun,I.A. Handbook of mathematical functions. National Bureau of Standards, Washington, 1964.

[2] Cox,D.R. & Miller,H.D. The theory of stochastic processes, Chapman & Hall, London, 1996.

[3] Daley,D.J. & Vere-Jones,D. An introduction to the theory of point processes. Vol. I . Springer, New York, 2003.

[4] DasGupta,A. Asymptotic theory of statistics and probability. Springer, New York, 2008.

[5] Lewis,P.A.W. & Shedler,G.S. Simulation of nonhomogeneous Poisson processes by thinning. Naval Research Logistics Quart. 26,3, 403-413, 1979.

[6] Streit,F. Detection of delays at the registration of events of a point process. 58. World Statistic Congress of the ISI, 2011, Dublin (23.August, on CD).

RENDICONTI DEL CIRCOLO MATEMATICO DI PALERMO
Serie II, Suppl. 84 (2012), pp. 259-266

A GLM approach for the customer satisfaction measurement in some bathing beaches of Messina province[1]

Agata Zirilli. Angela Alibrandi

1. Introduction

The measure of customer satisfaction is a relatively new concept for many companies whose interest, until recently, was addressed only to the data of income and assets (Giarelli, 2002). The customer satisfaction identification allows the relationship between business and users in order to understand needs and expectations and, therefore, to adequate products and services to customer expectation (Bogani, 2001).
In this work we focused our attention on customer satisfaction measurement in bathing establishments, by virtue of the growing interest that people show toward the seaside holidays. In recent years, port authorities and municipalities receive a very large number of requests for release of grant of beaches.
The bathing beach is a strictly summer service, it was initially created for hotels customers and was later extended to daily, weekly and monthly customers. There are many reasons for bathers to choose the bathing establishment: the existence of amenities and services (umbrellas, chairs, snacks, drinks, entertainment, etc...) and the cleanliness in the beach.
In this context, our goal is twofold: firstly, we propose to use the PLUM methodology for modeling ordinal response variables; this model class represents a methodologically adequate solution in the case of quality judgments, guarantying a good fit to data; on the other hand, we want to evaluate the customer satisfaction in the bathing establishments; in particular, we want to individuate the factors that significantly influence the global satisfaction level and to verify the possible dependence from these potential predictors.

[1] This note, though it is the result of a close collaboration, was specifically elaborated as follows: paragraphs 1, 5 and 6 by A. Zirilli and paragraphs 2, 3 and 4 by A. Alibrandi

2. The PLUM approach

PLUM (Polytomous Universal Model) is an extension of the general linear model to ordinal categorical data (Marija J. Norušis,2009; Lawson and Montgomery,2006). In ordinal logistic regression, the event of interest is observing a particular score or less; for the rating of three judges, we model the following odds:

Θ_1 = prob(score of 1)/prob(score greater than 1)

Θ_2 = prob(score of 1 or 2)/prob(score greater than2)

Θ_3 = prob(score of 1,2 or 3)/prob(score greater than 3)

The last category doesn't have an odds associated with it, since the probability of scoring up to and including the last score is 1. All of the odds are of the form:

Θ_j = prob(score $\leq$ j) / prob(score >j) that is equal to:

Θ_j = prob(score $\leq$ j) / (1- prob(score $\leq$ j).

Consequentially, the number of constants to be estimated in the model are equal to the number of categories of the response variable minus 1. (Amemiya, 1981). The ordinal logistic model for a single independent variable is:

$$ln(\Theta j) = \alpha j - \beta X \qquad (1)$$

where *j* goes from 1 to the number of categories minus 1. Larger coefficients indicate an association with larger scores. For a continuous variables, a positive coefficient indicates that as the values of the variables increase, the likelihood of large scores increases. An association with higher scores means smaller cumulative probabilities for lower scores, since they are less likely to occur. Each logit has its own αj term but the same coefficient β. That means that the effect of the independent variable is the same for different logit functions.

The ordinal logistic model is based on the assumption that there is a latent continuous outcome variable and that the observed ordinal outcome arises from the discretizing the underlying continuum into j- ordered groups (Agresti, 2002).

The basic form of the generalized linear model is

$$link(\gamma i) = \frac{\theta j - [\beta_1 x_1 + \beta_2 x_2 + ... + \beta_k x_k]}{\exp(\tau_1 z_1 + \tau_2 z_2 + ... + \tau_m z_m)} \qquad (2)$$

where:

γ_j is the cumulative probability for the *j*th category,

Θ_j is the threshold for the j-th category,

$\beta_1 \ldots \beta_k$ are the regression coefficients,

$x_1 \ldots x_k$ are the predictors;

k is the number of predictors;

$\tau_1 \ldots \tau_m$ are coefficients for the scale component

$z_1 \ldots z_m$ are the *m* predictors variables for the scale component.

The link function is, as it is known, the link between the random component and the systematic component

In PLUM procedure, there are 5 available different link functions:

Table 1: Link functions in PLUM procedure

Function	Form	Typical application
Logit	ln (y/1-y)	Evenly distributed categories
Complementary Log-log	ln (-ln (1-y))	Higher categories more probable
Negative log-log	-ln (-ln (y))	Low categories more probable
Probit	$\Phi^{-1}(y)$	Analyses with explicit normally distributed latent variable
Cauchit (Cauchy)	Tan (Π (y-0.5))	Outcome with many extreme values

3. The data

In this paper the data are derived from responses to a questionnaire, ad hoc designed to measure the satisfaction level of bathers towards the services provided by some bathing establishments, located on the Ionian coast of Messina province.

The sample consists of 309 bathers, aged between 16 and 58 years, present in the bathing area at the time of questionnaire administration.

Each bather gave its agreement, with reference to each item, on an ordinal scale consisting of five levels.

The survey was performed in the period July – August 2010, according to the technique of cluster sampling, that results justified by the considerable savings in terms of time/ cost.

The questionnaire was structured into four sections:

- an introductory registry section to obtain basic information on gender and age, place of residence and profession of the interviewees;
- a section about contextual factors, where the respondent is asked to express the personal reason for choosing the bathing establishment;
- a section on interest indicators, where the respondent is asked to express a personal judge, according to an ordinal growing scale, about some indicators of interest (staff courtesy and helpfulness, environment cleanliness, toilets usability, auxiliary services quality, structure accessibility, personal assessments about the costs sustainability);
- an overall judgment towards the services offered by the frequented bathing establishment.

Figure 1 shows the satisfaction mean levels of the interviewed with reference to the interest indicators.

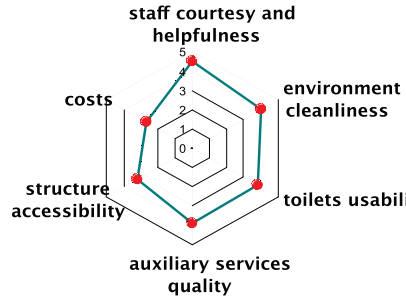


Figure 1 – Satisfaction mean levels for indicators

As we can see, the highest mean levels of satisfaction are found for "staff courtesy and helpfulness" and "environment cleanliness"; the lowest satisfaction, however, is referred to the "costs".

Table 2 shows the observed frequencies of the bivariate distributions of satisfaction levels for sex and age (that has been categorized in three classes).

In general, we note that the higher satisfaction assessments (4 and 5 response levels) are more numerous than the extreme dissatisfaction assessments (1 and 2 response levels). In particular, the most satisfied subjects are female and aged between 30 and 45 years.

Table 2: Absolute frequencies and percentages of bivariate distributions of sex and age class for satisfaction levels

		Satisfaction levels					
Factors		***1***	***2***	***3***	***4***	***5***	**Total**
Sex	M	0 *(0,0)*	11 *(3,6)*	42 *(13,6)*	57 *(18,4)*	14 *(4,5)*	**124 *(40,1)***
	F	2 *(0,6)*	13 *(4,2)*	45 *(14,6)*	93 *(30,1)*	32 *(10,4)*	**185**

							(59,9)
Age classes	≤30	1 *(0,3)*	5 *(1,6)*	24 *(7,8)*	37 *(12,0)*	16 *(5,2)*	**83 *(26,9)***
	30-45	1 *(0,3)*	10 *(3,2)*	27 *(8,7)*	59 *(19,1)*	21 *(6,8)*	**118 *(38,2)***
	>45	0 *(0,0)*	9 *(2,9)*	36 *(11,7)*	54 *(17,5)*	9 *(2,9)*	**108 *(35,2)***

4. Results

Initially we estimated all univariate models in order to individuate the factors that significantly influence the bathers satisfaction level measured on five level (Table 3); so, in our model the number of constants to be estimated is four. On the bases of the significant predictors, we estimated a multivariate model that allows to define the bathers' profile (Table 4). For each model we provide parameter estimations (coefficients, standard error and relative p-value).

Table 3: Results of univariate PLUM models estimation

Predictor	B	S.E	p	**Predictor**	B	S.E	p
Constant 1	-5,60	0.77	0.000	Constant 1	-5.22	0.71	0.000
Constant 2	-2.95	0.37	0.000	Constant 2	-2.57	0.22	0.000
Constant 3	-1.11	0.33	0.000	Constant 3	-0.72	0.15	0.000
Constant 4	1.20	0.33	0.000	Constant 4	1.59	0.17	0.000
Age	-0.01	0.01	0.070	Sex	-0.42	0.21	0.057
Constant 1	0.19	0.79	0.808	Constant 1	0.01	0.75	0.998
Constant 2	3.84	0.59	0.000	Constant 2	3.36	0.49	0.000
Constant 3	6.54	0.66	0.000	Constant 3	6.39	0.59	0.000
Constant 4	9.64	0.77	0.000	Constant 4	9.76	0.72	0.000
Staff courtesy	1.82	0.17	**0.000**	Env.cleanl.	1.94	0.16	**0.000**
Constant 1	1.60	0.41	0.002	Constant 1	-0.30	0.77	0.692
Constant 2	4.03	0.46	0.000	Constant 2	2.92	0.48	0.000
Constant 3	7.02	0.56	0.000	Constant 3	5.56	0.55	0.000
Constant 4	7.03	0.57	0.000	Constant 4	8.76	0.67	0.000
Toilet usab.	1.42	0.13	**0.000**	Auxil.serv.	1.73	0.15	**0.000**
Constant 1	-2.02	0.75	0.008	Constant 1	1.56	0.90	0.083
Constant 2	0.838	0.36	0.023	Constant 2	4.61	0.69	0.000
Constant 3	3.16	0.41	0.000	Constant 3	6.96	0.74	0.000
Constant 4	6.03	0.50	0.000	Constant 4	9.88	0.85	0.000
Struct.access.	1.11	0.12	**0.000**	Costs	2.49	0.24	**0.000**

[Dependent variable: bathers satisfaction, measured on five levels]

By examining the results of the univariate models, we can see that bathers satisfaction is significantly dependent on staff courtesy, environment cleanliness, toilet usability, auxiliary services, structure accessibility and costs. So, we estimated a multivariate PLUM model (Table 4) that allowed us to identify, in the complex pattern of variables, the statistically significant

predictors of bathers satisfaction. For this model, we report also the log-likelihood test and the relative significance.

Table 4: Results of multivariate PLUM models estimation

Predictor	B	S.E	Wald	p
Constant 1	7.69	1.30	34.63	0.000
Constant 2	14.44	1.43	100.21	0.000
Constant 3	19.44	1.78	126.50	0.000
Constant 4	24.43	2.06	148.35	0.000
Age	0.01	0.01	1.02	0.314
Sex	-0.74	0.27	7.20	**0.007**
Staff courtesy	0.66	0.21	9.68	**0.002**
Env. cleanlin.	1.20	0.22	31.18	**0.000**
Toil.usability	0.35	0.19	3.35	0.067
Auxil.services	0.53	0.21	5.88	**0.015**
Struct.access.	0.41	0.15	7.67	**0.006**
Costs	0.98	0.34	8.16	**0.004**
-2 Log-Likelihood=375.620		df=7	p=**0.000**	

At the multivariate approach, bathers satisfaction results significantly dependent on sex (the negative sign of the coefficient denotes an higher satisfaction for sex=0 i.e. female, than for sex=1 i.e.male), staff courtesy, environment cleanliness, auxiliary services, structure accessibility and costs; toilet usability is not a significant predictor.

We investigated the existence of possible interactions between the regressors, but in any case there were significant estimates of these effects, at the prefixed significance level (α=0.05).

5. Model fit estimation

Finally, we focused our attention on model fit estimation; taking into account the categorical nature of the response variable, we used the following index:

- Cox & Snellαs pseudo R-squared, expressed by:

$$R^2 = 1 - \left\{ \frac{L(M_{Intercept})}{L(M_{Full})} \right\}^{2/N} \qquad (3)$$

where:

M_{full} = model with predictors

$M_{intercept}$ = model without predictors

(= estimated likelihood.

It has a maximum value that is not 1: if the full model predicts the outcome perfectly and has a likelihood of one, Cox & Snell's is less than one.

- Nagelkerke pseudo R-squared, expressed by:

$$R^2 = \frac{1-\left\{\frac{L(M_{Intercept})}{L(M_{Full})}\right\}^{2/N}}{1-L(M_{Intercept})^{2/N}} \quad (4)$$

It is the ratio between the Cox & Snell R-squared and its maximum possible value, $1\text{-}L(M_{Intercept})^{2/N}$. If the full model perfectly predicts the outcome and has a likelihood of 1, it is equal to 1.

- McFadden pseudo R-squared, expressed by:

$$R^2 = 1-\frac{\ln \hat{L}(M_{Full})}{\ln \hat{L}(M_{Intercept})} \quad (5)$$

It is the ratio between the log-likelihood of the intercept model and the log-likelihood of the full model. A small ratio of log-likelihoods indicates that the full model is a far better fit than the intercept model. In Table 5 we show the values of the above mentioned tests, that denote an acceptable model fit estimation.

Table 5: Model fit estimations

Pseudo	**Cox & Snell's**	**Nagelkerke**	**McFadden**
R square	0.704	0.771	0.499

6. Final remarks

Focusing our attention on the obtained results, we can affirm that the statistical analysis showed a significant influence of some factors (sex, staff courtesy, environment cleanliness, auxiliary services, structure accessibility and costs) on bathers satisfaction that attempt the bathing establishment.

Among these significant predictors, environment cleanliness is the most remarkable satisfaction factor, as demonstrated by its higher significance. Moreover the women also seem to be more satisfied (especially aged between 30 and 45 years).

The uneasiness (particularly the structure accessibility and the costs) constitute factors in evident contrast with the attainment of elevated satisfaction standards.

References

AGRESTI A. (2002), Categorical data analysis (2nd edition). New York: Wiley.

AMEMIYA, T., (1981), Qualitative response models: a survey, Journal of Economic Literature 19, 1483-1536.

BOGANI G. (2001), La qualità del sistema dei processi realizzativi: i sistemi di gestione per la qualità, T. Conti, P. De Risi (a cura di), Manuale della qualità, Il Sole 24 ore, Milano.

GIARELLI G. (2002), Oltre la customer satisfaction: il problema di cogliere la complessità di un punto di vista, a cura di C. Cipolla, G. Giarelli, L. Altieri , Valutare la qualità in sanità, Franco Angeli, Milano.

LAWSON C., MONTGOMERY, C., (2006), Logistic Regression Analysis of Customer Satisfaction Data. Quality and Reliability Engineering International. 22, 971- 984.

MARIJA J. NORUŠIS. (2009). PASW Statistic 18. Statistical Procedures Companion. Paerson Education

Finito di stampare da
"Fotograf digital service"
Palermo, novembre 2012